CD4 T cells are both protective and pathologic in mice following ocular herpes simplex virus type 1 (HSV-1) infection

by

Andrew John Lepisto

B.A. Washington and Jefferson College, 1999

Submitted to the Graduate Faculty of

School of Medicine in partial fulfillment

of the requirements for the degree of
Doctor of Philosophy

University of Pittsburgh

2005

UNIVERSITY OF PITTSBURGH

FACULTY OF SCHOOL OF MEDICINE

This dissertation was presented

by

Andrew John Lepisto

It was defended on

June 1st, 2005

and approved by

JoAnne Flynn, Ph.D.
Associate Professor, Department of Molecular Genetics and Biochemistry

Olivera J. Finn, Ph.D.
Professor, Department of Immunology

Paul R. Kinchington, Ph.D.
Associate Professor, Department of Ophthalmology

Anuradha Ray, Ph.D.
Professor, Departments of Medicine and Immunology

Robert L. Hendricks, Ph.D.
Dissertation Director
Professor, Departments of Ophthalmology, Immunology, and Molecular Genetics and
Microbiology

ii

Copyright permission was granted for:

1. Xu M, Lepisto AJ, Hendricks RL. Co-stimulatory requirements of effector T cells at inflammatory sites. DNA and Cell Biology. 2002. May-June;21 (5-6):461-5.

2. Andrews and McMeel Publishers for Calvin and Hobbes comic strip

Copyright permission letters are on file with Andrew Lepisto.

CD4^{+} T cells are both protective and pathologic in mice following ocular herpes simplex virus type 1 (HSV-1) infection

Andrew John Lepisto

University of Pittsburgh, 2005

A major challenge to combating ocular herpes simplex virus type 1 (HSV-1) infection lies in controlling the protective and immunopathological potential of the immune system. Numerous studies have shown that the immune system, especially CD8 T cells, plays an integral role in the establishment and maintenance of viral latency. In contrast, CD4 T cells mediate an immunoinflammatory response in the infected cornea termed herpes stromal keratitis (HSK) that leads to scarring and blindness. Here we address several hypotheses related to the role of CD4 T cells following ocular HSV-1 infection.

First, we asked if stimulation through the costimulatory pair CD134/OX40L is required for the activation of CD4 T cells within the infected cornea and subsequent inflammation. Our findings established that both CD134 and OX40L are expressed in the cornea during HSK. However, blocking CD134/OX40L interactions did not alleviate HSK. Our second hypothesis was that HSV-specific CD4 T cells are required to initiate HSK, but bystander activation becomes important during the later, chronic stages of disease. To address this hypothesis we isolated and cloned CD4 T cells from infected corneas, demonstrated their reactivity to viral antigens, and confirmed their capacity to mediate HSK in nude mice. These cells will be used in future studies to investigate the relative role of antigen-specific and bystander activated CD4 T cells in HSK. Next, we tested the hypothesis that while CD4 T cells are the primary mediators of inflammation in the cornea, CD8 T cells can also mediate inflammation in their absence. Our

findings established that CD8 T cells can mediate HSK, but CD8 T cell-mediated HSK is transient and only induced when high doses of virus are used to infect the cornea.

We also tested our hypothesis that CD4 T cell help is required for the proper generation and maintenance of memory CD8 T cells at the site of viral latency. Our findings demonstrate that CD4 T cells control the contraction phase of the effector CD8 T cell response within the TG, the generation of CD8 memory precursors, and directly or indirectly influence viral genome burden within sensory neurons following ocular infection.

Acknowledgments

First and foremost, I want to thank my mother for all of her love, guidance, and wisdom that has made me the person I am today. Her determination to provide for our family instilled within me a drive to do my best at everything I attempt and to never give up. I would also like to thank my sister Liisa as her intelligence and drive to succeed helped me strive to always put forth my best effort. I would also like to thank my grandparents, Dan and Marge Zoltani and Miriam Lepisto and the rest of my family for all of their love and support.

I would like to thank my beautiful wife Laura for her unwavering support and love throughout graduate school. She has always been understanding of the trials and tribulations that comprise graduate school and has helped me persevere through all the rough times. I have enjoyed every day we have been together and I look forward to many more wonderful years ahead.

I would like to thank my advisor Robert L. Hendricks for his unwavering optimism in my work throughout graduate school. I could not have had a more supportive and motivating mentor than Bob. His scientific expertise is unparalleled and I am grateful to have learned under his tutelage.

I would also like to thank all of the past and present members of the Hendricks lab for all of their help in experimental design and brainstorming.

TABLE OF CONTENTS

LIST OF FIGURES

PREFACE

1.   Introduction

1.1.   General background

1.1.1.   Herpes simplex virus basics and epidemiology

1.1.1.1.   Epidemiology of HSV-1 and HSV-2

Herpes simplex viruses (HSV) are some of the most ubiquitous infectious agents in the world. Estimates of seroprevalence of HSV-1 in the United States alone exceed two-thirds of all people aged 12 or older (1). The prevalence steadily increases with age resulting in greater than 90% seropositivity in persons aged 70 or older. Seroprevalance of HSV-1 in the US is significantly higher in females (70.9%) compared to males (64.2%) and higher seropositivity is observed in Mexican Americans (85.1%) compared to African Americans (74.1%) and Caucasians (64.7%). Infection with HSV-1 usually occurs in the facial region; however recent evidence has shown that HSV-1 is an increasing cause of genital lesions (2-4). The most common manifestation of HSV-1 infection is the common cold sore or fever blister of the mouth or lip, which is a recurrent problem in many individuals and is due to the ability of the virus to persist in the host for the life of the individual. HSV-1 infection of the eye can result a blinding disease termed herpes stromal keratitis (HSK) and is a leading cause of infectious blindness in the US.

The seroprevalance of HSV-2 worldwide varies greatly among geographic area, with the highest incidence of HSV-2 infection found in areas of Africa and in some parts of the Americas, including the United States (5). The NHANES III study revealed a high percentage of HSV-2 positive individuals in the United States with the seroprevalance of HSV-2 in people 12 years and older at approximately 22%, corresponding to ~45 million infected individuals. This study

found a higher incidence of HSV-2 in women (25.6%) vs men (17.8%) and in African Americans (45.9%) vs Caucasians (17.6%). This number has risen dramatically since the late 1970s and represents a large public health issue especially if this number continues to rise as has been projected (6). It is important to note that both HSV-1 and HSV-2 infections result in infection for the life of the individual due to the inability of the host immune system to fully eliminate the virus.

1.1.1.2.   Viral structure and life cycle

HSV-1 is comprised of four basic parts; 1) a lipid envelope studded with at least 11 different varieties of glycoproteins important in viral binding and entry, 2) an amorphous tegument which contains proteins necessary for the initiation of viral transcription, 3) an icosadeltahedral capsid that surrounds the viral core, and 4) the core which contains the approximately 152 kbps dsDNA genome (7). All of these components together form an intact virion with an approximate diameter of 200nm. The large viral genome has been estimated to encode at least 84 different viral proteins which are produced in a sequential fashion during a lytic infection, a hallmark of HSV. The viral genes are sub-divided into several basic classes based upon the timing of their expression: immediate early (α or IE) genes, the early (β or E) genes, and the late (γ or L) genes.

The viral life cycle of a lytic infection begins with the virus binding to the surface of a cell followed by the viral envelope fusing with the plasma membrane and releasing the capsid and tegument proteins into the cytoplasm. Glycoproteins gB and gC are required for attachment, while gD is necessary for the actual entry of the virus into the cell. Tegument proteins are delivered into the cell immediately following viral fusion and entry and are important regulators of both host and viral transcription. One such tegument protein, vhs, immediately induces host

mRNA degradation within the cell during which time the viral capsid is transported to the nuclear pores. Once the viral capsid reaches the nuclear pore, viral DNA is released into the nucleus and α gene transcription is initiated. This initiation of α gene transcription is facilitated by another tegument protein, VP16, in concert with the host protein Oct-1. Most of the α gene products function to transactivate the next class of viral genes, the β genes, which are predominately involved in viral genome replication. Following viral nucleic acid synthesis, the γ genes are produced which are primarily structural proteins such as new capsids and glycoproteins, which are then used to package new virions. It is important to note that some γ genes are produced prior to viral DNA replication, hence these select genes are termed γ1 genes. One such γ1 gene of particular importance is glycoprotein B, which serves as the immunodominant antigen for the host CD8 T cell response in C57Bl/6 mice which will be discussed in greater detail later. All other γ genes that are produced after viral DNA replication are termed γ2 genes. The newly formed virion is then packaged and egresses from the cell thus completing the lytic viral life cycle.

1.1.1.3.   Lytic vs latent infection

In some cases, HSV infection does not result in destruction of the host cell, instead the virus enters into a latent state characterized by little to no detectable viral gene expression. This intriguing facet of HSV has been the focus of intense study by virologists for decades. Latent infections occur within sensory ganglia that innervate the site of primary infection. Viral DNA with the nuclei of these sensory ganglia becomes episomal and can persist in this state for the life of the individual. Very few viral transcripts are generated during latency, most notable the latency associated transcripts (LAT). This transcript has been shown to be expressed by some

neurons that contain viral DNA, however a definitive functional product of this transcript has not been identified (8-10).

More recently, HSV latency is being redefined due to the findings of several investigators that immediate early, early, and even late genes of the viral genome are indeed transcribed in latently infected mouse trigeminal ganglia (TG), the site of viral latency following ocular HSV-1 infection (11-14). One of the earliest studies by Coen's group showed viral mRNA for the IE gene ICP4 and the E gene TK are produced in latently infected TGs (11). This group also later showed that late gene transcripts for gC could be detected in latently infected mouse TG (12). More recently, Margolis' group confirmed the earlier works of Coen by showing transcripts for ICP4, TK and gC in latently infected TGs using in situ hybridization on numerous TG sections (14). This work illustrated how very rare it is possible to detect individual neurons that are actively producing viral transcripts, with their findings that only one neuron out of 10 latently infected TGs was positive for viral gene transcription (14). Additionally, this group showed that not only are viral genes being transcribed, but that viral gene proteins were produced in latently infected TGs, again at a very low incidence of one positive neuron out of 10 latently infected TGs.

Additional evidence for active viral gene expression during latency was shown by Sawtell in which 17% of latently infected ganglia were positive for viral proteins at 31 days post-infection (P.I.) (15). It is important to note that in those ganglia that were positive, only a single neuron out of the entire ganglion was positive for viral proteins. It was noted that the percentage of ganglia positive for viral protein decreased as the time P.I. increased to a point at which only 6.5% of ganglia were viral protein positive at 60 days P.I. The author of this study estimates that only one out of 90,000 latently infected neurons will produce viral proteins. Work by our group

has shown that latently infected neurons express IE (ICP4) and E (ICP8) proteins in ex vivo TG cultures (16). These observations lead us to hypothesize that viral gene transcription during latency results in the production of immuno-stimulatory antigens which in turn results in an active immune response that maintains viral latency. These concepts will be discussed in depth later.

In some cases, the virus switches from this latent state back to a lytic life cycle. This process is referred to as reactivation and ultimately results in recurrent disease at the site of initial infection due to production of new infectious viral particles within the sensory ganglia that travel back to that primary site and cause new lesions. Some stimuli for this reactivation include UV-B irradiation (17), hyperthermia (18) and stress (19-21), however a molecular understanding of how these stimuli results in reactivation remain unknown. It is important to note two key points about reactivation and how it differs from lytic life cycle. First, VP16, which is required for initial viral gene transcription during a lytic infection appears to be dispensable for reactivation in vivo (22). Secondly, ICP0 is required for efficient reactivation in vivo (23), while it is dispensable during lytic infection (24).

Historically, most virologists believed that the intrinsic nature of the host neuron regulates viral reactivation; however the concept that the host immune system plays an active role is now gaining support. This topic will be discussed in greater detail in a later section.

1.1.2. Structure of the eye and cornea

1.1.2.1. Basic anatomy of the eye

Initial infection of the surface of the eye by HSV-1 results in the infection and destruction of corneal epithelial cells. An additional consequence of corneal infection by HSV-1 is the virus gains access to nerve termini within the corneal epithelium resulting in viral spread to the

sensory ganglia that innervates the eye, the trigeminal ganglion (TG). It is here, within the TG, that the virus establishes a latent infection as previously mentioned.

The cornea is comprised of several layers beginning with the corneal epithelium that faces the external environment (25).
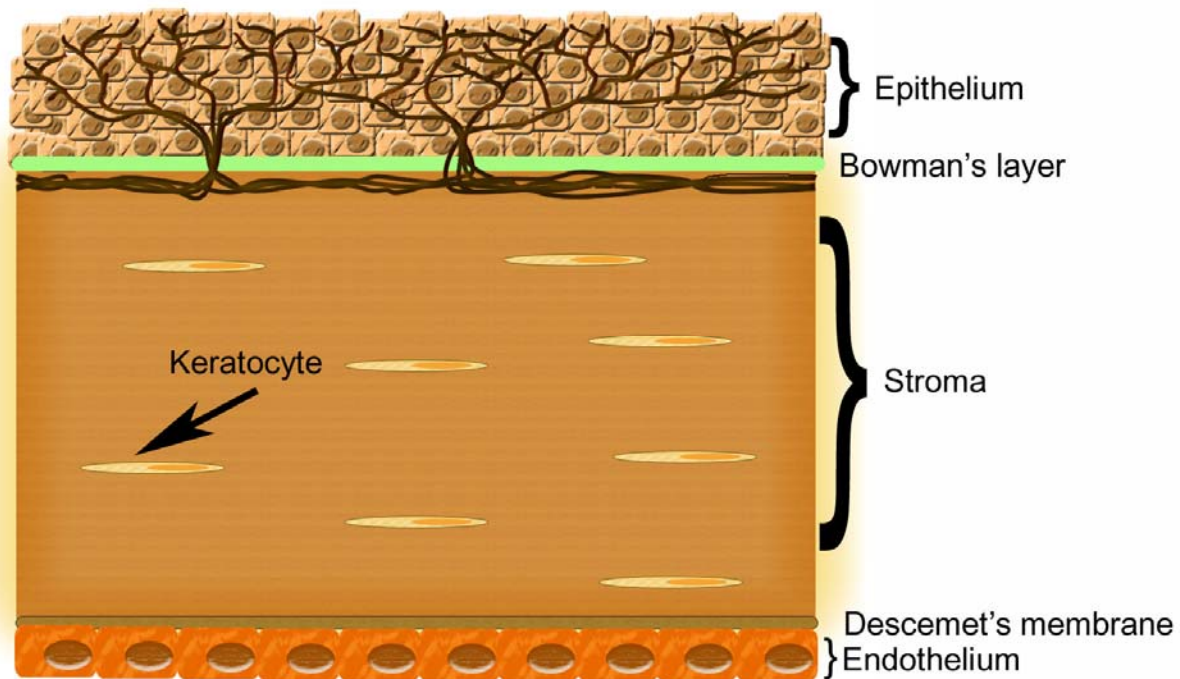
Figure 1: Cross section of the mouse cornea.
Note the innervation of the cornea as represented by brown lines extending into the epithelial layer..

The major functions of the corneal epithelium are; 1) Provide a mechanical barrier to foreign matter, 2) Maintain a barrier to the diffusion of water and solutes, and 3) create a transparent and smooth optical surface that the tear film can adsorb to. The corneal epithelium consists of five to seven layers of cells which sit upon a basement membrane. Immediately below the epithelial cell basement membrane lies Bowman's layer, which was thought to be found in humans but not in mice; however but more recent electron microscopy has shown that the corneas of mice do contain Bowman's layer (26).

Below Bowman's layer lies the stroma of the cornea. The stroma makes up approximately 90% of the thickness of the cornea and consists primarily of collagen fibers. The collagen fibers are uniform and small (250-300 angstroms) and are organized into bundles called lamellae. The lamellae are highly organized and are arranged parallel to the tear surface which results in corneal transparency. Other components of the corneal stroma are the keratocytes and the ground substance that fills in all the gaps between the lamellae. The ground substance consists of the proteoglycans keratin and chondroitin sulfate. The keratocytes function to maintain the collagen matrix of the cornea and are the cells responsible for scar formation as they transform into fibroblasts after injury and contribute to scar tissue formation.

Descemet's membrane lies below the stroma and is made by the endothelial layer. In contrast to Bowman's layer, Descemet's membrane can be regenerated following injury and is easily separated from the stroma. Upon endothelial cell injury, Descemet's membrane thickens; therefore one can use the thickness of this membrane as a record of previous episodes of disease. Below Descemet's membrane lies the corneal endothelium. The corneal endothelium acts as a selective permeability barrier which allows diffusion of nutrients into the cornea and, more importantly, pumps water out of the stroma to maintain a slightly dehydrated state that is necessary for visual acuity. The corneal endothelium is made up of a single layer of cells and has very little to no regenerative capacity. As an individual ages, some loss of endothelial cells occurs which is compensated by spreading and enlarging of the remaining endothelial cells.

The cornea is heavy supplied with sensory nerves by the first division of the trigeminal nerve by way of the long and short ciliary branches of the nasociliary nerve. The long ciliary nerves enter the eye near the optic nerve and travel through the suprachoroidal space anteriorly toward the cornea. The nerve fibers branch multiple times and lose their myelin sheaths before

entering the cornea at the limbus (27). The nerve fibers enter the cornea parallel to the corneal

surface at first, branch further and then turn 90° to proceed toward the corneal surface. Directly

below the epithelial layer, the nerve bundles form a dense subepithelial plexus. The fibers then

pierce Bowman's layer and terminate among the epithelial cells. The constant branching of the

nerve bundles while finding their way to the epithelium results in a very large number of nerve

endings within the cornea. In fact, the cornea is considered one of the most highly innervated

tissues in the body and some rough estimates as to the absolute number of nerve endings within a

normal human cornea exceeds 600,000 (27). The presence of such a vast number of nerve

endings within the corneal epithelium provides an ideal environment for the virus to gain access

to nerve termini and travel to the TG to establish a life long latent infection.

1.1.3.   Basics of an immune response

1.1.3.1.   Components of the immune system

Infection of a tissue is first realized by the immune system by the tissue resident

hematopoietic cells most notably the dendritic cell (DC). These highly specialized sentinel cells

attack and phagocytose foreign bodies including viruses and bacteria that have breached the

physical barriers of the body such as the skin. The presence of these cells is critical for the

initiation of an immune response since these cells are responsible for coordinating T cell

responses to pathogens within the draining lymph nodes. Acquisition of foreign antigen by DCs

in the periphery results in the differentiation and maturation of these DC ultimately resulting in

the migration of these cells to the local draining lymph nodes (DLNs). This is facilitated by up

regulation of cell surface markers such as CCR7 which help direct the antigen-laden DC to the

draining lymphoid tissue. The DCs that enter the DLNs arrest within the organ and display

antigens to circulating naive T cells that continually pass through looking for the antigen that their T cell receptor recognizes. Upon recognition of antigen, the naive T cell stops circulating and begins to divide and differentiate (28).

T cells can be divided into two basic subtypes based on expression of the surface coreceptors CD8 or CD4 (28). CD8 T cells are the body's main defense to viruses that infect cells and reside in the cytoplasm as they can directly lyse those infected cells. Based on this ability to kill virally infected cells, CD8 T cells are commonly referred to as cytotoxic T cells or CTLs; however these cells can also produce large amounts of inflammatory cytokines such as IFN-γ and TNF-α that contribute to pathogen eradication. Lysis of cells by CTLs can be mediated through several different mechanisms (29). One mechanism by which CTLs kill cells is through the perforin/granzyme pathway. Briefly, this process involves formation of a pore within the target cell membrane by perforin followed by entry of the granzymes into that target cell through the newly formed pore. These granzymes include granzyme A and B, both of which are serine proteases that target intracellular caspases resulting in cell death by apoptosis (30). Another mechanism used by CTLs to lyse cells is the Fas:FasL pathway. Activated CD8 T cells express high levels of FasL which trimerizes and binds to Fas expressed on target cells resulting in the death of that cell by apoptosis.

The other major subtype of T cell found in the body is the CD4 T cell. These cells are commonly referred to as helper T cells due to their integral role aiding in the activation and sometimes survival of other immune cells (28). These functions include helping B cell responses, resulting in production of antibody, and also in activation of macrophages, which allows these phagocytic cells to fully process engulfed material. Some of these helper functions are mediated through the production of cytokines such as IFN-γ, IL-2, and IL-4, while other helper functions

are mediated by direct cell to cell contact. CD4 T cells are divided into three subtypes based on their cytokine secretion profile and effector functions: Th1, Th2 and T_{reg} (regulatory T cells). Th1 cells produce IFN-γ and IL-2 and are responsible for stimulating the microbicidal activity of phagocytic cells such as macrophages. Additionally, Th1 cells can activate macrophages through cell to cell contact via CD40/CD154 interactions.

Th2 CD4 T cells function primarily to activate B cells responses, resulting in proper B cell differentiation and antibody secretion. Th2 CD4 T cells produce IL-4, IL-5 and IL-13, which are important for antibody isotype class switching and B cell proliferation (31). Th2 also provide signals to B cells through CD40:CD154 and CD134:OX40L interactions resulting in proliferation and antibody isotype class switching (28).

T_{reg} CD4 T cells are, as the name implies, down-regulators of ongoing immune responses through production of immunosuppressive cytokines including TGF-β and IL-10 (32). These cells are subdivided into several different populations, with the majority of recent work focusing on the $CD4^+CD25^+$ cells population.

1.1.3.2. Phases of an adaptive immune response

Initial infection at a peripheral site results in the activation of components of the innate immune system that can mobilize immediately to control the primary infection. These cells of the innate immune system include DCs (which take up antigen and travel to the DLNs to initiate an adaptive immune response), monocytes, and neutrophils (33). All of these cells of the innate immune system are good for the initial control of an infection, but generation of a potent adaptive immune response is usually necessary for complete eradication of the invading pathogen. Additionally, generation of immunological memory is restricted to the adaptive immune system, which results in protection from subsequent re-infection with the same

pathogen. The endpoint of an adaptive immune response is the generation of memory, but there are numerous phases of a typical adaptive immune response to a pathogen which include expansion of the T cells specific for an antigen, contraction of a vast majority of those cells after the antigen has been cleared from the individual, and then finally the establishment and maintenance of a stable memory T cell pool.

PRIMING

Dendritic cells laden with antigen collected from phagocytosed pathogens display specific epitopes of these pathogens on their surface in the context of major histocompatibility complexes (MHC) with in the DLNs. Naïve T cells specific for a particular antigen are quite rare, with some estimates that only 1 out of every 10^5 naïve T cells will be specific for a particular antigen (34). This contributes to the length of time necessary to initiate an adaptive immune responses and shows why the body needs the innate immune system to quell the initial infection until the adaptive immune response is ready.

T cells recognize antigen within MHC molecules on the antigen presenting cell (usually a dendritic cell) through their T cell receptor (TCR) expressed on the surface of the cell and are signaled to proliferate and differentiate. Activation of T cells requires not only stimulation through the TCR, but an additional costimulatory signal is required to prevent the T cells from entering an unresponsive state termed anergy (35) (Figure 2).
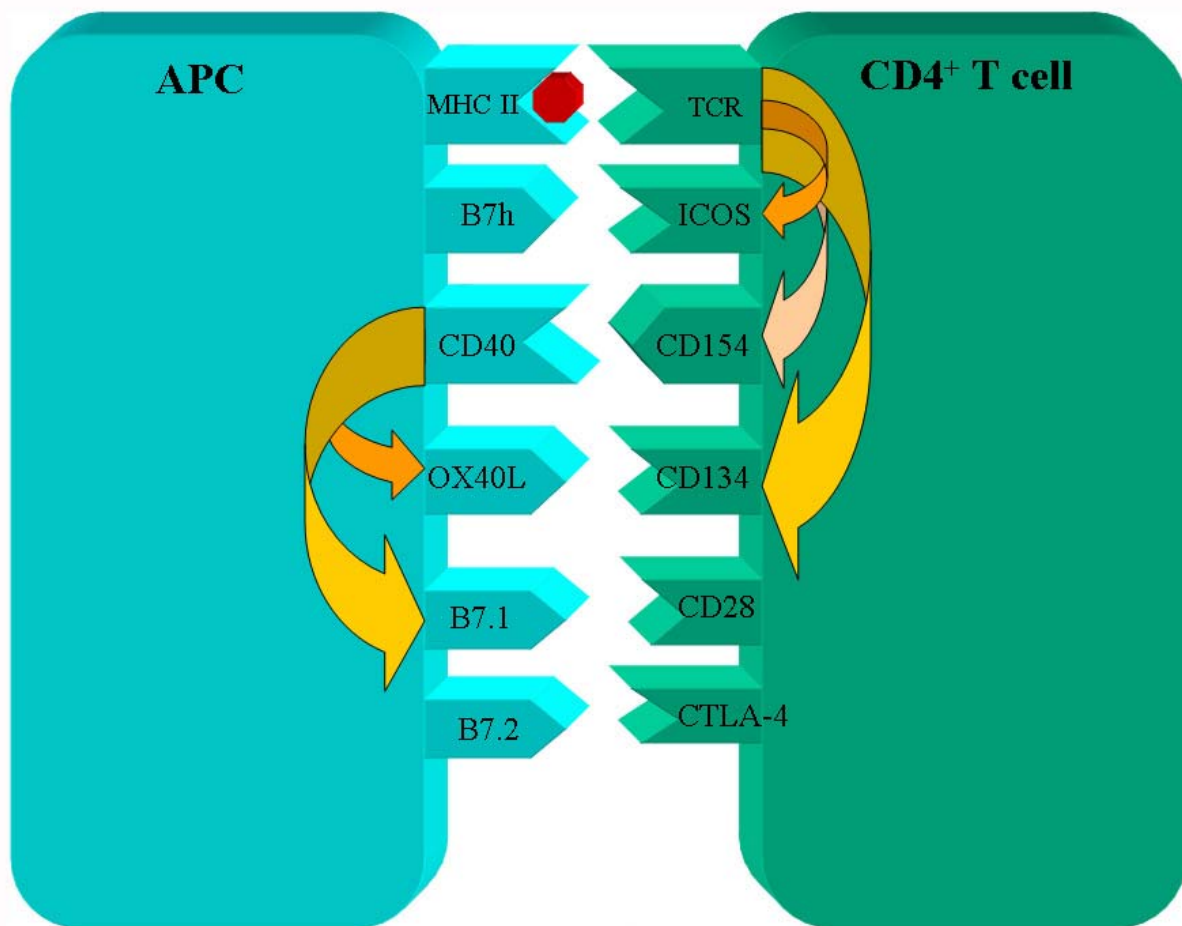
Figure 2: Common costimulatory molecules on CD4 T cells and antigen presenting cells.

The arrows show the cross regulation of the different costimulatory pairs. CD134, CD40L and ICOS are only expressed after stimulation through the TCR on the T cell. This figure is modified and borrowed with permission from (36).

This costimulatory signal can be provided by one of numerous costimulatory pairs expressed on the surface of the cell such as B7:CD28, CD40:CD154, CD134:OX40L just to name a few (37). The requirement for costimulation of T cells is not restricted to just naïve T cells during priming as numerous studies have shown a need for costimulation for effector T cell activation (36,38). The end result of naïve cell priming is clonal expansion of the antigen specific T cells which then differentiate into effector T cells and leave the lymphoid organ to travel to the

original site of inflammation. A list of surface markers used in this thesis along with the common names for some of theses markers in provided in Figure 3.

Surface molecule	Other names	Cell type expressed on	Function
B7.1	N/A	Antigen presenting cells	T cell costimulation
B7.2	N/A	Antigen presenting cells	T cell costimulation
CD11c	N/A	Some dendritic cells	Unknown
CD40	N/A	Antigen presenting cells	T cell costimulation
CD154	CD40L	CD4 T cells	T cell costimulation
CD134	OX40	CD4 T cells and some CD8 T cells	T cell costimulation
CD134L	OX40L	Antigen presenting cells	T cell costimulation
CD127	IL-7 receptor α chain	Naïve and memory CD4 and CD8 T cells	T cell survival
CD28	N/A	CD4 T cells and some CD8 T cells	T cell costimulation
CD137	4-1BB	CD4 T cells and CD8 T cells	T cell costimulation
DO11.10	Ova specific T cell receptor	CD4 T cells in DO11.10 transgenic mice	T cell receptor
CD69	N/A	Most lymphocytes	Unknown
B7h	B7RP-1	Antigen presenting cells	T cell costimulation
ICOS	Inducible costimulator	CD4 T cells and CD8 T cells	T cell costimulation

Figure 3: CD designations and common names.

CONTRACTION

Following eradication of the invading pathogen, the vast majority of the effector T cells die via apoptosis in a process called contraction (39). This contraction phase prevents host tissue damage by elimination of those cells producing inflammatory mediators. The factors that control contraction are becoming clearer (39). It appears that contraction can occur in the absence of perforin, however IFN-γ appears to play a pivotal role (39-41). These studies showed elevated numbers of antigen specific CD8 T cells in the absence of IFN-γ as far out as 150 days P.I., while the majority (75%) of antigen specific CD8s were eliminated by D +10 P.I. in WT mice. A potential concern in this study was the persistence of virus in the IFN-γ knockout mice, suggesting antigen load may also regulate contraction. This was addressed in a subsequent study and showed antigen clearance does not appear to be absolutely required for T cell contraction (42,43). CD95 (fas) appears to be dispensable for T cell contraction following LCMV infection (44), but there exists some controversy as to what role, if any, TNF plays in contraction (44,45).

It is interesting to note a recent publication that re-examined the need for perforin and IFN-γ during contraction using a model system in which CD8 T cells themselves are not needed for pathogen clearance (46). The authors did not find as dramatic of an effect of IFN-γ deficiency on T cell contraction as has been reported, however they did observe slightly delayed contraction in the absence of IFN-γ. Unpublished work in our lab indicates that removal of IFN-γ results in accelerated contraction of HSV specific CD8 T cells, contrary to the results of Harty and colleagues (39,40,47).

T CELL MEMORY

Not all effector T cells die during contraction, instead a small percentage (5-10%) of the cells survive and become a stable pool of memory T cells that are capable of responding to re-infection with the same pathogen with greater fervor than that observed following initial infection. For the sake of this thesis, I will restrict my discussion to memory CD8 T cells. Currently, much more is known about CD8 T cell memory development, however numerous groups are beginning to unravel the intricacies of CD4 T cell memory development (48).

A question that has represented a major hurdle to immunologists for years is how can we identify that small subpopulation of effector cells that will survive contraction and become memory T cells? This question has been recently answered by two different groups looking for cell surface expression of markers found only on the small population of effectors that are memory precursors. One such marker is the CD8αα homodimer, first identified by Madakamutil et al (49,50). The authors show that CD8αα is expressed on the small subset of effector cells that persist following contraction. The authors also showed that signaling through CD8αα appears to be necessary for proper memory T cell development since mice unable to express the CD8αα homodimer exhibited low numbers of memory T cells following infection (49).

These findings are very similar to those of Kaech et al that identified IL-7Rα (CD127) as a marker that identifies memory precursors within an effector pool (51) (depicted in figure 3). This finding of CD127 on memory precursor cells is not surprising given earlier work showing IL-7 signals are necessary for memory T cell development (52). The authors show that adoptive transfer of CD127$^+$ cells results in a long lasting pool of cells in naïve animals that can effectively protect from a rechallenge while CD127$^-$ cells do not persist and are unable to protect from rechallenge (51). Signaling through CD127 results in increased expression of the anti-apoptotic molecules Bcl-2 and Bcl-xl (51), thus suggesting IL-7Rα$^+$ effector cells survive contraction due to signaling through IL-7Rα which results in protection from apoptosis. This may not be necessarily true since several reports have shown that overexpression of bcl-2 and bcl-xl does not completely protect all effector cells from cell death (53,54), suggesting additional effects of IL-7 signaling must occur that protect these memory precursors from death. It is interesting to note that Madakamutil et al found IL-7Rα expression on cells expressing CD8αα (49).
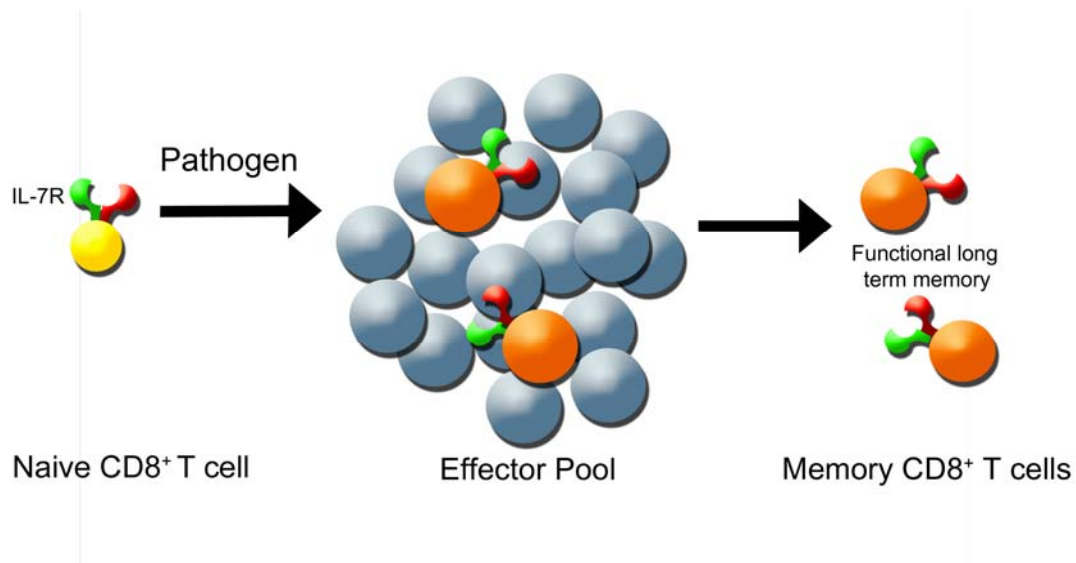
Figure 4: IL-7Rα (CD127) expression on effector cells marks memory T cell precursors.
Naïve T cells express CD127 as do memory T cells. During the expansion phase, only 5-10% of all effector cells express CD127 which are the precursor memory T cells.

Memory CD8 T cells are subdivided into two populations which are termed effector memory (T_{em}) and central memory (T_{cm}) (55). These two populations are divided based upon several criteria including tissue localization, production of cytokines, and cell surface expression of CD62L and CCR7. What are the major differences between these subtypes and effector cells? Both T_{cm} and T_{em} express high levels of CD44, CD122, IL-15Rα, and CD127. T_{cm} localize to lymphoid tissues especially the spleen, while T_{em} are found predominately in non-lymphoid tissues, but can also be located in the spleen. Related to their tissue localization patterns, T_{cm} express high levels of CD62L and CCR7, markers that allow for migration into lymphoid tissue, while T_{em} do not express either marker. Some theories as to the localization of these two types of memory cells predict that T_{em} are present in nonlymphoid tissues to immediately combat a reinfection during which time T_{cm} can expand and give rise to effector T cells that can flood into the infected tissue and help fully eliminate the pathogen (56).

Another fundamental difference between T_{em} and T_{cm} relates to their ability to produce cytokines following rechallenge. Initial studies examining the differences between T_{em} and T_{cm} showed T_{em} were selectively better at producing IFN-γ and TNF-α compared to T_{cm}. Additionally, the T_{em} were immediately cytolytic which was not observed in T_{cm}(57). More recent studies however have shown that T_{em} and T_{cm} appear to be equally capable of producing both IFN-γ and TNF-α following antigen restimulation, while T_{cm} are the predominant cell type that make IL-2 (58,59). In contrast to previous findings (57), a recent study showed that both T_{em} and T_{cm} were equally efficient at cell killing (58). That same study showed equivalent proliferative capacity of the T_{em} and T_{cm} following restimulation. This aspect of T cell memory remains controversial and is under intense study by several groups.

Controversy exists as to which subpopulation is the 'better' memory cell in terms of ability to respond to rechallenge. Recent work showed superior protection of T_{cm} vs T_{em} in eliminating both a systemic and a localized infection (58), however others argues that T_{em} are better memory cells (60). The apparent contradiction between these two studies may lie in the infection model used as some studies use systemic infections, while others studied mucosal infection. It is apparent that we are far from understanding the full process of memory T cell development and protection.

The lineage development of effector memory and central memory also remains controversial. Historically, two different models were put forth to explain how T_{em} and T_{cm} are generated and maintained; 1) a linear model (56) of naive$\rightarrow$effector$\rightarrow$T$_{cm}\rightarrow$T$_{em}$ and 2) naive$\rightarrow$effector then a split (61) into the two separate populations of T_{cm} and T_{em}. More recently, a very different model has been suggested in which naive$\rightarrow$effector$\rightarrow$T$_{em}\rightarrow$T$_{cm}$ occurs (58). This model has been challenged by Lefrancois' group in which they show that this phenomenon only

occurs when adoptively transferring cells into mice and does not occur following a normal infection. They also showed decreasing the input numbers of adoptively transferred cells results in very different transitions between memory populations (personal communication A. Marzo). This data from Lefrancois' lab predicts initial precursor frequency and competition for resources dictates the actual lineage transition of memory T cells in vivo. These different models are depicted in figure 5.
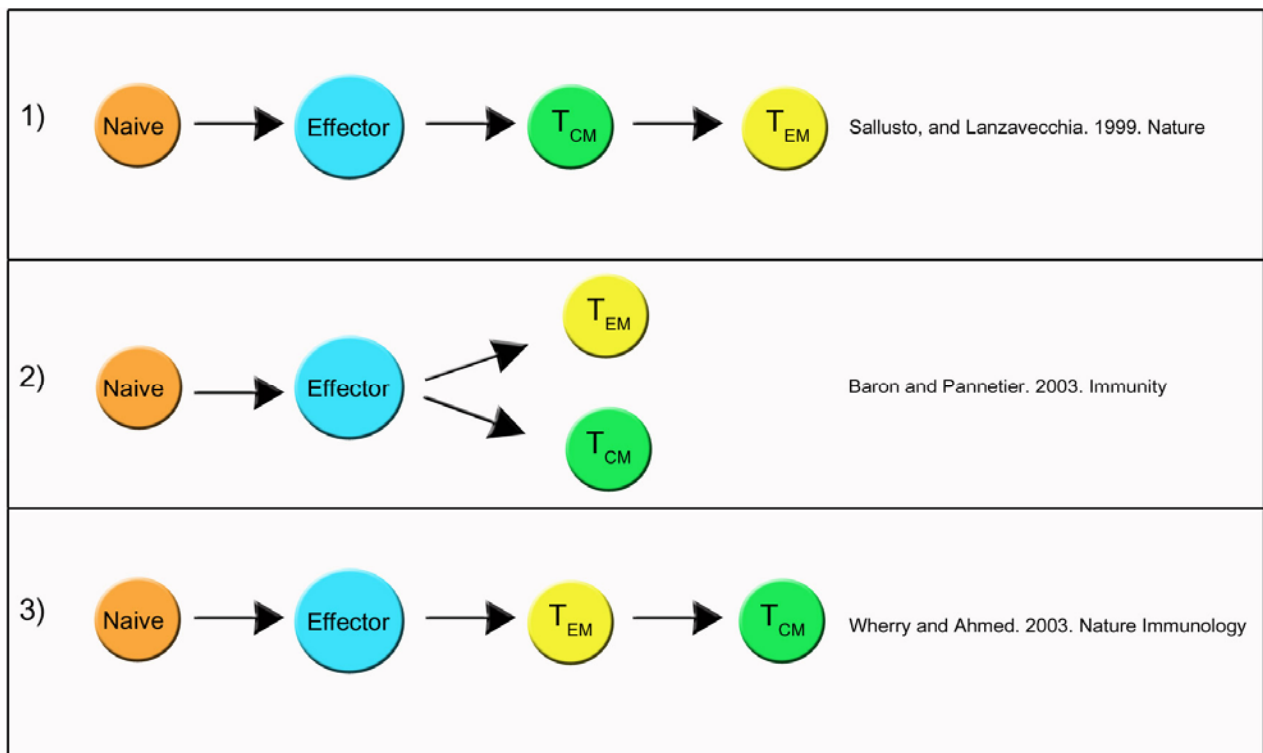
Figure 5: Models of memory CD8 T cell differentiation.

The fundamental problem with making sense of these studies is the different models used by each group. In the most extreme cases, the model naive→effector then a split into the two separate populations of T_{cm} and T_{em} was identified using human cells, while the studies showing a linear differentiation of memory cells (scenario 3 in figure 5) were performed in mice. There exists the real possibility that memory T cell development differs dramatically between mice and

humans and this difference will obviously influence our ability to interpret these seemingly contradictory data.

Once memory T cells are generated, how do they persist in vivo? Seminal studies in the field established that memory T cell do not require MHC interactions to persist (for both CD8 and CD4 memory T cells) (62,63); instead it appears that certain cytokines including IL-7 and IL-15, regulate the ability of memory CD8 T cells to survive for extended periods of time (64,65). Additionally, there is some evidence that other cell types (CD4 T cells) may regulate/maintain CD8 T cell memory (66). This maintenance of CD8 T cell memory by CD4 T cells will be discussed later.

1.1.4. Immune response to ocular HSV-1

Now given the basics of a typical immune response, how does the body combat an ocular HSV-1 infection?

1.1.4.1. The good

Initial infection of the corneal surface induces migration of Langerhans cells (LC) into the central cornea, which is normally devoid of dendritic cells (67). This migration of LCs into the cornea results in the acquisition of viral antigens by those LCs, which then travel to the draining lymph nodes (DLNs) to present antigen to naïve T cells. Some reports indicate that the actual presentation of viral antigens is mediated by a lymph node resident DC and not by the migrating DCs, however this is following a footpad infection and may not reflect what occurs following ocular infection (68). During the period of time necessary for the induction of an adaptive immune response, the cornea is infiltrated by a wave of neutrophils (PMNs) that effectively

eliminate the virus replicating in the epithelial cells of the cornea (69,70). Numerous studies have shown that this wave of PMNs functions to eliminate infectious virus from the cornea by approximately 4-6 days P.I. (69,70). It is also noteworthy that this wave of PMNs is not accompanied by a T cell infiltrate, subsides after a few days, and does not cause appreciable opacification of the cornea.

A consequence of primary HSV-1 infection of the eye is the virus gains access to the nerve endings within the highly innervated corneal epithelium. Once inside the nerve endings, the virus is able to travel via retrograde axonal transport to the trigeminal ganglion (TG). Here the virus briefly replicates, and then enters a latent state. Interestingly, it appears that the virus is capable of reaching the TG within 24 hours of initial infection of the surface of the eye (71). The elimination and control of the virus in the TG is mediated by in part the innate immune system. Heavy infiltration of macrophages and $\gamma\delta$ T cells is observed within the TG 5-7 days post-infection (P.I.) (72-74). This infiltration of large numbers of innate immune cells is accompanied by the production of antiviral cytokines TNF-α and IFN-γ along with nitric oxide (NO). Previous work has shown that this early production of IFN-γ is contributed by $\gamma\delta$ T cells (74) and possibly NKT cells (75,76), while TNF-α and nitric oxide are produced by infiltrating macrophages (74). Work by Simmons' group clearly demonstrated that NKT cells play a necessary role in the clearance of the virus and may contribute to the IFN-γ found early in the TG (75,76). IFN-γ and TNF-α appear to be critical in controlling initial viral replication and spread within the TG as depletion of these cytokines resulted in increased viral replication (74) and infection of IFN-γ KO mice resulted in encephalitis (77). Additionally, both TNF-α and IFN-γ regulate migration of inflammatory cells into the TG (74). Depletion studies show increased viral titers and spread within the TG when either $\gamma\delta$ T cells (73), macrophages (74) or NK/NKT cells (in a zosteriform

model) (75) are depleted prior to infection, thus highlighting the role of the innate immune system in the initial clearance of the virus. More recent data also shows a critical role of TNF-α in the initial control of ocular HSV-1 using TNF deficient mice (78). This study showed increased mortality and viral titers in TNF deficient mice following ocular infection. The potential role of neutrophils (PMN) in control of viral within the TG is less understood. One study showed increased viral titers and increased mortality of HSV infected mice when neutrophils were depleted prior to infection (70), but others have found the TG to be devoid of PMNs (72).

The contribution of the adaptive immune system to the initial control of viral replication within the TG has been extensively explored. Seminal studies by Metcalf et al showed nude mice, which are deficient in T cells, do not survive initial infection, thus indicating a necessary role for T cells in the initial control of viral replication (79). Additionally, SCID mice deficient in both T cells and B cells also fail to control the virus and die of encephalitis within two weeks post infection (80,81), again stressing the necessary role of adaptive immunity in control of HSV-1 infection in the TG. It does appear however that the virus can establish a latent infection in some neurons in the absence of CD8 T cells, as has been shown in SCID mice, however these mice all ultimately die from encephalitis (82,83).

Understanding of which T cell subset is important for the control of initial viral replication within the TG was first addressed by Simmons and Tscharke, who showed increased neuronal cell death and increased viral spread in mice depleted of CD8 T cells (84). Additionally, adoptive transfer of CD8 T cells to nude mice results in survival of these mice following ocular HSV-1 infection (80). Another study showed a necessary role for CD8 T cells in the control of initial infection in mice and that the virally encoded ICP47 does play an

important role in the mouse system (85). Some reports have shown that either CD8 or CD4 T cells can mediate initial clearance of the virus from the TG and protect animals from encephalitis (86), while others have shown only CD8 T cells can mediate protection from encephalitis (80). The differences in these findings may lie in the strain of virus used to infect mice as the virulence of different strains of HSV-1 varies dramatically. In contrast, several studies argue that CD4 T cells represent the major T cell type involved in the initial control of HSV-1 infection (87-89) and these findings are supported by some of the data presented within this document.

Following the initial control of viral replication within the TG, some components of the immune system remain in the TG seemingly for the life of the animal (72,90-92). In fact, T cells have been recovered from latently infected TGs greater than 90 days P.I. (72). Importantly, this persistence of immune cells within latently infected TGs is also observed in humans (93). Additional analysis of these CD8 T cells within latently infected TGs show that these cells can prevent viral reactivation in ex vivo TG cultures at least in part through production of IFN-γ (16,94). More recent studies have shown that the CD8 T cells that are recovered from latently infected TGs of C57Bl/6 mice recognize the immunodominant viral glycoprotein gB epitope gB$_{498-505}$ (90) and express CD69, a marker for recent activation. This study also provided compelling evidence for the formation of an immunological synapse between CD8 T cells and neurons, again supporting the notion that CD8 T cells play an active role in the maintenance of viral latency.

In addition to the persistence of immune cells within latently infected TGs, several groups have observed persistent inflammatory cytokine expression within latently infected TGs (92,95-97). It is interesting to note that this persistent cytokine expression during latency was reduced by treatment with acyclovir, suggesting the adaptive immune system is actively monitoring and

responding to low-level viral gene expression during latency (96). In addition to inflammatory cytokine transcripts in latently infected TGs, chemokine transcripts for MIP-1α, MIP-1β, MCP-1 and RANTES (all chemokines that chemoattract T cells) were recovered from latently infected TGs, providing additional support for an active immune response during viral latency (98).

These findings of immune cell persistence and continual inflammatory cytokine/chemokine production during latency strongly support a model of 'tug-of-war' between the adaptive immune system and the virus throughout latency in which the virus is constantly trying to reactivate from latency but is shut down by the host immune system.

1.1.4.2.   The bad

The immune response to ocular HSV-1 infection is not always beneficial. It is obvious that a potent immune response to the virus is critical for the control of the virus in the TG as mice deficient in T cells succumb to infection due to spread of the virus to the central nervous system and eventual encephalitis as discussed. The situation within the cornea is much different. Following infection of the eye with HSV-1, neutrophils (PMN) infiltrate the eye and clear the virus (69,70). There is some evidence that other cell types, including macrophages (99), and $\gamma\delta$ T cells (100), may play a role in viral clearance. In HSK susceptible mice, a second, more robust immune infiltrate of PMNs and (also T cells) occurs in the absence of live virus resulting in immunopathology. This immunopathology results in opacification of the cornea and blindness and is called herpes stromal keratitis (HSK) (figure 4).
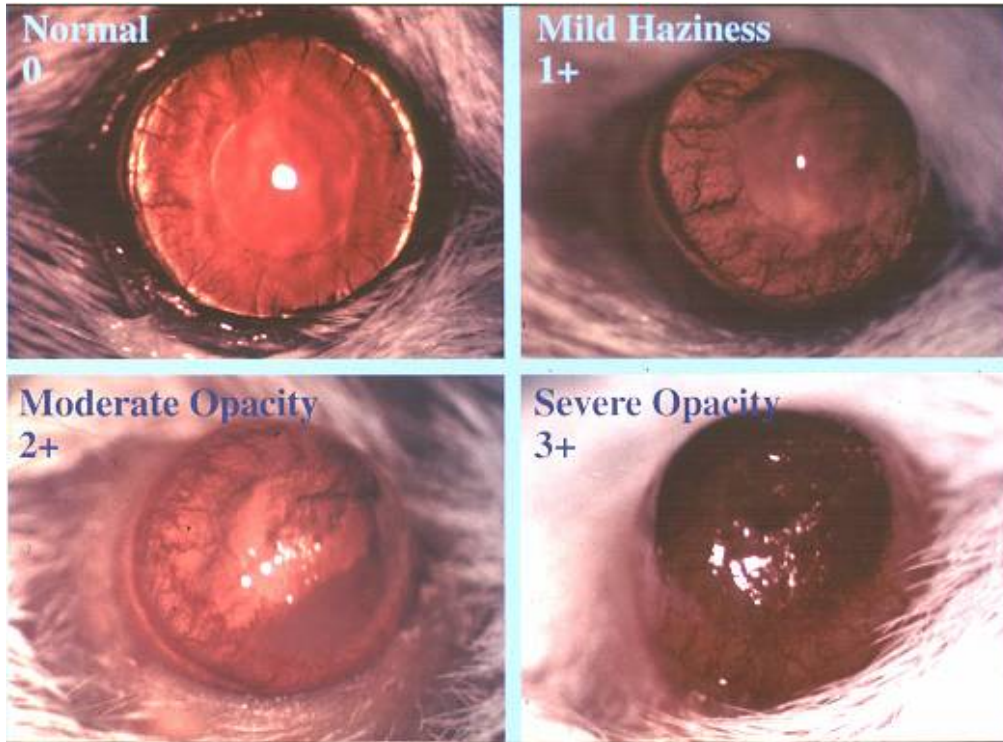
Figure 6: Herpes stromal keratitis (HSK) in BALB/c mice.

Clinical HSK begins in mice approximately 8-10 days post-infection (P.I.) and reaches maximal severity around D15 P.I. HSK is scored based upon level of opacity within the cornea with a score of 3.0 representing blindness.

Current understanding of the immunologic process that ultimately culminates in HSK within the cornea has been accomplished through the use of a mouse model. Some of the earliest work by Metcalf, et al showed that T cells play a critical role in HSK as nude mice did not develop HSK following ocular infection (79). Subsequent studies showed that adoptive transfer of T cells into nude mice restored HSK development indicating T cells mediate HSK (101). Several groups then examined which T cell subset was responsible for HSK using in vivo antibody depletion of either CD4 or CD8 T cells within immunocompetent mice, with most studies concluding that CD4 T cells are the T cell subset responsible for HSK when using the RE strain of HSV-1 (102,103). Additionally, adoptive transfer of either HSV-immune CD4 or naïve CD4 T cells into SCID mice induced HSK in these normally HSK resistant mice (80). Further

work revealed that the CD4 T cells that mediate HSK are of the Th1 phenotype and that Th1 cytokines play a crucial role in the development of HSK as in vivo neutralization of these cytokines reduced HSK incidence and severity (104-107). In fact, work by our group showed that these Th1 cytokines are required throughout HSK as neutralization of either IL-2 or IFN γ after HSK had already become clinically evident caused disease regression (106).

Further characterization of HSK has shown that while Th1 type CD4 T cells serve to regulate inflammation, polymorphonuclear leukocytes (PMNs) are responsible for the tissue destruction that results in the corneal opacity indicative of clinical HSK. Our lab has previously shown that IFN-gamma produced by the Th1 CD4 T cells upregulates PECAM expression on endothelial cells, which facilitates PMN extravasation into the cornea (105). Further, we have shown that IL-2 production in the cornea during HSK creates a chemotactic gradient for PMNs and maintains the survival of those cells (106). It should be noted that natural killer cells may play a role in HSK as depletion of these cells reduced HSK severity (108).

Another important factor in HSK is the role that antigen-presenting cells play in disease development. A study on Langerhans cells (LC) strongly suggests that these cells play a critical role in the activation of the CD4 T cells that mediate disease in the cornea. Mice treated with UV-B irradiation, which depletes LC in the central cornea, prior to infection showed significantly decreased incidence and severity of HSK compared to non-LC depleted mice (109)**.**

1.2. Background to specific aims

1.2.1. Costimulation during HSK

A study by our lab suggests that the CD4 T cells that infiltrate the cornea and regulate disease require re-stimulation by LC in the cornea in order to cause disease (38). This led to

attempts to modulate the activation of the CD4 T cells within the cornea in the hope of alleviating disease (36). One such attempt focused on blocking costimulatory interactions in the cornea, specifically targeting B7:CD28 interactions and showed that blocking B7.1:CD28 interaction within the cornea prevented the development of HSK (38). This study supports the hypothesis that CD4 T cells that enter the cornea and mediate HSK require reactivation within the cornea to cause disease, presumably by Langerhans cells as suggested (36).

Other candidate targets for costimulatory blockade that may prove beneficial to alleviating HSK are CD40:CD154 and CD134:OX40L, both TNF family members. CD40/CD154 interactions have been shown to be important for production of IL-12 and IL-18 (110-112) by antigen-presenting cells (APC). This reciprocal activation produces the robust Th1 CD4$^+$ T cell response that is required for the eradication of many viral and bacterial infections. However, a recent study examining the role of local CD40/CD154 interactions within the cornea showed a minimal role of these interactions in HSK development (113). CD134 is a member of tumor necrosis factor receptor superfamily (TNFR) that includes CD40 (114). CD134 expression is limited to activated CD4 and CD8 T cells in both mice and humans (115-117). OX40L is a member of the tumor necrosis factor (TNF) family and is expressed on dendritic cells (DC) (117,118), B cells (119), endothelial cells (120), and T cells (121). Neither CD134 nor OX40L are expressed on resting cells; rather they are expressed only after T cell (CD134) or APC (OX40L) activation (115-118).

An attractive feature of CD134:OX40L as a target for immune modulation lies in the finding that CD134 is selectively expressed on activated T cells isolated from inflammatory sites in a number of diseases such as experimental allergic encephalomyelitis (EAE), rheumatoid arthritis, and graft versus host disease (GVHD) (122-124). Manipulation of CD134:OX40L

interactions (either by blocking CD134:OX40L binding or selectively depleting CD134 expressing cells) represents a potentially powerful method for down-modulating a harmful immune response without causing peripheral suppression of the immune system (125,126). This makes CD134 a better target than CD28 for immunosuppression by targeting an inducible molecule rather than the constitutively expressed CD28. In support of this theory, blockade of CD134:OX40L interactions resulted in an alleviation of several inflammatory diseases in mice including rheumatoid arthritis (RA), experimental autoimmune encephalomyelitis (EAE) and graft versus host disease (GVHD) (122,123,127).

Work in section 4.1 of this thesis tests our hypothesis that CD134/OX40L interactions are critical for the activation of pathogenic CD4 T cells during HSK. We show that this costimulatory interaction is not required for HSK development either within the cornea or systemically.

1.2.2.   Specificity of CD4 T cells present in the corneas of mice with HSK

Numerous studies have investigated the inflammatory infiltrate present in human corneas with HSK. These studies identified virus-specific CD4 T cells in humans and showed that these cells produce both Th1 and Th2 cytokines in response to viral antigens, but not to corneal autoantigens (128). Subsequent studies by this group, using a larger cohort of patients, showed both CD4 and CD8 T cells could be found within corneas of people with HSK (129). They showed again that the T cells present in those corneas reacted to viral antigens but not to corneal autoantigens. Other studies confirmed the presence of virus specific CD4 T cells in human corneas with HSK, and have even begun identifying specific viral tegument proteins UL21 and UL49 as the specific proteins recognized by these CD4 T cells in the cornea (130).

We show in section 4.2 that CD4 T cells recovered from the corneas of mice with HSK are virus specific, produce IFN-γ following stimulation, transfer HSK to the normally HSK resistant nude mice, and protect those nude mice from encephalitis.

1.2.3.   Contribution of CD8 T cells to HSK

Most work on HSK in mouse models has concluded that CD4 T cells are the primary regulator of disease following HSV-1 RE strain infection (80,102,103). Contrary to these studies, our lab has shown that the infiltrate induced following corneal infection with HSV-1 KOS strain consists of CD8 T cells (103). Several other groups have shown a role for CD8 T cells in HSK, with some finding that in vivo depletion of CD8 T cells following HSV-1 RE strain infection results in accelerated/more severe HSK, suggesting a regulatory role for CD8 T cells in the disease (102). More recently, several articles have re-examined the role of CD8 T cells in the pathogenesis of HSK. Studies in the normally HSK resistant C57Bl/6 mouse strain revealed that CD8 deficiency caused these normally resistant mice to now develop HSK supporting previous work suggesting CD8 T cells play a regulatory role in limiting HSK severity (86). Additional studies showed more severe HSK in CD8 deficient BALB/c mice, a strain of animal that is normally HSK susceptible (131), following corneal infection using the KOS strain of HSV-1. This work using the HSK susceptible mouse strains suggests again that CD8 T cells normally function in a regulatory fashion to limit HSK in vivo. More recently, studies performed in transgenic Bl/6 mice indicate that virus specific CD8 T cells are not found within corneas with active HSK, instead only virus non-specific CD8 T cells could be recovered from HSK lesions (132). This work suggests a pathologic role for virus-nonspecific CD8 T cells in HSK progression at least in C57Bl/6 transgenic animals.

Further complicating the relative role of CD4 and CD8 T cells in HSK in mice is work by Harvey Cantor's group, which argues that HSK with the RE strain of HSV-1 is mediated by an innate immune system mechanism only, with T cells playing no role in HSK (133). This claim was based upon the observation that CD4 depleted RAG2$^{-/-}$ DO11.10 mice (CD4 T cells within these mice can only recognize Ova) developed HSK following HSV-1 RE ocular infection. It has been shown however that HSK lesions in RAG2$^{-/-}$DO11.10 mice and immunocompetent mice involve very different immune mechanisms (134). These RAG2$^{-/-}$ DO11.10 mice are unable to control initial viral replication within the cornea following primary ocular HSV-1 infection while immunocompetent animals do control the initial viral infection in the eye. Additionally, if RAG2$^{-/-}$DO11.10 mice are treated with acyclovir following primary infection, these mice do not develop HSK further illustrating that HSK in these mice is viral pathology induced and not immunopathologic as is seen in immunocompetent mice (134). These RAG2$^{-/-}$DO11.10 mice therefore do not represent an appropriate model to address the role of T cells in the etiology of HSK.

We show in section 4.3 of this thesis that CD8 T cells can mediate HSK in the absence of CD4 T cells; however the disease is more transient. Additionally, we show that CD8 T cells that infiltrate the cornea of CD4 deficient mice are activated and virus specific.

1.2.4.   CD4 T cell regulation of the CD8 T cell response in the TG

In general, most studies have shown that CD4 T cells are dispensable for the primary CD8 T cell response in lymphoid tissues (135-138). These studies have employed techniques such as tetramer staining to show that the initial expansion (priming) of CD8 T cells is CD4 independent and have exposed flaws with some previous work that concluded CD4 T cells were necessary for

primary CD8 T cell generation. Previous work concluded that primary CD8 T cell responses are sometimes CD4 dependent (138,139), but the techniques available at these time required an extended secondary restimulation to address functionality, resulting in data that addressed secondary responses instead of primary responses. These findings are by no means absolute as several reports have revealed decreased primary CD8 T cell responses in the absence of CD4 T cells (140,141). Both of these studies show decreased numbers of antigen specific CD8 T cells at nonlymphoid sites such as the lung following infection when CD4 T cells were absent. Interestingly, Marzo et al showed that only specific pathogens require CD4 T cells to generate optimal primary CD8 T cell responses. This study revealed a reduced percentage of antigen specific CD8 T cells in the lungs of CD4 depleted animals only when those mice were infected with VSV but not with *Listeria monocytogenes* (140). This reduction may reflect decreased priming of CD8 T cells or may also suggest decreased recruitment of CD8 T cells into nonlymphoid tissues. Additional work illustrating a necessary role for CD4 T cell help for primary CD8 T cell responses is work by Serbina et al that described a conditional effect on the primary CD8 T cell response in the absence of CD4 T cells. They showed no defect in primary CD8 T cells expansion, migration or ability to produce IFN-γ in the absence of CD4 T cells, but they did observe reduced cytolytic ability of these primary effector CD8 T cells(142).

One of the most fascinating areas of memory T research is the role of CD4 T cells in the generation and maintenance of memory CD8 T cells. Several prominent articles have recently emerged showing CD4 T cells are absolutely required for the generation of effective CD8 T cell memory in several different model systems that include both noninflammatory and infectious antigens (135-137,143). The general conclusion from these studies was that CD4 T cells provide a critical signal to CD8 T cells during priming that is vital for these CD8 T cells to develop into

functional memory cells that can respond to a secondary challenge (138). In contrast to these findings, one study has reported that functional memory CD8 T cells can develop in the absence of CD4 cells (140).

So what is this mystery signal provided to CD8 T cells during priming that imparts on them the ability to be good memory T cells? The answer to this question may be TRAIL expression (144). This study shows that 'helpless' CD8 T cells, but not 'helped' CD8 T cells, produce soluble TRAIL following restimulation. The authors showed TRAIL receptor is expressed on both 'helped' and 'helpless' CD8s T cells, therefore production of soluble TRAIL by 'unhelped' CD8 T cells and the subsequent death of large numbers of CD8 T cells might explain why some investigators have found decreased proliferative capacity of CD8 T cells following restimulation in a CD4 deficient environment (135-137,143).

In contrast, these results with TRAIL production do not appear to function following infection of CD4 deficient mice with murine gamma herpes virus. Work by Doherty's group with murine γ herpes virus (MHV-68 or γHV-68) has shown that proper effector and memory CD8 T cells are generated in CD4 deficient mice, but the mice eventually die several months P.I. (145). It has been reported that similar numbers of functional virus specific CD8 T cells are present in CD4 deficient hosts (146,147) and understanding of why these animals succumb to infection is unclear. This model of gamma herpes virus infection involves an additional variable not included in most model systems in that the pathogen enters a latent state and may represent more of a chronic or persistent infection.

Bevan's group has presented a completely different case of when CD4 T cell help is needed for CD8 T cell memory. They argue that CD4 T cells are not needed during CD8 T cell priming, instead they are required for the maintenance of CD8 T cell memory over time (66,138). This

31

study shows that memory CD8 T cells adoptively transferred into CD4 deficient host wane over time, suggesting a constant need for CD4 T cell help during memory. This model also shows that the CD4 T cells that are providing help to the memory CD8 T cells are doing it in an antigen independent manner, but what kinds of signals or cytokines that these CD4 T cells provide to the memory CD8 T cell remains enigmatic.

1.2.4.1. Acute versus chronic/latent infection

An important consideration when addressing T cell responses and memory is whether the pathogen is cleared from the animal. Most groups studying CD8 T cell memory development rely on models of acute infection such as LCMV or a genetically engineered pathogen that expresses a specific epitope that allows the investigators to follow the antigen specific population through the course of the response. It is therefore problematic to apply results from these models to infections that result in a chronic or latent infection, such as with HSV-1 infection. As described, there is strong support for an ongoing immune response during viral latency, based upon inflammatory cytokine secretion and activation markers on immune cells present at the site of viral latency (148,149). How does a persistent or latent infection influence the development of T cell memory? There exists ample evidence that a chronic infection can result in the exhaustion of CD8 T cell responses characterized as either a shift in immunodominance, functional impairment or even deletion of the CD8 T cells (150-159). There appears to be a range of exhaustion which is based upon the antigen load (155). From work done in LCMV infection, the order of CD8 T cell exhaustion begins with loss of IL-2 secretion (low antigen load), then loss of TNF-α secretion (medium antigen load), then loss of IFN-γ secretion (high antigen load) and then finally death or deletion (very high antigen load) of the CD8 T cells. It is important

therefore when dealing with a chronic or latent infection, as is observed in HSV-1 infection, to be aware of the possibility of CD8 T cell exhaustion.

Several of these studies illustrating CD8 exhaustion also involve CD4 deficiency, such as in HIV infection (157-159). It should be noted that functional defects in CD8 T cells responses can occur in CD4 competent animals, thus illustrating CD8 T cell exhaustion can occur either in the presence (155,157,160) or absence (158,161) of CD4 T cell help. In fact, one group argues that infection of CD4 deficient mice with a chronic strain of LCMV results in the "worst possible scenario"(162) in terms of CD8 T cell exhaustion.

This question of how CD4 T cells regulate the development of CD8 T cell memory during a persistent or latent infection may prove to be very challenging (138). This is due in part to the additional variable of decreased antibody production in CD4 deficient hosts. The author admonishes that too often we neglect the unintentional consequence of decreased antibody production that occurs when addressing the role of CD4 T cell help (for CD8 responses) through CD4 depletion. This may be most evident in studies of HIV in which conclusions that suggest the declining ability of CD8 T cells to control the virus is due to the loss of a CD4 T cell help signal to those CD8 T cells. An alternative explanation is loss of CD4 numbers hinders the ability of the individual to produce antibodies to the shifting antigen of the virus resulting in reduced viral control (138).

We show in section 4.4 that CD4 T cells are important regulators of the contraction phase of the effector CD8$^+$ T cell response and in the generation of CD8 memory precursors in the TG. Additionally we provide evidence that CD4 T cells either directly or indirectly influence viral genome copy number within the TG.

2.   Specific Aims

The following summarizes the specific goals that were set forth for my thesis project, and the progress that was made in my studies.

Specific Aim 1: Determine the role of OX40/OX40L interactions in the cornea in relation to the development of HSK.

Hypothesis: CD134/OX40L interactions within the cornea are required for HSK development.

Past work in our lab has shown that blocking B7.1 costimulatory interactions in the cornea results in alleviation of inflammatory infiltration into the cornea and markedly reduced HSK. This led us to investigate the role of another costimulatory interaction CD134/OX40L in HSK. We determined that CD134/OX40L costimulation was not required within this setting by blocking this interaction both systemically and locally within the cornea with blocking reagents (soluble CD134 receptor and an antagonist anti-OX40L antibody) at different times both before and after ocular infection with HSV-1.

Specific Aim 2: Characterize CD4 T cells present in the corneas of mice with HSK.

Hypothesis: CD4 T cells that initiate HSK recognize viral antigens, however bystander activated CD4 T cells propagate disease.

Previous studies identified CD4 T cells as critical players in the development of HSK in mice, however the specificity and functionality of those CD4 T cells remains relatively unexplored. To better understand the role of CD4 T cells in the development of HSK, we generated CD4 T cell clones from corneas of mice with active HSK, and demonstrated their reactivity to viral antigens and their ability to transfer HSK to nude mice that are normally resistant to HSK. These cells will be used in future studies to characterize the relative involvement of HSV-1 specific versus bystander activated $CD4^+$ T cells in HSK.

Specific Aim 3: Determine if CD4 T cells are absolutely required for HSK development in mice.

Hypothesis: Although $CD4^{\pm}$ T cells are the primary mediators of HSK, in their absence, CD8 T cells can mediate disease.

Studies in our lab have shown that depletion of CD4 T cells in A/J mice prior to infection significantly reduced, but did not completely eliminate HSK. This finding, coupled with the fact that T cell deficient animals do not develop HSK, suggests that CD8 T cells may also be capable of mediating HSK. This is consistent with findings in humans that CD4 and CD8 T cells are recovered from the corneas of patients with HSK. Our findings established that $CD8^+$ T cells can mediate a transient HSK in $CD4^+$ T cell-deficient mice.

Specific Aim 4: Explore the direct or indirect involvement of CD4 T cells in maintaining HSV-1 latency within the trigeminal ganglion.

Hypothesis: CD4 T cells control the generation and maintenance of properHSV-specific CD8 T cell memory, and might also directly influence viral gene expression during latency.

3.   Materials and Methods

3.1.   Mice and virus infection

Female wild type (WT) BALB/c mice (Frederick Cancer Research Center, Frederick, MD), CD4^{-}

[/-] BALB/c mice (kindly provided by Pat Stuart, Washington University, St Louis) (163) and

C57BL/6 mice (Jackson Laboratory, Bar Harbor, ME) were used at 6-8 wk of age in all

experiments.   All mice were anesthetized by intraperitoneal injection of 2 mg of ketamine

hydrochloride and 0.04mg of xylazine (Phoenix Scientific, St. Joseph, MO) in 0.2ml of HBSS

(Biowhittaker, Walkersville, MD).   Topical corneal infection was performed by scarification of

the central cornea 15 times with a sterile 30-gauge needle in a crisscross pattern, and applying

3μl of RPMI (Biowhittaker, Rockland, ME) containing varying doses of HSV-1. The RE strain

of HSV-1 used was grown in Vero cells, and intact virions were purified on OptiPrep[TM]

gradients according to the manufacturer's instructions (Accurate Chemical & Scientific Corp.,

Westbury, NY), and stored at -80°C.   The concentration of plaque-forming units (pfu) of HSV-1

was determined in a standard virus plaque assay.   All experimental procedures were reviewed

and approved by the University of Pittsburgh Institutional Animal Care and Use Committee

(IACUC).

3.2.   Monitoring of HSV-1 corneal and skin disease

Corneal disease was monitored in a masked fashion by slit-lamp examination on alternate days

after HSV-1 corneal infection.   By 2 days after infection, BALB/c mice uniformly exhibited

dendritic-shaped corneal epithelial lesions that healed by 4 days post-infection (P.I.).   HSK was

characterized by corneal opacity and neovascularization beginning approximately 7 days after

HSV-1 corneal infection. Opacity and neovascularization developed concurrently, and were monitored by slit-lamp examination. HSK was scored (see figure 4) on the basis of opacity as 1+, mild corneal haze; 2+, moderate opacity; 3+, severe opacity obscuring the iris; or 4+, corneal perforation.

3.3. Whole mount cornea immunofluorescence staining

Mice were euthanatized by halothane inhalation and the corneas excised. Any attached lens, conjunctiva, iris and excess limbal tissue were removed from the corneas. The corneal stroma and epithelium were then separated after a 20 minute incubation at 37°C in PBS containing 20 mM EDTA. The following general procedure was used for all antibodies, with the exception of CD11c and OX40L. After separation, the corneal stromas were fixed for 30 minutes at 4°C in 1% paraformaldehyde-PBS followed by extensive washing with PBS. After fixation, the corneal tissue was blocked for 20 minutes at 37°C with 10 µg/mL Fc-Block diluted in PBS-BGEN (PBS containing 3% BSA, 0.25% gelatin, 5 mM EDTA, and 0.025% Nonodet-P40, a nonionic detergent). After the blocking step, corneal tissue was incubated overnight at 4°C with 100 µL primary antibody (1–5 µg/mL) diluted in PBS-BGEN. The tissue was then washed 5 times, 5 minutes each, with PBS. Tissues stained with fluorescently labeled primary antibody were fixed again with 1-4% paraformaldehyde-PBS, for 30 minutes, at 4°C, rinsed with PBS, placed on slides, mounted with Immu-Mount mounting medium (Shandon, Pittsburgh, PA), and coverslipped. Alternatively, tissues that were reacted with a biotinylated primary antibody were further incubated with 100 µL of fluorescently labeled streptavidin (1–2.5 µg/mL) diluted in PBS-BGEN for 1 hour at 37°C. This was followed by five washes of 5 minutes each with PBS, fixation, and mounting onto slides. For visualization of CD11c staining, tyramide amplification

was performed with a kit (TSA Direct; NEN, Boston, MA) according to the manufacturer's recommendations. In brief, tissue to be reacted with the CD11c antibody was blocked with 10 µg/mL Fc-Block, 10% human serum, and 10% goat serum diluted in TNB buffer (1M Tris-HCl, 0.15M NaCl, and 0.5% "Blocking Reagent" supplied with the TSA Direct Kit). The tissue was reacted in sequential incubation and washing steps with unlabelled CD11c antibody (1 µg/mL), followed by biotinylated goat anti-hamster IgG (5 µg/mL), streptavidin-HRP (1:100), and the fluorophore tyramide (1:50). All antibody incubations were performed in TNB buffer. Endogenous peroxidase activity in the tissue was quenched with 3% H_2O_2 before staining. For OX40L staining, the corneas were washed after PFA fixation in 1X PBS and then were added to the blocking reagent normal goat serum (NGS) for 20 minutes at 37° C. The corneas were incubated with CD134-human F_c fusion protein (provided by Andrew Weinberg, Oregon Health Sciences Center) at 1µg/ml for 1 hour at 37°C. The corneas were then washed five times with 1X PBS and then were added to goat anti-human IgG biotin for 1 hour at 37° C. The corneas were washed again five times in 1X PBS and then incubated with streptavidin-Cy3 at 37° C for one hour. Following the one hour incubation, the corneas were washed five times with 1X PBS and then mounted onto slides using Immu-mount and visualized using confocal microscopy. All slides were examined by fluorescence microscopy on a 1 x 70 microscope (Olympus, Tokyo, Japan) equipped with a confocal imaging system (Radiance Plus; Bio-Rad, Hercules, CA). Digital images were captured using the scanning confocal laser and the accompanying software (Lasersharp 2000; Bio-Rad).

3.4.   Reagents and Antibodies

Reagents for whole mount staining: DMEM and penicillin-streptomycin, BioWhittaker (Walkersville, MA); fetal bovine serum (FBS), Hyclone (Logan, UT); bovine serum albumin (BSA) and bovine gelatin, Sigma (St. Louis, MO); goat serum, Atlanta Biologicals (Norcross, GA); EDTA, Fisher Scientific (Fair Lawn, NJ); NP-40, Calbiochem (La Jolla, CA); paraformaldehyde, Electron Microscopy Sciences (Fort Washington, PA); ketamine hydrochloride and xylazine, Phoenix Pharmaceutical, Inc. (St. Louis, MO); halothane, Halocarbon Laboratories (River Edge, NJ).

A list of antibodies used for corneal whole mount staining, corneal/TG flow is provided in figure 6. To visualize $gB_{498-505}$ specific CD8 T cells, Dimer-X reagent from BD Pharmingen was used. Briefly, we loaded the emtpy Dimer-X reagent with gB peptide the day before each experiment. We combined 0.3325 ul of gB peptide (stock concentration was 2mg/ml) with 5ul of Dimer-X reagent (stock concentration is 0.1 mg/ml) for each tube that would be stained for $gB_{498-505}$ specific cells. We then used 5ul of that dimer-X:gB peptide mixture per staining tube along with other surface antibodies. All stains done in the TG using Dimer-X:gB reagent were incubated for one hour at 4° C.

reagent	Source	Catalog Number	amount used	isotype	clone	Application
Dimer X PE (H-2K^b:Ig)	BD PharMingen	552944	0.5ug (peptide loaded)	mouse IgG1λ	N/A	Flow cytometry
PE anti-CD8α	BD PharMingen	553033	0.2 μg	rat IgG2aκ	53-6.7	Flow cytometry
APC-Cy7 anti-CD8α	BD PharMingen	557654	0.2 μg	rat IgG2aκ	53-6.7	Flow cytometry
FITC anti-CD8β.2	BD PharMingen	553040	0.5 μg	rat IgG1κ	53-5.8	Flow cytometry
PE anti-CD4	BD PharMingen	553049	0.2 μg	rat IgG2aκ	RM4-5	Flow cytometry
PE anti-mouse I-A/I-E	BD PharMingen	557000	0.2 μg	rat IgG2bκ	M5/114.15.2	Flow cytometry
FITC anti-CD69	BD PharMingen	557392	0.5 μg	hamster IgG1λ	H1.2F3	Flow cytometry
PerCP anti-CD45	BD PharMingen	557235	0.2 μg	rat IgG2bκ	30-F11	Flow cytometry
PE-Cy7 anti-CD4	BD PharMingen	552775	0.2 μg	rat IgG2aκ	RM4-5	Flow cytometry
APC anti-CD127	eBioscience	17-1271-82	0.2 μg	rat IgG2aκ	A7R34	Flow cytometry
APC anti-DO11.10 TCR	Caltag	MM7505	0.1 μg	mouse IgG2a	KJ1-26	Flow cytometry
FITC anti-DO11.10 TCR	Caltag	MM7501	0.1 μg	mouse IgG2a	KJ1-26	Flow cytometry
APC anti-Ly6C/G (Gr-1)	Caltag	MRM3005	≤0.2 μg	rat IgG2b	RM6-8C5	Flow cytometry
APC anti-IFN gamma	BD PharMingen	554413	0.2 μg	rat IgG1	XMG1.2	Flow cytometry
biotin anti-OX40	BD PharMingen	559862	0.5 μg	rat IgG1κ	OX-86	Flow cytometry
Vβ TCR screening panel	BD PharMingen	557004	varies	varies	N/A	Flow cytometry
FITC anti-CD4	Caltag	MCD0401	3ug/ml final conc.	rat IgG2aκ	RM4-5	Corneal whole mount
Alexa 488 anti-mouse I-A/I-E	Labeled in house	41CM13	1:500 dilution of stock	rat IgG2b	M5/114.15.2/TIB-120	Corneal whole mount
FITC anti-cd11c	BD PharMingen	553801	used tyramide amplification	hamster IgG1κ	HL3	Corneal whole mount
biotin anti-CD45	BD PharMingen	553077	5ug/ml final conc.	rat IgG2bκ	30-F11	Corneal whole mount
biotin anti-OX40	BD PharMingen	559862	2-6μg/ml final conc.	rat IgG1κ	OX-86	Corneal whole mount
hOX40-hFc	From Andrew Weinberg	N/A	6ug/ml final conc.	N/A	N/A	Corneal whole mount
Cy-3 goat anti-human	Jackson Immunoresearch	109-165-098/36CM13	1:50 dilution of stock	N/A	N/A	Corneal whole mount
Streptavidin Cy3	Jackson Immunoresearch	016-160-084	2μg/ml final conc.	N/A	N/A	Corneal whole mount
Avidin- FITC	BD PharMingen	554057	5μg/ml final conc.	N/A	N/A	Corneal whole mount

Figure 7: Antibodies used for flow cytometry and whole mount corneal staining.

3.5. Preparation of corneal single cell suspension

At various times after HSV-1 corneal infection, mice were scored for HSK and corneas were removed, and incubated with PBS-EDTA to separate the epithelial layer. Individual corneal stromas were rinsed, cut into quarters, treated with collagenase type I (84 units/cornea; Sigma, St. Louis, MO) for 1.5-2 hrs at 37 ^{o}C, and triturated until no apparent tissue fragments remained. The single cell suspension of each cornea was then filtered through a 40μm cell strainer cap (Becton Dickinson Labware), washed once with flow buffer (1X PBS + 0.1% sodium azide + 1% FCS) and then stained for surface markers.

3.6. Preparation of trigeminal ganglion single cell suspension

At various times after HSV-1 corneal infection, mice were sacrificed and both TGs were removed (in the case of C57Bl/6 mice both eyes are infected and therefore both TGs were used, in BALB/c mice only one eye was infected, thus only one TG was removed). Both (or individual TGs in the BALB/c mice) TGs were treated with collagenase type I (40 units/TG; Sigma, St. Louis, MO) for 1 hr at 37 $^{\circ}$C, and triturated until no apparent tissue fragments remained. The single cell suspension of each TG was then filtered through a 40μm cell strainer cap (Becton Dickinson Labware), and washed. In the case of C57Bl/6 mice, both TGs were digested together in 100ul of collagenase per TG and then exactly one half of the volume was removed (one TG equivalent), filtered through a 40μm cell strainer cap (Becton Dickinson Labware) and subjected to flow cytometric analysis, while the other half was used for viral genome copy number. After staining, cells were fixed in 1% paraformaldehyde (PFA, Electron Microscopy Sciences, Fort Washington, PA) and analyzed on a FACSAria (Becton Dickinson) using FACSDIVA data analysis software. The entire extract of each individual TG was analyzed to provide an estimate of the absolute number of marker positive cells per TG.

3.7. Quantitation of leukocyte populations in corneal cell suspensions

Single cell suspensions of individual corneas (one cornea/tube) were prepared on the designated day after HSV-1 infection, incubated with anti-mouse CD16/ CD32 (Fcγ III/II Receptor (2.4G2, BD PharMingen) to prevent nonspecific binding of fluoresceinated mAbs, and then stained for various leukocyte surface markers for 30 minutes at 4° C. After staining, cells were fixed in 1% paraformaldahyde (PFA, Electron Microscopy Sciences, Fort Washington, PA) and analyzed on a FACSAria (Becton Dickinson) using FACSDIVA data analysis software. The

entire extract of each individual cornea was analyzed to provide an estimate of the absolute number of marker positive cells per cornea. All flow staining was performed in flow wash buffer which is 1X PBS + 0.1% sodium azide + 1% FCS.

3.8.   Bone marrow derived dendritic cell (BMDC) preparation

Bone marrow was isolated from the femurs of naïve BALB/c mice, incubated with a final concentration of 5ug/ml anti-CD3 (clone 145-2C11 to deplete T cells), 5ug/ml anti-CD4 (clone GK1.5 to deplete CD4 T cells), 5ug/ml anti-CD8 (clone 2.43 to deplete CD8 T cells), 5ug/ml of anti Gr-1 (clone RB6-8C5 to deplete neutrophils), 5ug/ml anti-Mac-1 (clone TIB-128 to deplete macrophages), 5ug/ml of anti-B220 (to deplete B cells) and anti-Ia (clone TIB-120 to deplete antigen presenting cells) for one hour on ice. The cells were incubated in the antibodies in Cedarlane Cytotoxicity media (RPMI-1640 with 25mM Hepes buffer and 0.3% bovine serum albumin). After the one hour, cells were washed once with Cytotoxicity media, and then incubated with rabbit complement (Cedarlane) for 1 hour at 37° C. The rabbit complement was prepared first by adding 1ml of sterile water to the lyophilized complement, then dilute that 1:8 in cytotoxicity media. Sterile filter that solution and then use 8mls of that sterile complement to resuspend the pellet of cells that were incubated with the antibodies. After the one hour incubation, the cells were washed with complete DC media and then live cells were purified by ficol separation (Atlanta Biologicals I40650). Cell were counted, and then cultured in 10ng/ml GM-CSF (Granulocyte monocyte colony stimulating factor, R&D Systems catalog # 415-ML) and 10ng/ml SCF (Stem cell factor, R&D Systems catalog # 455-MC) and 2ME for 3 days at a concentration of $2X10^5$ cells per ml (10^6 cells per well of a 6 well plate). Cells were fed with fresh media containing GM-CSF and SCF after 3 days, and nonadherent cells were harvested on day 6. These nonadherent cells were then cultured at a concentration of $2X10^5$ cells per ml in

complete DC media containing 10ng/ml GM-CSF, 10ng/ml IL-4, and 10ng/ml TGF-β for an additional 3-4 days to generate immature Langerhans-like cells that were used for CD4 T cells stimulations.

Media used for all DC culture is complete DC media: RPMI + 1% sodium pyruvate (Stock used from Invitrogen, 100mM), 10% fetal calf serum, 1% MEM non-essential amino acids (stock from Invitrogen, 10mM), 25ul HEPES (Stock used from Cambrex Bioscience 1M), 2mM L-glutamine (Cambrex, add 10 mls of stock 200mM to each 1L of RPMI), and 100U/ml penicillin and 100ug/ml streptomycin.

3.9.   Generation of viral antigen loaded DCs for CD4 stimulations

Following the incubation of DCs in GM-CSF, IL-4, and TGF-β, the cells were then purified using standard MACS separation for cd11c. After cd11c purification, 6 X10^6 cells (in a total volume of 1ml) were aliquoted into a 1.5 ml siliconized microfuge tube. 100μl of the different lysates were added into each tube and incubated for 1 hr at 37° C. At the end of the one hour incubation, all of the cells (6X10^6) were plated into a 6 well plate supplemented with GM-CSF (1ul/ml) in a final volume of 5 mls of complete DC media and then incubated for 1 hour at 37°. At the end of the one hour incubation, LPS (2ul/ml with final concentration being 200ug/ml), TNF-α (1ul/ml with a final concentration being 10ng/ml) and GM-CSF (1ul/ml with a final concentration being 10ng/ml) were added and the cells were cultured/matured overnight at 37° C. The following day, the cells were scraped from each well using a 500ul pipet tip, washed, counted and then combined with CD4 T cells for ELISA stimulations.

Alternatively, following the incubation with lysates in the 1.5 ml tubes, DCs were combined with the maturation stimuli (LPS, TNF-α, and GM-CSF) and then directly plated into

the appropriate wells of either a 48 well or 96 well plate overnight. The following day, all the wells were washed twice with Iscoves media to remove residual LPS and TNF-α and then T cells were added to the wells along with fresh media and 2-ME (final concentration of 5×10^{-5} M).

3.10. Vero cell lysate generation

The HSV-1 antigens were extracted from Vero cells (3.5×10^6/ml) 1, 5, 10 hours after RE HSV-1 infection (multiplicity of infection of 4). Confluent flasks of Vero cells were infected at an MOI of 4 for one hour, washed twice with Vero growth media (DMEM supplemented with: 10% FCS, 1% HEPES (stock used from Cambrex Bioscience 1M), 0.1 mM nonessential amino acids (stock from Invitrogen, 10mM), 1mM sodium pyruvate (stock from Invitrogen, 100mM), L-glutamine (2mM) 100U/ml penicillin and 100ug/ml streptomycin) and then incubated for either 4 hours or 9 hours to generate the 5 hour and 10 hour lysates, respectively. One flask that had been infected for one hour only was immediately harvested and processed to generate the 1 hour Vero cell lysate. The extraction of viral antigens from the infected Vero cells involved 3 freeze/thaw cycles, two 2 min homogenization cycles using the Retsch MM 300 Mixer Mill homogenizer, UV inactivation for 10 minutes at 5cm, and clarification by centrifugation at 200Xg.

3.11. Stimulation and analysis of IFN-γ production by corneal CD8 and CD4 T cells

MKSA cells (a SV40-transformed BALB/c mouse kidney fibroblast cell line kindly provided by Dr. Robert Bonneau, Pennsylvania State University College of Medicine) were infected at an MOI of 5 for 1 hour at 37°C, the cells were washed twice with MKSA media (DMEM supplemented with: 5% FCS, 2% HEPES (stock used from Cambrex Bioscience 1M),

L-glutamine (2mM) 100U/ml penicillin and 100ug/ml streptomycin) and then further incubated for 4 hours. The cells were then harvested and $1x10^6$ HSV-infected MKSA cells were used to stimulate the CD8$^+$ T cells in each digested cornea. Alternatively, BMDC were pulsed overnight with an extract from Vero cells that were infected with HSV-1 for 10 hours and $0.25x10^5$ BMDC were used to stimulate CD4$^+$ T cells in each cornea.

The corneal cells (both CD4 and CD8s) were stimulated for 6 hours in the presence of Golgiplug and assayed for intracellular IFN-γ production using BD Pharmingen's intracellular cytokine staining protocol.

3.12. Stimulation and analysis of IFN-γ production by T cells in the TG

Intracellular IFNγ stains were carried out using cytofix/cytoperm kit with Golgiplug™ (BD Pharmingen) in accordance with the manufacturer's instructions. Briefly, individual TG from C57Bl/6 mice were incubated with 0.5×10^6 stimulator cells and Golgiplug™ for 6 hours at 37°C. Stimulator cells were the B6WT3 fibroblast cell line transfected to produce the gB$_{498-505}$ peptide (B6/T-350gB) (164) and were also pulsed with gB$_{498-505}$ peptide at a concentration of 2ug/ml in DMEM supplemented with 10% FCS for 30 minutes at 37° C for one half hour and then washed. After the 6 hrs incubation, the cells were stained for cell surface markers and intracellular cytokines followed immediately by flow cytometric analysis. For BALB/c TGs, MKSA cells (a SV40-transformed BALB/c mouse kidney fibroblast cell line kindly provided by Dr. Robert Bonneau, Pennsylvania State University College of Medicine) were infected at an MOI of 5 for 1 hour at 37°C, the cells were washed twice with MKSA media and then further incubated for 4 hours. The cells were then harvested and different numbers of HSV-infected MKSA cells were used to stimulate the CD8$^+$ T cells in each digested BALB/c TG.

3.13. Corneal viral titers

Following HSV-1 corneal infection, the corneal surfaces of WT and CD4$^{-/-}$ BALB/c mice were swabbed on days +2, +4, +6, +8 with sterile Weck-Cel surgical spears (Medtronic Solan, Jacksonville, FL), spears were placed in 0.5 ml RPMI, and frozen at -80° C until assayed. For viral titers, 1:2, 1:10, 1:50, and 1:250 dilutions of the samples were plated onto confluent Vero cells, incubated for 1 hour at 37° C, and then plaque assay media containing 0.5% methylcellulose was added. The cultures were incubated for 72 hours, fixed with formalin, stained with crystal violet and plaques were counted with the aid of a dissecting microscope.

3.14. T cell line (THSK3.30) generation

A total of 30 infected BALB/c corneas were removed from D+11 infected mice and the epithelial sheets, ciliary body, iris and conjunctiva were removed and discarded. The stroma was digested into a single cell suspension using Liberase Blendzyme (stock concentration of 3.5 mg/ml) diluted 1:50 in RPMI with no fetal calf serum. We used 100ul of the diluted Blendzyme per cornea. The resulting single cell suspension was filtered through a 50um cell strainer and washed with Iscoves complete media (Iscoves Modified Dulbecco's Medium supplemented with 10% Fetal Calf Serum, 100U/ml penicillin and 100ug/ml streptomycin, and 2-mercaptoethanol (2-ME) at a final concentration of $5X10^{-5}$ M). The cells were then washed with MACS beads buffer (2mM EDTA and 0.5% BSA in 1X PBS) and incubated with anti-CD4 coated MACS beads for 15 minutes at 4 degrees Celsius. The cells were washed with MACS beads buffer and then added to a standard MACS column and the CD4 T cells were collected. These CD4 T cells were then cultured at 37° C in one well of a 48 well plate in Iscoves media with 10ng/ml IL-15 for 3 days. After 3 days, the cells were stimulated with $2X10^6$ irradiated (3000 rads) BALB/c

splenocytes plus 1ug/ml anti-CD3 and 10ng/ml IL-15 for 3 days. After this stimulation, the cells were washed with Iscoves media and cultured in Iscoves plus 25 U/ml of rIL-2, 5ng/ml of rIL-7 and 2-ME ($5X10^{-5}$ M) still in a single well of a 48 well plate. Five days later the cells were fed with fresh Iscoves media containing 25 U/ml of rIL-2 and 5ng/ml rIL-7 and 2-ME ($5X10^{-5}$ M).

3.15. T cell clones generation

The THSK3.30 cell line was cloned by limiting dilution in 60 well Terasaki plates (Nunclon catalog #163118). $4X10^4$ irradiated splenocytes were combined with differing numbers of T cells per well (we chose 10, 5, 1, and 0.3 cells per well). Final volume per well in the Terasaki plates was 10ul. Master mixes of T cells and splenocytes were prepared and then supplemented with IL-2 (25 U/ml), IL-7(5ng/ml) and 2 ME ($5X10^{-5}$ M) and then 10ul of those master mixes were added to each well in the Terasaki plates. Note that the T cell line (THK3.30) was stimulated the day before we cloned them using splenocytes and anti-CD3/anti-CD28.

For the 10 T cells per well: 7000 T cells were combined with 28 X 10^6 irradiated splenocytes along with IL-2 (500U/ml), IL-7 (5ng/ml) and 2ME ($5X10^{-5}$ M) in a final volume of 7mls. 10ul of this mixture was added to each well, which resulted in 10 T cells per well and 4 X 10^4 splenocytes per well. This solution provided enough cells for ten full plates.

For the 3 T cells per well: 2100 T cells were combined with 28 X 10^6 irradiated splenocytes along with IL-2 (500U/ml), IL-7 (5ng/ml) and 2ME ($5X10^{-5}$ M) in a final volume of 7mls. 10ul of this mixture was added to each well, which resulted in 3 T cells per well and 4 X 10^4 splenocytes per well. This solution provided enough cells for ten full plates.

For the 1 T cell per well: 700 T cells were combined with 28 X 10^6 irradiated splenocytes along with IL-2 (500U/ml), IL-7 (5ng/ml) and 2ME ($5X10^{-5}$ M) in a final volume of 7mls. 10ul of this

mixture was added to each well, which resulted in 1 T cell per well and 4 X 10^4 splenocytes per well. This solution provided enough cells for ten full plates.

For the 0.3 T cells per well: 210 T cells were combined with 28 X 10^6 irradiated splenocytes along with IL-2 (500U/ml), IL-7 (5ng/ml) and 2ME ($5X10^{-5}$ M) in a final volume of 7mls. 10ul of this mixture was added to each well, which resulted in 0.3 T cells per well and 4 X 10^4 splenocytes per well. This solution provided enough cells for ten full plates.

The plates were examined for cell growth every few days and once good cell growth was observed, cells were transferred a 96 well plate. After the cells grew in the 96 well plate, they were transferred to a 48 well pate and so on until they were plated in 6 well plates.

3.16. Maintenance of T cell line/clones

The T cell line and clones were propagated using a cycle of stimulation, feeding, and then rest. For stimulation using irradiated splenocytes, two separate solutions were prepared: A and B. The two solutions are prepared in equal volumes and equal amounts of each solution were added to each well of cells to be stimulated. Solution A contains Iscoves media plus anti-CD3 (from Bluestone's lab ATCC) and anti-CD28 (clone 37.51) both at a final concentration of 2ug/ml. Solution B contains irradiated splenocytes (3000 rads), IL-15 @ 2X desired final concentration (20ng/ml) and IL-12 @ 2X desired final concentration (4ng/ml). All media was removed from the cells and solution A was added to the cells and incubated for 10 minutes at 4° C. Then solution B was added directly to the cells and solution A. After combining the two solutions with the cells, the final concentrations of the cytokines IL-15 and IL-12 were 10ng/ml and 2ng/ml, respectively. The numbers of irradiated splenocytes added was based upon the size of the well that the T cells were grown in. For each well of a 6 well plate, we added 10-15 X 10^6 irradiated splenocytes per well and for 12 well plates we add 5-7 $X10^6$ irradiated splenocytes per

well. Final volume for each well in a 6 well plate is 5mls, final volume for each well in a 12 well plate is 3mls, final volume for each well in a 24 well plate is 2mls, final volume for each well in a 48 well plate is 1ml and final volume for each well in a 96 well plate is 0.2 mls. T cells are stimulated for 3 days and then they are fed. 2ME was included in all cultures at ($5X10^{-5}$ M).

The feeding and expansion phase is achieved by removing all cells in the well, followed by Ficol separation of live cells (if necessary) and re-plating in fresh media containing IL-2 (500U/ml) and IL-7 (5ng/ml). Alternatively, one half of the media can be removed and then add back media with 2X concentration of IL-2 and IL-7 so that the final concentration of these cytokines is still 500U/ml for IL-2 and 5ng/ml for IL-7. Cells are fed again after 3 to 4 days with fresh media and cytokines. Cells go through one stimulation, two feed cycles, and then a rest cycle, and then the stimulation is done again.

The rest phase involves removal of all media (Ficol cells again to obtain live cells if needed) and then add back fresh media containing IL-15 at 10ng/ml final concentration. Cells are usually rested for a period of 3 to 4 days and then are stimulated as described.

3.17. ELISA testing of T cell line/clones for viral reactivity

For initial testing of clones set 1 and 2, stimulations were set up in 48 well plates. For identification of viral specificity using 1, 5, 10 hr viral lysates, stimulations were performed in 96 well plates. The exact conditions are as follows:

48 well plates: 2×10^5 of each T cell clone was combined with 10^5 viral antigen loaded BMDCs. This protocol was used to test THSK3.30 cell line specificity and all of the initial characterization of clones set 1 and 2. Final volume in each well of a 48 well plate is 1ml.

96 well plates: $1X10^5$ T cells were combined with 5×10^4 DCs viral antigen loaded DCs. Final volume in each well of a 96 well plate is 200 ul.

Instead of using purified DCs from bone marrow, we also used bulk splenocytes as stimulators of the T cell clones. This was performed in a 96 well plate and we added 2×10^5 T cells with 10^6 irradiated naïve splenocytes per well. We also added the different Vero cell lysates into each well (usually between 10-100ul lysates per well) with the final volume per well being 200ul. For all ELISA stimulations, we used Iscoves media supplemented with 2ME (5×10^{-5} M).

3.18.   Generation of UV-inactivated HSV-1 RE

HSV-1 RE was placed under a UV light source at a distance of 5 cm for 10 minutes. This was performed in the tissue culture hood to maintain sterility. Place the virus to be inactivated in a small plastic Petri dish and remove the lid to inactivate. The UV inactivated virus was tested by standard plaque assay on Vero cells to confirm full inactivation has occurred.

3.19.   ELISA detection of IFN-γ in supernatants

Microtiter plates (DYNEX IMMULON® 4HBX, Thermo Labsystems, Franklin, MA) were coated overnight with primary anti-cytokine capture Ab. The plates were washed and blocked with 1% BSA in PBS. The supernatant fluids and standards were added and incubated at room temperature for 2 h. The plates were washed again, secondary biotinylated anti-cytokine detection Ab was added and incubated at room temperature for 1 h. The plates were then washed and developed with strepavidin-horseradish peroxidase (BD Pharmingen, San Diego, CA) and its substrate ((3,3' 5,5'-Tetramethylbenzidine Base, GIBCO BRL, Gaithersburg, MD). The colored reaction product was measured with an enzyme immunoassay plate reader at 450 nm. The amount of cytokine in each supernatant was extrapolated from a standard curve. The capture/detection Abs were as follows: IFN-γ, R4-6A2 (from ATCC)/polyclonal goat anti-mouse

IFN-γ (R&D systems, Inc., Minneapolis, MN). The detection sensitivity was 5.6 pg/ml for IFN-γ.

3.20. ELISA setup for DO11.10 CD40L KO vs WT draining lymph nodes

The DLN (cervical and submandibular lymph nodes) were excised 5, 7, and 9 days after HSV-1 infection, and single cell suspensions were prepared in assay medium (RPMI 1640 plus 5%FCS, 10mM HEPES buffer, and antibiotics). CD4$^+$ T cells and CD11c$^+$ DCs were isolated by two rounds of magnetic separation using MACS mouse CD4 (L3T4) and MACS mouse CD11c (N418) MicroBeads, respectively according to the manufacturer's instructions (Miltenyi Biotec Inc., Auburn, CA). The purified CD4$^+$ T cells (5 x 10^5) were cultured in 96-well round bottom plates (Becton Dickinson, Franklin Lakes, NJ) with CD11c$^+$ DCs (2.5 x 10^4) and UV-inactivated RE strain HSV-1 (UV-HSV, 5 x 10^7 final PFU/ml). The cultures were incubated at 37 ^{o}C for 72 hrs, and cytokine content of supernatant fluids was measured in a standard ELISA.

3.21. Real time PCR for viral genome copy number

DNA extraction protocol:

C57Bl/6 mice that were previously infected with 3X10^5 PFu HSV-1 RE, were sacrificed and both TGs were removed and digested with collagenase type I (40 units per TG in a volume of 100ul per TG). After the digestion, exactly one half of the volume was used for flow cytometry and the other half was used for DNA extraction using a Qiagen Miniprep kit. Briefly, the one TG equivalent (which is in ~100 ul of collagenase) was spun down at 15,800 X g. The pellet was then resuspended in 200ul of 1X PBS. We then followed the directions in the Qiagen DNeasy kit (the protocol for "Purification of Total DNA from cultured Animal Cells" part of the booklet). Total DNA was eluted from the column with a single wash of 100ul of DNase free

water. These DNA samples were stored at -80° C for at least 2-3 days and then DNA concentration was determined by diluting the DNA samples 1:10 in water in a 384 well spectrophotometer plate and DNA concentrations were determined on a SPECTRAmax[384] spectrophotometer (Sunnyvale, CA). Aliquots of DNA were prepared from each TG by removing 100ngs of total DNA from the original samples followed by bringing the total volume up to 100ul so that the final concentration is 1ng/ul. The aliquots were stored at -80° C for at least one day.

Real time PCR\reaction setup:

The total numbers of wells that will be used is determined, keeping in mind that each sample (including unknowns, standards, and negative controls) will be run in duplicate. Standards consist of 10^4 and 10^3 of gH plasmids. The Master mix (TaqMan Universal PCR Master Mix: Part number 4304437 from Applied Biosystems) and gH primer probe mixture (ABI) were combined into a master mix following these calculations:

1. Master Mix (x+3)∗22.5ul where x = total number of wells

2. gH primer/probes (x+3)∗2.5ul where x = total number of wells

All reagents were protected from light and then 25ul of the above mixture was aliquoted into each well of a 96 well optical assay plate. Negative control wells consisted of 25μl of water plus 25μl of the master mix/gH primer probe mixture. Positive control wells consisted of 25ul of the gH plasmid positive controls plus 25μl of the master mix/gH primer probe mixture. 25 ul of each unknown DNA sample (total of 25ng of DNA) was added to the wells containing 25μl of the master mix/gH primer probe mixture. The plate was then centrifuged at 1000 rpm for 1 minute, covered with foil and incubated at 4° C for 1 hour.

Real Time PCR machine run:

An ABI Prism 7700 Sequence Detector was used, running 96-well plates at 50 μL / well final volume. Instrument control and data analysis were made using the default settings of the supplied Primer Express v. 1.5a software. Each assay comprised duplicate measurements of both DNA and control (water) at 25 ng of DNA per well. This sample was mixed with the appropriate primer-probe set and TaqMan 2 x PCR Mastermix. A primer-probes set for the viral gene gH was designed and custom-synthesized by the ABI Assays-by-Design service.

3.22.   Reverse transcriptase-PCR for OX40L mRNA in corneal samples

Briefly, individual corneas were removed and placed in sterile PBS. An autoclaved stainless steel bead was added and the corneas were mechanically disrupted using a Retsch MM300 Mixermill (Qiagen catalog number 85110). RNA was then purified from the resulting cell suspension using a Qiagen RNeasy kit. Following elution of RNA, the sample was treated with the Ambion DNase kit and then reverse transcription (RT) was performed. Following RT, the resulting cDNA was amplified using OX40L specific primers as reported (165,166). OX40L #1:   ATGGAAGGGGAAGGGGTTCAACC   and   OX40L   primer   #2: TCACAGTGGTACTTGGTTCACAG. Both primers were purchased from Sigma-Genosys. The resulting OX40L fragment is 596 bps.

3.23.   Statistics

The differences in HSK severity and the differences in cornea cellular infiltrations between WT and CD4 deficient mice were analyzed by an unpaired *t* test. The difference in incidence of disease between WT and CD4 deficient mice was analyzed by Fisher's exact test. All statistical analysis of TG populations between WT and CD4 deficient mice were analyzed by an unpaired *t* test.

4.   Results

4.1.   Do CD134/OX40L interactions play a role in herpes stromal keratitis (HSK)?

Past work in our lab has shown that costimulatory interaction through B7/CD28 within the cornea are critical for the development of HSK (38). We therefore hypothesized that other costimulatory interactions such as CD134/OX40L would also be required for the development of HSK. This is based on the finding that stimulation through CD134 is as potent a stimulus to the CD4 cell as the signal though CD28 (126,167).

4.1.1.   Cells within mouse corneas with HSK express CD134 (OX40) and OX40L (OX40L).

First we wanted to identify if cells within the corneas of mice with HSK express CD134 (CD134) or OX40L. The prediction is that CD4 T cells will express CD134 while DCs would be the cell type expressing OX40L. Figure 8 shows CD4 T cells within the corneas of mice with HSK express CD134, while figure 9 shows OX40L is expressed on CD45^{+} MHC class II^{-} cd11c^{-} cells. The identification of CD134 on CD4 T cells is consistent with the literature, but a lack of OX40L^{+} DCs (cd11c) was surprising. Even more surprising was the finding that OX40L is not expressed by MHC class II expressing cells in the cornea. CD134 expression in the cornea was first observed at D+3 post-infection, while OX40L expression was not identified until D+7-D+10, usually with the onset of HSK. This is consistent with the literature suggesting expression of OX40L is the limiting factor in CD134/OX40L interactions and signaling (126).
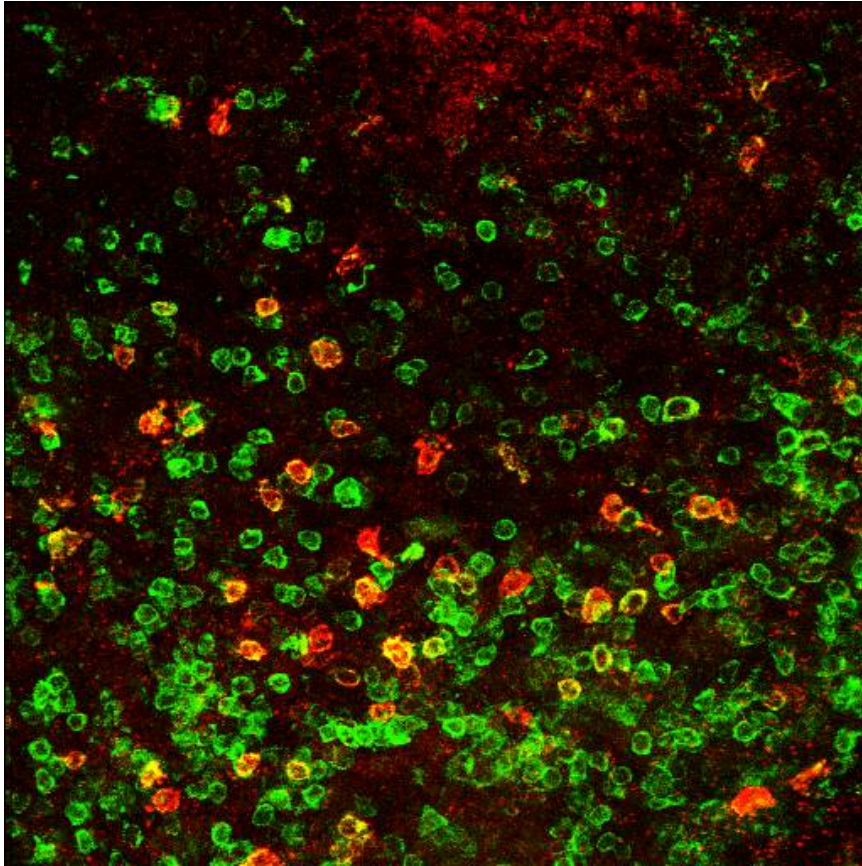
Figure 8: CD134 is expressed on CD4 T cells in the corneas of mice with HSK.

BALB/c mice were infected with 10^5 PFU of HSV-1 RE. Corneas were removed from mice 14 days P.I., the iris, ciliary body, lens, conjunctiva, and epithelium were removed and discarded. The stromal layer of the cornea was then stained with a biotin-labeled antibody to CD134 followed by staining with avidin-Cy3 and a FITC labeled antibody to CD4.
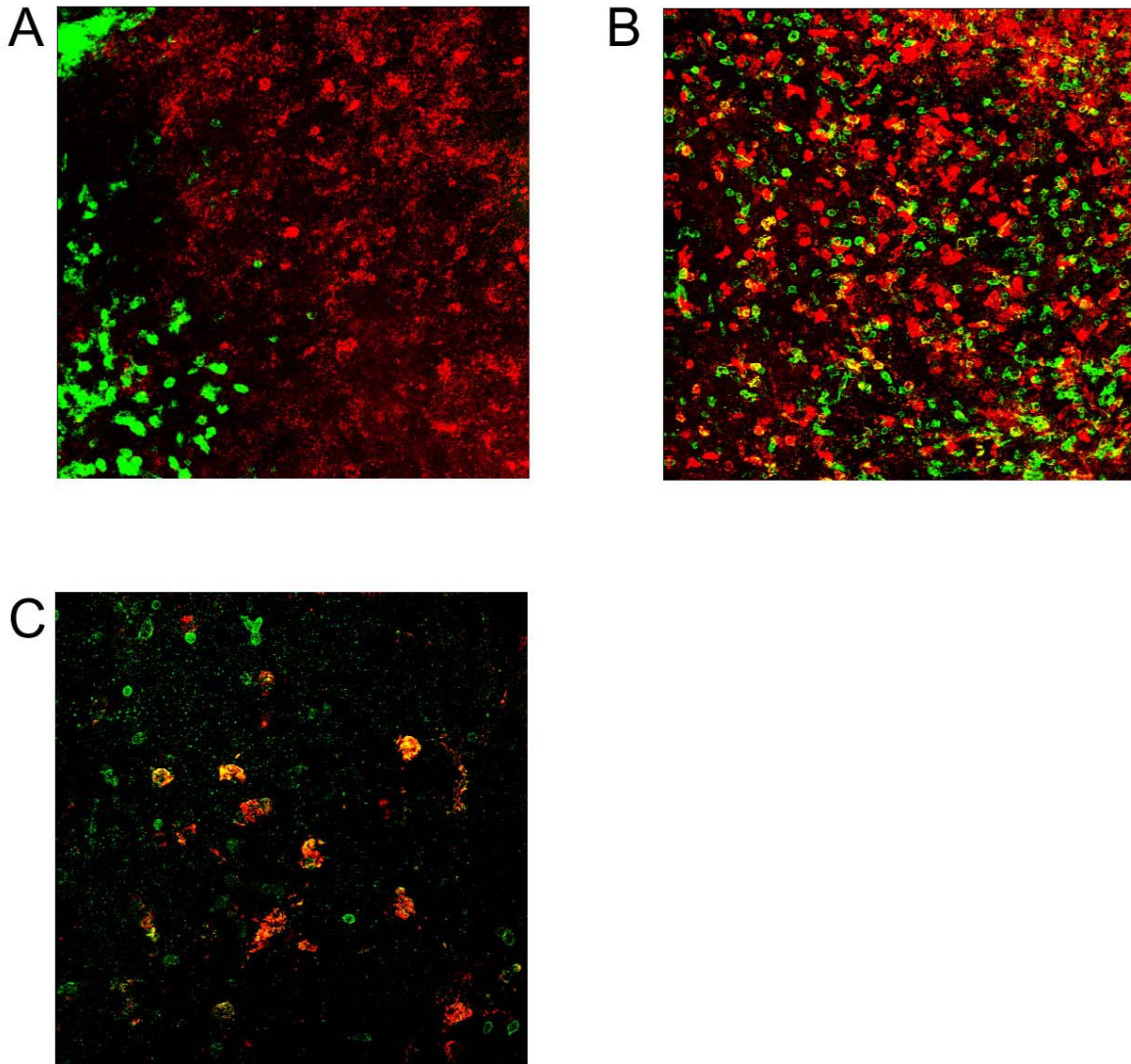
Figure 9: OX40L is expressed on CD45$^+$MHC class II$^-$ cd11c$^-$ cells in corneas with HSK.

BALB/c mice were infected with 10^5 PFU of HSV-1 RE. Corneas were removed from mice 14 days P.I., the iris, ciliary body, lens, conjunctiva, and epithelium were removed and discarded. The stromal layer of the cornea was then stained for OX40L using an Cy3 labeled CD134 fusion protein (as described in the materials and methods) and a FITC labeled antibody to cd11c (A), an alexafluor 488-labeled antibody to MHC class II (B), or a FITC labeled antibody to CD45 (C). OX40L$^+$ cells costained for CD45 but not for cd11c or MHC class II.

To confirm the OX40L staining, the corneas of mice with HSK were tested for OX40L mRNA (figure 10). mRNA for OX40L was reproducibly found in infected corneas, but not in uninfected corneas. The positive control was RNA isolated from OX40L transfected cells.
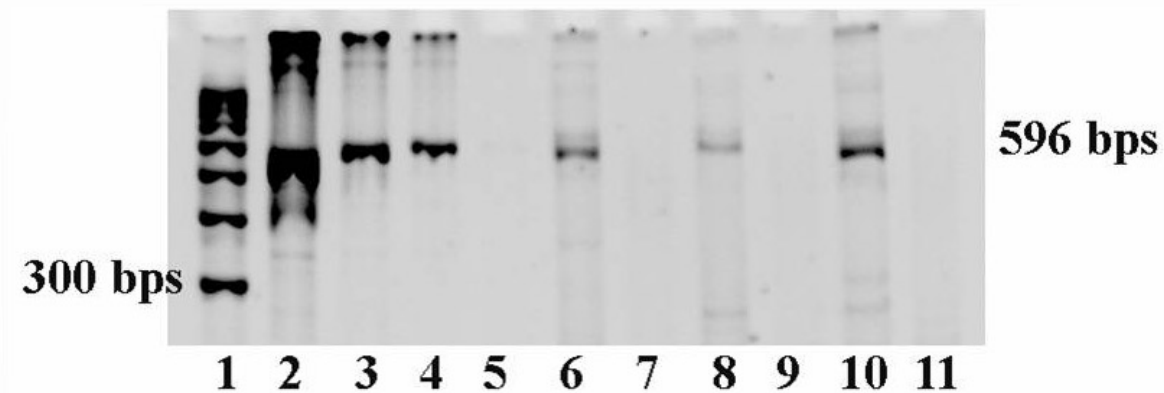
1. 100 bp ladder
2. 5 ul of cDNA from OX40L transfectants
3. 1 ul of cDNA from OX40L transfectants
4. 0.5 ul of cDNA from OX40L transfectants
5. 5 ul from OX40L transfectants –RT
6. D15 P.I. Cornea 1A+ RT
7. D15 P.I cornea 1A – RT
8. D15 P.I. Cornea 1B +RT
9. D15 P.I. Cornea 1B – RT
10. D15 P.I. 2 corneas +RT
11. D15 P.I. 2 corneas – RT

Figure 10: OX40L mRNA is present in corneas with HSK.

BALB/c mice were infected with 10^5 PFU of HSV-1 RE. Corneas were removed from mice 15 days P.I., the iris, ciliary body, lens, conjunctiva, and epithelium were removed and discarded. mRNA was isolated from the stromal layer of the cornea using a Quiagen miniprep kit and then reverse transcribed to cDNA. OX40L specific primers were used to detect OX40L cDNA within those corneal samples. Positive control was mRNA from OX40L transfected cells and negative controls were corneas with no RT. Expected band size for OX40L is 596 bps.

To better identify the percentage of CD4 T cells that express CD134 within the corneas of mice with HSK, corneas were digested with collagenase and stained for CD4 and CD134 (figure 11). Approximately 15% of CD4 T cells in the corneas of mice with HSK stained positive

for CD134. This is consistent with the pattern of immunofluorescence observed in figure 8 and indicates that CD4 T cells in the cornea during HSK express this costimulatory marker.
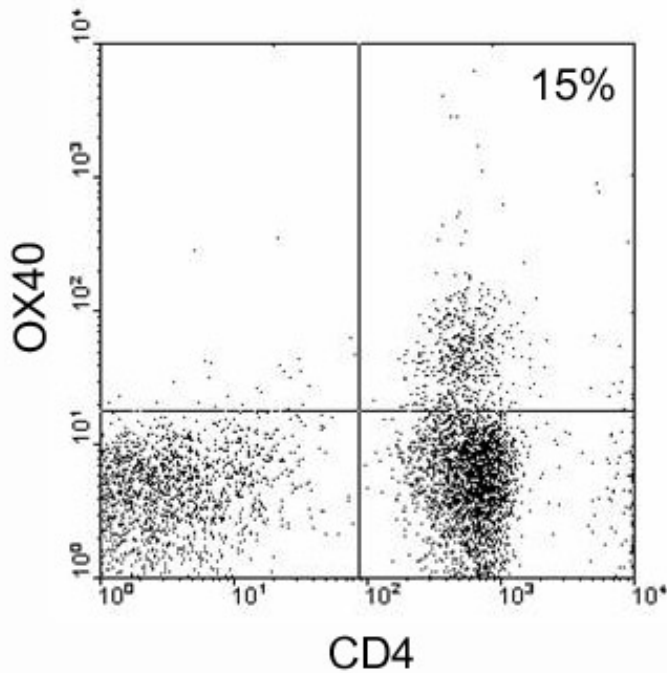
Figure 11: CD4 T cells express CD134 in corneas of mice with HSK.

BALB/c mice were infected with 10^5 PFU of HSV-1 RE. Corneas were removed from mice 14 days P.I., the iris, ciliary body, lens, conjunctiva, and epithelium were removed and discarded. The stromal layer of the cornea was then digested and the resulting single cell suspension was stained with anti-CD4 and anti-CD134 antibodies. We found that 15% of the CD4 T cells within the corneas of mice with HSK express CD134.

4.1.2. Are CD134/OX40L interactions required for HSK?

Given our findings of both CD134 and OX40L expression within corneas with HSK, we next asked whether these interactions were absolutely necessary for HSK development by treating mice with a blocking antibody to OX40L (RM134L). This antibody has shown efficacy in alleviating several different inflammatory diseases such as rheumatoid arthritis and graft versus host disease (122,127). The first set of experiments tested whether CD134/OX40L

interactions are needed during the priming phase of the response by treating mice with 0.5 mg of RM134L intraperitoneally (I.P.) starting one day prior to infection and then again on +1, +3, +5, +7 P.I. (figure 12). This treatment regimen did not affect the incidence or severity of HSK, suggesting CD134/OX40L interactions are dispensable during the priming phase.
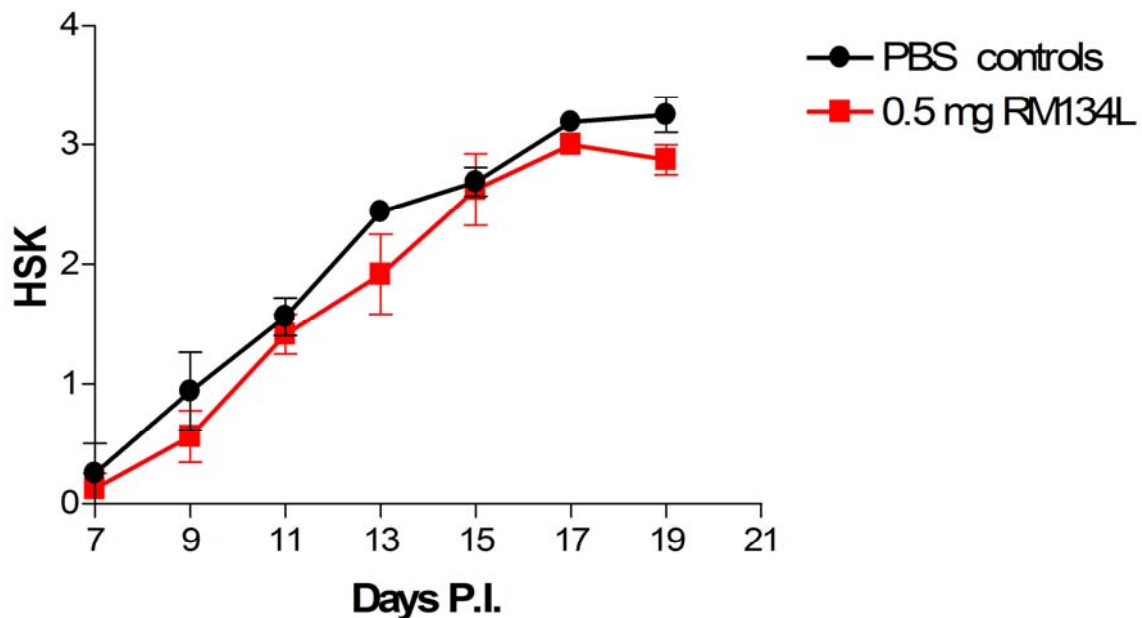
Figure 12: CD134/OX40L interactions are not needed during T cell priming.
BALB/c mice were treated with 0.5 mg of RM134L antibody, an antibody that blocks CD134/OX40L interactions, one day before infection and then on D+1,+3,+5,+7. Mice were infected with 10^5 PFU of HSV-1 RE. Mice were scored for HSK incidence and severity starting on D7 and then every other day thereafter through day 19 P.I. Data are expressed as either the mean ± standard error HSK score of HSK of four mice per group.

The role of CD134/OX40L interactions locally within the cornea was then addressed. We treated BALB/c mice with RM134L locally via subconjunctival injection (figure 13), but found no beneficial effects of treatment on HSK incidence or severity. Blockade of CD134/OX40L interactions using a fusion protein (figure 14) composed of mouse CD134 coupled to mouse Fc (123,126) was also ineffective at reducing HSK incidence or severity.
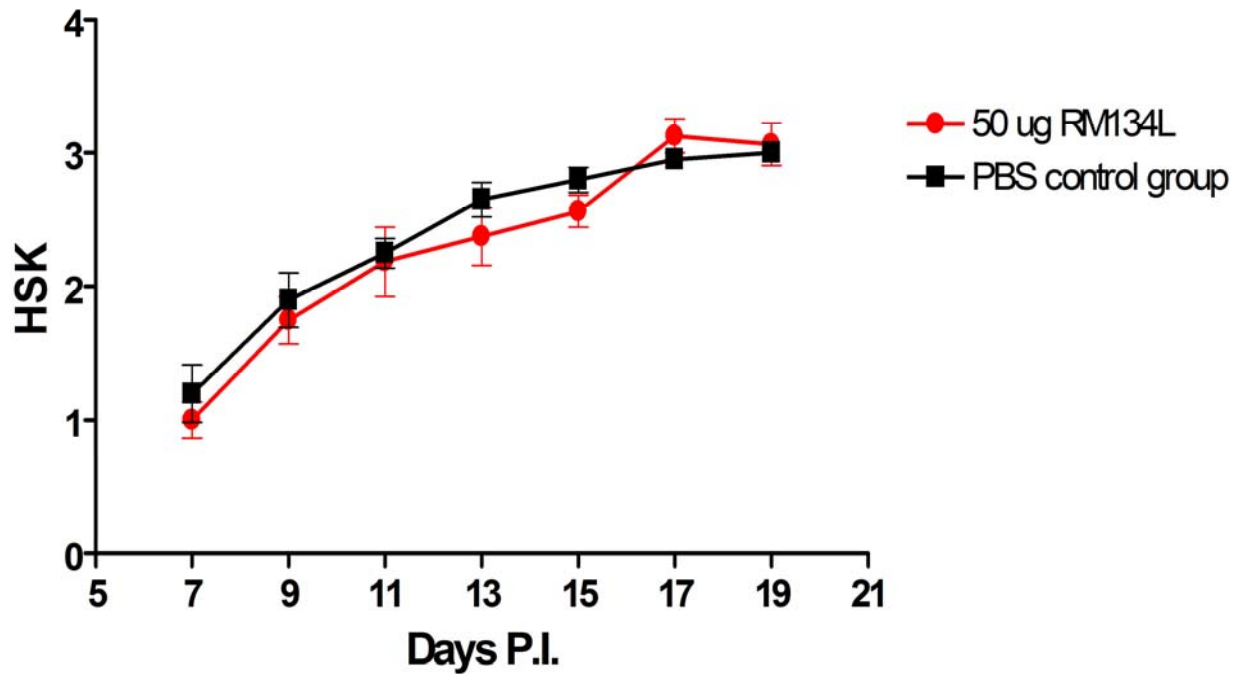
Figure 13: Local blockade of CD134/OX40L interactions with RM134L does not alleviate HSK.

BALB/c mice were infected with 10^5 PFU of HSV-1 RE. Five mice were injected with 50ug of RM134L subconjunctivally starting on day 7 P.I. and then every other day thereafter through D19 P.I. HSK incidence and severity was assessed every other day from D7 through D21. Data are expressed as either the mean ± standard error HSK score of HSK of 5 mice per group.
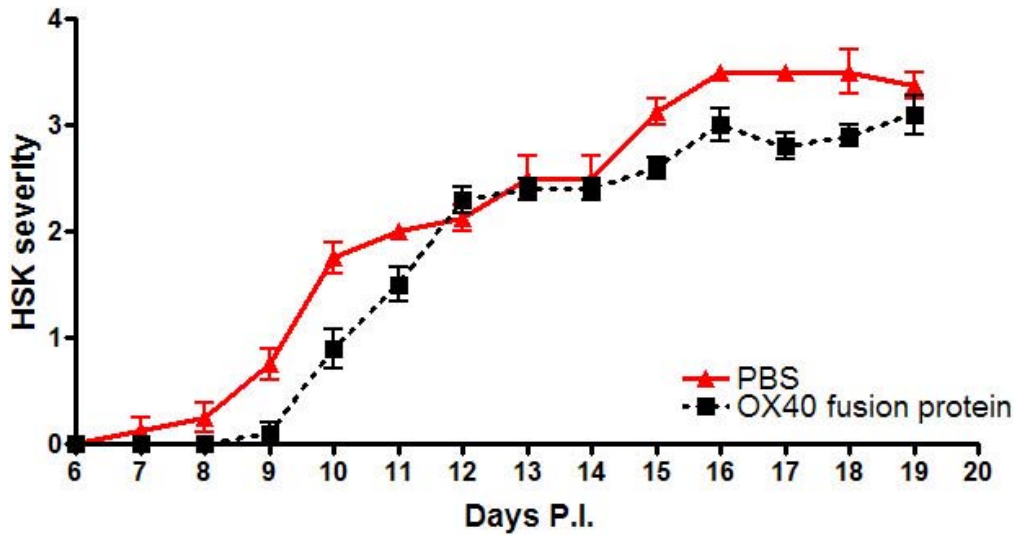
Figure 14: Local blockade of CD134/OX40L interactions with an CD134-fusion protein does not alleviate HSK.

BALB/c mice were infected with 10^5 PFU of HSV-1 RE. Five mice were injected with 10ug of CD134 fusion protein subconjunctivally starting on day +5 P.I. and then every other day thereafter through D19 P.I. Control mice were injected with PBS alone. HSK incidence and severity was assessed every day from D6 through D19. Data are expressed as either the mean ± standard error HSK score of HSK of 5 mice per group.

To confirm that subconjunctival treatment was indeed resulting in deposition of RM134L within the corneal stroma, corneal sections from mice that were injected with RM134L (a rat anti-mouse OX40L antibody) or injected with PBS were stained with a Cy-3 labeled anti-rat antibody. As can be seen in figure 15, the RM134L subconjunctival injections did result in antibody deposition within the cornea. This data provides confirmation that the treatment strategy did result in blocking antibody within the cornea, however CD134:OX40L interactions within the cornea are not needed for HSK.
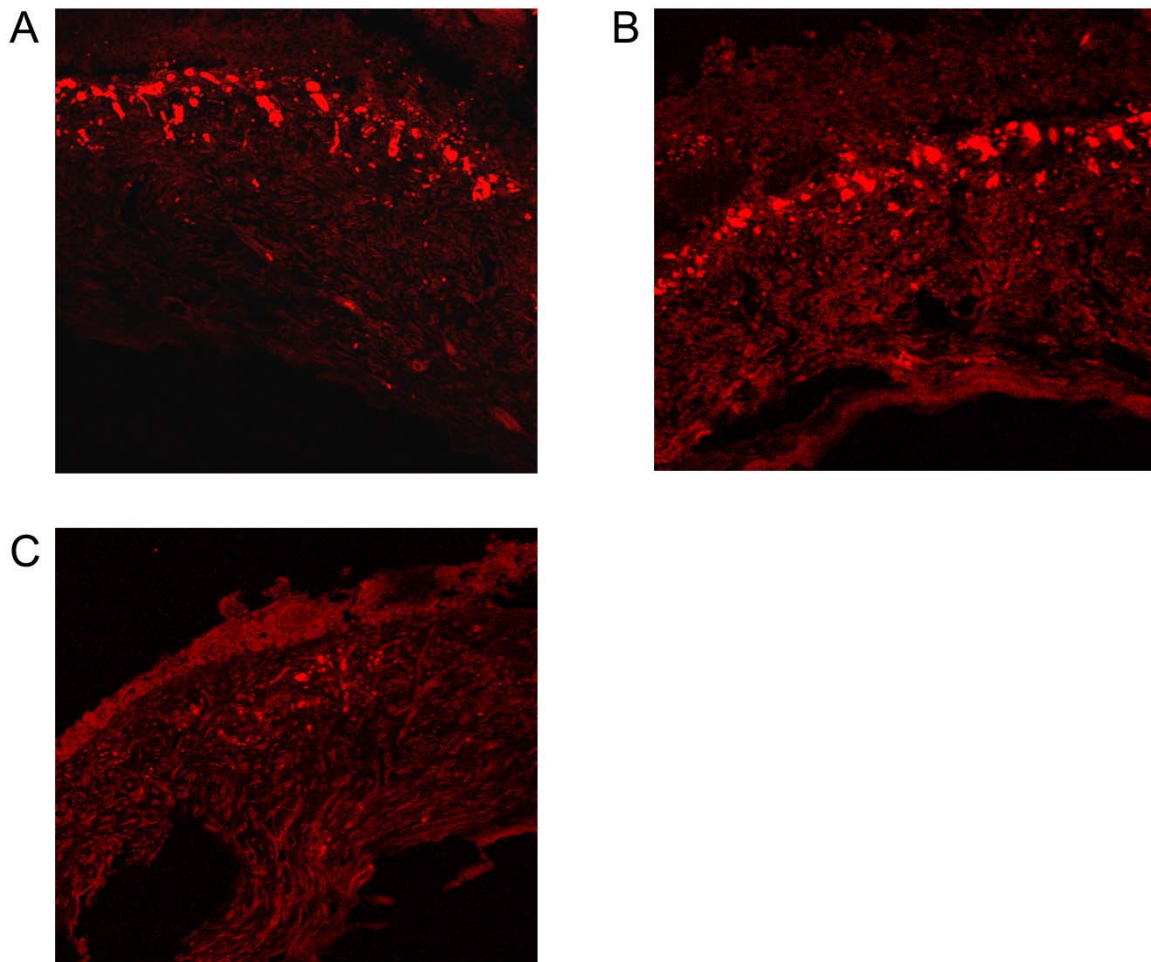
Figure 15: Subconjunctival injection of RM134L results in deposition of antibody with the cornea.

BALB/c mice were infected with 10^5 PFU of HSV-1 RE. Mice were subconjunctivally injected with either RM134L (A,B) or PBS (C) on days 7,9,11,13,15,17,19. On day 19, the eyes were enucleated, embedded in a paraffin block and sections were then stained with an anti-rat antibody that was Alexafluor 546 (red) labeled. RM134L is a rat anti-mouse OX40L antibody. Sections from mice that were injected with RM134L show positive staining with the anti-rat antibody (A,B), while PBS controls showed no positive staining.

The expression pattern of CD134 on CD4 T cells is restricted to later stages of activation, and some reports indicate that CD134/OX40L interactions are involved in CD4 T cell migration (168,169). Based on these findings, mice were treated systemically with RM134L starting on day 5 P.I. and then again on days 6, 7, and 8. This treatment regimen will deliver blocking antibody during the late stages of CD4 T cell activation within the LNs and also at a time when CD4 T cell migration into the cornea would be just starting. This treatment did not result in alleviation

of HSK (figure 16), which suggests CD4 T cells are not using CD134/OX40L to migrate into the cornea to mediate HSK. As a final test for a role for CD134/OX40L interactions in HSK, the infectious dose used for infection was reduced (based on our findings in section 4.3) and mice were treated starting just before onset of disease on day 7 and then throughout to peak disease at D+14. In one experiment, a dramatic decrease in the incidence of HSK (figure 17A) was observed in RM134L treated mice, however this effect was not reproducible (figure 17B).
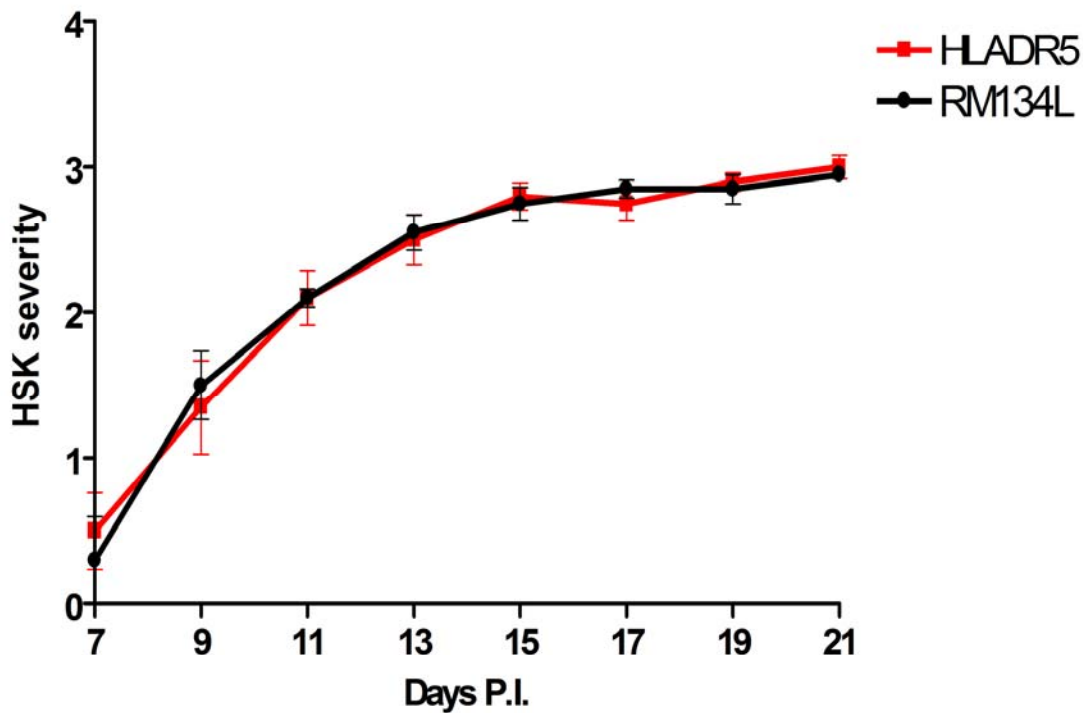
Figure 16: Treating with RM134L on days 5,6,7,8 P.I. does not alleviate HSK.

BALB/c mice were infected with 10^5 PFU of HSV-1 RE. Five mice were treated with either 0.5 mg of RM134L I.P. or 0.5 mg of a control antibody (HLA-DR5) on days +5,+6,+7,+8 P.I. Mice were monitored for HSK starting on D+7 and then every other day through D+21. RM134L treatment did not affect incidence or severity of disease in these mice. Data are expressed as either the mean ± standard error HSK score of HSK of five mice per group.
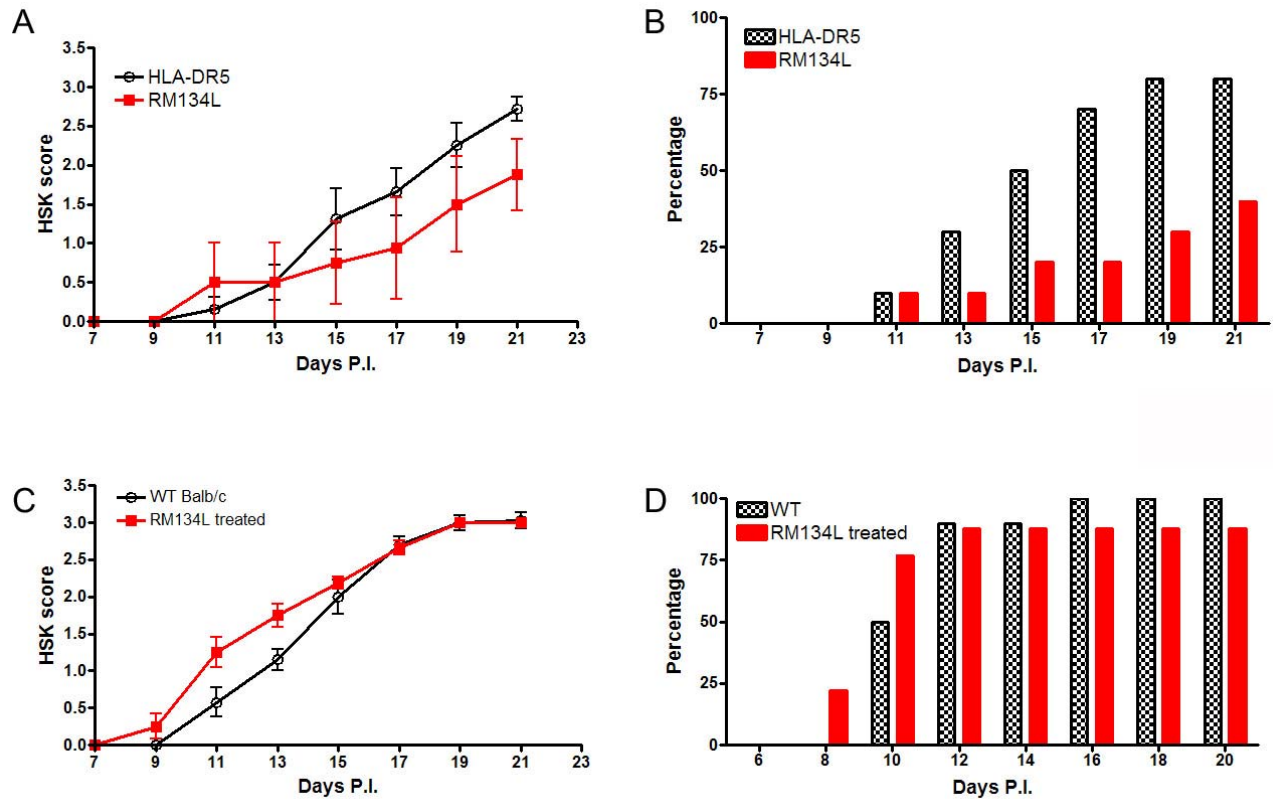
Figure 17: Blockade of CD134/OX40L interactions after low dose HSV-1 infection in BALB/c mice does not reproducibly alleviate HSK.

Mice were ocularly infected with 10^3 PFU of HSV-1 RE. Mice were systemically treated with 0.5 mg of RM134L or control antibody (A,B) or were left untreated (C,D) by I.P. injection on days 7, 9, 11, 13, 15 P.I. Data in A and C are shown only for those mice that developed HSK. Data are expressed as either the mean ± standard error HSK score (A,C) or incidence of HSK (B,D) of ten mice per group.

A potential concern with the inability to block HSK using RM134L is that the antibody may not be functional. To confirm that this antibody is indeed functional, cells transfected to express OX40L were pre-incubated with the RM134L that was used for all in vivo blocking experiments or with an isotype matched control antibody and then stained with a commercially available antibody to OX40L. This experiment (figure 18) showed that pretreatment with RM134L (used in all of the in vivo blocking experiments) inhibited binding of the commercially available anti-OX40L antibody and confirms that the preparation of RM134L used in our studies is functional.
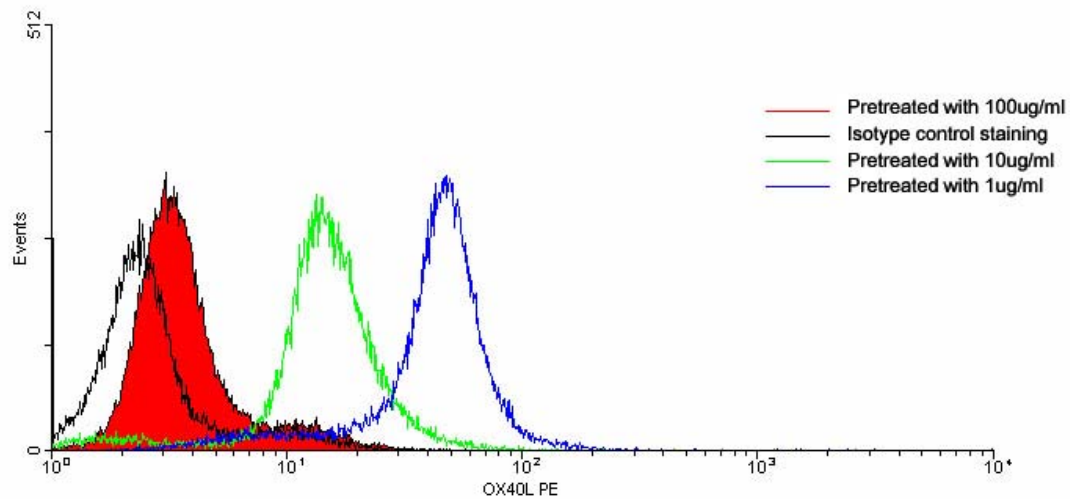
Figure 18: The RM134L antibody used for in vivo blocking experiments is functional.

OX40L expressing L5178Y cells were pretreated with differing concentrations of RM134L antibody used for in vivo blocking experiments for 30 minutes on ice and then stained with an anti-OX40L antibody.

The overall conclusion from these studies is that CD134/OX40L interactions are not required for HSK development in BALB/c mice.

4.2.   What is the antigen specificity of CD4 T cells within the corneas of mice with HSK?

As described, numerous studies have concluded that CD4 T cells are responsible for HSK. There is however some dissention as to the mechanism by which these CD4 T cell mediate disease. HSK has been described as an autoimmune disease mediated through molecular mimicry (170), while others argue that HSK is mediated by bystander activation (171) of CD4 T cells. Our hypothesis is that virus specific CD4 T cells initiate HSK, while bystander activated cells propagate the disease once it has begun. This hypothesis is supported by the findings in humans that virus specific T cells can be expanded from human corneas that have been removed due to HSK (128-130). To test our hypothesis that virus specific CD4 T cells play a necessary role in the initiation of HSK, we began by generating and characterizing a CD4 T cell line from

the corneas of BALB/c mice with HSK. This cell line allowed us to directly test whether virus specific CD4 T cells could mediate HSK.

4.2.1. Corneal cell line from mice with HSK exhibits viral reactivity

Thirty corneas were removed from BALB/c mice that had HSK at D11 P.I. CD4 T cells were purified from the corneas and grown in culture for several weeks to establish a cell line designated THSK3.30. Viral specificity of the T cell line was assessed by stimulating that cell line with UV-inactivated HSV-1 RE in an ELISA. Figure 19 clearly shows that the cell line contains virus specific cells.

THSK 3.30 cell line
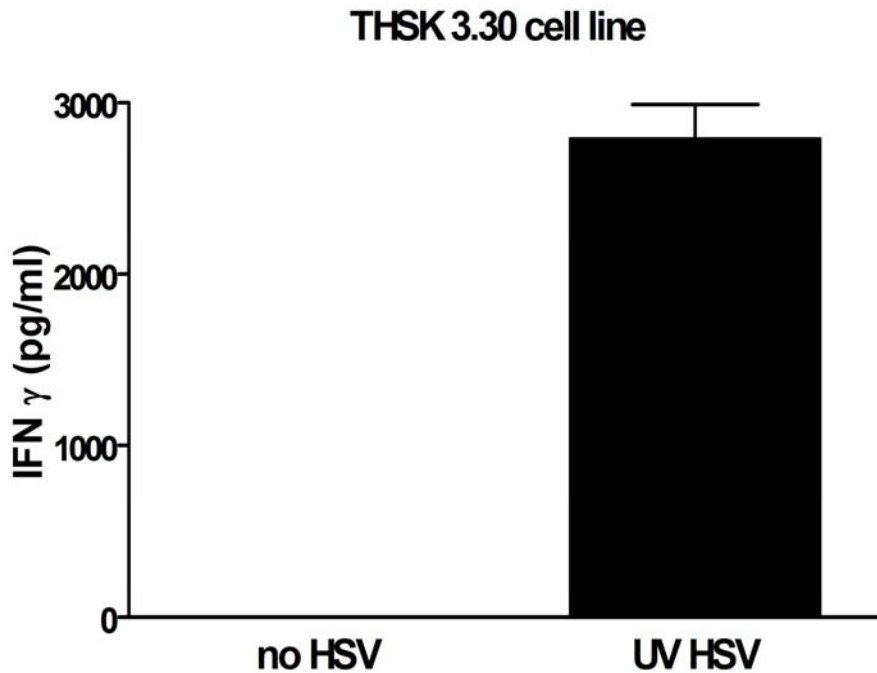
Figure 19: A CD4 T cell line grown out of corneas with HSK is virus reactive.

BALB/c mice were infected with 10^5 PFU of HSV-1 RE. CD4 T cells were purified from corneas of mice with HSK at D+11 P.I. (as described in the Material and Methods) and were cultured until a stable cell line was established. This cell line was stimulated with UV-inactivated HSV pulsed DC (UV HSV) or unpulsed DC (no HSV) for 72 hrs and supernatants were collected and assayed for IFN-y by standard ELISA.

4.2.2. CD4 T cell clones were generated from the THSK3.30 cell line

To better characterize the role of virus specific CD4 T cells in HSK, two sets of T cell clones (figures 20 and 21) were generated from the THSK3.30 cell line by limiting dilution as described in the materials and methods. Some of the T cell clones generated from the cell line showed high viral reactivity as defined by IFN-γ production in a standard ELISA. It is of note that some of the T cell clones generated from THSK3.30 showed very little virus specificity while others produced very large amounts of IFN-γ.
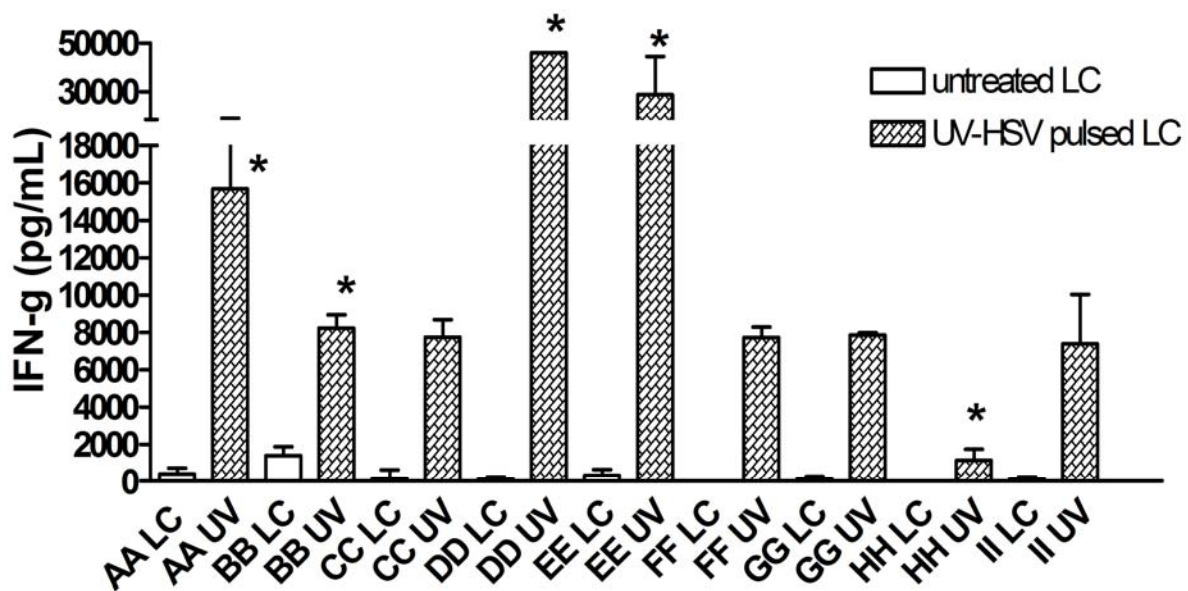
Figure 20: T cell clones generated from the THSK3.30 cell line are virus specific and produce IFN-γ.

Individual clones (AA through II) were stimulated with UV inactivated HSV pulsed Langerhans cells (UV) or with unpulsed control Langerhans cells (LC) for 72 hrs and then culture supernatants were collected and assayed for IFN-γ by standard ELISA. Clones that were chosen for further study are marked with an asterisk.
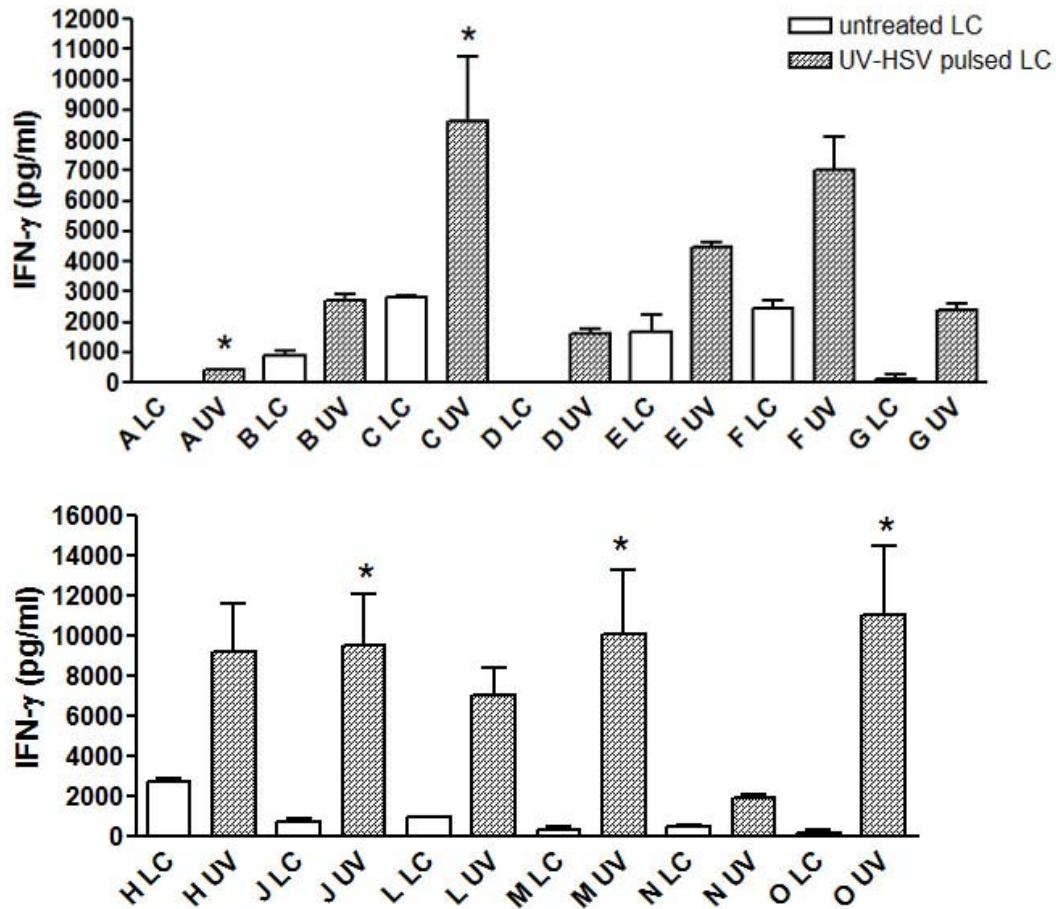
Figure 21: T cell clones generated from the THSK3.30 cell line are virus specific and produce IFN-γ.

Individual clones were stimulated with UV inactivated HSV pulsed Langerhans cells (UV) or with unpulsed control Langerhans cells (LC) for 72 hrs and then culture supernatants were collected and assayed for IFN-γ by standard ELISA. Clones that were chosen for further study are marked with an asterisk.

Five clones from each group were chosen for further study; from clones group one we chose AA, BB, DD, EE, HH and from clones group two we chose A, C, J, M, O. Clones A and HH were chosen as negative controls for future experiments since they exhibited low viral reactivity. These findings are very similar to those in humans in which virus specific CD4 T cells can be grown out of human corneas with HSK (128,129,172).

4.2.3. What class of viral proteins are recognized by the clones?

To better understand the antigen specificity of the T cell clones, cell lysates were generated from infected Vero cells. The time of infection was varied with the goal of stopping viral replication at different times post infection thus taking advantage of the sequential nature of gene expression of HSV-1. Figure 22 gives a depiction of the different time point lysates and what class of viral genes would be expected to be highest at that time.
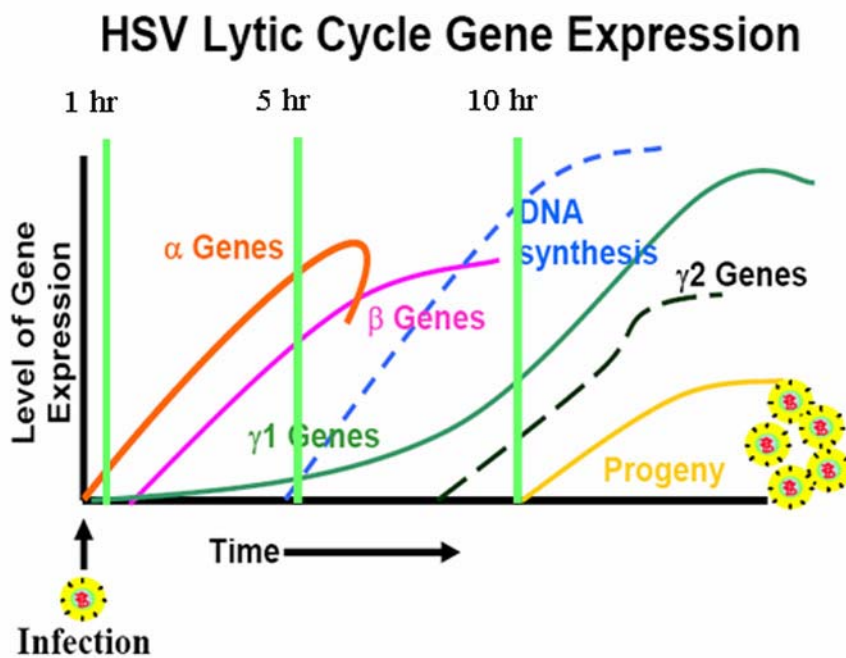
Figure 22: Viral lysate generation for gene class expression study.

Green bars designate the different time points of viral cell lysates that we generated for initial identification of the antigen specificity of the T cell clones.

Extracts obtained at the different time points (1, 5, and 10 hrs) were used determine the antigen specificity of the different T cell clones. The results shown in figure 23 suggest the CD4 T cell clones recognize an early or late protein since they responded best to the 5 and 10 hour lysates. This would be consistent with the findings of several groups that reported CD4 T cells in

mice recognize gD (173,174). This data is challenging to interpret due to the large background production of IFN-γ observed when stimulating the T cell clones with control uninfected lysates, however the general trend, especially with clone O, is that the clones respond best to late time point lysates suggesting specificity for an early or late viral protein (figure 23) .
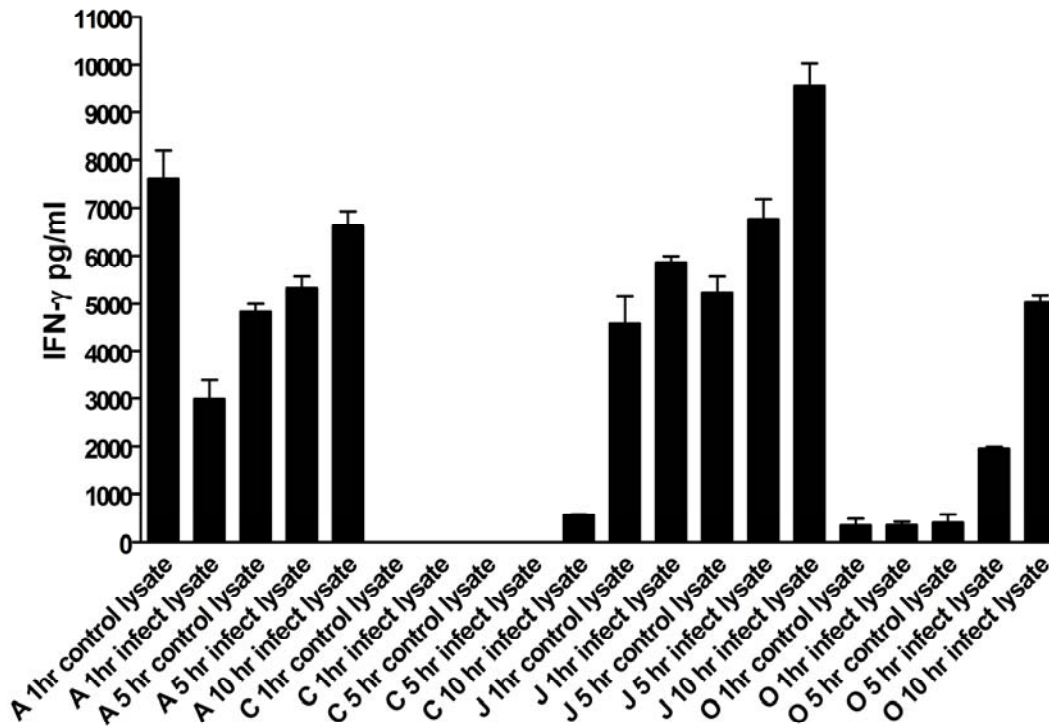
Figure 23: CD4 T cell clones produce IFN-γ in response to early/late proteins.

10^5 of each clone was incubated with $0.2X10^5$ viral-antigen loaded LCs (labeled as 1 hr, 5hr, or 10 hr infect lysate) or with control lysate loaded LCs (labeled as 1hr, 5hr, or 10hr control lysate) that were prepared the day before as described in the materials and methods. The cells were stimulated for 72 hrs and culture supernatants were collected and assayed for IFN-γ by standard ELISA.

4.2.4.　　T cell Receptor β chain usage of the clones

Studies in both mice and humans have reported a skewing of the T cell receptor β chains in HSK lesions (172,175-178). The Vβ TCR expression of the CD4 T cell clones was tested and all of the clones expressed Vβ 8.3 (data not shown). To identify if this skewing of Vβ T cell receptor usage is observed in the corneas of mice with HSK, we stained for Vβ 8.3 and Vβ8.1.2

on CD4 T cells directly out of the corneas of mice with HSK (figure 24). The Vβ8.3 usage of corneal CD4$^+$ T cells cells (11-12%) was not significantly different from that of CD4$^+$ T cells from the LNs of naïve BALB/c mice (figure 25) suggesting that there is not a particular skewing towards Vβ 8.3 within the cornea. This was surprising given the dramatic skewing of the clones and may reflect selective outgrowth of select Vβ expressing CD4 T cells during the generation of the cell line or clones. Alternatively, Vβ expression on CD4 T cells was not tested on day 11 P.I. corneas with HSK, which was the time P.I. at which the THSK3.30 cell line was generated. It is conceivable that Vβ 8.3 cells predominate the corneas early in HSK and therefore the skewing observed in the T cell clones reflects this initial preponderance of Vβ 8.3 cells in the corneas at D+11 P.I.
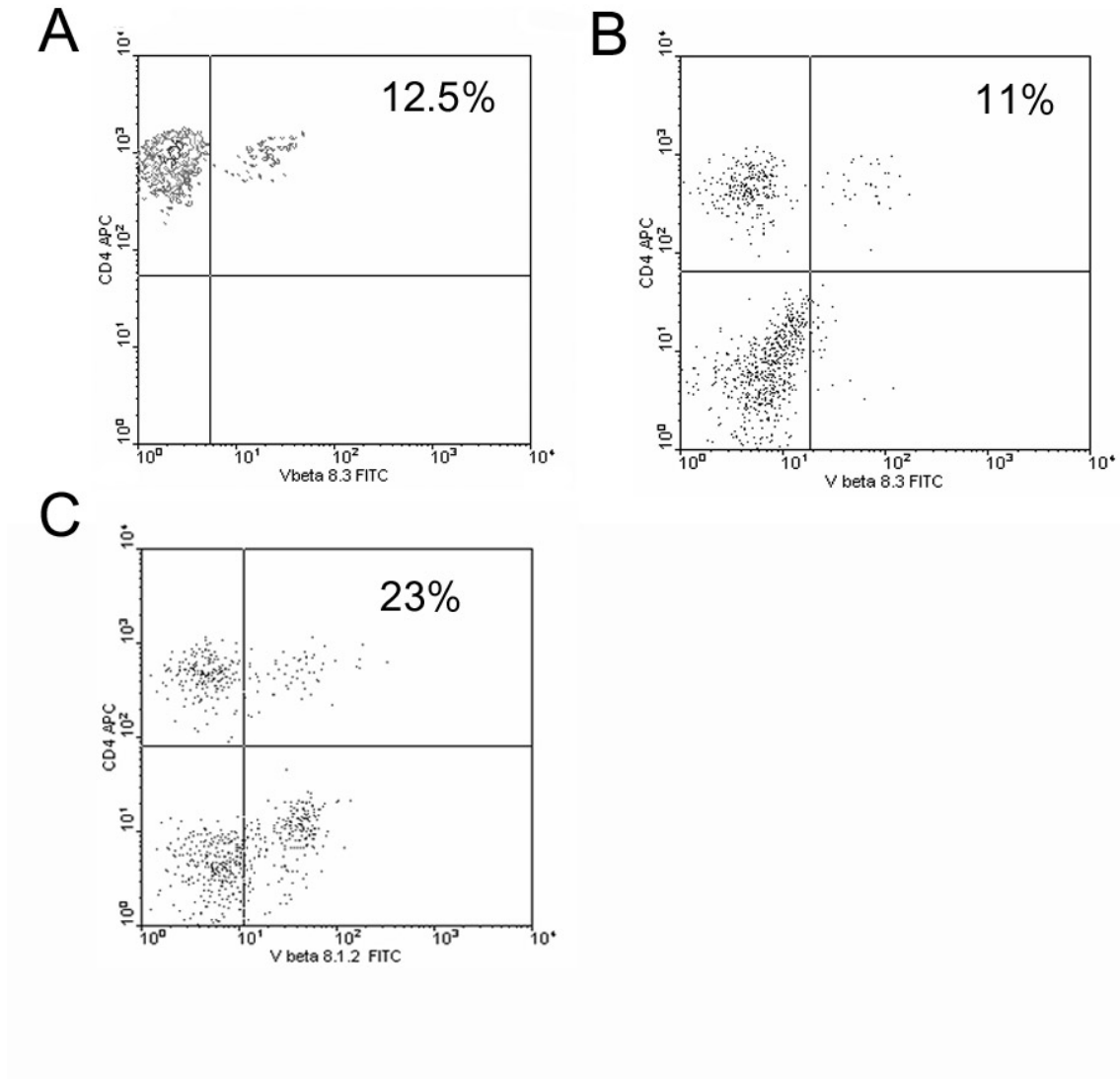
Figure 24: 12% of CD4 T cells in corneas with HSK express Vβ 8.3.

BALB/c mice were infected with 10^5 PFU of HSV-1 RE. Corneas were removed from mice 14 days P.I. (A) or 24 days P.I. (B), (C) and the iris, ciliary body, lens, conjunctiva, and epithelium were removed and discarded. The stromal layer of the cornea was then digested and the resulting single cell suspension was stained with anti-CD4 and anti-Vβ 8.3 antibodies (A,B) or with anti-Vβ 8.1.2 (C) antibodies. The percentage in the upper right hand quandrant is the percentage of CD4 T cells that stained positive for either Vβ 8.3 or Vβ 8.1.2.
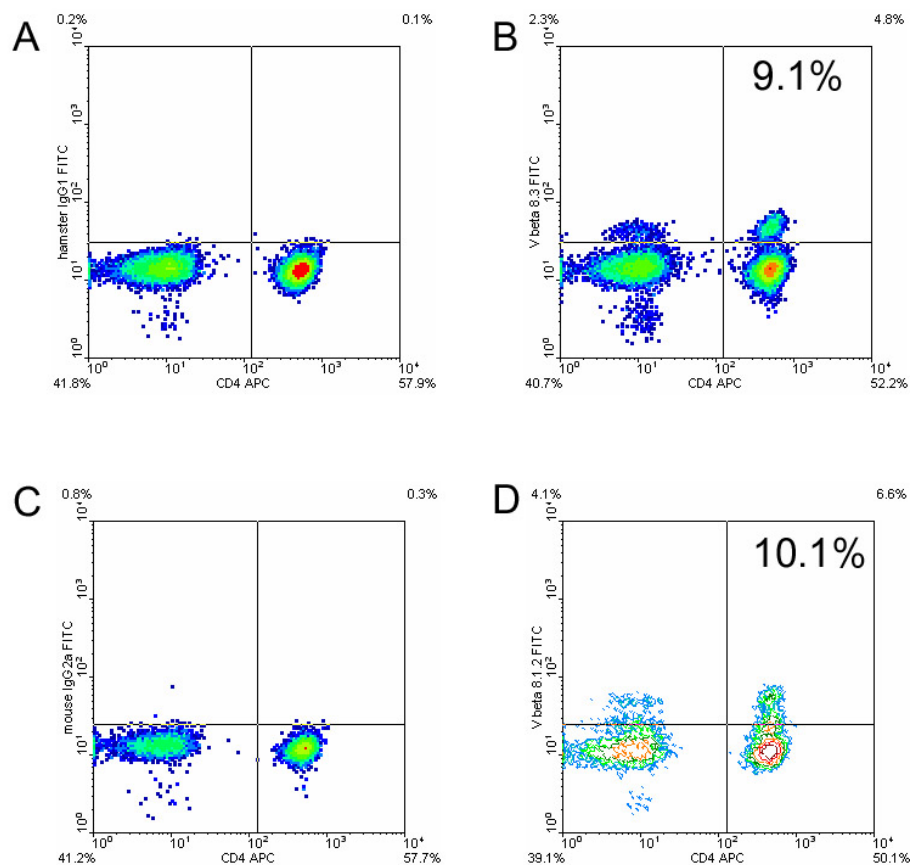
Figure 25: Vβ expression on CD4 T cells in naïve BALB/c mice LNs.

WT naïve BALB/c mice were sacrificed and all LNs in the neck were removed and stained for CD4 and Vβ 8.3 (B) or Vβ 8.1.2 (D). Appropriate controls for each Vβ antibody (hamster IgG1 for Vβ 8.3 and mouse IgG2a for Vβ 8.1.2) are shown in (A) and (B). Percentages in the upper left quadrant are the percentages of CD4 T cells expressing that particular Vβ chain of the T cell receptor.

4.2.5.   Clone AA can induce HSK, provide protection from encephalitis, and reduce skin disease in HSV-1 infected nude mice

Based on the findings that the CD4 T cell clones are virus specific, one might predict that these cells could induce HSK in mice. Nude mice provide a working model to test this hypothesis. These mice are normally resistant to HSK (79) but when immune T cells are adoptively transferred into nude mice they develop corneal disease (101) . Clone AA was chosen for adoptive transfer studies based on its high production of IFN-γ in response to viral stimulation. This CD4 T cell clone was injected into nude mice 6 days P.I. via tail vein injection

(figure 26). Adoptive transfer of this clone resulted in HSK in some mice and protection from periocular skin disease. The protection from skin disease is consistent with the proper migration of the CD4 T cells into the skin around the eye where production of IFN-γ has been shown to be protective (104). Interestingly, nude mice adoptively transferred with clone AA exhibited increased survival compared to RPMI injected mice and mice that were transferred with bulk CD4 T cells from the DLNs (figure 26C).
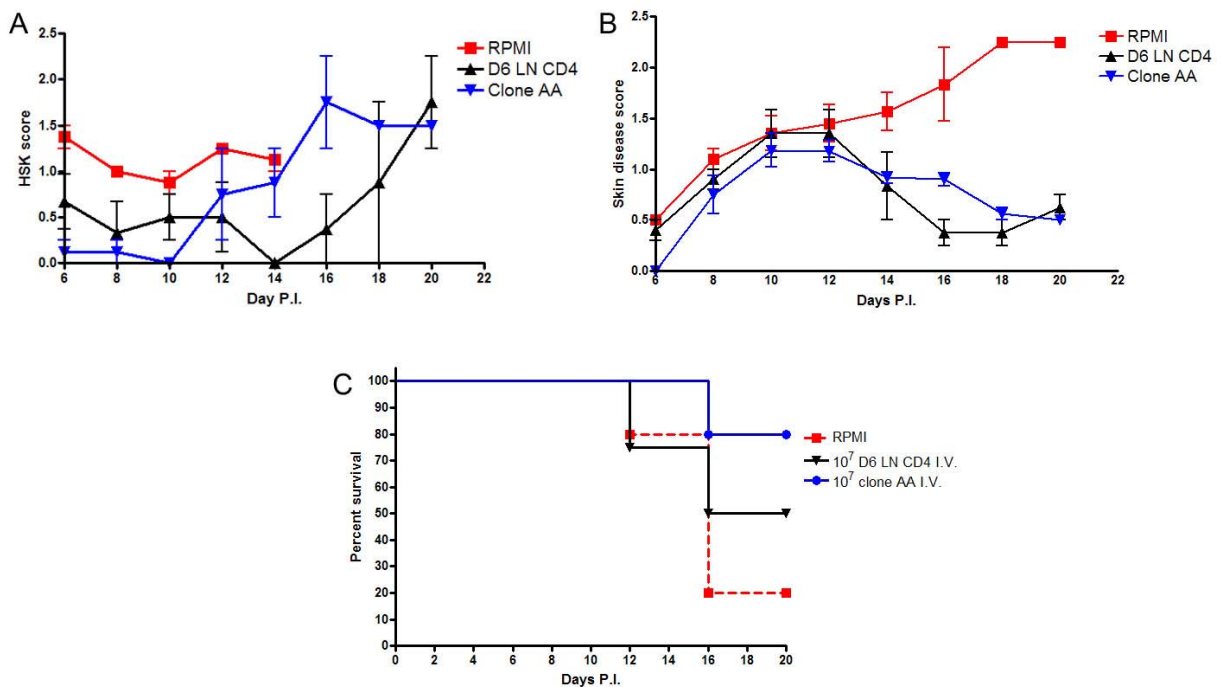
Figure 26: Adoptive transfer of CD4 T cell clone AA induces HSK in nude mice.

BALB/c nude mice were infected with 10^5 PFU of HSV-1 RE. On day 6 P.I., 10^7 cells of clone AA or 10^7 CD4 T cells from the DLNs of D6 infected BALB/c mice were transferred via tail vein injection into those infected nude mice. As a negative control, some mice were injected with RPMI alone. We monitored HSK incidence and severity (A), periocular skin disease (B), and survival of the mice (C) through day 20. Data are expressed as the mean ± standard error HSK score of HSK (A), mean± standard error periocular skin disease score (B) or survival (C).

Proper migration of the adoptively transferred cells was confirmed by removing both the TGs and corneas of nude mice that received an adoptive transfer and staining for CD4 T cells (figure 27). There is some evidence that CD4 T cells play a direct role in the elimination of virus

(88,89). This data showed efficient migration into both the TG and cornea of nude mice adoptively transferred with clone AA (figure 27). It was interesting to note that CD4 T cells could be recovered from the TGs of mice adoptively transferred with either clone AA or with bulk D+6 DLN CD4 T cells, however the protective effect of those cells on the survival of the nude mice was most apparent with clone AA (figure 26C).
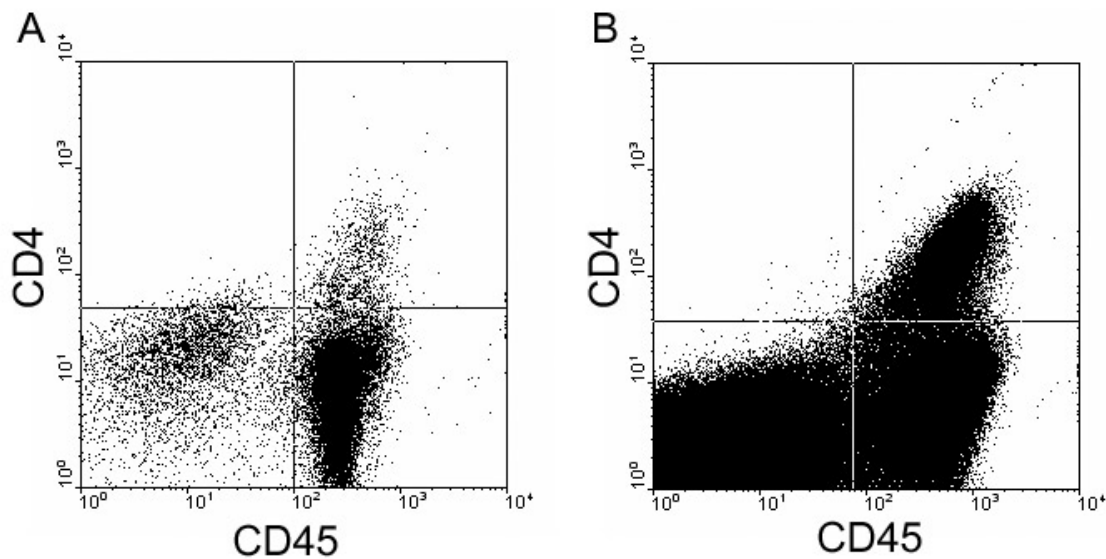
Figure 27: Adoptively transferred clone AA migrates into the cornea and TG of nude mice
One nude mouse that had received an adoptive transfer of clone AA on day +6 P.I. was sacrificed on D+16 P.I. and the cornea (A) and TG (B) of this mouse was digested with collagenase and stained for CD45 and CD4.

These results show that virus specific CD4 T cells isolated from the corneas of mice with active HSK can induce HSK in the normally HSK resistant nude mouse. This is strikingly similar to numerous studies in humans in which virus specific CD4 T cells can be recovered from corneas with HSK and therefore validate our hypothesis that virus specific CD4 T cells can

mediate HSK in our mouse model. The relative role of other CD4 T cells such as bystander activated cells and autoreactive cells is still not fully understood.

4.2.6. What role do virus non-specific CD4 T cells (bystander activated cells) play in our model of HSK?

The hypothesis that HSK occurs due to a bystander activated "cytokine storm" has been proposed. In support of this model, transgenic T cell receptor mice that are incapable of recognizing viral antigens or corneal antigens for that matter, still develop HSK (81,134,171,179,180). Our hypothesis is that virus specific CD4 T cells initiate HSK, which then produce inflammatory chemokines/cytokines that recruit/activate virus non-specific (bystander) cells to propagate the disease. We tested whether the bystander activated cells that may contribute to HSK require costimulation via CD40/CD154 interactions. To this end we utilized DO11.10$^+$ mice that had been backcrossed onto CD154 KO mice. CD4 T cells in DO11.10$^+$ mice express a transgenic TCR specific for ovalbumin. These mice provide a good model to address what role the bystander CD4 T cells play in HSK initiation or progression. Previous work has shown that DO11.10$^+$ mice develop HSK with similar kinetics to WT mice (81) as do CD154 deficient mice (113), therefore any reduction in HSK severity or kinetics would be due to the costimulatory blockade of bystander CD4 T cells. To determine whether bystander activation of CD4$^+$ T cells in corneas with HSK require CD40 costimulation, wild type and CD154 KO DO11.10$^+$ BALB/c mice were infected. We found that DO11.10$^+$ CD154 KO mice consistently exhibited delayed HSK kinetics compared to WT mice (figure 28A), suggesting bystander activated CD4 T cells are dependent on CD40/CD154 costimulation to mediate HSK.

To confirm that the reduced kinetics of disease observed in DO11.10$^+$ CD154 KO mice was not due to lack of CD154 costimulation, we compared CD154 KO mice to CD154 KO

DO11.10[+] mice and again observed a reduction in the kinetics of HSK in the DO11.10[+] CD154 KO mice (figure 28B and C). This finding strongly suggests that bystander cells require stimulation through CD40/CD154 to mediate HSK. An additional control would be to address whether intact DO11.10[+] mice also show reduced HSK compared to WT. Indeed we found that DO11.10[+] mice exhibited decreased kinetics of disease compared to WT mice, suggesting the decrease in HSK severity in CD154 KO DO11.10[+] mice (Figures 28 A-C) is most likely a result of decreased numbers of viral antigen specific CD4 T cells in those mice. This is contradictory to previous work that reported DO11.10[+] mice develop HSK with identical kinetics to WT BALB/c mice, but is consistent with our hypothesis that virus specific CD4 T cells initiate HSK. Since DO11.10 mice contain fewer potentially HSV reactive naïve CD4 T cells, it is not surprising that the kinetics of HSK is delayed in these mice.
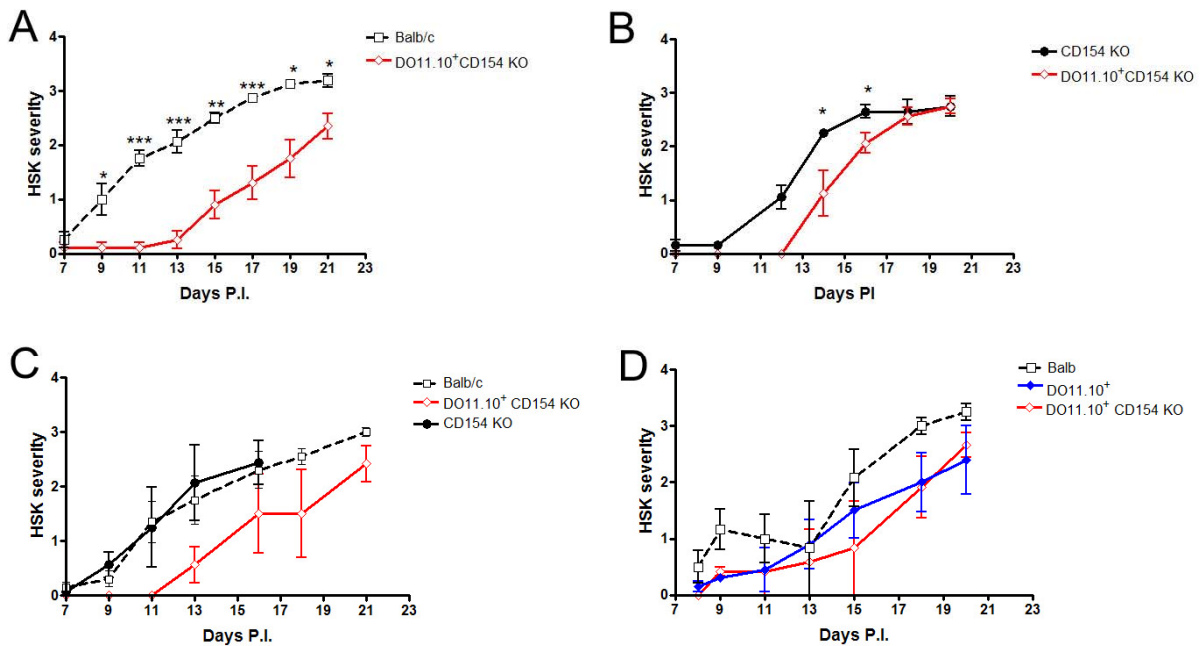
Figure 28: HSK kinetics and severity in BALB/c, DO11.10[+] BALB/c, CD154 KO BALB/c, and DO11.10[+] CD154 KO BALB/c mice.

Groups of animals were infected with $1X10^5$ PFU of HSV-1 RE and monitored for HSK severity and incidence through day 21 P.I. Data are represented as mean±SEM HSK score.

The ability of transgenic CD4 T cells (expressing a TCR that is incapable of recognizing viral antigens) to infiltrate the corneas of DO11.10[+] CD154 KO mice with HSK was then tested (Figure 29). Corneas were removed from DO11.10[+] CD154 KO mice at D21 P.I., digested with collagenase, and then stained for CD45, CD4 and the clonotypic TCR using a KJ1-26 antibody. KJ[+] CD4 T cells were found in the eyes of the DO11.10[+] CD154 KO as shown in Figure 29 and is consistent with recent studies (81,134). This data suggests that CD4 T cells that are incapable of recognizing viral antigens migrate into the corneas of DO11.10[+] CD154 KO mice where they may contribute to HSK.
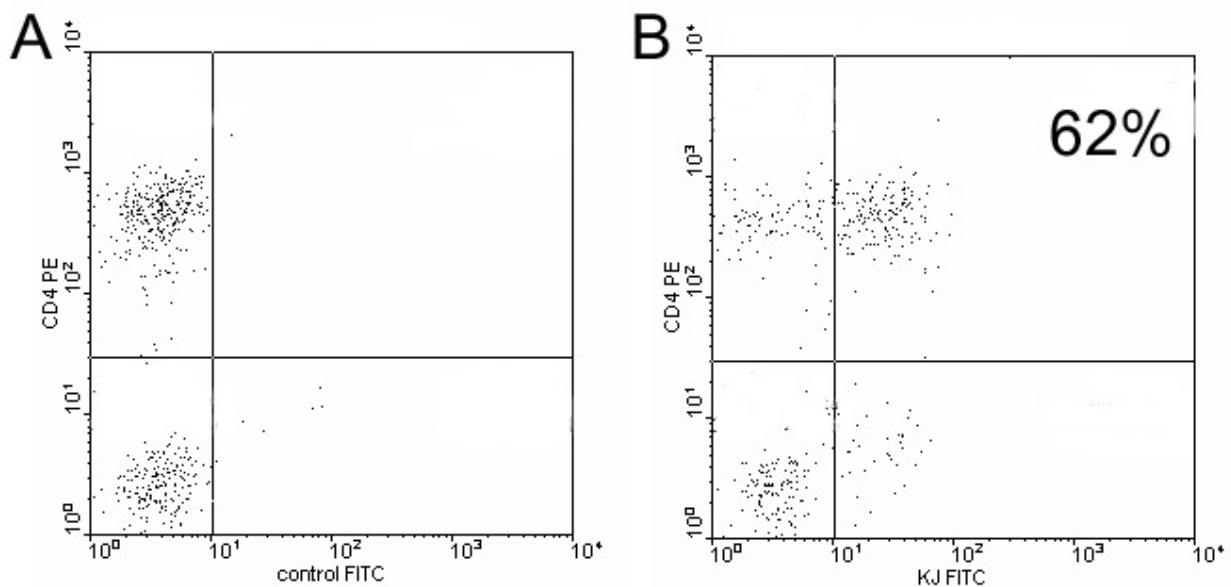
Figure 29: KJ[+] CD4 T cells can be recovered from the corneas of DO11.10[+] CD154 KO mice with HSK.

DO11.10[+] CD154 KO mice were infected with 10^5 PFU of HSV-1 RE. Corneas were removed from mice 21 days P.I. and the iris, ciliary body, lens, conjunctiva, and epithelium were removed and discarded. The stromal layer of the cornea was then digested and the resulting single cell suspension was stained with anti-CD4 and anti-KJ1.26 antibodies. The percentage in the upper right hand quandrant is the percentage of CD4 T cells that stained positive for the clonotypic TCR.

77

The activation status of the bystander CD4 T cells (KJ$^+$) present in the corneas of transgenic mice was then determined. A large proportion of the CD4 T cells expressing the clonotypic TCR also expressed the activation marker CD69 in the corneas of DO11.10$^+$ CD154 KO (figure 30). We found that 44% of all the CD4 T cells present in the corneas of DO11.10$^+$ CD154 KO mice with HSK were positive for both KJ and for CD69. This shows that bystander activated CD4 T cells can infiltrate the corneas of DO11.10$^+$ CD154 KO mice and become activated presumably via inflammatory cytokines. These activated bystander CD4 T cells may be capable of producing inflammatory cytokine such as IL-2 and IFN-γ that contribute to HSK severity and progression (104).
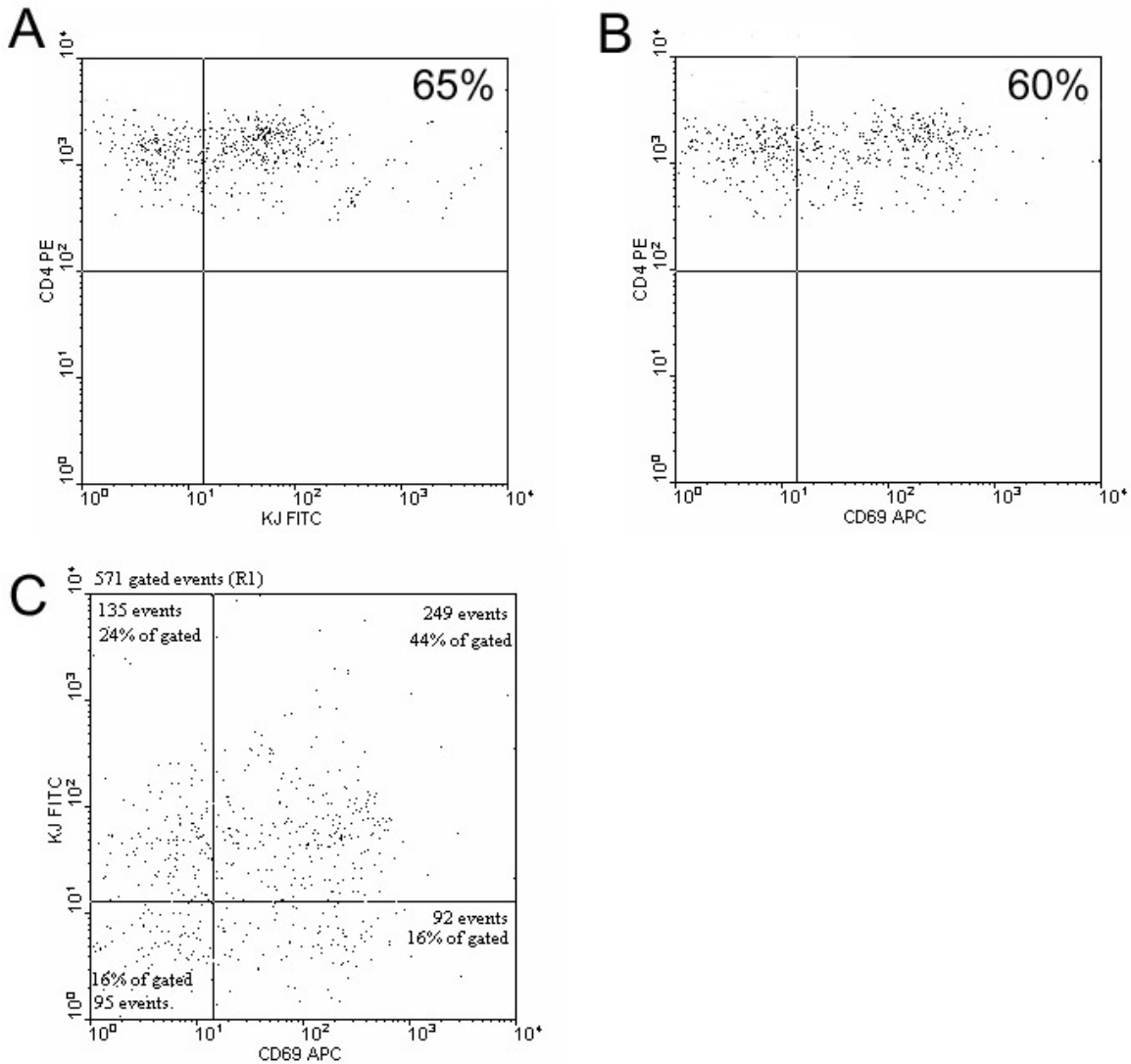
Figure 30: KJ[+] CD4 T cells present in the corneas of DO11.10[+] CD154 KO mice at D22 P.I. are activated.

DO11.10 CD40L KO mice were infected with 10[5] PFU of HSV-1 RE. On day 22 P.I., Corneas were removed from mice and the iris, ciliary body, lens, conjunctiva, and epithelium were removed and discarded. The stromal layer of the cornea was then digested and the resulting single cell suspension was stained with anti-CD4, anti-KJ1.26, and anti-CD69 antibodies. The percentage in the upper right hand quadrant is the percentage of CD4 T cells that stained positive for the clonotypic TCR (A), or for CD69 (B). In (C), the data shows CD69 and KJ expression on all of the gated CD4 T cells in the cornea.

Studies were then performed to test whether the delay in HSK kinetics observed in CD40L KO DO11.10 mice is due to delayed generation of viral specific CD4 T cells in the

DLNs of the DO11.10 CD40L KO mice. Draining lymph nodes were removed from WT and DO11.10 CD40L KO mice on days 5, 7, 9 P.I., CD4 T cells were purified and were then stimulated with DCs and UV-inactivated HSV for 3 days. At the end of the three days supernatants were assayed for IFN-γ (figure 31). At all time points analyzed, CD4 T cells from the DLNs produced contained significantly fewer virus specific CD4 T cells in the CD40L KO DO11.10 mice.
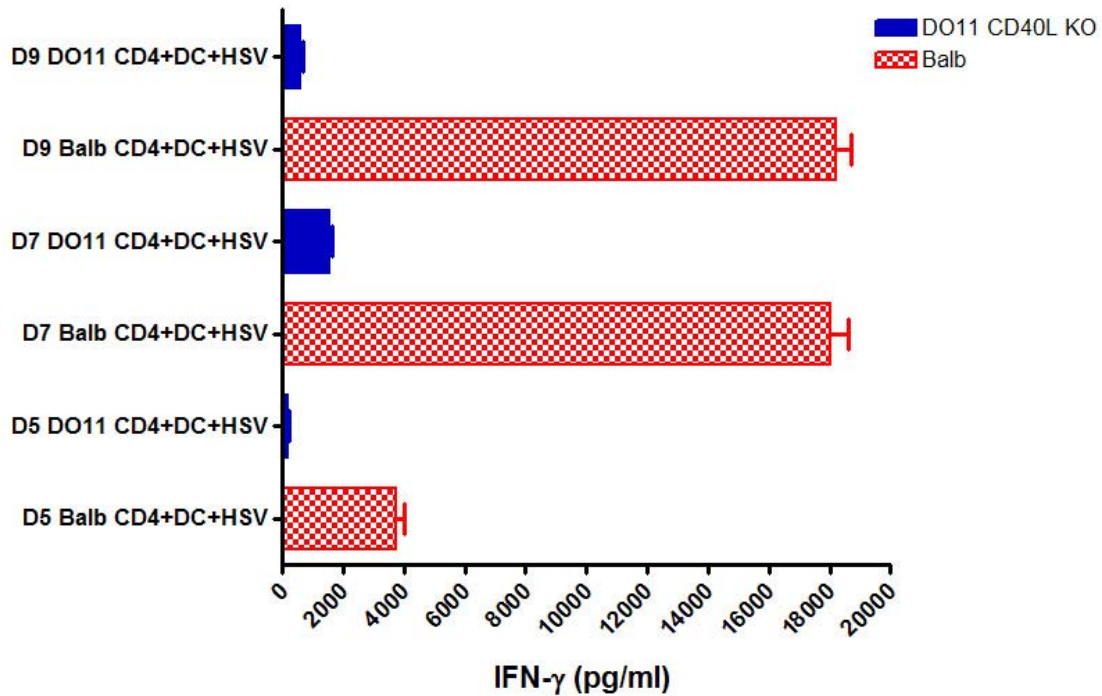
Figure 31: DO11.10$^+$ CD154 show reduced generation of virus specific CD4 T cells in the DLNs at Days 5, 7, and 9 P.I.

BALB/c and DO11.10 CD40L KO mice were infected with 10^5 PFU HSV-1 RE. On days 5, 7 and 9, the entire set of DLNs from either WT or DO11.10 mice were removed, counted and then both cd11c$^+$ and CD4$^+$ cells were MACS purified. 5×10^5 CD4 T cells were combined with 2.5×10^4 cd11c$^+$ DCs along with UV-inactivated HSV-1 RE in each well of a 96n well plate. The cells were stimulated for 72 hours and then tested for IFN-γ in the supernatant by standard ELISA. Data are represented at mean ± SEM pg/ml of IFN-γ.

These data are consistent with our hypothesis that virus specific CD4 T cells initiate HSK, while bystander activated CD4 T cells propagate it once it has been established (see discussion).

We argue that the slower kinetics of HSK in CD40L KO DO11.10 mice (and also in the intact DO11.10 mice) is a result of reduced numbers of virus specific CD4 T cells that are necessary for the rapid initiation of HSK. It should be noted that CD40L KO mice develop HSK with similar kinetics to WT mice, but the cytokine profile within the DLN is skewed in the absence of CD40:CD40L signaling (113).

4.3.   Are CD4+ T cells absolutely required for HSK?

Following our findings that the virus specific T cell clone AA could induce HSK in the normally HSK resistant nude mouse, we next wanted a cleaner model to further characterize the clones since nude mice invariably die following ocular HSV-1 infection (figure 26C) (79). Since CD4$^+$ T cells are thought to play a requisite role in HSK, CD4-deficient mice should show reduced or no HSK following corneal infection. Surprisingly, when infected with a high dose (1x10^5 pfu) of HSV-1 RE, CD4 KO BALB/c mice developed HSK with early kinetics and incidence similar to that of WT BALB/c mice (figure 32). However, HSK in CD4 KO mice was transient, with declining severity beginning around 2 weeks P.I.. By day 29, many of the CD4 KO mice exhibited clear corneas with the only remaining signs of the previous inflammation being residual, highly attenuated blood vessels. This was in contrast to the WT mice in which severe HSK uniformly persisted throughout the observation period. We also tested anti-CD4 treated mice for their susceptibility to HSK and found similar results to that of CD4 KO mice (figure 33). This was performed to confirm that the disease occurring in the KO mice is not due to one of the aforementioned problems with CD4 KO mice (181,182).
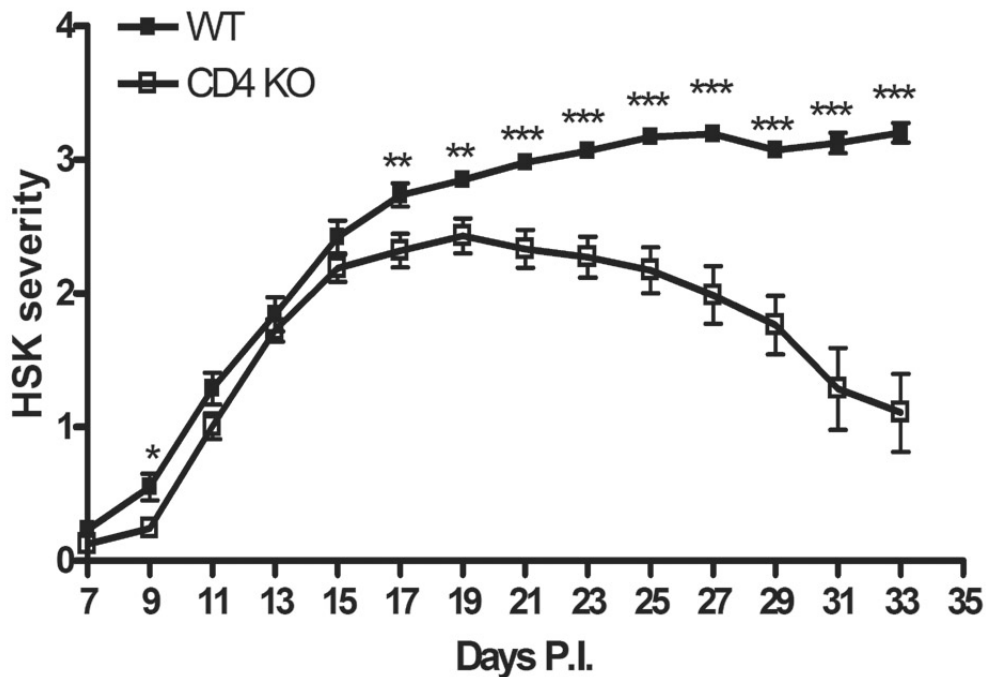
Figure 32: CD4 knockout (CD4 KO) mice infected with a high dose of HSV-1 RE develop transient HSK.

The corneas of WT and CD4 KO BALB/c mice were infected with 1×10^5 PFU of HSV-1 RE, and HSK severity was monitored by a masked observer with a slit-lamp biomicroscope. The incidence of disease was 90% in the WT mice and 84% in CD4 KO. Data shown only for those mice that developed HSK. Pooled data from 4 separate experiments (n=20 mice/group) are expressed as the mean ± standard error HSK score. Significant (**, p<0.01; ***, p<0.001) group differences were observed at all times after 17 days P.I. as assessed by an unpaired Student's *t* test.
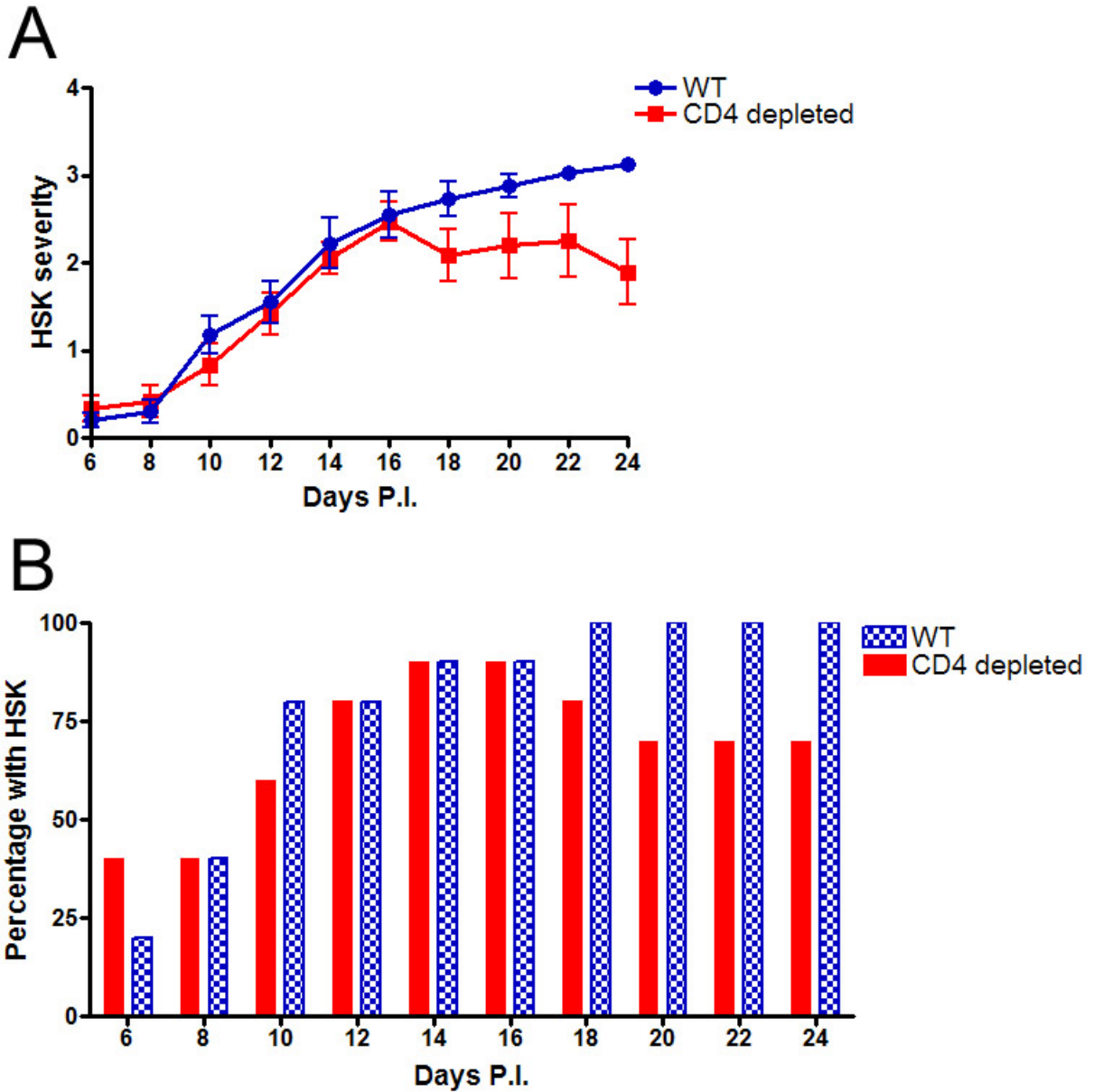
Figure 33: CD4 depleted mice infected with high dose HSV-1 RE develop transient HSK.

The corneas of WT and CD4 depleted BALB/c mice (treated with 0.15 mgs of anti-CD4 Ab on days -2, +1, +5, +8, +15) were infected with 1×10^5 PFU of HSV-1 RE, and HSK severity was monitored by a masked observer with a slit-lamp biomicroscope. Data is shown only for those mice that developed HSK. Data are expressed as the mean ± standard error HSK score (A) or percentage of mice with HSK (B) above a score of 0.5

To determine what cell type might mediate HSK in CD4-deficient mice, corneas from

WT and CD4 KO animals were digested and analyzed by flow cytometry as described in the

materials and methods. The inflammatory infiltrate in the infected corneas of WT mice 14 days P.I. consisted primarily of neutrophils (80-90% of CD45$^+$ cells) and CD4$^+$ T cells (~10% of CD45$^+$ cells), with few if any CD8$^+$ T cells (< 1% of CD45$^+$ cells) present (Figure 34). Although the clinical score of HSK was similar at 14 days P.I. in WT and CD4 deficient mice, the overall infiltrate (CD45$^+$ cells) was significantly higher in the CD4 KO mice (figure 34). Neutrophils were also the dominant leukocyte population in infected corneas of CD4 deficient mice, but in these mice a prominent population of CD8$^+$ T cells (~5-10% of CD45$^+$ cells) was also observed.

Around the time HSK reached maximum severity (day 14 P.I.), the CD69 activation marker was expressed on 20-25% of CD8$^+$ T cells in corneas of CD4 deficient mice, and on 25% of CD4$^+$ T cells in the corneas of WT mice (figure 35A). To assess the antigen specificity and function of T cells in the infected corneas 14 days P.I., dispersed corneal cells were stimulated with HSV-1 antigen-pulsed DCs (to stimulate HSV-1 specific CD4$^+$ T cells in WT corneas), or with HSV-1 infected, MHC class I compatible MKSA cells (to stimulate HSV-1 specific CD8$^+$ T cells in corneas of CD4 KO mice). As illustrated in Figure 35B, 15-20% of the CD4$^+$ T cells in corneas of WT mice, and 5-10% of CD8$^+$ T cells in corneas of CD4-deficient mice produced IFN-γ in response to viral antigens. Thus, a substantial portion of CD4$^+$ T cells in infected corneas of WT mice, and CD8$^+$ T cells in the infected corneas of CD4-deficient mice were activated, HSV-1 specific, and capable of producing IFN-γ when stimulated with HSV-1 antigens.
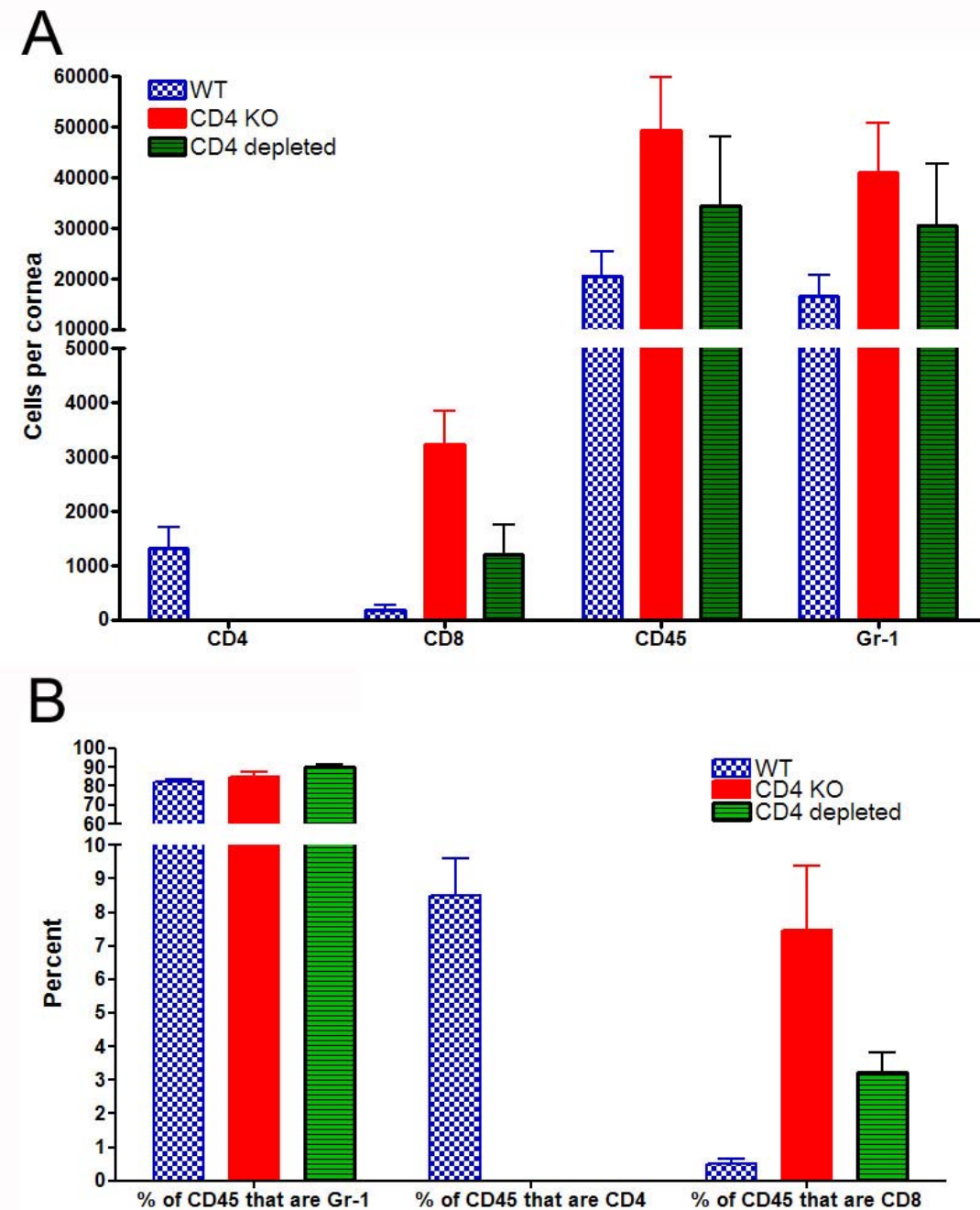
Figure 34: Composition of the corneal infiltrate 14 days after infection.

WT, CD4 KO and CD4 depleted mice were infected with $1x10^5$ PFU of HSV-1 RE, individual corneas with HSK were removed on D14 P.I., and single cell suspensions were stained with antibodies to CD45, CD4, CD8, and Gr-1 (A&B). Infiltrate data (A-B) are pooled from two experiments with four individual mice per group.
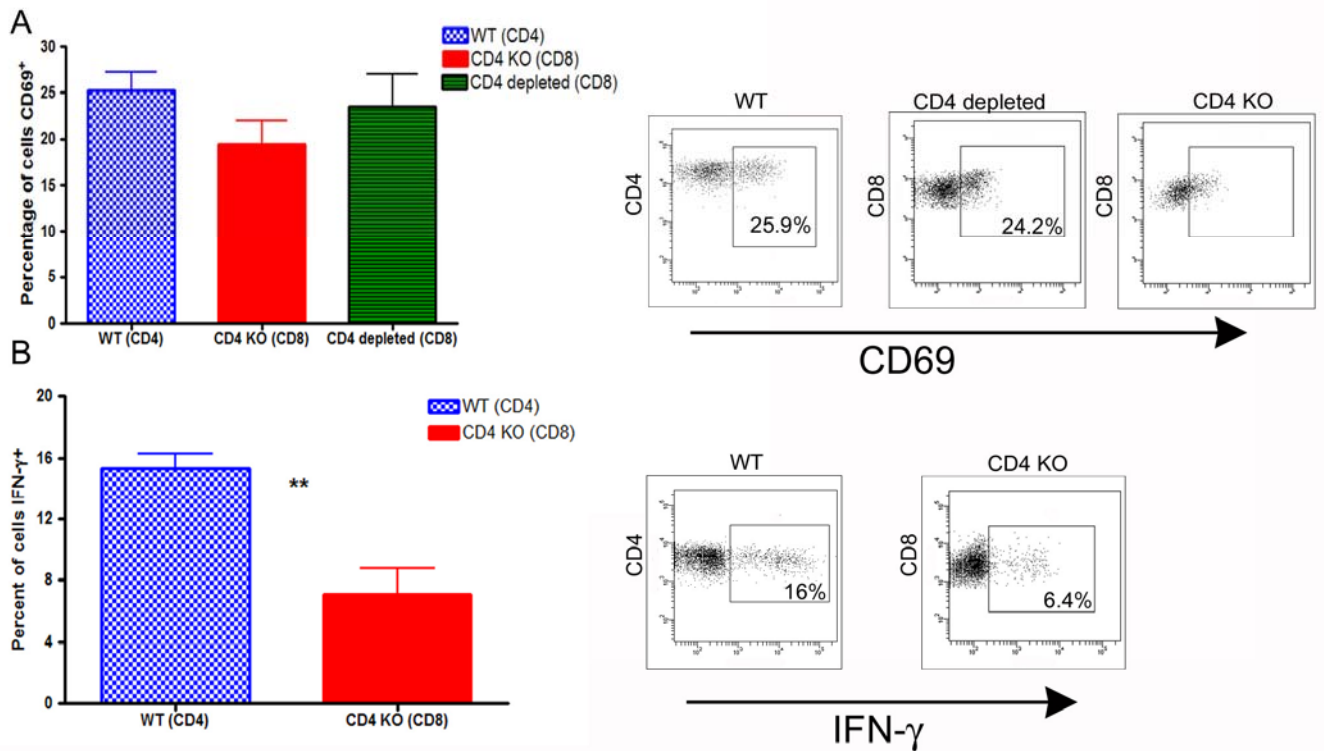
Figure 35 CD8 T cells present in the corneas of CD4 deficient mice are activated and produce IFN-γ in response to viral stimulation.

WT, CD4 KO and anti-CD4 treated mice were infected with 1×10^5 PFU of HSV-1 RE, individual corneas with HSK were removed on D14 P.I., and single cell suspensions were stained with antibodies to CD45, CD4, CD8, and for CD69 (A) and analyzed by flow cytometry. Alternatively, individual corneas were simulated for 6 hours in the presence of Golgiplug© with either viral antigen-pulsed bone marrow-derived DCs for CD4 T cell stimulation, or with HSV-infected MKSA cells for CD8 stimulation. The corneal cells were then stained for surface markers CD45, CD4, CD8 and for intracellular interferon gamma and analyzed by flow cytometry (B). Infiltrate data (A) are pooled from two experiments with four individual mice per group. For intracellular cytokine staining (B), data are from two experiments with two individual mice per group. Asterisks indicate a significant ($*$, $p < 0.05$; $**$, $p < 0.01$) difference between WT and CD4 KO mice, as assessed by an unpaired Student's t test.

The severe HSK (>3+) in WT mice persisted through day 35 P.I., even though the number of CD4$^+$ T cells and neutrophils declined significantly (compare Fig. 36A with Fig. 34A). However, the percentage of activated (CD69$^+$) CD4$^+$ T cells in infected corneas of WT mice at 35 days (48.6 ± 4.0, Fig. 36B) was significantly higher than that seen at 14 days P.I. (25.3 ± 2.0, Fig. 35A). Thus, chronic HSK appears to be more closely related to the persistent activation of

CD4$^+$ T cells than to the actual magnitude of the inflammatory infiltrate. At 35 days P.I., leukocytes were virtually undetectable in corneas of CD4-deficient mice in which HSK regressed below a score of 1+ (not shown). In contrast, corneas of CD4-deficient mice that still expressed > 2+ level of HSK had neutrophil counts that were as high or higher than those observed in corneas of WT mice with 3+ HSK (Fig. 36A). However, CD8$^+$ T cells were no longer detectable in the inflamed corneas of CD4-deficient mice. Thus the regression of inflammation in CD4-deficient mice is characterized by a loss of CD8$^+$ T cells, followed by a gradual reduction in neutrophils and attenuation of blood vessels.
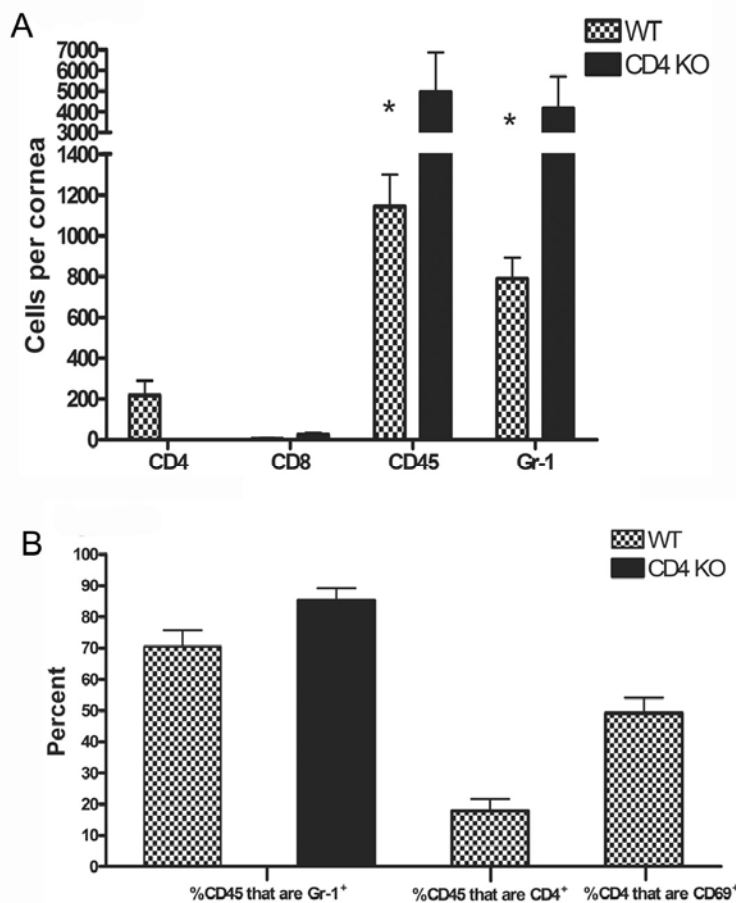
Figure 36 Composition of the corneal infiltrate 35 days after infection.

WT and CD4 KO mice were infected with $1x10^5$ PFU of HSV-1 RE, individual corneas with HSK were removed on D35 P.I., and single cell suspensions were stained with antibodies to CD45, CD4, CD8, Gr-1 and for CD69 and analyzed by flow cytometry. Infiltrate data (A-B) are from five individual mice per group. Asterisks indicate a significant (*, $p < 0.05$) difference between WT and CD4 KO mice, as assessed by an unpaired Student's *t* test.

To identify whether HSK was CD4 T cell independent at all viral doses, WT and CD4-deficient mice were infected with decreasing doses of HSV-1 and monitored for the development of HSK. In WT mice, HSK developed over a wide range of HSV-1 doses; with 80-100% incidence and similar kinetics and severity at infectious doses ranging from $1x10^5$ to $5x10^2$ PFUs of HSV-1. In contrast, the incidence of disease began to decline in CD4-deficient mice at an infectious dose of $5x10^3$ PFU, reaching a 20-30% incidence at the lowest dose tested (figures 37

and 38). Thus, the capacity of CD8^{+} T cells to promote transient HSK requires high doses of HSV-1 that are of questionable physiologic relevance. At low infectious doses HSK is largely CD4^{+} T cell-dependent.
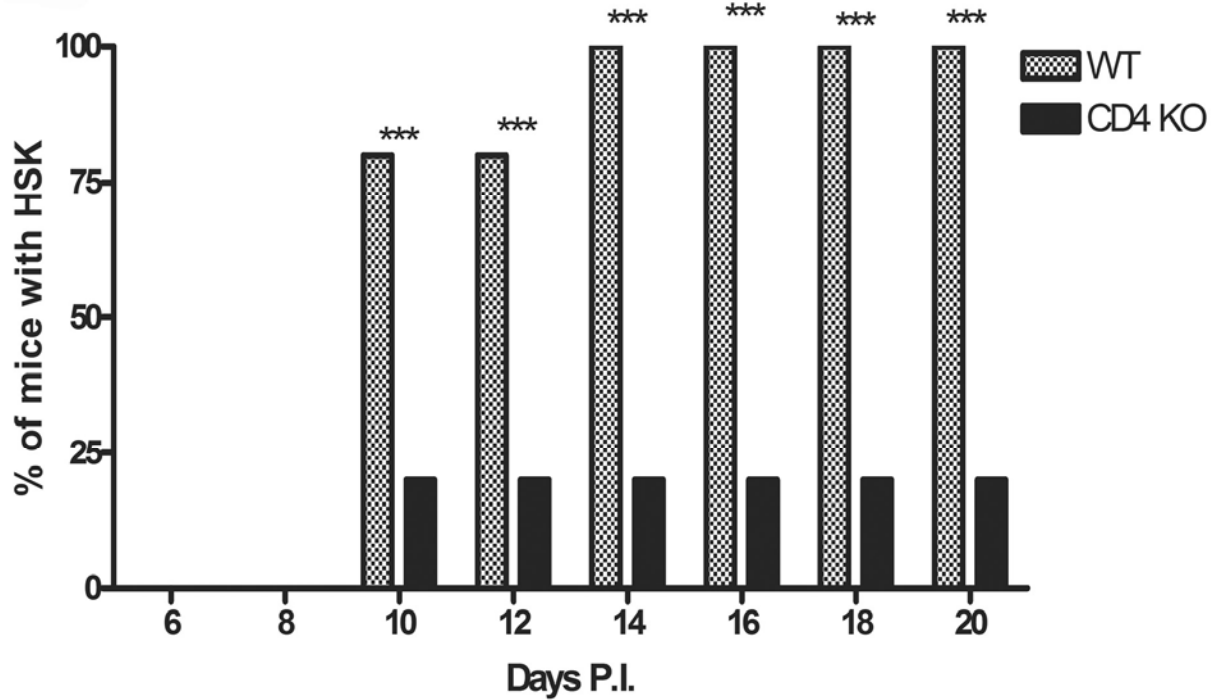
Figure 37 CD4 T cells are required for HSK development following low dose infection.

WT BALB/c and CD4 KO mice were infected with 5×10^2 PFU of HSV-1 RE and were monitored for HSK using a slit lamp microscope. Data are from a representative experiment that was repeated twice with similar results. Asterisks indicate a significant (∗∗∗, p<0.001) difference in the incidence of disease between WT and CD4 KO mice as assessed by Fisher's exact test.
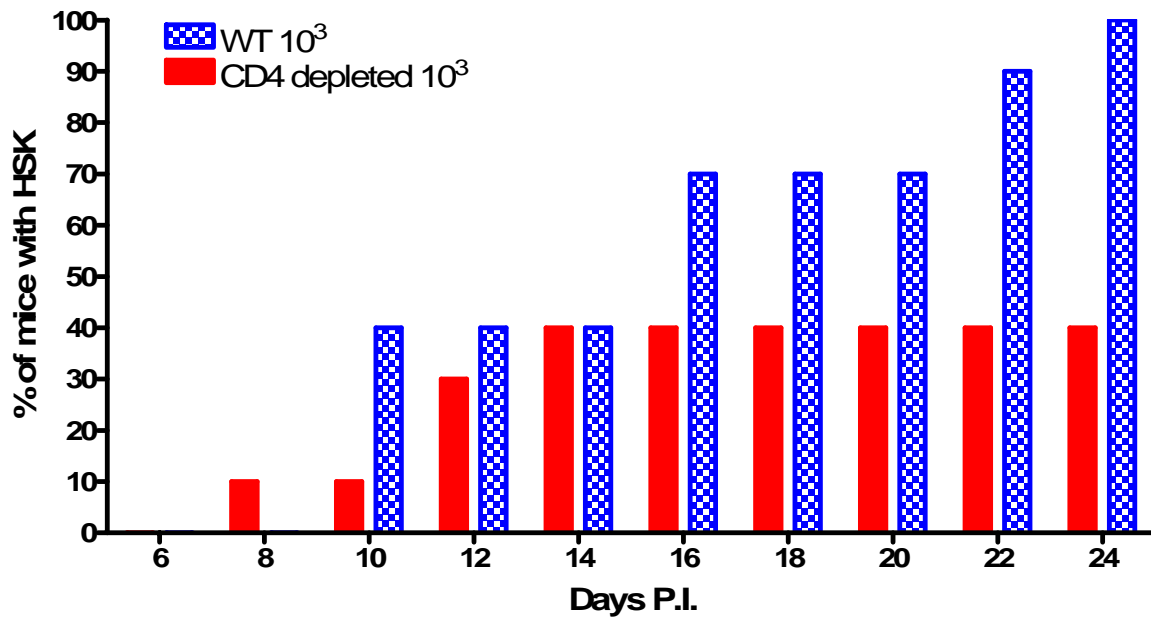
Figure 38 CD4 T cells are required for HSK development following low dose infection.

WT BALB/c and CD4 depleted mice were infected with 10^3 PFU of HSV-1 RE and were monitored for HSK using a slit lamp microscope.

To rule out the possibility that uncontrolled virus replication contributed to pathology in CD4$^+$ T cell-deficient mice (134), HSV-1 was quantified in swabs of infected corneas of CD4-deficient and WT BALB/c mice on days 2, 4, 6, and 8 days P.I. As shown in figure 39, HSV-1 was cleared from the corneas of CD4 KO and WT mice with similar kinetics. No infectious virus was detectable in corneal swabs from either mouse strain beyond 6 days P.I.
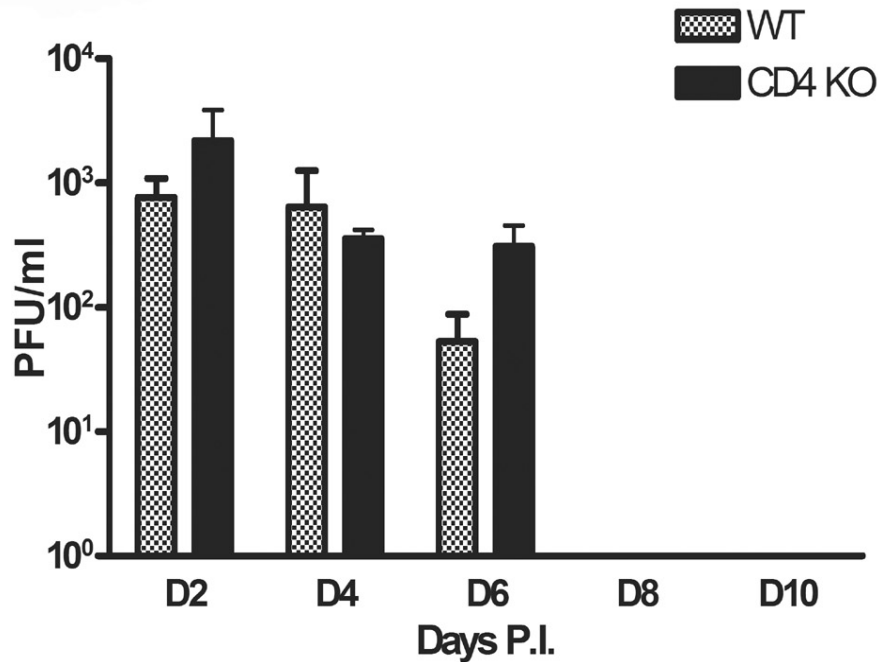
Figure 39 CD4 KO mice clear infectious virus from the cornea with similar kinetics to WT mice.

WT and CD4 KO mice were infected with $1X10^5$ PFU of HSV-1 RE and the corneas were swabbed with a sterile surgical spear on days 2,4,6,8,10 P.I. and assayed for live viral by standard plaque assay. Data represent mean±SEM of virus titer in eye swabs and are from five individual animals for each group at each time point.

One plausible explanation for the decreased incidence of disease following low dose infection in CD4 KO mice may be that the initial priming of CD8 T cells within the draining lymph nodes is reduced or even absent following low dose infection. The DLNs of CD4 KO mice infected with high dose HSV-1 RE (10^5) and low dose HSV-1 RE (10^3) were compared by flow cytometry. This revealed that low dose infection results in a smaller expansion of CD8 T cells in the DLNs compared to high dose infection (figure 40A). Additionally, there was a large drop in the percentage of CD8 T cells that were CD69 positive within the DLNs of low dose infected mice (figure 40B) compared to high dose infection. This may explain the reduced incidence of HSK in low dose infected CD4 KO mice. We have not yet tested whether a similar trend will hold true in the DLNs of WT BALB/c infected with a low dose of HSV-1 RE.
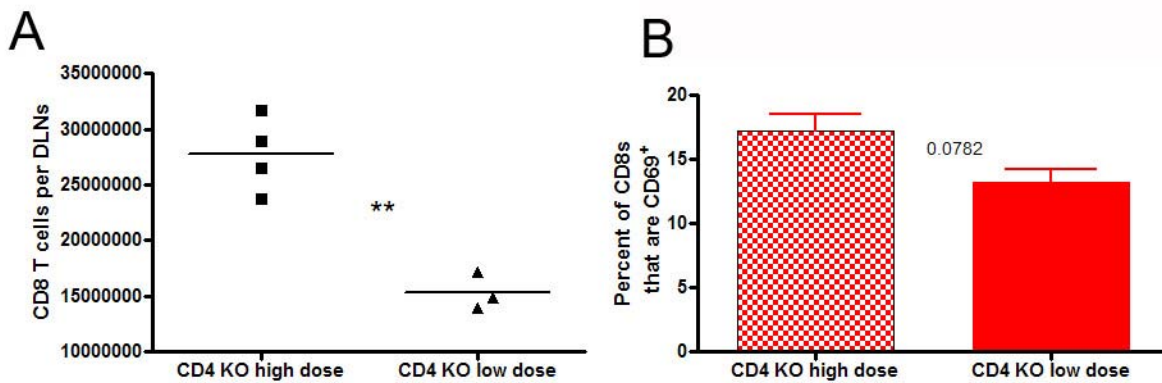
Figure 40 Low dose infection of CD4 KO mice results in lower CD8 T cell numbers in the DLNs at D+6 P.I. compared to high dose infection.

BALB/c CD4 KO mice were infected with either 10^5 or 10^3 PFU of HSV-1 RE on one eye. On day +6 P.I., all of the draining lymph nodes from the neck of each mouse were collected, counted and stained for CD8 and CD69. Asterisks indicate a significant (*, $p < 0.05$; **, $p < 0.01$) difference between WT and CD4 KO mice, as assessed by an unpaired Student's *t* test.

4.4.   Do CD4 T cell regulate CD8 T cell responses in the TG?

As discussed in the introduction, the role of CD4 T cell help in CD8 T cell responses is a topic of intense study (138). Data from our laboratory and others suggests that HSV-1 specific effector CD8$^+$ T cells are required for survival of primary infection (84), and memory CD8$^+$ T cells play an important role in maintaining the virus in a latent state (16,90,94,148,149). We hypothesized that efficient generation of effector and memory CD8 T cells is dependent on CD4 T cell help. To this end, we used CD4 KO mice on the BALB/c background along with transiently CD4 depleted C57Bl/6 mice and analyzed different times P.I. for changes in CD8 T cell phenotype and functionality. Additionally, we tested whether a lack of CD4 T cells affected viral latency.

4.4.1.   In BALB/c mice

Following infection of Balb/c CD4 KO mice, a striking loss of CD8 T cells in the TG over time was observed. This started to become apparent at D22 P.I. and then became a statistically significant reduction at 35 days P.I. (figure 34A). This reduction in CD8 T cell numbers suggested a requisite need for CD4 T cell help either early during priming in order to generate good memory CD8 T cells as suggested (135-137,161), or may reflect a need for CD4 T cell help for the maintenance of memory CD8 T cells during latency (66). First, it was important to reproduce these findings in CD4 depleted mice as CD4 KO mice have been shown to have several compensatory mechanisms not found in WT mice such as MHC class II restricted CD8s (182) and CD4$^-$CD8$^-$ Class II restricted 'CD4 wannabe' cells (181,183). A much more dramatic decline in the numbers of CD8 T cells in the CD4 depleted BALB/c mice compared to control BALB/c mice was observed, with statistically significant drops in the numbers of CD8 T cells evident by D+14 P.I. (figure 41B). The lack of a significant difference between WT and CD4 depleted mice at D+33 may be due to the fact that CD4 T cells are beginning to recover in those mice around D+33, as evidenced by very low numbers in the TG and some recovery in the spleen.
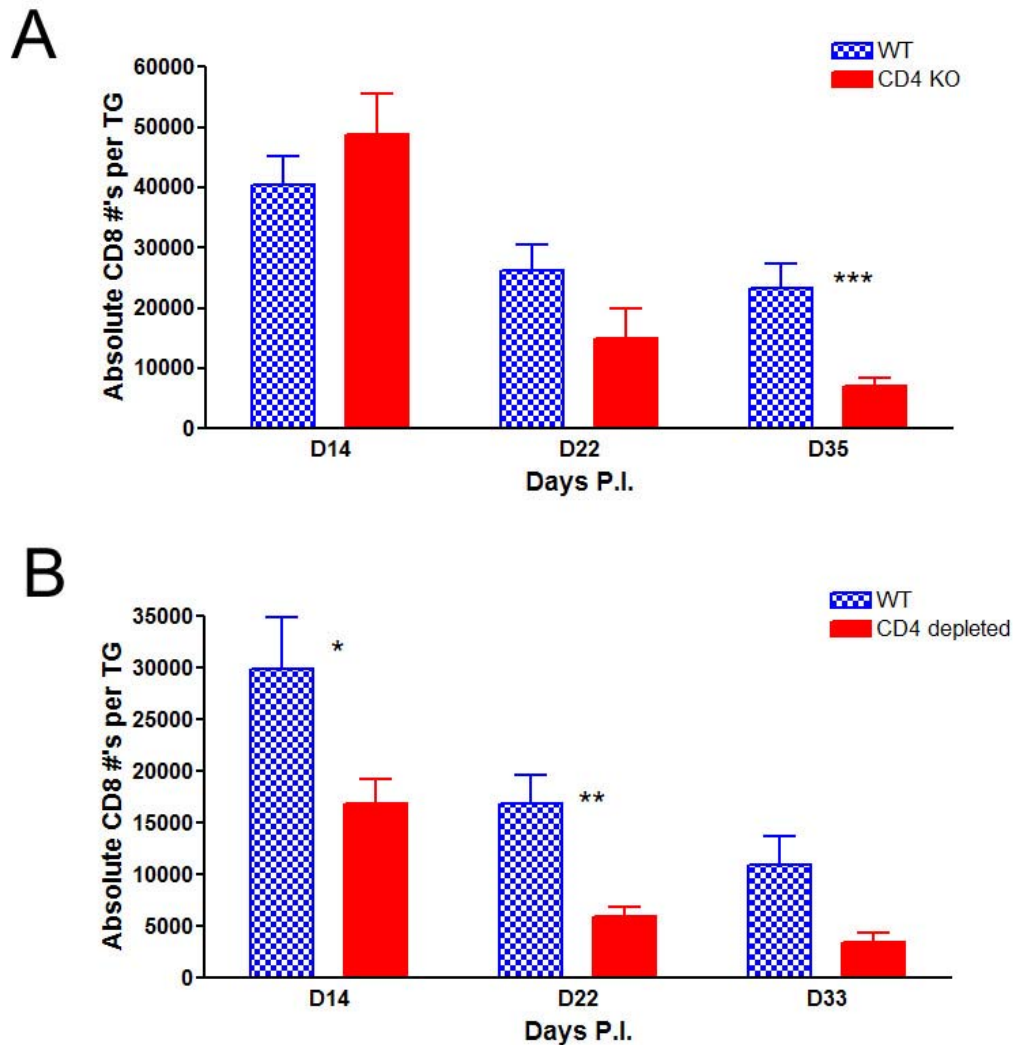
Figure 41 CD4 deficiency in BALB/c mice results in a gradual decline in the numbers of CD8 T cells in the TG.

WT BALB/c ,CD4 KO BALB/c, and CD4 depleted BALB/c mice were infected with $1X10^5$ PFU of HSV-1 RE and then sacrificed at different times P.I. TGs form each animal were digested and stained for CD45 and CD8. Data represent mean±SEM number of cells per TG. Asterisks indicate a significant (*, $p < 0.05$; **, $p < 0.01$; ***, $p<0.001$) difference between WT and CD4 deficient mice, as assessed by an unpaired Student's t test. For CD4 depleted mice: day 14, n=4 mice for WT and n=5 mice for CD4 depleted, day 22, n=3 WT mice and 4 CD4 depleted mice, day 33, n=8 WT mice and n=5 CD4 depleted. For CD4 KO data, day 14 n=5 WT mice and n=5 CD4 KO mice, day 22 n=4 WT mice and n=5 CD4 KO mice, day 35 n=5 WT mice and 12 CD4 KO mice.

Expression of the activation marker CD69 and a memory marker CD127 (IL-7Rα) on the

infiltrating CD8s in the TGs of WT and CD4 depleted mice was examined (this analysis was not

performed in CD4 KO BALB/c mice). These results clearly demonstrate a reduction in the

numbers and percentage of CD8 T cells that express the memory marker CD127 in CD4 depleted

BALB/c mice at all times tested, however CD69 expression was more consistent between the

WT and CD4 depleted mice (figure 42).
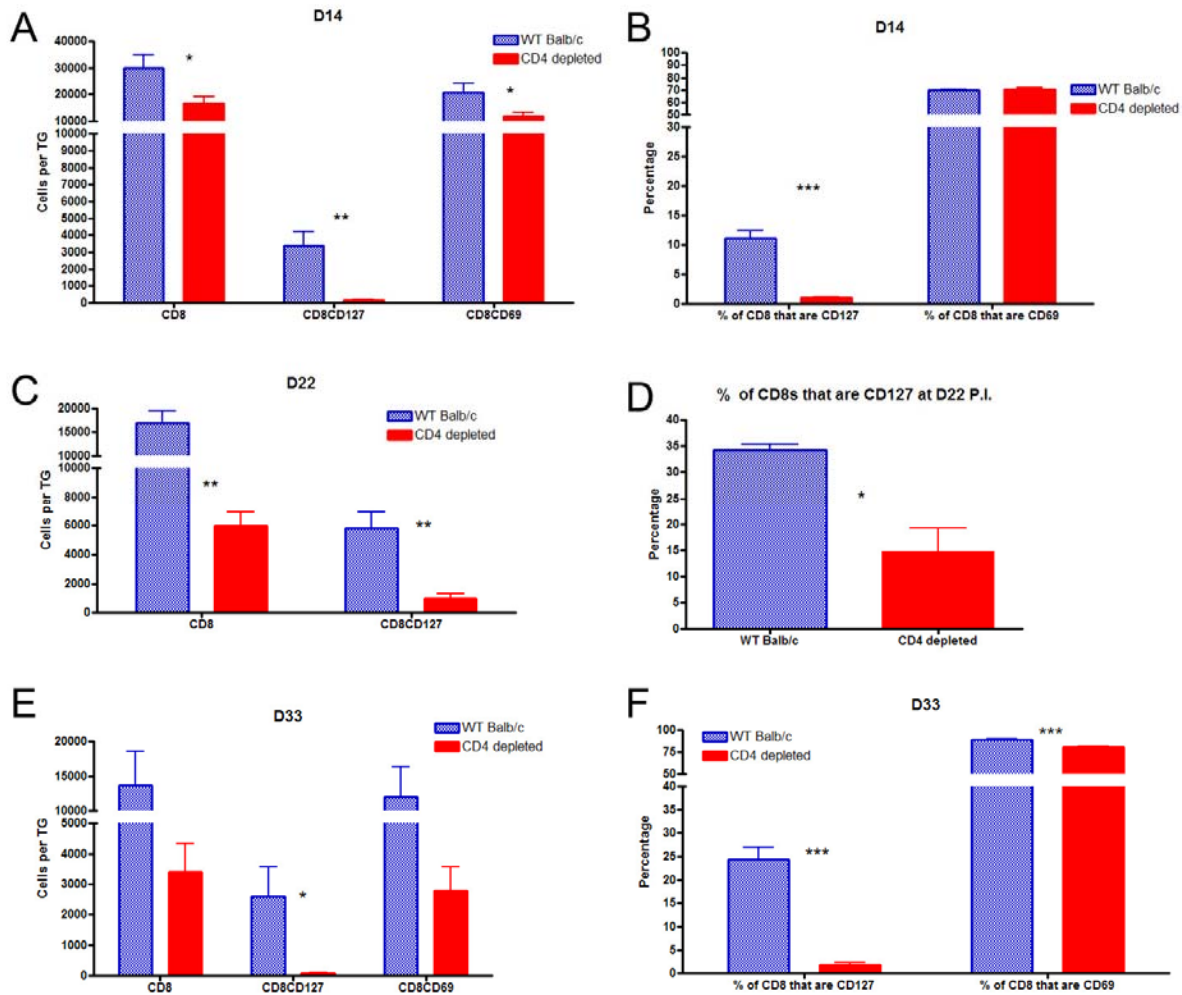
Figure 42: Reduced CD127 expression on CD8 T cells in the TG of CD4 depleted BALB/c mice.
WT BALB/c and CD4 depleted BALB/c mice (treated with 0.15 mgs of GK1.5 on days -2, +1, +5, +8) were infected with $1X10^5$ PFU of HSV-1 RE unilaterally and then sacrificed at different times P.I. Individual TGs from each animal were digested and stained for CD45 and CD8. Data represent mean±SEM number of cells per TG or mean percentage of cells±SEM expressing each marker. Asterisks indicate a significant (*, $p < 0.05$; **, $p < 0.01$; ***, $p<0.001$) difference between WT and CD4 depleted mice, as assessed by an unpaired Student's t test. At day 14, n=4 mice for WT and n=5 mice for CD4 depleted. At day 22, n=3 WT mice and 4 CD4 depleted mice. At day 33, n=8 WT mice and n=5 CD4 depleted.

Note the low expression of CD127 on CD8 T cells in CD4 depleted animals. Very recent work has shown that CD4 deficiency can result in decreased expression of CD127 on CD8 T cells (153,184,185). To test whether this reduction in CD127 was caused by an absence of CD4 T cells early during priming or later during latency, BALB/c mice were depleted of CD4 cells with a single injection of anti-CD4 on D-2 (labeled as early CD4 depleted), which resulted in a transient depletion of CD4 T cells (through D+12), or were depleted of CD4 T cells on days +28, +30, +32 (labeled as late CD4 depleted) (Figure 43). We found that the absence of CD4 T cells early during priming resulted in a statistically significant decrease in the percentage of CD8 T cells expressing CD127 or CD69, which was not found when CD4 T cells were depleted late during latency (figure 43C). An interesting observation is that late term CD4 depletion in the BALB/c mice resulted in what appeared to be a decline in the absolute numbers of CD8 T cells (figure 43A), however comparisons of absolute numbers is challenging in this experiment due to the low N value and a large amount of variability between animals in the same group.
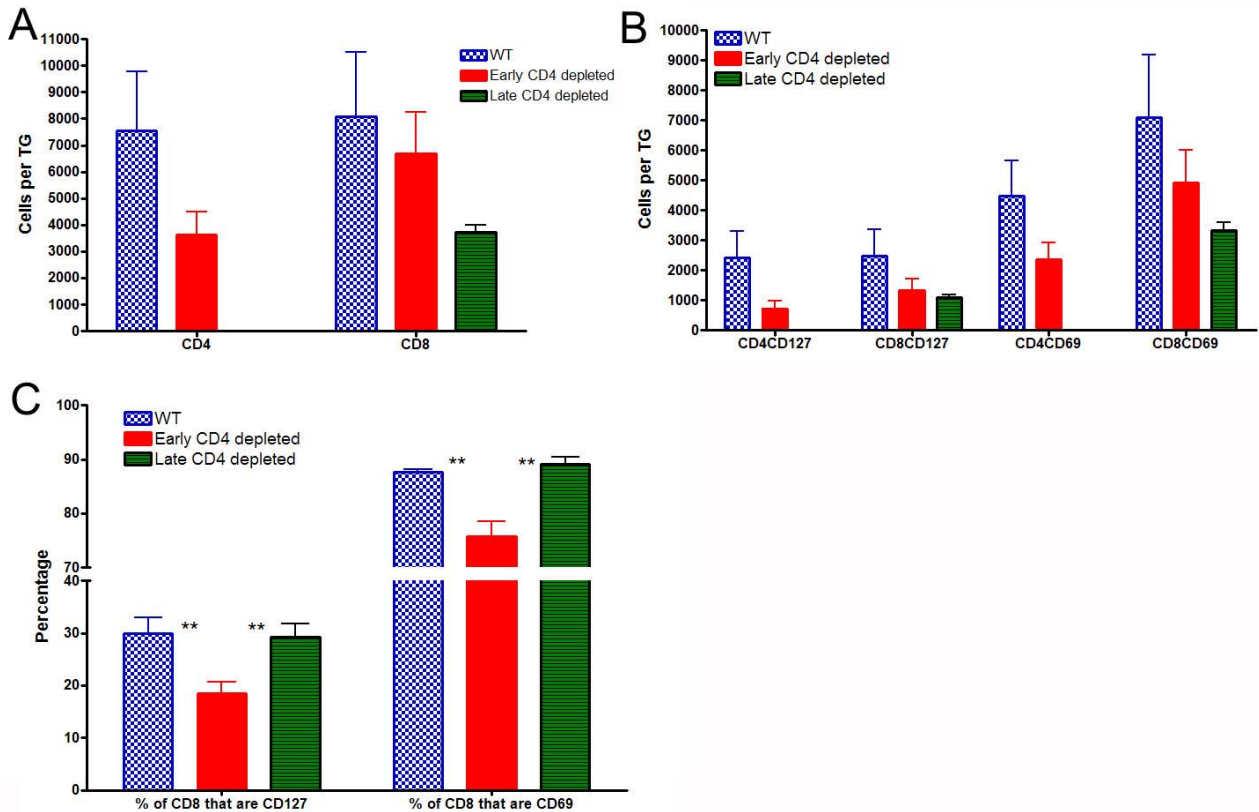
Figure 43: Depletion of CD4 T cells during priming, but not during latency, results in decreased expression of CD127 and CD69 on CD8 T cells in the TG of BALB/c mice.

WT BALB/c and CD4 depleted BALB/c mice (treated with 0.15 mgs of GK1.5 on days -2 = early depleted, or with 0.15 mgs GK1.5 on days +28, +30,+32 = late depleted) were infected with $1X10^5$ PFU of HSV-1 RE unilaterally and then sacrificed on day +33. Individual TGs from each animal were digested and stained for CD45, CD8, CD69 and CD127. Data represent mean±SEM number of cells per TG (A, B) or mean±SEM of percentage positive for each marker. Asterisks indicate a significant (*, $p < 0.05$; **, $p < 0.01$; ***, $p<0.001$) difference between WT and CD4 depleted mice, as assessed by an unpaired Student's *t* test. In (C), There was a significant difference between WT and early CD4 depleted mice, and again between early CD4 depleted mice and late depleted mice, but there was significant difference between WT and late CD4 depleted mice. This data was generated from 4 WT mice, 5 early CD4 depleted mice and 4 late CD4 depleted mice.

The reduced numbers of CD8 T cells in the TGs of CD4 depleted BALB/c mice at D+14 may be a result of a decreased proliferative capacity of CD8 T cells in the DLNs early after infection. To test this, WT BALB/c and CD4 depleted BALB/c (treated with 0.15 mgs of GK1.5 on days -2, +1, +5, +8) mice were infected with $1X10^5$ PFU of HSV-1 RE and were given BrdU on days 6 and 7 P.I. The mice were sacrificed on D+8 P.I. and the numbers of CD8 T cells and

BrdU incorporation in the CD8 T cells in the DLNs was examined. This study revealed no apparent effect on the initial CD8 T cell expansion in DLNs of CD4 depleted mice (figure 44). This is consistent with most of the primary literature that argues that generation of the primary CD8 effector population is CD4 T cell independent (135-138).
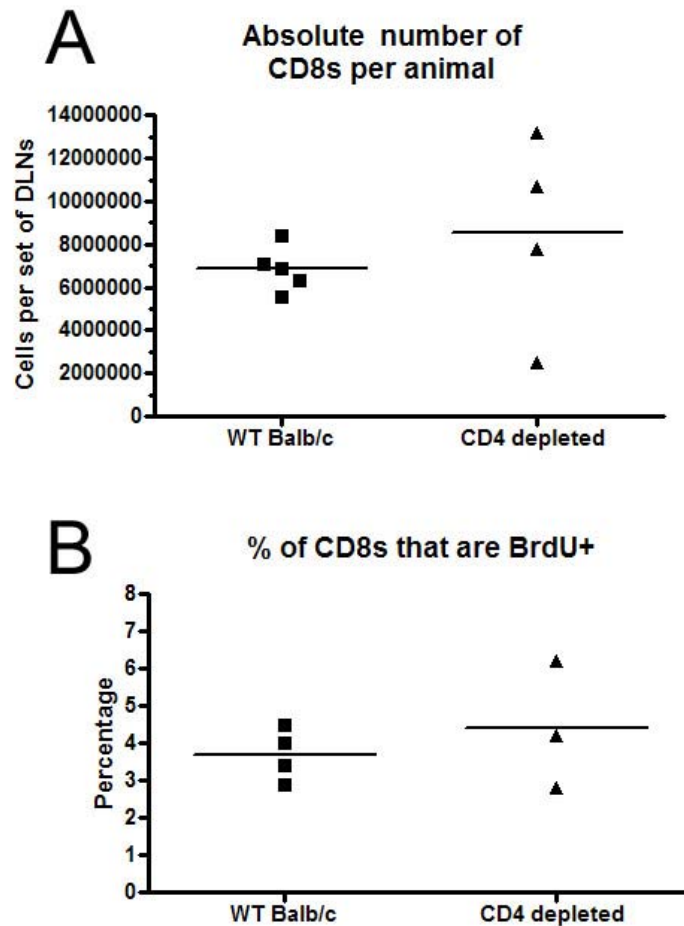
Figure 44: CD4 depletion does not affect the proliferation of primary CD8 T cells in the DLNs at day +8 P.I.

WT and CD4 depleted BALB/c mice were infected with 10^5 PFU of HSV-1 RE. On days +6 and +7 P.I., the mice were treated with 1 mg of BrdU by I.P. injection. On day +8 P.I., the draining lymph nodes were removed and stained for CD8 and BrdU.

The drawback to using BALB/c mice for these studies is the lack of tetramer reagents to analyze the virus antigen specific CD8 T cell population. We developed an assay to test for antigen specific CD8 T cells in the TGs of BALB/c mice by intracellular cytokine staining. HSV-1 RE infected MKSA cells were used as CD8 T cell stimulators to test what percentage of CD8 T cells within the TGs of BALB/c mice respond to viral antigens. 10^6 HSV infected MKSA cells yielded the best stimulation at D+13 P.I. (figure 45) and this was shown again at D+22 P.I. (figure 46). Unfortunately, no comparison between WT BALB/c mice and CD4 KO/depleted BALB/c mice was performed, but nevertheless this assay will be very useful for future studies.
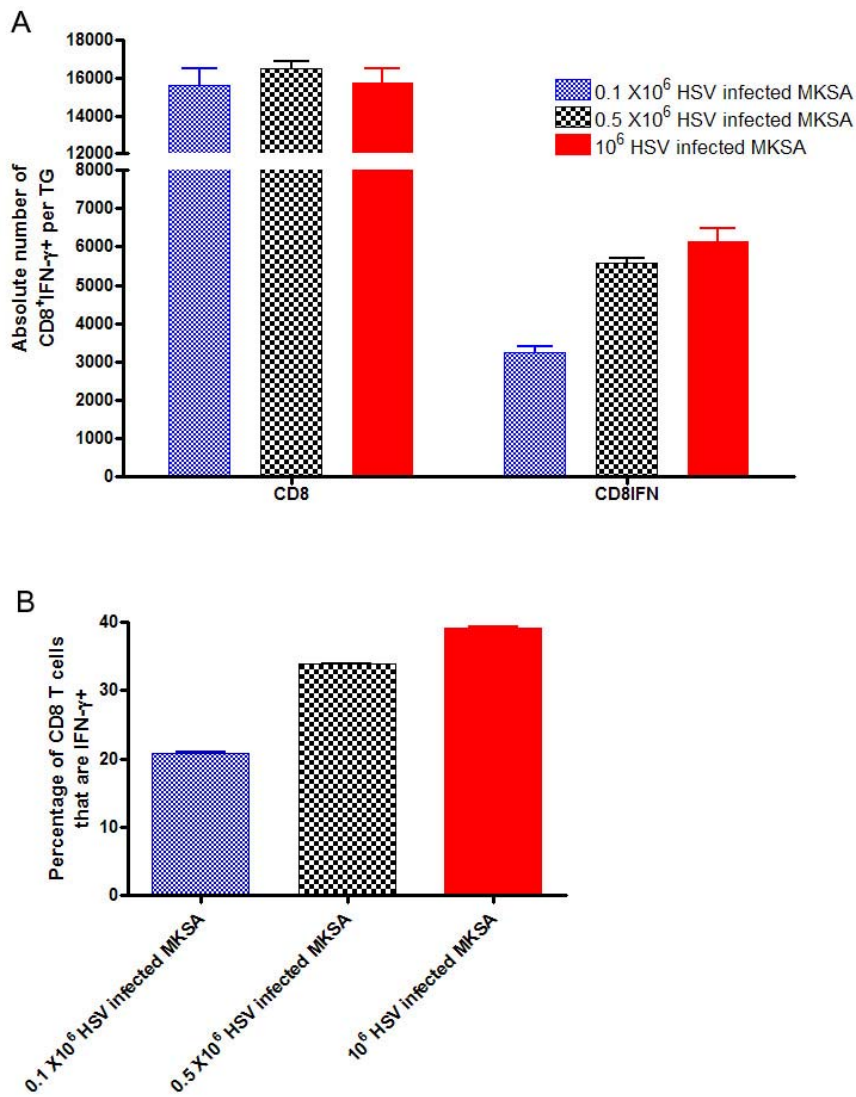
Figure 45: CD8 T cells in the TG of Balb/c mice at D+13 P.I. respond to viral antigens and produce IFN-γ.

BALB/c mice infected with 10^5 PFU of HSV-1 RE. On day 13 P.I., TGs were removed, digested and then incubated with varying numbers of HSV-1 infected MKSA cells in the presence of Golgiplug for 6 hours. Mean absolute cell numbers±SEM (A) and mean percentage of cells producing IFN-γ±SEM (B) are shown. Cells were then stained for surface markers and intracellular IFN-γ following BD PharMingen's protocol. Data were generated from 2 Tgs for each group.
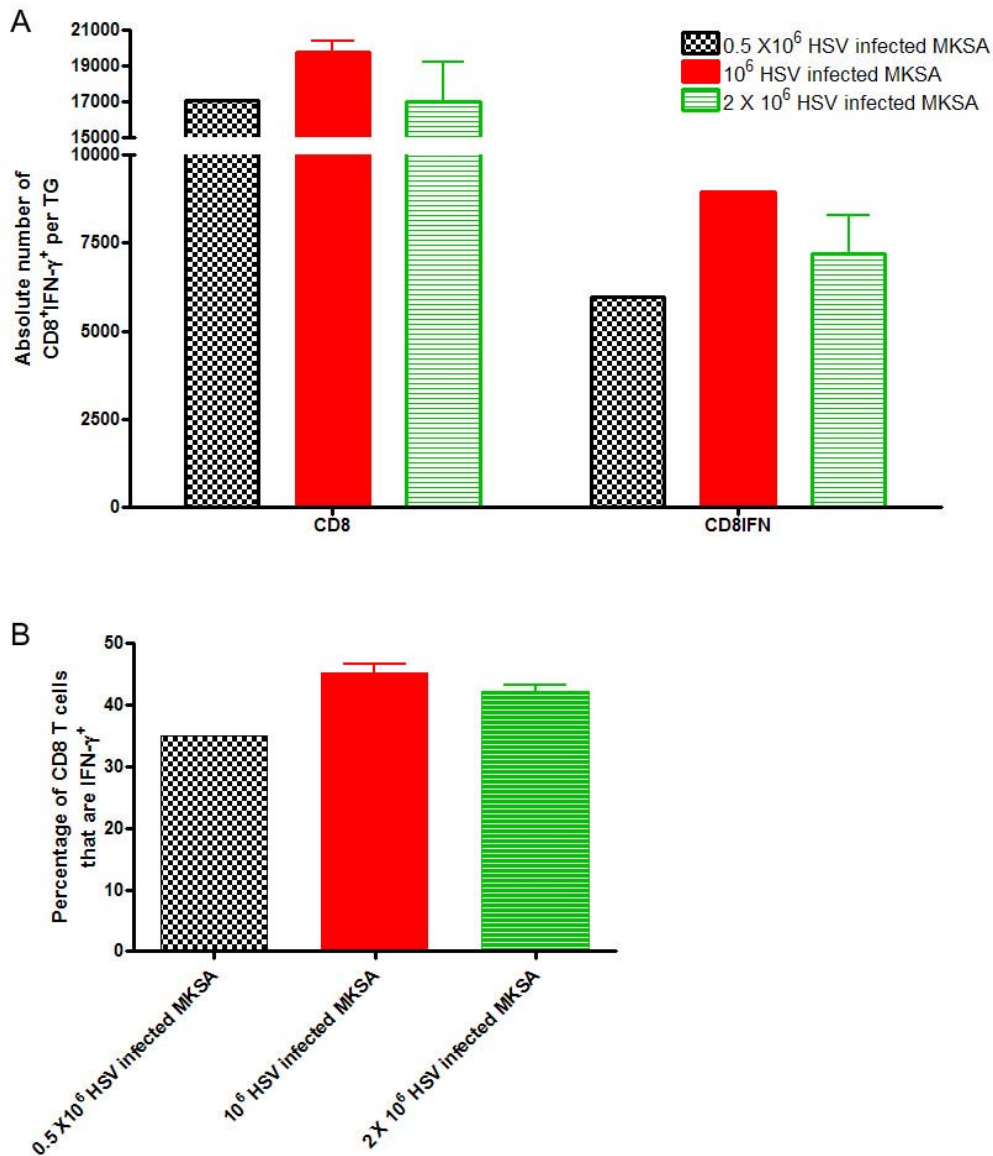
Figure 46: CD8 T cells in the TG of Balb/c mice at D+20 P.I. respond to viral antigens and produce IFN-γ.

BALB/c mice infected with 10^5 PFU of HSV-1 RE. On day 22 P.I., TGs were removed, digested and then incubated with varying numbers of HSV-1 infected MKSA cells in the presence of Golgiplug for 6 hours. Cells were then stained for surface markers and intracellular IFN-γ following BD PharMingen's protocol. Mean absolute cell numbers±SEM (A) and mean percentages of cells producing IFN-γ ±SEM (B) are shown. Data were generated from 2 TGs for each group.

4.4.2. In C57Bl/6 mice

The drawback to analysis of CD8 T cells in BALB/c mice is the inability to detect virus specific CD8 T cells due to a lack of an appropriate CD8 T cell epitope in the BALB/c haplotype. We therefore moved from CD4 deficient BALB/c mice into CD4 deficient C57Bl/6 mice in which an immunodominant epitope is known and has been used in our model (90).

The studies began in CD4 KO C57Bl/6 mice and two time points were examined, D+38 P.I. and D+67 P.I. (figure 47). At both time points tested no statistically significant differences in the absolute numbers of total CD8 T cells or the absolute numbers of gB$_{498-505}$ specific CD8 T cells between the WT C57Bl/6 and the CD4 KO C57Bl/6 mice was observed, however a statistically significant difference in the percentage of CD8 T cells that were gB$_{498-505}$ specific at both time points was identified.
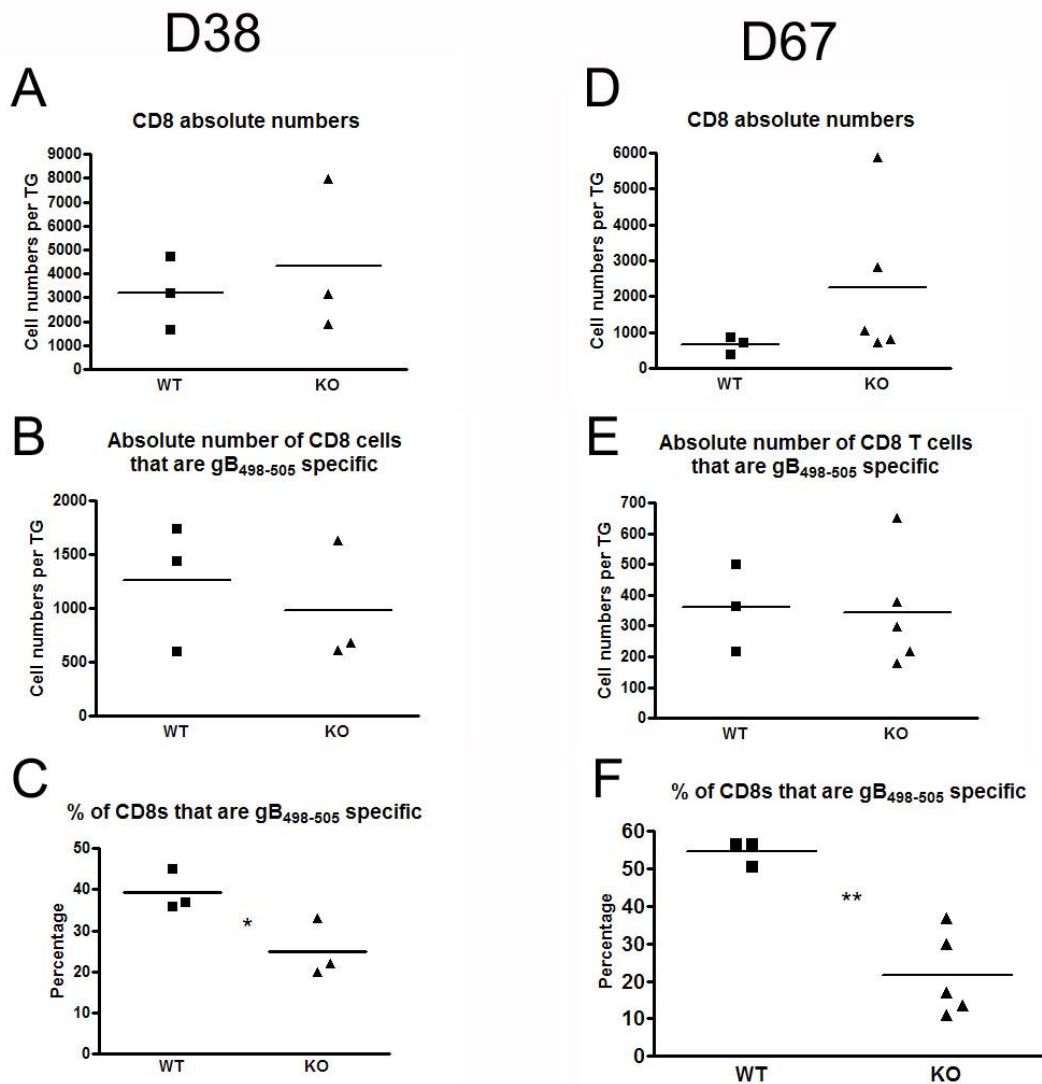
Figure 47: Similar numbers of virus specific CD8 T cells are present in the TGs of WT C57Bl/6 and CD4 KO C57Bl/6 mice at days 38 and 67 P.I.

Both eyes of WT and CD4 KO C57Bl/6 mice were infected with 3×10^5 PFU of HSV-1 RE. The mice were sacrificed on either day +38 P.I.(A-C) or D+67 P.I. (D-F) and both TGs were removed, digested into a single cell suspension and then one TG equivalent was subjected to flow cytometry. Mean absolute cell numbers±SEM (A,B,D,E) and mean percentages of cells expressing each marker ±SEM (C,F) are shown. Asterisks indicate a significant (*, $p < 0.05$; **, $p < 0.01$; ***, $p<0.001$) difference between WT and CD4 deficient mice, as assessed by an unpaired Student's *t* test.

As discussed in the introduction, several articles have exposed important compensatory mechanisms found in CD4 KO mice that are not normally observed in WT mice (181,182). Subsequent experiments were performed in CD4 depleted animals to avoid these potential

problems. 0.15 mg of anti-CD4 antibody (GK1.5) was administered I.P. to C57Bl/6 mice 2 days prior to infection ($3X10^5$ PFU of HSV-1 RE per eye) and then again on D+1, +5, +8 and then weekly P.I. Mice were sacrificed at different times P.I. and the phenotype and in some cases the functionality of the CD8 T cells within the TG were analyzed.

4.4.2.1.   Does CD4 deficiency during priming affect initial expansion and migration of effector T cells into the TG?

To address whether CD4 deficiency results in a defect in the early effector CD8 T cell population in the TG, mice were depleted of CD4 T cells on days -2, +1, +5 and then sacrificed on D+8 P.I. The TGs were removed, digested, and analyzed by flow cytometry (Figure 48). In addition, CD8 T cell functionality within the TG was tested by intracellular cytokine staining (Figure 49). Analysis of the infiltrate data (Figure 48) revealed that CD4 depletion did not result in decreased numbers of $gB_{498-505}$ specific CD8 T cells in the TG at D+8 P.I., however an overall increase in the total numbers of CD8 T cells in the TG suggesting a possible role of regulatory T cells that appear to only affect the virus non-specific T cells. Additionally, reduced numbers and percentage of $gB_{498-505}$ specific CD8 T cells expressing CD127 (IL-7Rα), a marker for memory T cell precursors (51), was observed in CD4 deficient mice. Interestingly, a concomitant increase in the numbers and percentage of $gB_{498-505}$ specific CD8 T cells expressing CD69, a marker of recent activation in the CD4 depleted TGs, was found in CD4 depleted animals.
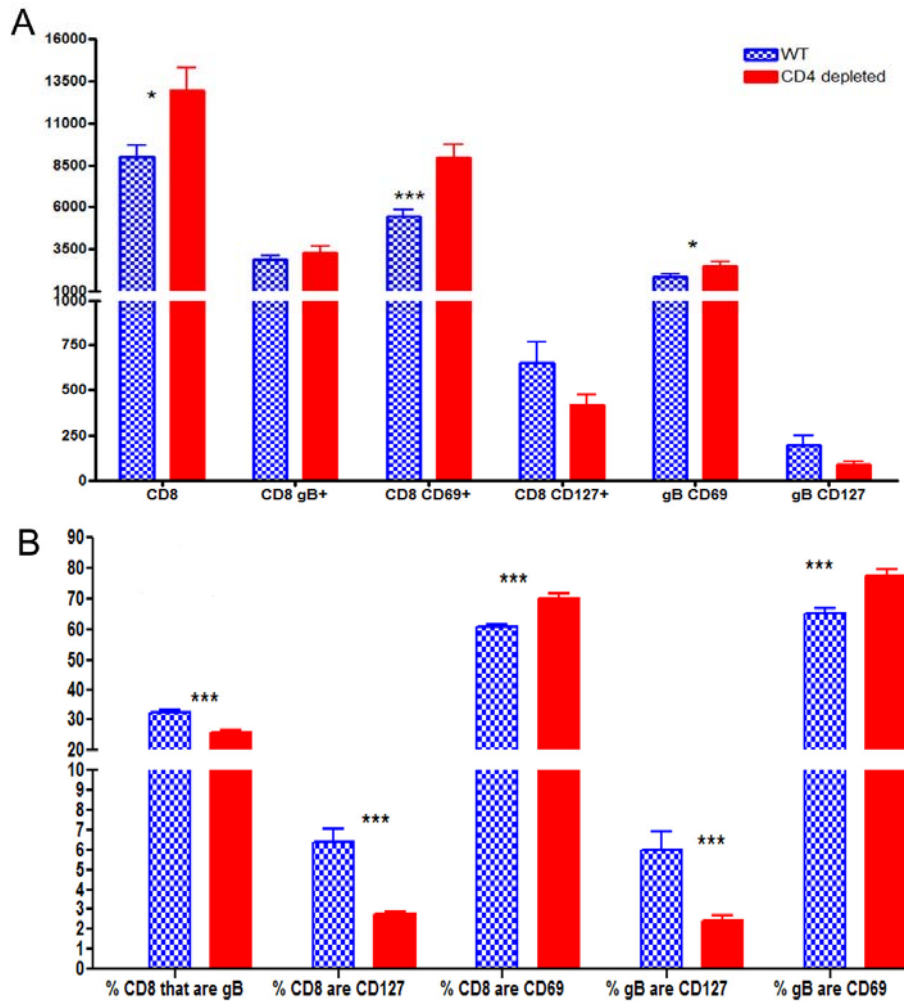
Figure 48: CD4 depletion reduces the generation of virus specific memory precursors in the TG.

Both eyes of WT and CD4 depleted C57Bl/6 mice (injected with 0.15 mgs of GK1.5 on days -2, +1, +5) were infected with 3×10^5 PFU of HSV-1 RE. The mice were then sacrificed on day +8 P.I. and both TGs were removed, digested into a single cell suspension and then one TG equivalent was subjected to flow cytometry. Mean absolute cell numbers±SEM (A) and mean percentages of cells expressing each marker ±SEM (B) are shown. Asterisks indicate a significant (∗, $p < 0.05$; ∗∗, $p < 0.01$; ∗∗∗, $p<0.001$) difference between WT and CD4 deficient mice, as assessed by an unpaired Student's *t* test.

The functional capacity of the CD8 T cells present in the TGs of WT and CD4 depleted mice at D+8 was tested by intracellular cytokine staining (figure 49). This data must be interpreted carefully since upon first glance, there is a significant decrease in the percentage of CD8 T cells within the TGs of CD4 depleted mice producing IFN-γ compared to WT TGs. This

initially suggests that there is a functional defect in the ability of the effector CD8 T cells to produce IFN-γ in the absence of CD4 T cell help. This is not true since this assay is examining the percentage of total CD8 T cells that can produce IFN-γ in response to viral antigens and the data in figure 44 clearly shows that the percentage of CD8 T cells that are viral antigen specific (gB$_{498-505}$ specific) is reduced in CD4 depleted mice. This reduction in the percentage of gB$_{498-505}$ specific CD8 T cells in the TG of CD4 depleted mice results in a reduced percentage of IFN-γ producing CD8 T cells seen in figure 48. Direct comparison of the absolute numbers of CD8 T cells that are producing IFN-γ between the WT and CD4 depleted mice, reveals no significant difference in the numbers of IFN-γ^{+} CD8 T cells between the WT and CD4 depleted mice (see figure 49A).
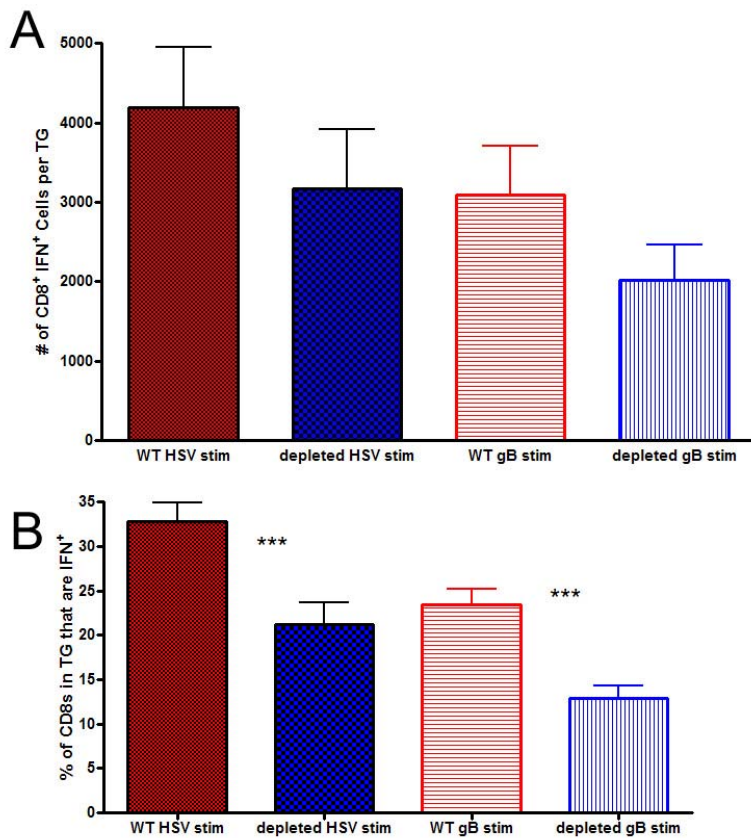
Figure 49: CD4 depletion does not significantly affect the number of IFN-γ producing CD8 T cells in the TG 8 days P.I..

Both eyes of WT and CD4 depleted C57Bl/6 mice (injected with 0.15 mgs of GK1.5 on days -2, +1, +5) were infected with $3X10^5$ PFU of HSV-1 RE. The mice were then sacrificed on day +8 P.I. and both TGs were removed, digested into a single cell suspension and then one TG equivalent was stimulated with either 0.5×10^6 HSV-infected B6WT3 cells (HSV stim) or with 0.5×10^6 gB peptide pulsed gB transfected B6WT3 cells for 6 hours in the presence of Golgiplug and then stained for intracellular IFN-γ by flow cytometry. Absolute cell numbers±SEM (A) and percentages±SEM of cells producing IFN-γ (B) are shown. Asterisks indicate a significant (*, $p < 0.05$; **, $p < 0.01$; ***, $p<0.001$) difference between WT and CD4 deficient mice, as assessed by an unpaired Student's t test. In (B), significant differences were observed between WT and CD4 depleted mice stimulated with either HSV targets or with gB targets.

The mean fluorescence intensity (MFI) of the IFN-γ+ CD8 T cells revealed a statistically significant decrease in the MFI of the CD8 T cells in the CD4 depleted mice compared to WT (figure 50). This suggests that on a per cell basis, virus specific CD8 T cells generated in a CD4 deficient environment are reduced in the amount of IFN-γ that they can produce.

107

Figure 50: CD8 T cells in the TGs of CD4 depleted mice produce less IFN-γ per cell than WT.
Both eyes of WT and CD4 depleted C57Bl/6 mice (injected with 0.15 mgs of GK1.5 on days -2, +1, +5) were infected with $3X10^5$ PFU of HSV-1 RE. The mice were then sacrificed on day +8 P.I. and both TGs were removed, digested into a single cell suspension and then one TG equivalent was stimulated with 0.5×10^6 gB peptide pulsed gB transfected B6WT3 cells for 6 hours in the presence of Golgiplug and then stained for intracellular IFN-γ by flow cytometry. The resulting IFN-γ$^+$ population was gated and the mean fluorescence intensity of that IFN-γ$^+$ population was determined. Asterisks indicate a significant (*, $p < 0.05$; **, $p < 0.01$; ***, $p<0.001$) difference between WT and CD4 deficient mice, as assessed by an unpaired Student's t test.

Our conclusion is that effector virus specific CD8 T cells can be generated in our model in the absence of CD4 T cells, although they appear to be slightly impaired in the amount of IFN-γ each cell can produce. This is consistent with most studies showing primary CD8 T cell responses can be generated in the absence of CD4 T cell help. The reduced functionality of the CD8 T cells in their ability to produce IFN-γ may result in delayed viral control, which will be addressed later in this thesis.

4.4.2.2. Does CD4 deficiency affect CD8 T cell contraction within the TG?

The next set of experiments tested whether the contraction phase of the immune response in the TG was affected by CD4 T cell deficiency. Previous work in our lab has identified D+8 as

the peak response in the TG, with contraction occurring immediately thereafter (unpublished observations). D+14 P.I. was chosen to address the contraction phase in WT and CD4 depleted mice (figure 51). A significant drop in the absolute numbers of $gB_{498-505}$ specific CD8 T cells in CD4 deficient mice at D+14 P.I. was observed. This suggests that the contraction phase is greatly accelerated in the absence of CD4 T cell help within the TG. Additionally, a statistically significant decrease in both the percentage and absolute number of $gB_{498-505}$ specific CD8 T cells expressing CD127 at D+14 in CD4 deficient mice was found. This decrease in CD127 expression was accompanied by an increase in the percentage of $gB_{498-505}$ specific CD8 T cells that express CD69, indicating that along with the decline in the numbers of memory precursor cells ($CD127^+$), CD4 deficient mice had a concomitant increase in the numbers of activated effector cells ($CD69^+$).
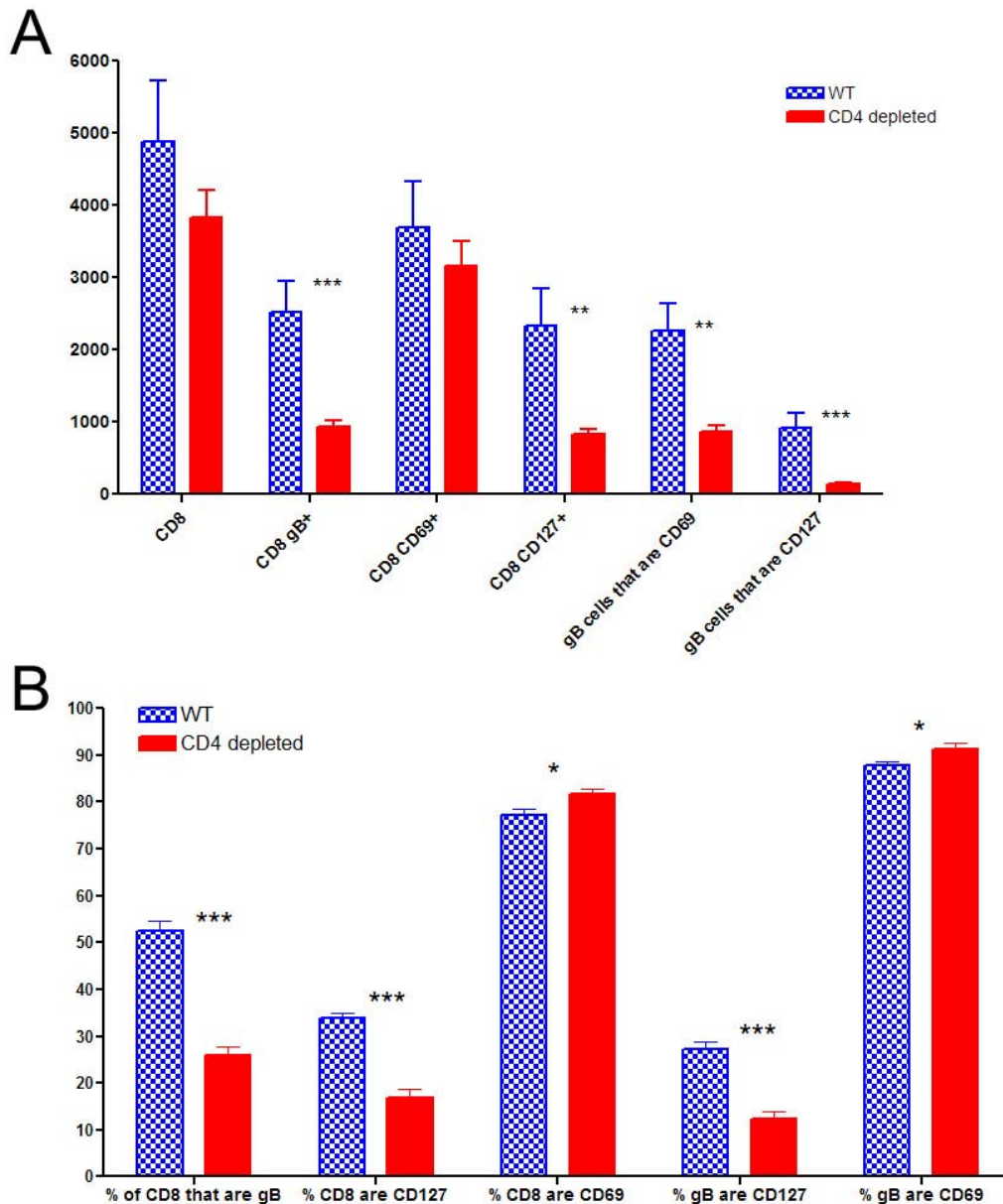
Figure 51: Contraction phase of gB$_{498-505}$ specific CD8 T cells is accelerated in CD4 depleted mice.

Both eyes of WT and CD4 depleted C57Bl/6 mice (injected with 0.15 mgs of GK1.5 on days -2, +1, +5, +8) were infected with $3X10^5$ PFU of HSV-1 RE. The mice were then sacrificed on day +14 P.I. and both TGs were removed, digested into a single cell suspension and then one TG equivalent was subjected to flow cytometry. Mean absolute cell numbers±SEM (A) and percentages of cells±SEM expressing each marker (B) are shown. Asterisks indicate a significant ($*$, $p < 0.05$; $**$, $p < 0.01$; $***$, $p<0.001$) difference between WT and CD4 deficient mice, as assessed by an unpaired Student's t test.

Defects in CD8 T cell phenotype and function were tested at D+19 P.I (figure 52) in CD4 deficient mice, a time point at which contraction is nearly complete. Again, reduced numbers and percentages of gB$_{498-505}$ specific CD8 T cells expressing CD127 was found which further confirms the lack of proper memory T cell development in CD4 deficient mice.
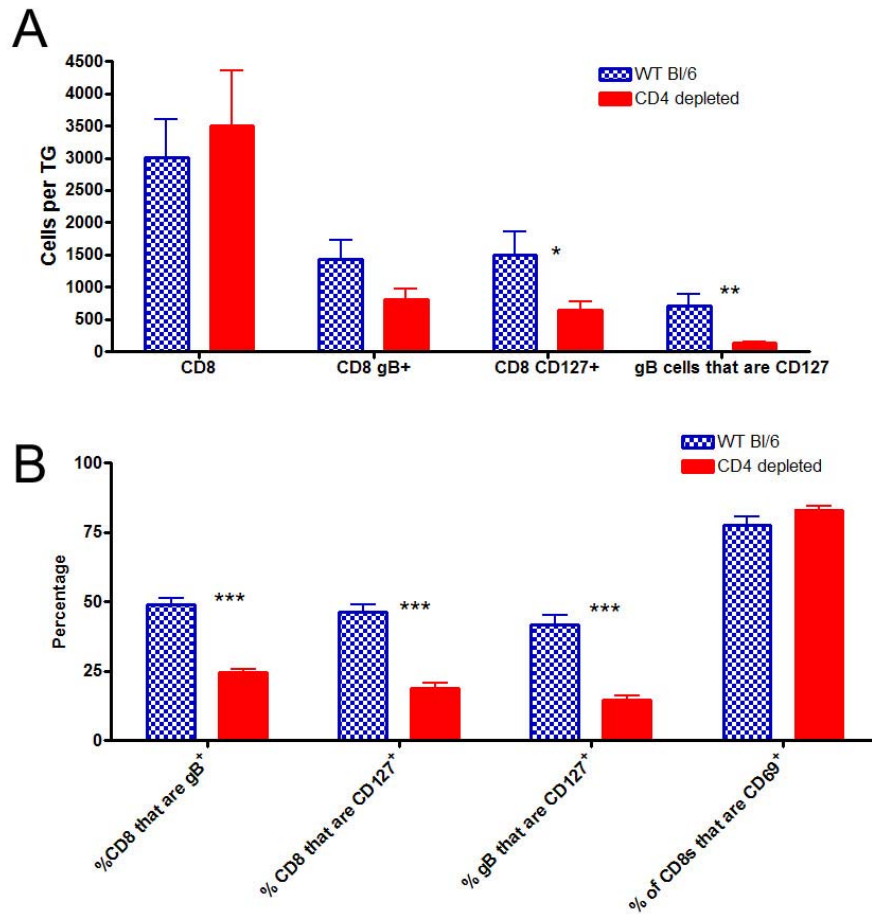
Figure 52: CD4 depletion results in defective generation of memory precursor CD8 T cells at D+19 P.I.

Both eyes of WT and CD4 depleted C57Bl/6 mice (injected with 0.15 mgs of GK1.5 on days -2, +1, +5, +8) were infected with 3X10^5 PFU of HSV-1 RE. The mice were then sacrificed on day +19 P.I. and both TGs were removed, digested into a single cell suspension and then one TG equivalent was subjected to flow cytometry. Mean absolute cell numbers±SEM (A) and percentages of cells±SEM expressing each marker (B) are shown. Asterisks indicate a significant (*, $p < 0.05$; **, $p < 0.01$; ***, $p<0.001$) difference between WT and CD4 deficient mice, as assessed by an unpaired Student's *t* test.

In addition to the changes in phenotype of the CD8 T cells in the TG of CD4 deficient mice at D+19, a decrease in the percentage of CD8 T cells producing IFN-γ in CD4 depleted mice (figure 53) was identified similar to the day +8 P.I. data (see figures 49 and 50). Even though the percentage has decreased, this is due to the reduction in the percentage of CD8 T cells that are gB$_{498-505}$ specific in the total infiltrate as was the case at D+8 P.I.
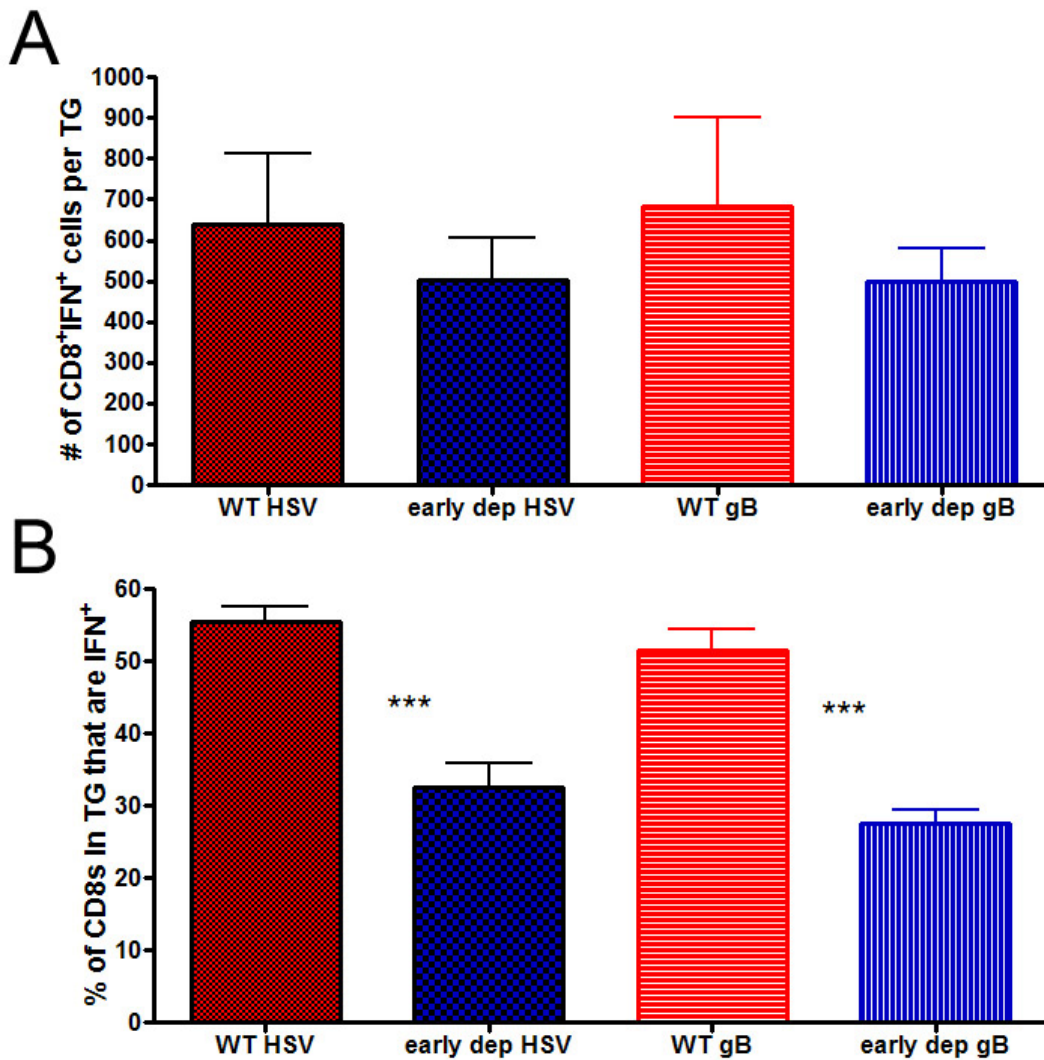
Figure 53: Equivalent numbers of CD8 IFN-γ cells are found in the TGs of CD4 depleted mice at D+19 P.I.

Both eyes of WT and CD4 depleted C57Bl/6 mice (injected with 0.15 mgs of GK1.5 on days -2, +1, +5, +8) were infected with 3X10^5 PFU of HSV-1 RE. The mice were then sacrificed on day +20 P.I. and both TGs were removed, digested into a single cell suspension and then one TG equivalent was stimulated with either 0.5 X 10^6 HSV-infected B6WT3 cells (labeled as HSV) or with 0.5 X 10^6 gB peptide pulsed gB transfected B6WT3 cells (labeled as gB) for

6 hours in the presence of Golgiplug and then stained for intracellular IFN-γ by flow cytometry. Absolute cell numbers±SEM (A) and percentage±SEM of cells producing IFN-γ (B) are shown. Asterisks indicate a significant (*, $p < 0.05$; **, $p < 0.01$; ***, $p<0.001$) difference between WT and CD4 deficient mice, as assessed by an unpaired Student's t test. In (B), significant differences were observed between WT and CD4 depleted mice stimulated with either HSV targets or with gB targets.

Analysis of the MFI of the CD8$^+$IFN-γ$^+$ cells in the CD4 depleted mice at D+19 P.I. revealed a significant reduction compared to WT mice (figure 54). This suggests that virus specific CD8 T cells in CD4 depleted mice are less capable of producing as much IFN-γ per cell as WT mice, as was seen at D+8 P.I.. Whether this drop in the amount of IFN-γ is physiologically relevant is not known.
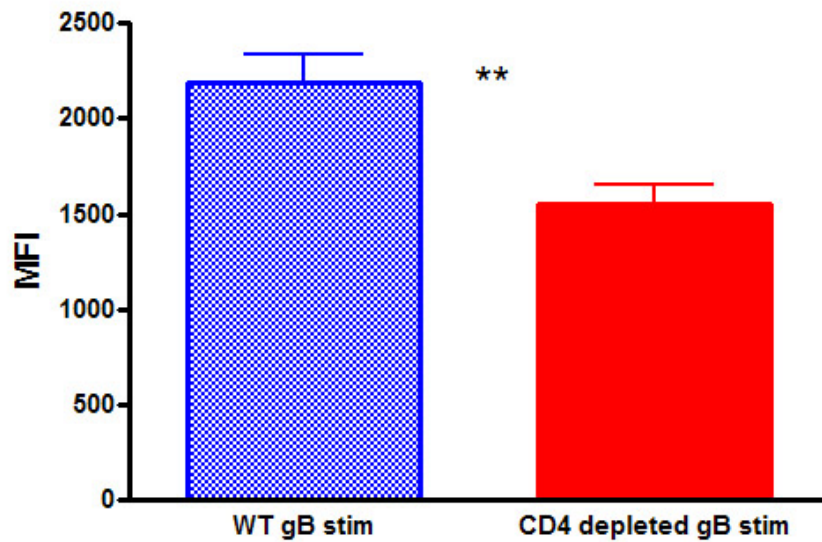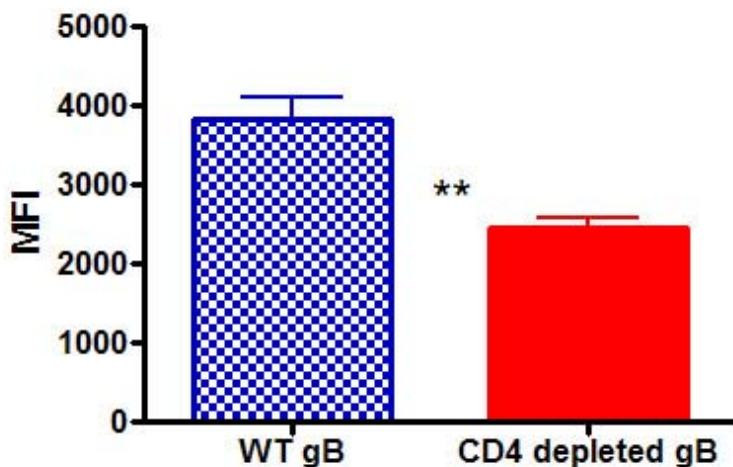

Figure 54: CD8 T cells in the TGs of CD4 depleted mice produce less IFN-γ per cell than WT mice at D+19 P.I.

Both eyes of WT and CD4 depleted C57Bl/6 mice (injected with 0.15 mgs of GK1.5 on days -2, +1, +5, +8) were infected with $3X10^5$ PFU of HSV-1 RE. The mice were then sacrificed on day +20 P.I. and both TGs were removed, digested into a single cell suspension and then one TG equivalent was stimulated with 0.5 X 10^6 gB peptide pulsed gB transfected B6WT3 cells for 6 hours in the presence of Golgiplug and then stained for intracellular IFN-γ by flow cytometry. The resulting IFN-γ$^+$ population was gated and the mean fluorescence intensity of that IFN-γ$^+$ population was determined. Asterisks indicate a significant (*, $p < 0.05$; **, $p < 0.01$; ***, $p<0.001$) difference between WT and CD4 deficient mice, as assessed by an unpaired Student's t test.

4.4.2.3. Does CD4 depletion during priming result in defective CD8 T cell phenotype during latency?

The D35 P.I. time point was chosen to identify whether CD4 depletion during priming would have a long lasting effect on the CD8 T cells. At this time point we observed an interesting phenomenon. When CD4 T cell depletion was not maintained following infection (using only a D-2, +1, +5, +8 treatment regimen), CD4 T cells recovered in most mice between D+32 and D+35. Coincident with CD4 T cell recovery was a massive infiltration of CD8 T cells into the TG (figure 55). This was found not only in the TG, but also in other tissues including the lung (figure 56). If CD4 T cell depletion is maintained, this influx of cells into the TG does not occur.

Low expression of CD127 on the $gB_{498-505}$ specific CD8 T cells was again seen at D+35 P.I. in CD4 depleted mice compared to WT (figure 55). Interestingly, the absolute number of $gB_{498-505}$ specific CD8 T cells at D+35 P.I. in constantly CD4 depleted animals was similar to the absolute numbers in WT mice even though CD4 deficiency caused such a dramatic acceleration of contraction in the CD4 depleted animals at D+14 P.I. (figure 51).
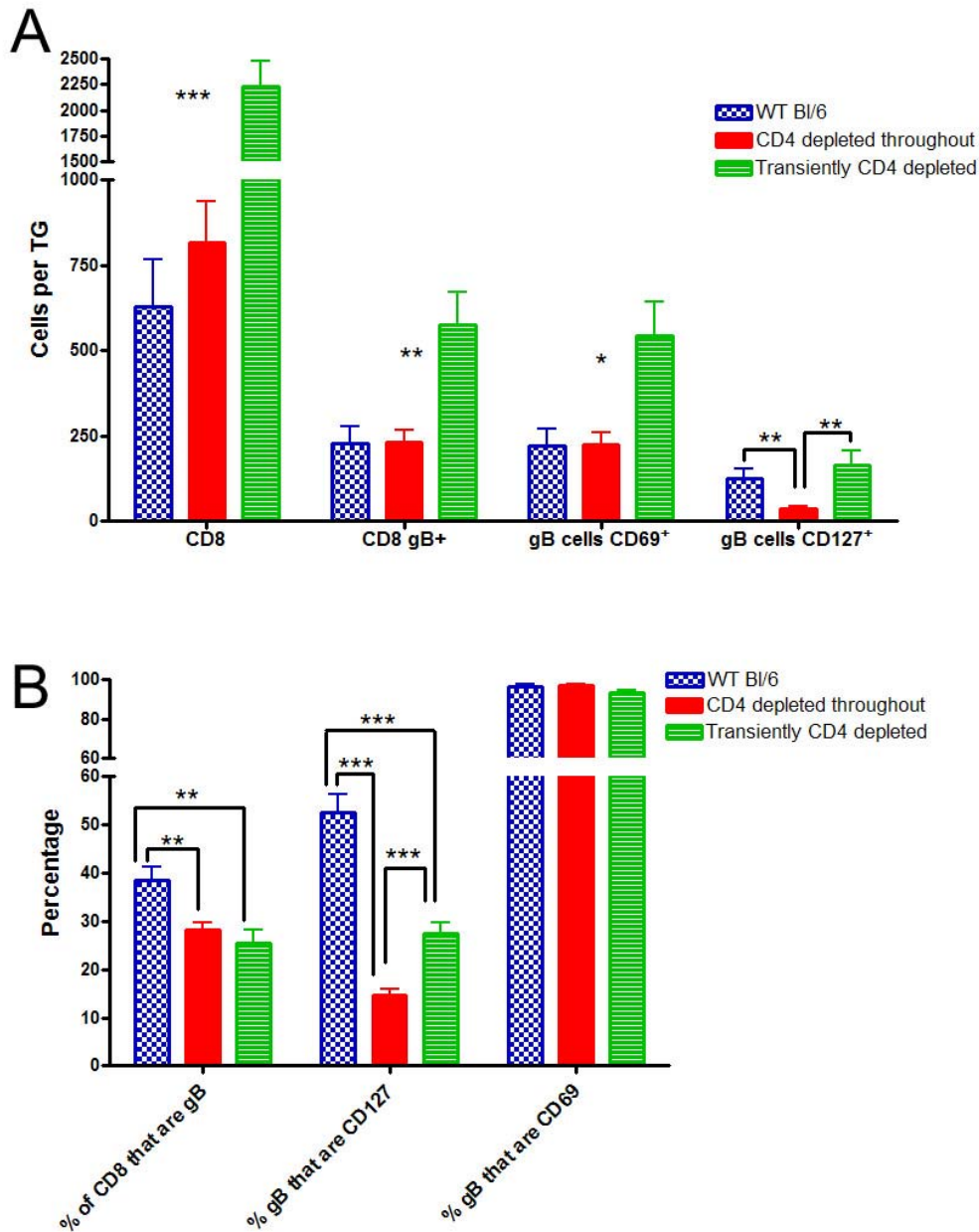
Figure 55: Transient CD4 depletion, but not continuous depletion, results in CD4 replenishment and massive infiltration of CD8 T cells into the TG of mice at D+35.

Both eyes of WT and CD4 depleted C57Bl/6 mice (injected with 0.15 mgs of GK1.5 on days -2, +1, +5, +8 for transiently depleted mice and on days -2, +1, +5, +8, +15, +22, +29 for throughout depleted mice) were infected with 3×10^5 PFU of HSV-1 RE. The mice were then sacrificed on day +35 P.I. and both TGs were removed, digested into a single cell suspension and then one TG equivalent was subjected to flow cytometry. Mean absolute cell numbers±SEM (A) and mean percentages of cells±SEM expressing each marker (B) are shown. Asterisks indicate a significant ($*$, $p < 0.05$; $**$, $p < 0.01$; $***$, $p<0.001$) difference between WT and CD4 deficient mice, as assessed by an unpaired Student's t test.
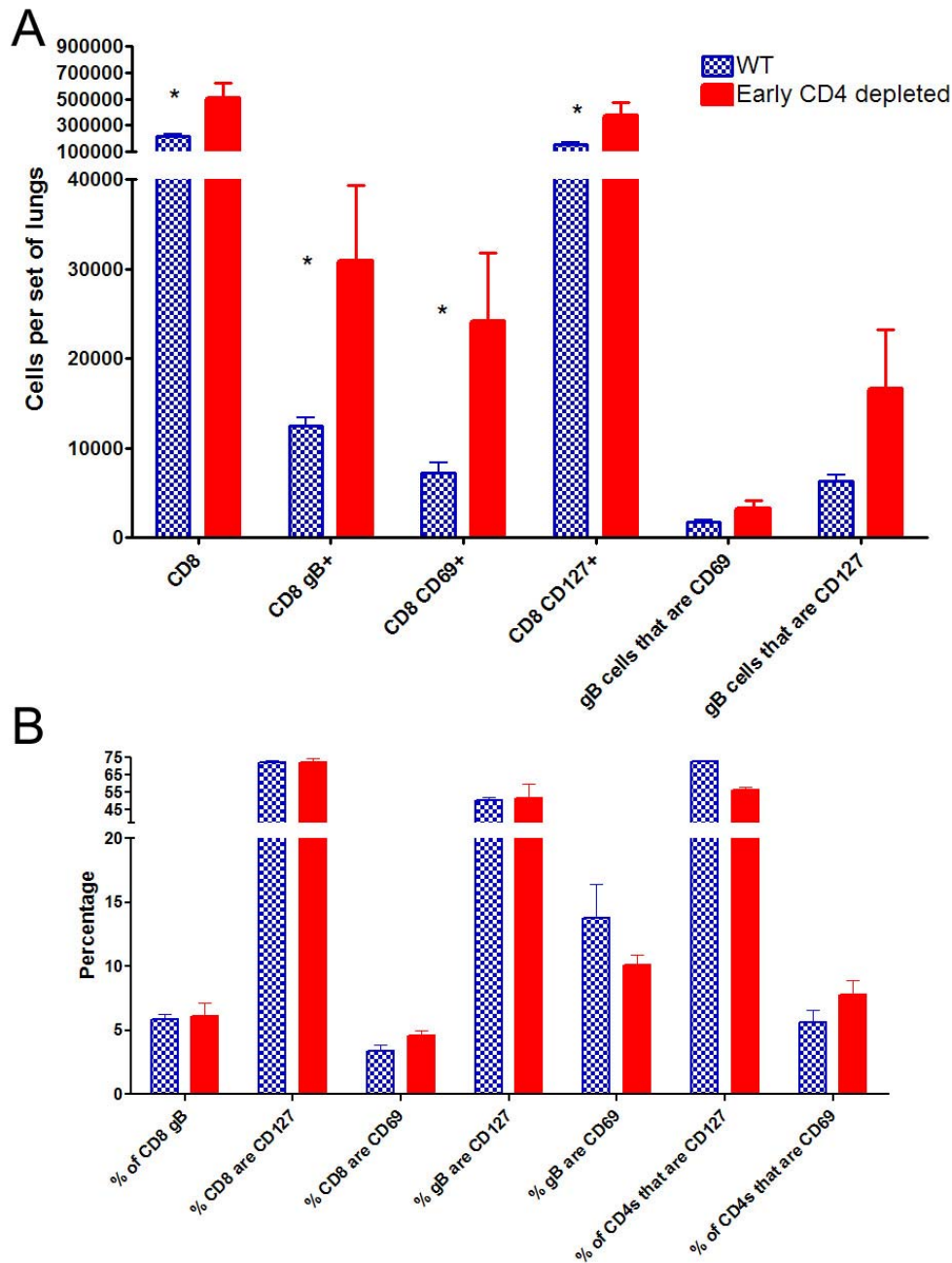
Figure 56: Recovery of CD4 T cells in CD4 depleted mice results in massive T cell infiltration into the lung .

Both eyes of WT and CD4 depleted C57Bl/6 mice (injected with 0.15 mgs of GK1.5 on days -2, +1, +5, +8 for early depleted mice) were infected with $3X10^5$ PFU of HSV-1 RE. The mice were then sacrificed on day +35 P.I. and the lungs were removed, digested into a single cell suspension and then subjected to flow cytometry. Mean absolute cell numbers±SEM (A) and mean percentages of cells±SEM expressing each marker (B) are shown. Asterisks indicate a significant (*, $p < 0.05$; **, $p < 0.01$; ***, $p < 0.001$) difference between WT and CD4 deficient mice, as assessed by an unpaired Student's t test. Five animals were used from each group

Given the findings of increased numbers of CD8s in the TG following CD4 T cell recovery, it was important to identify when this recovery occurs. A large cohort of mice was depleted with anti-CD4 antibody on days -2, +1, +5, +8 and then those mice were sacrificed on days +23, +26, +29, +32 P.I. The goal of these experiments was to identify when and where the massive expansion in the CD8 T cells is occurring when CD4 T cells recover from antibody depletion. One prediction could be that CD8 T cell are expanding in the draining lymph nodes or spleen upon CD4 T cell recovery and then migrating into the TG resulting in the large accumulation observed at D+35 P.I. An alternative explanation may be that the large numbers of CD8 T cells in the TG at D+35 is a result of infiltration of CD4 T cells into the ganglion, which results in proliferation of the CD8 T cell already present in the TG.

Approximately 20% of mice had CD4 recovery in the lymphoid organs at D+23 P.I., but by day +26 P.I., CD4 T cell recovery had occurred in 100% of mice (in the lymph nodes and spleens). Interestingly, CD4 recovery in the TG was very sporadic, with 20% (1 out of 5 tested) of mice showing CD4 recovery in the TG at D+23, 20% (2 out of 10 tested) at D+26, 14% (1 out of 7 tested) at D+29, and 40% (2 out of 5 tested) at D+32. At D35, 100% of all mice transiently depleted of CD4 T cells exhibited CD4 T cell recovery in the TG. This indicates a very rapid recovery occurring in most mice between D+32 and D+35. It is important to note that there was not a large increase in the numbers or percentage of $gB_{498-505}$ specific CD8 T cells in the LNs or spleen at any time suggesting the large numbers of $gB_{498-505}$ specific CD8 T cells in the TG at D+35 in the transiently depleted mice is due to expansion within the ganglion.

The ability of CD8 T cells to produce IFN-γ at D+35 P.I. was tested in transiently CD4 depleted mice (treated with anti-CD4 on days -2, +1, +5, +8 only) (figure 57). It is difficult to interpret the ability of CD8 T cells in the TGs of transiently depleted mice for their ability to

produce IFN-γ due to the massive increase in the numbers of CD8 T cells within the TGs of transiently depleted mice (see figure 55). This data is quite interesting in that it shows that a large number/percentage of the CD8 T cells in the TG following CD4 T cell recovery are indeed virus specific CD8 T cells (figure 57).
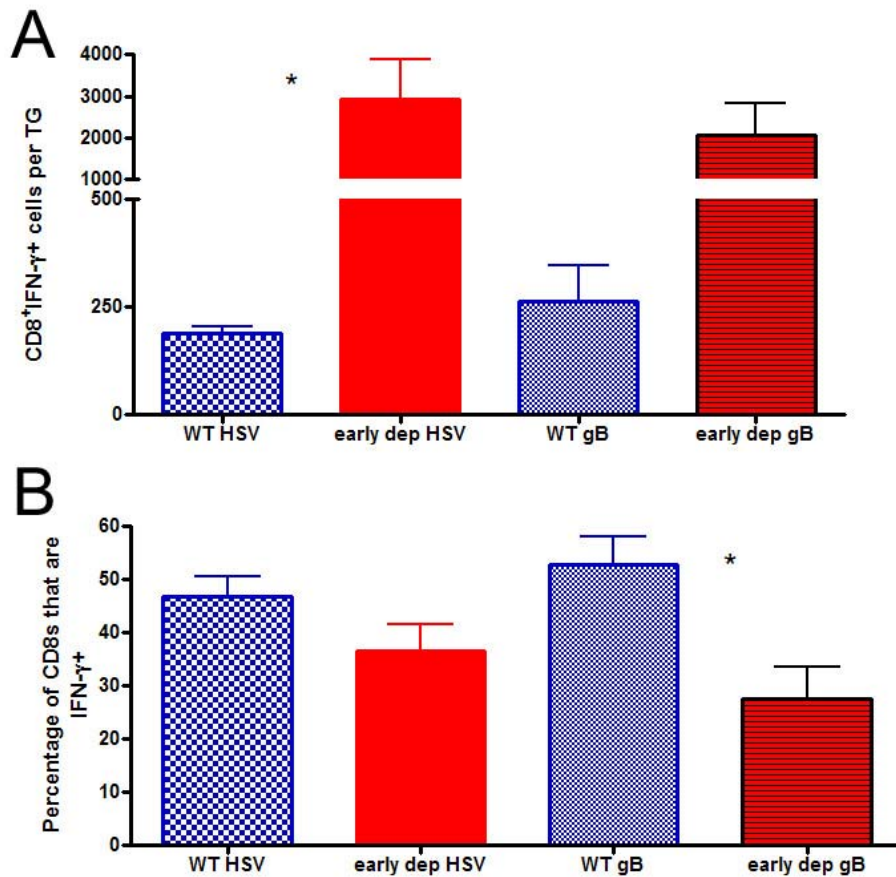
Figure 57: D35 IFN-γ production between WT and transiently depleted mice.

Both eyes of WT and CD4 depleted C57Bl/6 mice (injected with 0.15 mgs of GK1.5 on days -2, +1, +5, and +8) were infected with 3×10^5 PFU of HSV-1 RE. The mice were then sacrificed on day +35 P.I. and both TGs were removed, digested into a single cell suspension and then one TG equivalent was stimulated with either 0.5×10^6 HSV-infected B6WT3 cells (labeled on graph as HSV) or with 0.5×10^6 gB peptide pulsed gB transfected B6WT3 (labeled on graph as gB) cells for 6 hours in the presence of Golgiplug and then stained for intracellular IFN-γ by flow cytometry. Mean absolute cell numbers±SEM (A) and mean percentages of cells±SEM producing IFN-γ (B) are shown. Asterisks indicate a significant (*, $p < 0.05$; **, $p < 0.01$; ***, $p < 0.001$) difference between WT and CD4 deficient mice, as assessed by an unpaired Student's t test.

The ability of CD8 T cells in mice depleted of CD4 T cells throughout to produce IFN-γ was examined (figure 58). Again, similar to D+8 and D+19, a decrease in the percentage of CD8s producing IFN-γ was observed in the CD4 depleted mice which reflects a decrease in the percentage of gB$_{498-505}$ specific CD8s found in the CD4 depleted mice and therefore does not reflect a decrease in the ability of CD8 T cells generated in the absence of CD4 T cells to produce IFN-γ in response to viral antigens. Additionally, the Golgiplug used in this particular experiment may not have been effective as the percentage of cells that are IFN-γ are greatly reduced compared to other experiments at this time point.
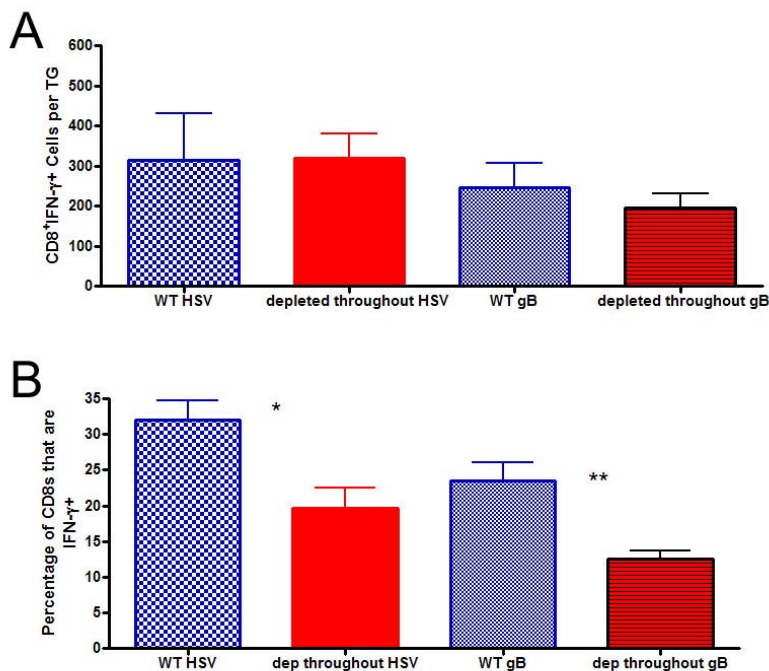
Figure 58: Equivalent numbers of IFN-γ^+ CD8 T cells in WT and CD4 depleted throughout mice at D+35.

Both eyes of WT and CD4 depleted C57Bl/6 mice (injected with 0.15 mgs of GK1.5 on days -2, +1, +5, +8, +15, +22, +29) were infected with $3X10^5$ PFU of HSV-1 RE. The mice were then sacrificed on day +35 P.I. and both TGs were removed, digested into a single cell suspension and then one TG equivalent was stimulated with either 0.5 X 10^6 HSV-infected B6WT3 cells (labeled on graph as HSV) or with 0.5 X 10^6 gB peptide pulsed gB transfected B6WT3 (labeled on graph as gB) cells for 6 hours in the presence of Golgiplug and then stained for intracellular IFN-γ by flow cytometry. Mean absolute cell numbers±SEM (A) and mean percentages of cells±SEM producing

IFN-γ (B) are shown. Asterisks indicate a significant (*, $p < 0.05$; **, $p < 0.01$; ***, $p<0.001$) difference between WT and CD4 deficient mice, as assessed by an unpaired Student's t test.

4.4.2.4.   Does CD4 depletion result in reduced control of viral latency?

We next tested whether the ability of the immune system to maintain HSV-1 latency was perturbed in the absence of CD4 T cells. Previous work using a murine gammaherpesvirus 68 (MHV-68) model of CD4 deficiency illustrated progressive loss of control of latent virus in CD4 KO mice ultimately resulting in the death of those mice (145-147). Viral genome copy number was determined using a sensitive real time PCR method at several time points including D+8, D+14, and D+35 for WT mice and mice depleted throughout (figure 59). At all time points P.I., increased viral genome copy number was found in CD4 depleted mice compared to WT mice.
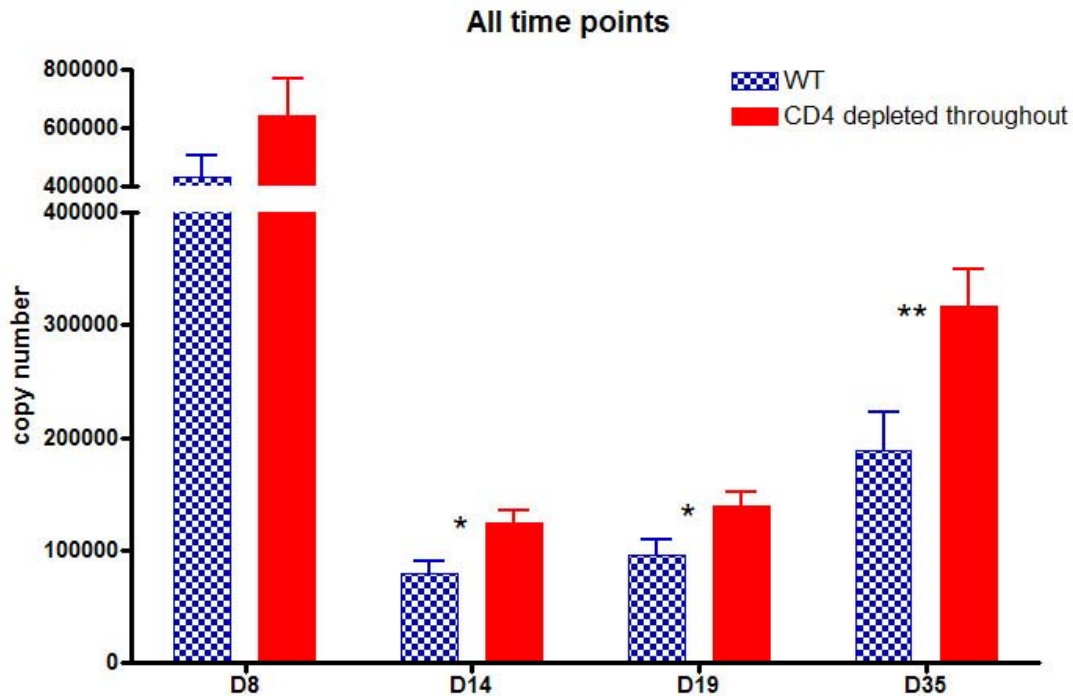
Figure 59: CD4 depletion results in increased viral genome copy number in the TG of C57Bl/6 mice.

Both eyes of WT and CD4 depleted C57Bl/6 mice (injected with 0.15 mgs of GK1.5 on days -2, +1, +5, +8, +15, +22, +29) were infected with $3X10^5$ PFU of HSV-1 RE. The mice were then sacrificed on days +8, +14, +19, and +35 P.I. and both TGs were removed, digested into a single cell suspension and then total DNA was purified from one TG equivalent. Asterisks indicate a significant (*, $p < 0.05$; **, $p < 0.01$; ***, $p < 0.001$) difference between WT and CD4 deficient mice, as assessed by an unpaired Student's *t* test. Data represent mean viral genome copy number±SEM.

4.4.2.5. Kinetics of CD8 T cells in WT and CD4 depleted animals

To better observe the phenotypic changes of CD8 T cells that occur in CD4 depleted mice over time compared to WT data was combined from previous experiments and additional data from time points between D+19 and D+35 was added. The absolute numbers of CD8 T cells and $gB_{498-505}$ specific CD8 T cells over time is shown in figure 60. This figure clearly shows the accelerated contraction phase of the $gB_{498-505}$ specific CD8 T cells that occurs in the CD4

depleted mice compared to WT controls, however as noted previously, the memory CD8 pool is

identical in WT and CD4 depleted mice.
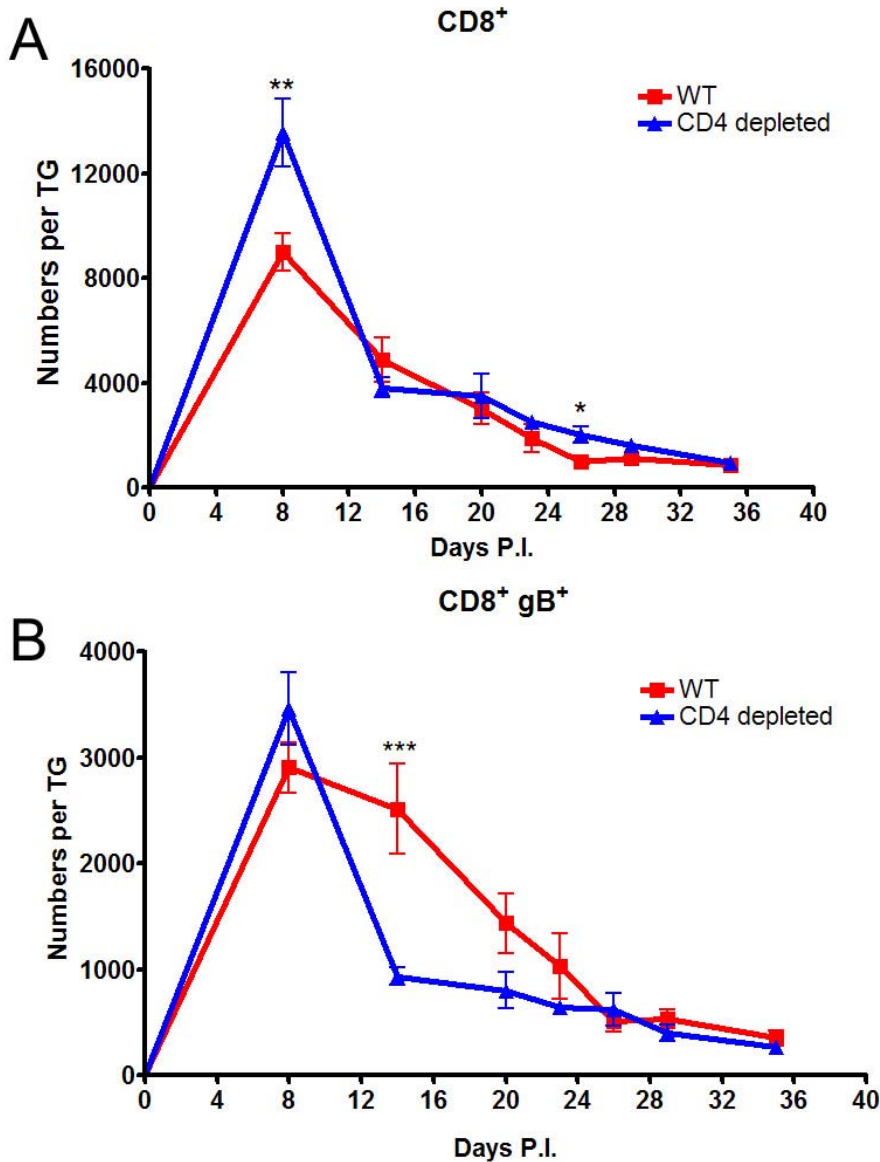
Figure 60: Kinetics of CD8 T cells within the TG of HSV-1 infected C57Bl/6 mice.

Both eyes of WT and CD4 depleted C57Bl/6 mice (injected with 0.15 mgs of GK1.5 on days -2, +1, +5, +8, +15, +22, +29) were infected with $3X10^5$ PFU of HSV-1 RE. The mice were then sacrificed on different days P.I. and both TGs were removed, digested into a single cell suspension and then one TG equivalent was subjected to flow cytometry. Mean absolute cell numbers±SEM are shown. Asterisks indicate a significant (*, $p < 0.05$; **, $p < 0.01$; ***, $p<0.001$) difference between WT and CD4 deficient mice, as assessed by an unpaired Student's *t* test.

One major finding of this work is the reduction in the expression of CD127 on $gB_{498-505}$ CD8s T cells in the absence of CD4 T cells. This was apparent at every time point tested and when this data is graphed kinetically, several important observations can be made (figure 61). First, CD4 depleted animals never develop the normally high percentage of $CD127^+$ $gB_{498-505}$ specific CD8s that are observed in the WT mice. Additionally it was surprising to find that the $gB_{498-505}$ specific CD8 T cells that express CD127 went through the typical three phases of an immune response; expansion, contraction and homeostasis. Both of these observations are clearly depicted in figure 61. Additionally, the level of expression of CD127 on memory T cells was much lower (in terms of MFI and separation from the negative population) than what has typically been reported following an acute infection, however a recent article examining CD127 expression following a persistent infection reports reduced MFI of CD127 on memory CD8 T cells (153,184). Figure 62 shows representative dot plots of $gB_{498-505}$ specific CD8 T cell expression of CD127 over time.
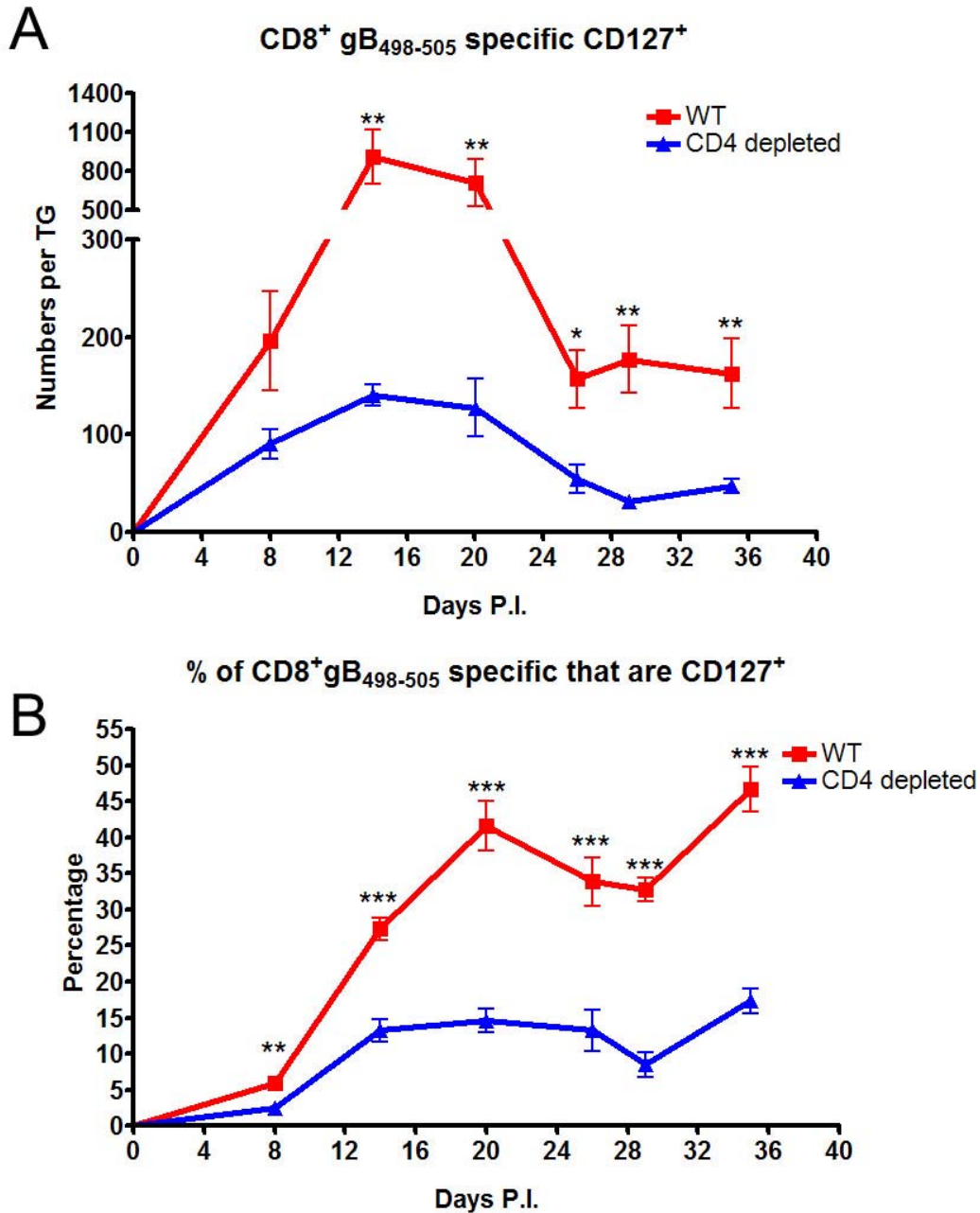
Figure 61: Kinetics of CD127 expression within the TGs of WT and CD4 depleted C57Bl/6 mice.

Both eyes of WT and CD4 depleted C57Bl/6 mice (injected with 0.15 mgs of GK1.5 on days -2, +1, +5, +8, +15, +22, +29) were infected with $3X10^5$ PFU of HSV-1 RE. The mice were then sacrificed on different days P.I. and both TGs were removed, digested into a single cell suspension and then one TG equivalent was subjected to flow cytometry. Mean absolute cell numbers±SEM (A) and mean percentage of cells±SEM expressing CD127are shown. Asterisks indicate a significant (*, $p < 0.05$; **, $p < 0.01$; ***, $p<0.001$) difference between WT and CD4 deficient mice, as assessed by an unpaired Student's *t* test.

124
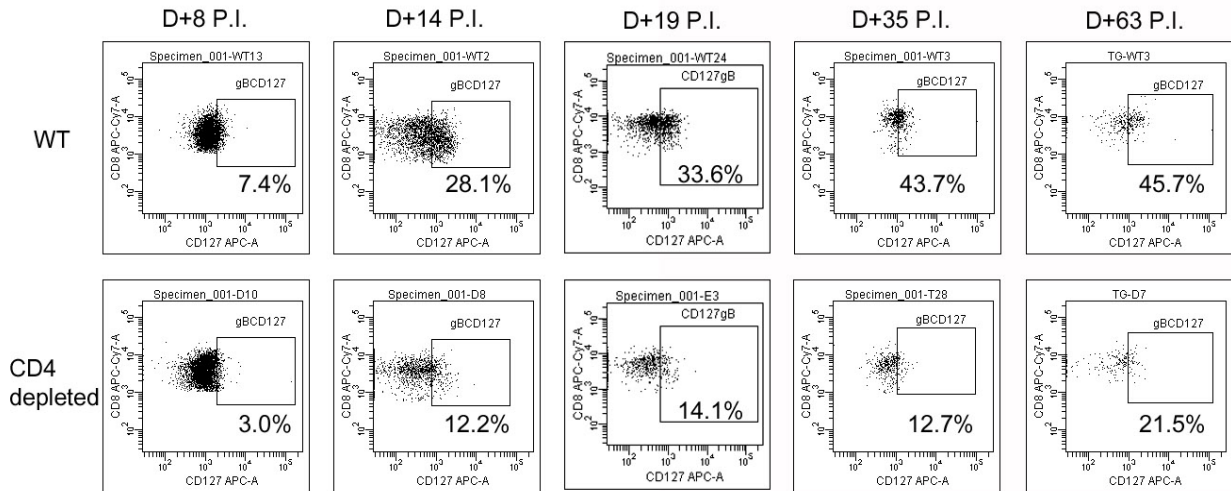
Figure 62: CD127 expression on gB$_{498-505}$ specific CD8 T cells in the TGs of C57Bl/6 mice.

Both eyes of WT and CD4 depleted C57Bl/6 mice (injected with 0.15 mgs of GK1.5 on days -2, +1, +5, +8, +15, +22, +29, +36, +43, +50, +57) were infected with 3X10^5 PFU of HSV-1 RE. The mice were then sacrificed on different days P.I. and both TGs were removed, digested into a single cell suspension and then one TG equivalent was subjected to flow cytometry. Numbers in each dot plot are the percentage of gB$_{498-505}$ specific cells positive for CD127.

4.4.2.6.   Are CD4 T cells required during viral latency?

The next question we wanted to address is whether CD4 T cells play any role in the maintenance of viral latency as has been shown for CD8 T cells (16,90). The prediction that CD4 T cells are actively involved in the maintenance of viral latency is supported by the observation of large numbers of activated CD4 T cells within the TGs of latently infected mice (figure 63). In most cases, CD4 T cells are more numerous than CD8 T cells during viral latency.
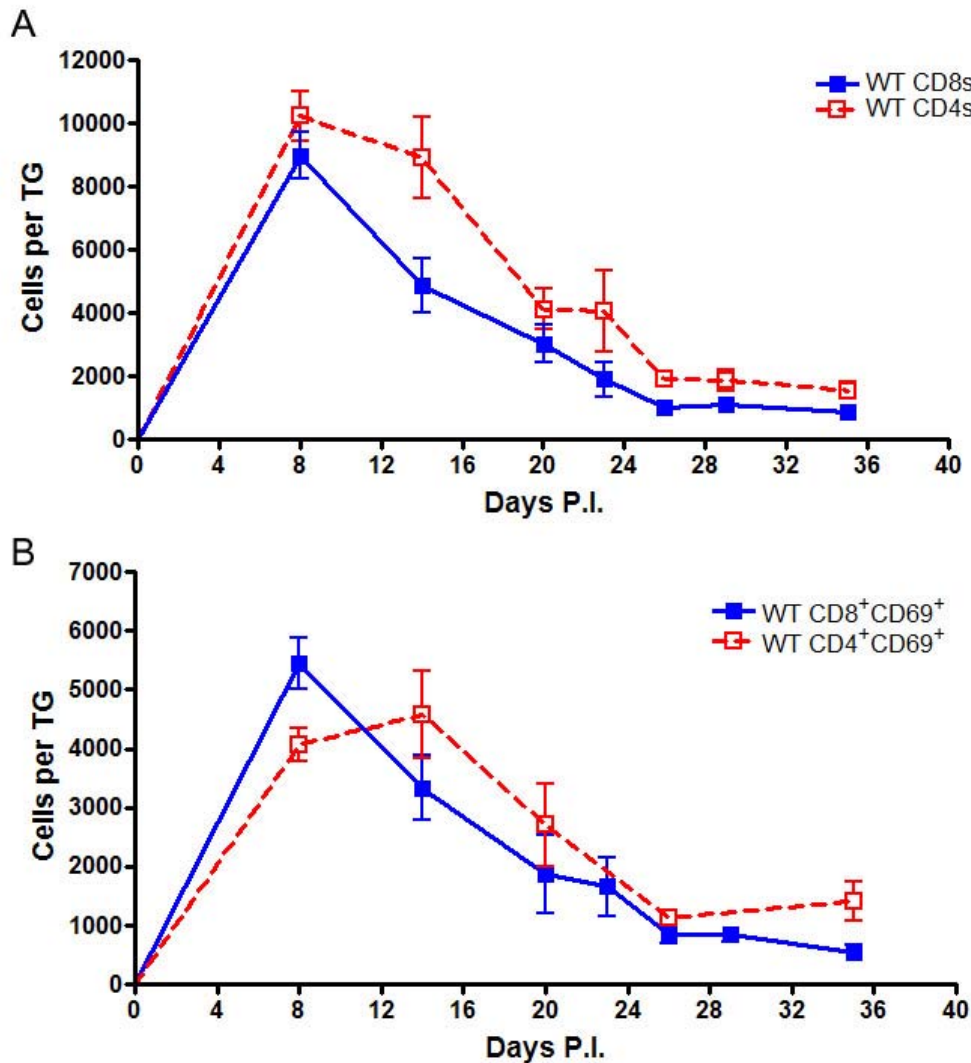
Figure 63: CD4 T cells outnumber CD8 T cells in TGs of C57Bl/6 mice after ocular HSV-1 infection.

Both eyes of WT mice were infected with $3X10^5$ PFU of HSV-1 RE. The mice were sacrificed on different days P.I. and both TGs were removed, digested into a single cell suspension and then one TG equivalent was subjected to flow cytometry. Mean absolute cell numbers±SEM are shown.

The stimulus for the activation of the CD4 T cells in the TG is unknown; however a large number of MHC class II positive cells within latently infected TGs are found. Interestingly, at least three populations of MHC class II^{+} cells are detected in the TGs of Bl/6 mice at D+17 P.I. (figure 64). These MHC class^{+} cells are likely to provide stimulation for CD4 T cells during latency and this is consistent with the notion that CD4 T cells may play an active role during

126

viral latency either through the production of IFN-γ or possibly by maintaining anti-viral CD8 T

cells (16,90).
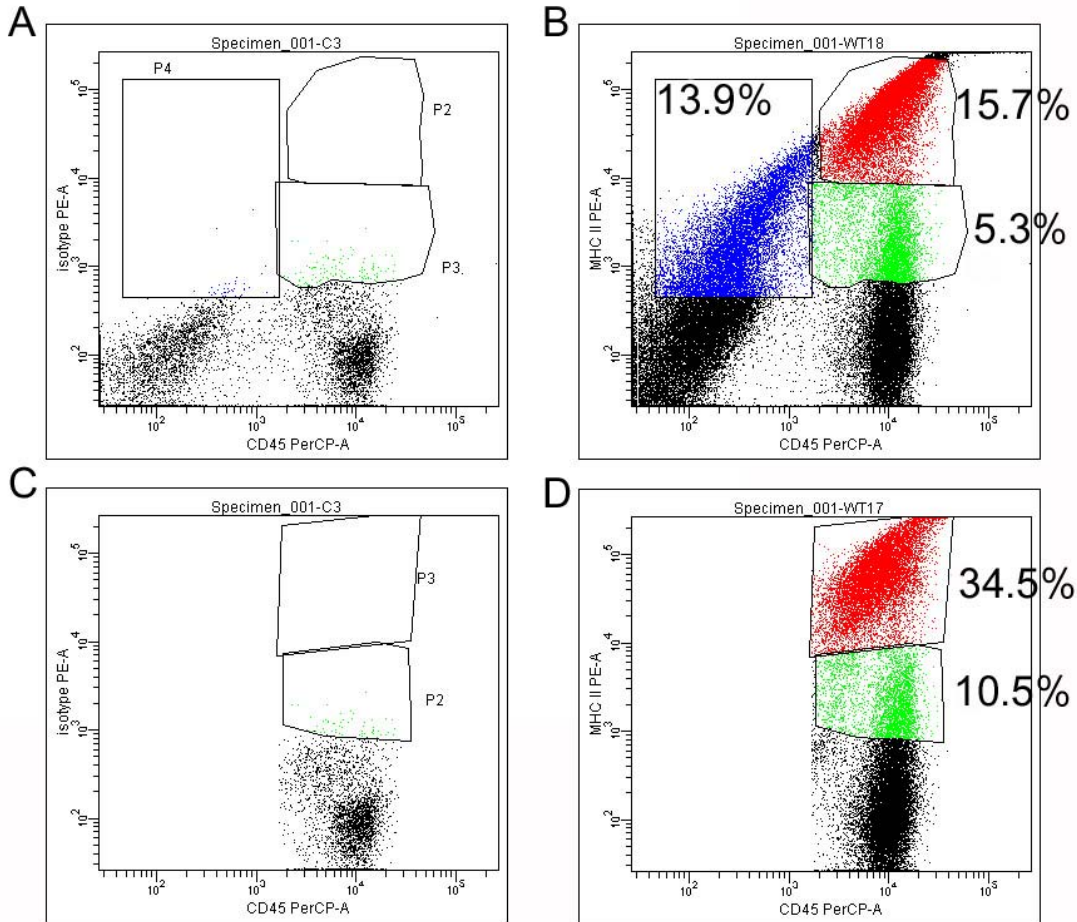
Figure 64: A large population of MHC class II⁺ cells are present in C57Bl/6 TGs at D+17 P.I.

Both eyes of WT mice were infected with $3X10^5$ PFU of HSV-1 RE. The mice were sacrificed on day +18 P.I. and both TGs were removed, digested into a single cell suspension and then one TG equivalent was subjected to flow cytometry. Dot plots in (A,B) were gated only on the live cell population in FSC/SSC and percentages shown in (B) indicate the percent of total cells positive for MHC class II. Dot plots in (C,D) were gated on the live cell population and then on CD45 positive cells. The percentages shown in (D) indicate the percent of CD45⁺ cells that are positive for MCH class II.

Recent work has shown that the maintenance of memory CD8 T cells requires CD4 T cell

help (66). To test if this hypothesis is valid in our model, CD4 T cells were depleted from

latently infected mice and the phenotype and functionality of the CD8 T cells in the TG was examined. CD4 T cells were depleted starting one week prior to the experiment (figure 65) and did not result in any appreciable effects on the CD8 T cell response.
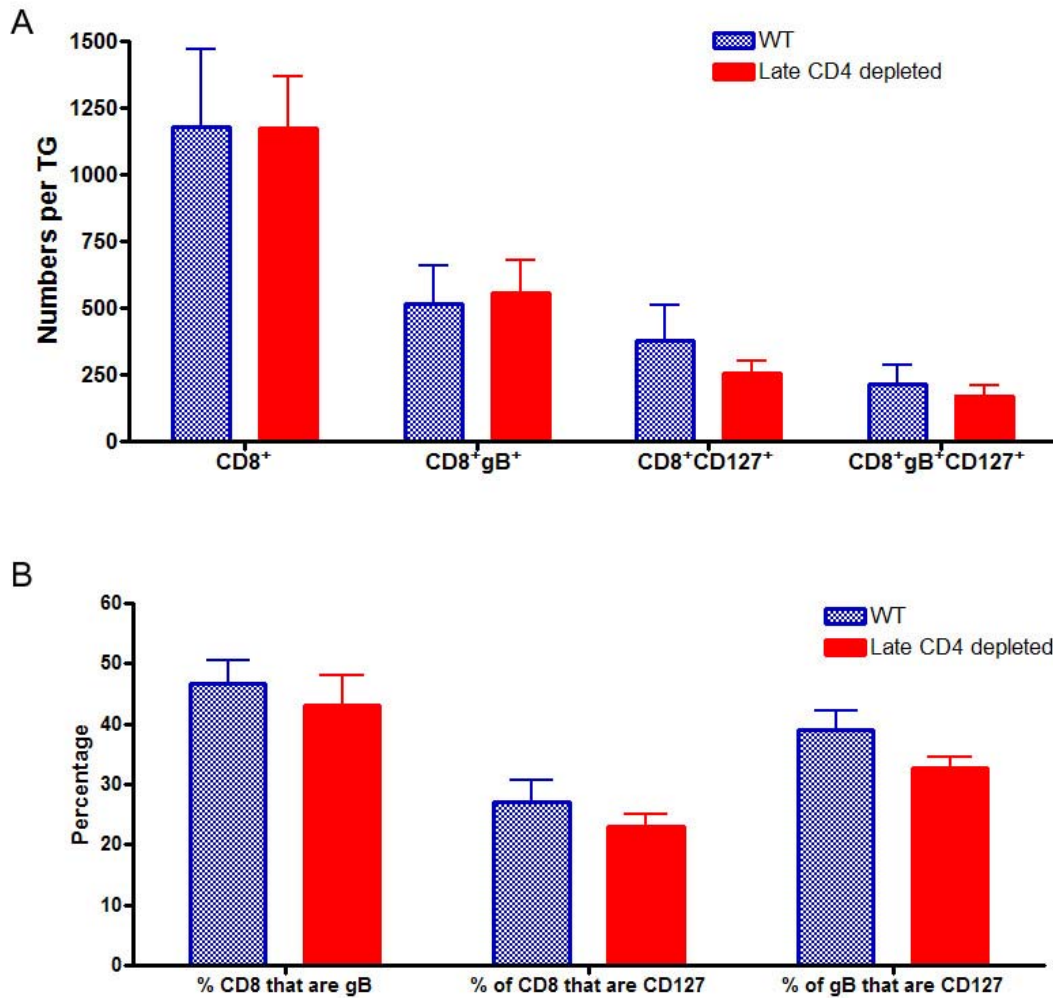
Figure 65: Depletion of CD4 T cells during latency does not affect CD8 T cell phenotype.

Both eyes of WT and CD4 depleted C57Bl/6 mice (injected with 0.15 mgs of GK1.5 on days +28, +30, +33) were infected with $3X10^5$ PFU of HSV-1 RE. The mice were then sacrificed on day 35 P.I. and both TGs were removed, digested into a single cell suspension and then one TG equivalent was subjected to flow cytometry. Mean absolute cell numbers±SEM (A) and mean percentages of cells expressing each marker ±SEM (B) are shown. Asterisks

indicate a significant (*, $p < 0.05$; **, $p < 0.01$; ***, $p<0.001$) difference between WT and CD4 deficient mice, as assessed by an unpaired Student's *t* test.

The functionality of CD8 T cells after CD4 depletion during latency was tested by intracellular cytokine staining. CD4 T cells were depleted starting on day +28 P.I. and then every other day through D+35 P.I. Depletion of CD4 T cells for one week during latency did not affect the ability of the CD8 T cells to produce IFN-γ in response to viral antigens.
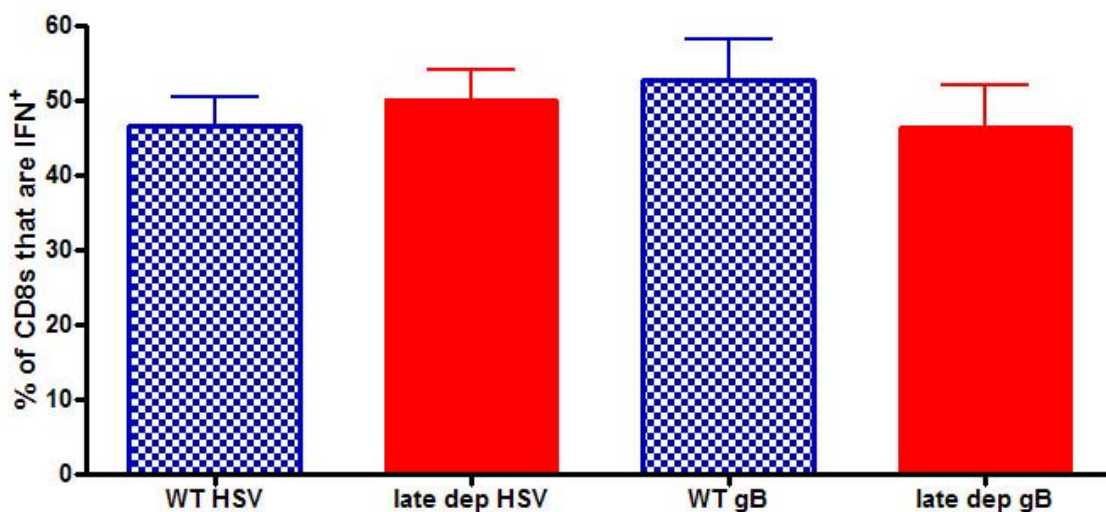
Figure 66: Depletion of CD4 T cells from day 28 through day 35 P.I. does not affect the functionality of virus specific CD8 T cells in the TG.

Both eyes of WT and CD4 depleted C57Bl/6 mice (injected with 0.15 mgs of GK1.5 on days +28, +30, +33) were infected with $3X10^5$ PFU of HSV-1 RE. The mice were then sacrificed on day +35 P.I. and both TGs were removed, digested into a single cell suspension and then one TG equivalent was stimulated with either 0.5×10^6 HSV-infected B6WT3 cells (labeled on graph as HSV) or with 0.5×10^6 gB peptide pulsed gB transfected B6WT3 (labeled on graph as gB) cells for 6 hours in the presence of Golgiplug and then stained for intracellular IFN-γ by flow cytometry. Mean percentages of cells±SEM producing IFN-γ are shown. Asterisks indicate a significant (*, $p < 0.05$; **, $p < 0.01$; ***, $p<0.001$) difference between WT and CD4 deficient mice, as assessed by an unpaired Student's *t* test.

One could argue that depletion of CD4 T cells for only one week is too short of a period of time to assess the effects of CD4 T cell on the maintenance of CD8 T cell memory. To test this, mice were depleted of CD4 T cells for two weeks during latency and then CD8 T cell phenotype (figure 67) and functionality (figure 68) was tested. The possible concern in the

generation of this data is that depletion began at a time when contraction is still occurring (depletion was started on day +15 P.I. and then on days +17, and +19, +22, +29). Depletion of CD4 T cells during latency had minimal effect on CD8 T cell phenotype and functionality.
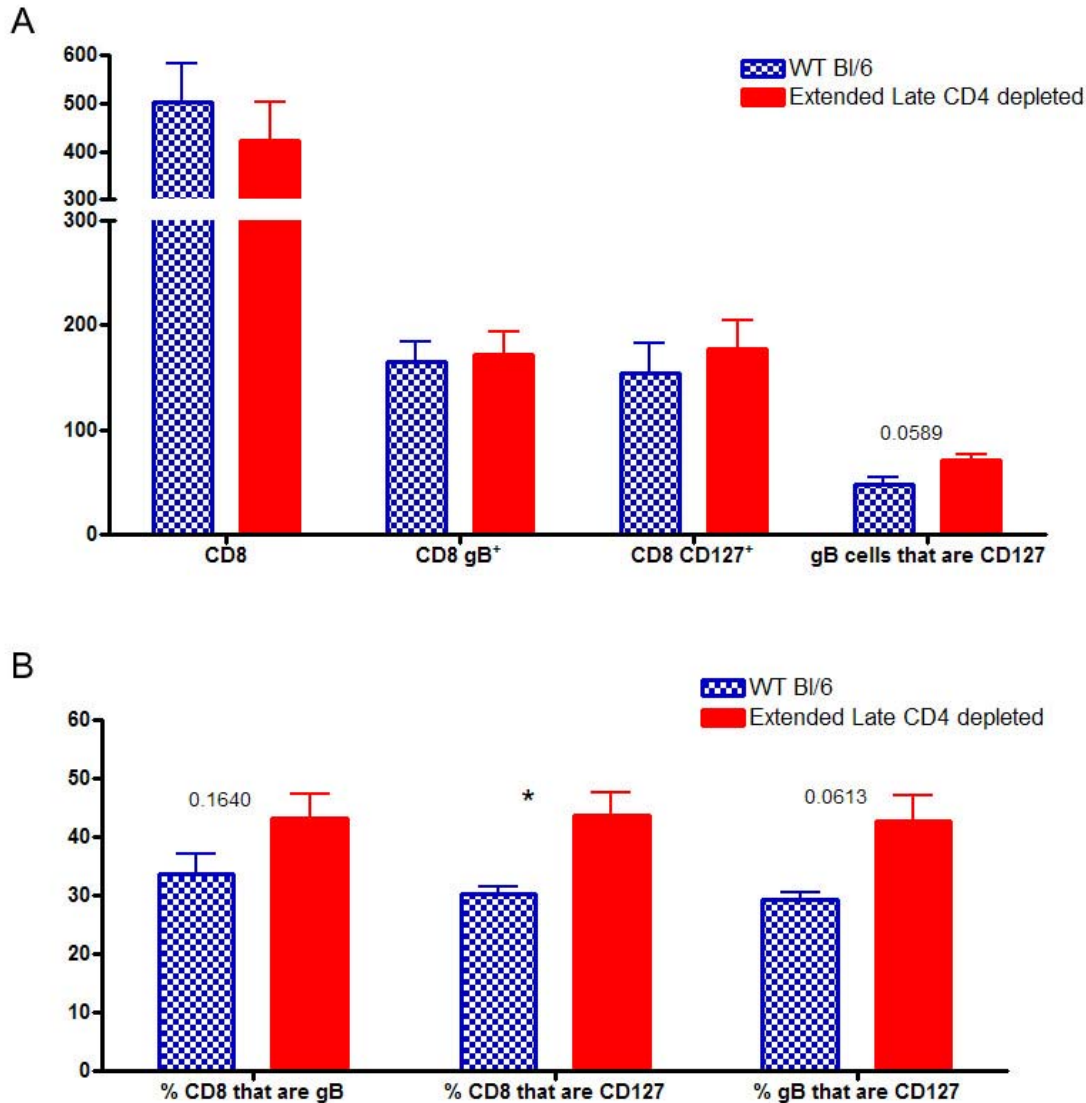
Figure 67: Extended late term depletion results in increased expression of CD127.

Both eyes of WT and CD4 depleted C57Bl/6 mice (injected with 0.15 mgs of GK1.5 on days +15,+17,+19,+22,+29) were infected with 3×10^5 PFU of HSV-1 RE. The mice were then sacrificed on day +35 P.I. and both TGs were removed, digested into a single cell suspension and then one TG equivalent was subjected to flow cytometry. Mean absolute cell numbers±SEM (A) and percentages of cells±SEM expressing each marker (B) are shown. Asterisks indicate a significant (∗, $p < 0.05$; ∗∗, $p < 0.01$; ∗∗∗, $p < 0.001$) difference between WT and CD4 deficient mice, as assessed by an unpaired Student's t test.
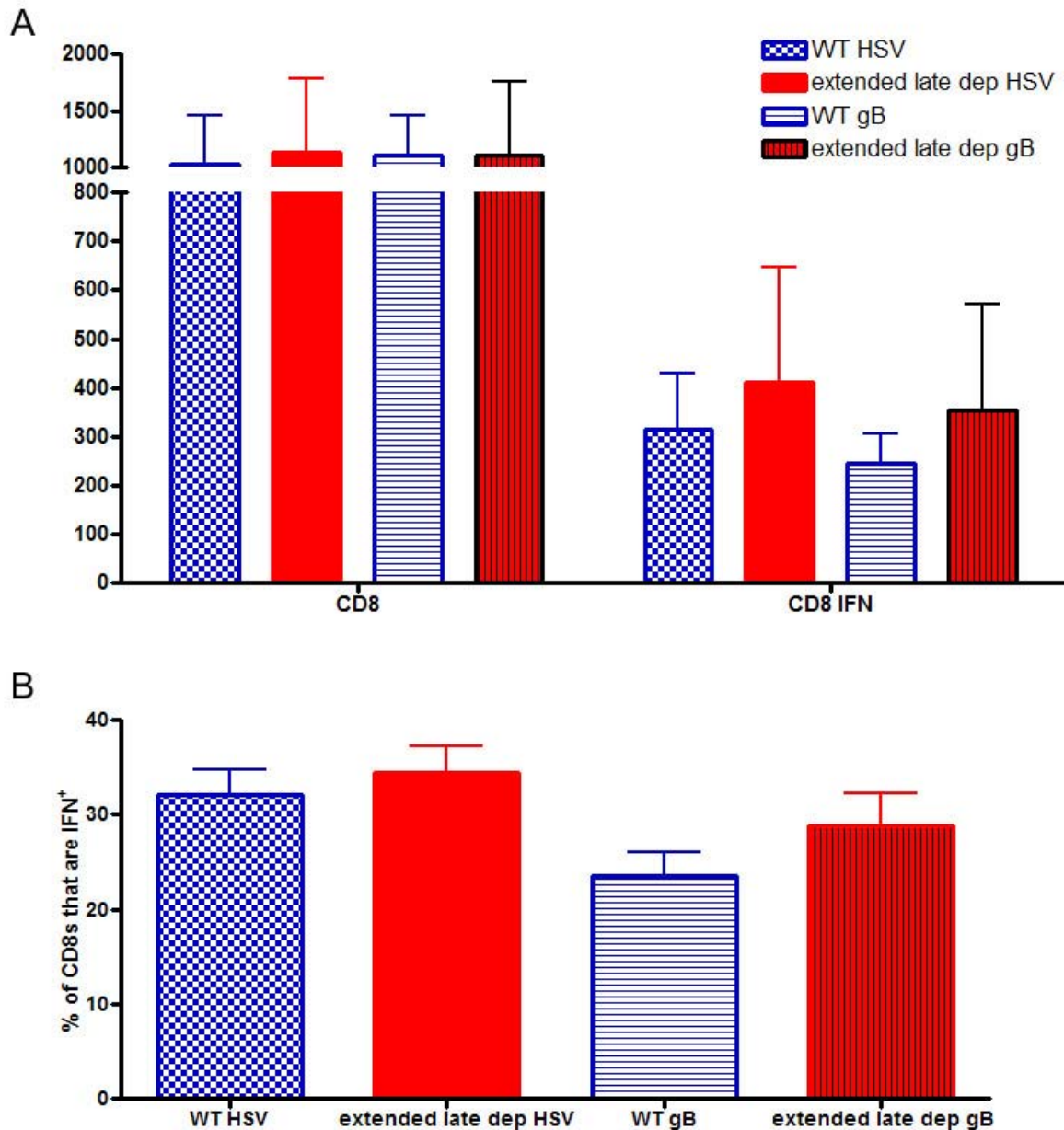
Figure 68: Depletion of CD4 T cells from D15 through D35 does not affect the ability of CD8 T cells in the TG to respond to viral antigens.

Both eyes of WT and CD4 depleted C57Bl/6 mice (injected with 0.15 mgs of GK1.5 on days +15,+17,+19,+22,+29) were infected with $3X10^5$ PFU of HSV-1 RE. The mice were then sacrificed on day +35 P.I. and both TGs were removed, digested into a single cell suspension and then one TG equivalent was stimulated with either 0.5×10^6 HSV-infected B6WT3 cells (labeled as HSV) or with 0.5×10^6 gB peptide pulsed gB transfected B6WT3 cells (labeled as gB) for 6 hours in the presence of Golgiplug and then stained for intracellular IFN-γ by flow cytometry. Absolute cell numbers±SEM (A) and percentages±SEM of cells producing IFN-γ (B) are shown. Asterisks indicate a significant (*, $p < 0.05$; **, $p < 0.01$; ***, $p<0.001$) difference between WT and CD4 deficient mice, as assessed by an unpaired Student's t test.

This data demonstrates that CD4 T cells are not absolutely required for the maintenance of CD8 T cell numbers, phenotype or functionality in C57Bl/6 mice during latency. A potential limitation of these studies is that one or two week CD4 depletion is not a sufficiently long enough time period to observe the effects of CD4 deficiency on CD8 T cell responses. Additionally, it would be important to identify if any changes in viral genome copy number is observed in mice depleted of CD4 cells during latency.

5.   Discussion

The short story of Dr. Jekyll and Mr. Hyde provides an interesting metaphor for the immune response to ocular HSV-1 infection. On one hand (Dr. Jekyll), the immune system does its job following the initial infection in the eye of recruiting PMNs into the eye to eliminate the invading virus. This helpful role of the immune response results in the elimination of the cytopathic virus from the surface of eye, however the virus is a bit quicker than the host and gains access to the numerous nerve termini in the corneal epithelium, where it is then able to travel to the trigeminal ganglion. Again the immune response can be compared to the benevolent Dr. Jekyll, in that the TG is heavily infiltrated by host immune cells, specifically γδ T cells and macrophages, which are able to eliminate this viral invader. This elimination is not complete, as the virus enters a state of latency, characterized by low level gene expression that the host immune system is unable to completely eliminate. The virus is capable of reactivating after a stressor, resulting in new live infectious virus that can travel back to the site of initial infection.

While control of the virus is occurring in the TG, Mr. Hyde makes his entrance in the cornea. After the first wave of PMNs clear the initial virus from the eye, they disappear and the eye appears to be saved. In both mice and humans, however, a second more robust wave of PMNs begins to enter the cornea. In our mouse model this begins around 7-10 days P.I. and also includes the infiltration of T cells. This aberrant immune infiltration into the cornea in the absence of live virus results in immunopathology in the eye and is termed herpes stromal keratitis (HSK). These PMNs and T cells contribute to corneal blindness by their mere presence and the production of collagenases and other proteolytic enzymes by the PMN culminating in the breakdown of the highly organized collagen matrix that composes the cornea stroma. In addition,

disruption of the endothelium during HSK results in increased hydration of the cornea, which also likely contributes to the disease.

Given these findings, one must be careful when attempting to reduce the immunopathology in the cornea by immunosuppression, more specifically one must be careful not to suppress the positive effects of the immune system in the TG. We cannot treat the infected individual suffering from HSK with a <u>systemic</u> immunosuppressant, since numerous studies have shown that the immune system is important in the control of the virus when it is in a latent state within the TG. Based on these facts, the common treatment for HSK is local steroid treatment coupled with antiviral medication. The steroid drops that are placed on the eye can help eliminate the immunopathology in the eye without affecting the protective immune response in the TG.

5.1.   Can CD134/OX40L interactions be targeted for alleviation of HSK?

Previous work in our lab has shown that effector CD4 T cells that infiltrate infected corneas of mice require B7.1:CD28 costimulation to mediate HSK (38). This provided the first demonstration that effector T cells require costimulation within an inflammatory site (36). CD28 is constitutively expressed by CD4 T cells (and some CD8 T cells), making it undesirable for immune modulation in HSV-1 infection, since T cells can play both a positive and negative role following ocular HSV-1 infection. An alternative would be to target a molecule that is expressed only on activated T cells. Additionally, treatment at the site of immunopathology would reduce the inflammation, without affecting the protective cells present at others sites. Targeting an inducible marker would also spare naive T cells that may be necessary for future infections. Ideally, this molecule would be expressed only on pathogenic T cells that infiltrate the cornea and mediate HSK. The molecule CD134 was targeted for several reasons; CD134 is expressed only on activated CD4 T cells, blockade of CD134/OX40L interactions alleviates numerous

inflammatory diseases, CD134/OX40L blockade does not appear to appreciably affect CD8 T cell responses (which are important for the maintenance of viral latency in the TG (16,90)), and signaling through CD134 is as potent a T cell stimulus as CD28 signaling, which has been shown to be necessary for HSK (38,125). We hypothesized that CD134/OX40L interactions are required for pathogenic CD4 T cell activation within the cornea, and that blockade of CD134/OX40L would ameliorate clinical HSK.

Both CD134 and OX40L were expressed within the corneas of mice with HSK (figures 5-8). In agreement with previous work, CD134 was exclusively expressed on CD4 T cells (figures 8 and 11). $CD4^+CD134^+$ cells were detected in the corneas of mice as early as 3 days P.I. with peak numbers observed at D+14. The observation of $CD134^+$ cells as early as D+3 P.I. is very surprising as peak expression of CD134 on naïve CD4 T cells occurs 48 hours post-TCR engagement (116,186). This data suggests that activated CD4 T cells migrate into the cornea very rapidly after infection. An alternative explanation is that there may be a very small population of resident CD4 T cells in the normal cornea; however this is unlikely as work in our lab has shown an absence of CD4 T cells in uninfected mouse corneas (67). At the peak expression of CD134 (D+14), most CD134 expression was restricted to CD4 T cells, based upon both whole mount cornea staining and flow cytometry analysis. A significantly lower proportion of CD4 T cells in infected corneas expressed CD134 (15%, Figure 11) than expressed another activation marker, CD69 (25%, Figure 34). Notably, the frequency of $CD134^+$ cells closely approximated the frequency of $CD4^+$ T cells that produced IFN-γ when stimulated with viral antigens (~15%, Figure 35). This is consistent with the notion that CD134 expression is regulated by TCR signaling, whereas CD69 expression reflects both antigen specific and bystander activation. In agreement with this hypothesis is the observation that corneas of

D011.10 mice with HSK contain both Ova-specific and non-Ova-specific CD4$^+$ T cells that express CD69 (figure 30). Additionally, the percentage of CD4 T cells that express Vβ8.3 in the corneas of mice with HSK is very similar again to the percentage of CD4 T cells that express CD134 and are virus specific. We propose that virus specific CD4 T cells in the corneas of mice with HSK express both CD134$^+$ and Vβ8.3$^+$.

Interestingly, expression of OX40L differed from our expectations based on current literature. OX40L costained only with CD45 but not with cd11c or MHC class II. This was surprising since expression of OX40L is reported to be restricted to antigen presenting cells such as dendritic cells, macrophages and B cells (125). Expression of OX40L was not observed in the cornea until day +7 P.I., with peak numbers observed at D+14 P.I., which is consistent with a recent review that suggests that OX40L expression is the limiting factor in CD134/OX40L interactions in vivo (187). The lack of expression of OX40L on antigen presenting cells was discouraging and suggested that CD134/OX40L interactions may not be necessary for the activation of CD4 T cells in the cornea during HSK.

It is interesting to speculate why antigen presenting cells do not express OX40L in the cornea. Previous work has clearly shown that other costimulatory molecules are expressed by antigen presenting cells in the cornea including B7.1 and B7.2 (38), so why is OX40L excluded? It is feasible to propose that the activation needed to induce expression of OX40L on antigen presenting cells in the cornea is higher than for other costimulatory molecules such as B7.1. It is very possible that the amount of viral antigen present in the cornea during HSK is very low and is probably supplied to antigen presenting cells through nerve termini from the latently infected TG (134). The expression of OX40L on MHC class II$^-$ cells might suggest that the cell type expressing OX40L in the cornea is the resident corneal macrophage population described by

Brissette-Storkus et al (67). This study clearly demonstrated a resident population of CD45$^+$cd11b$^+$F4/80$^+$ cells that are MHC class II$^-$, however the authors did not address costimulatory molecule expression on those cells. Notably, OX40L has been demonstrated on cd11b$^+$ cells (123), therefore it is plausible that the cell type expressing OX40L in vivo during HSK is this resident macrophage population that is CD45$^+$ but MHC class II$^-$.

Given the fact that both CD134 and OX40L are expressed in corneas during HSK, in vivo blocking experiments were performed to address if HSK can be alleviated by CD134/OX40L blockade. Several strategies were developed to test our hypothesis that CD134/OX40L interactions are required for the development of HSK. To rule out a possible effect on the inductive phase of the immune response to HSV-1, mice received systemic treatment prior to corneal infection with an antagonist anti-OX40L antibody (RM134L). This antibody has been shown to be effective at alleviating numerous inflammatory diseases including experimental autoimmune encephalomyelitis (168), colitis (188), graft versus host disease (127), and rheumatoid arthritis (122). Systemic treatment with RM134L during T cell priming did not reduce the incidence or severity of HSK (figure 12). This data suggested that CD134/OX40L interactions are not needed during the inductive phase of the CD4$^+$ T cell response to HSV-1, consistent with most literature indicating CD134/OX40L interactions take over after B7/CD28 interactions have occurred (125). To address the requirement for CD134-OX40L interaction locally in the cornea during development of HSK, mice received subconjunctival injections every other day (day 7-19 pi) of 50µg of either with RM134L or a soluble CD134 fusion protein. Although the antibody effectively diffused into the cornea (Figure 15), it did not have a palliative effect on HSK (figures 13 and 14).

In another series of experiments, CD134/OX40L interactions were disrupted systemically starting right before disease onset (figure 16). This treatment strategy was used in the attempt to block effector CD4 T cell migration into the cornea since CD134/OX40L interactions have been shown to be critical for migration of effector CD4 T cells into inflammatory sites (168). Again, this treatment strategy failed and no beneficial effects of RM134L treatment on HSK incidence or severity was detected (figure 16).

As a final attempt to ameliorate HSK, CD134/OX40L interactions were disrupted following a reduced infectious dose that has been shown to cause CD4-dependent disease (figures 37 and 38). In one experiment, a reduction in the incidence of HSK in RM134L treated mice was observed, but this result was not reproducible (figure 17).

We conclude that even though both CD134 and OX40L are expressed within corneas of mice with HSK, these interactions are dispensable for disease development similar to CD40/CD40L interactions (113). Nonetheless, these findings will form the basis for future studies testing the efficacy of cocktails of reagents capable of blocking multiple potentially redundant costimulatory interactions within the infected cornea. Such combined treatments might prove efficacious in ameliorating this potentially blinding immunoinflammatory reaction.

5.2. What is the antigen specificity of CD4 T cells infiltrating the corneas of mice with HSK?

Currently, at least three mechanisms have been proposed to explain CD4 T cell involvement in HSK (189). These include bystander activation (171,179,190), molecular mimicry/autoimmunity (133,170,191,192), and virus specific activation. Both bystander activation and molecular mimicry have been shown in the mouse model, however a role for virus specific activation has not been identified. When CD4$^+$ T cells were expanded from human corneas with HSK, virus specific, but not autoreactive CD4 T cells were recovered

(128,129,172), while reactivity to corneal antigens (autoreactivity) has been shown to not occur (129). The role of bystander activated cells in human HSK is currently unknown.

HSK is a CD4+ T cell-mediated immunopathologic process that is regulated in part by Th1 cytokines. One approach to determining a role for HSV-1 specific CD4+ T cells in this process is to determine if such cells are present in corneas with HSK, and if they produce Th1 cytokines when stimulated directly ex vivo with HSV-1 antigens. This was the case in human corneas and now we have found it to be true in our mouse model as shown by the generation and characterization of virus specific CD4 T cell clones from mice with HSK.

The finding that all of the virus specific CD4 T cell clones express a single Vβ is similar to human studies (172) and could be explained by one of two possibilities. First, this may be due to a selective outgrowth of Vβ8.3$^+$ CD4 T cells during the initial generation of the cell line. In support of this, the original cell line (THSK3.30) exclusively expresses Vβ 8.3. The reason why this TCR expressing cell type would be selectively grown out during culture is unknown. It should be noted that the T cell line was expanded using a polyclonal stimulus (anti-CD3 and anti-CD28 stimulation), which should not result in selective outgrowth of a particular clone.

A second alternative is that Vβ 8.3 cells are virus specific and predominate in the corneas of mice with HSK at the very early stages of HSK, and are slowly 'diluted' out at disease progresses (depicted in figure 69). This might explain the skewing of the T cell line THSK 3.30 to Vβ8.3 since the cell line was started from corneas of mice at D+11 P.I., a time at which HSK has just started to develop. We propose that virus specific CD4 T cells that infiltrate the eye (depicted in red in figure 69) express Vβ 8.3 and are the prominent TCR Vβ cell type present in the cornea during the very early stages of HSK (days 7-11). As disease progresses (D+14 and later), and viral antigen availability decreases, the inflammatory cytokines and chemokines

produced by the virus specific CD4 T cells (Vβ 8.3[+]) recruit virus non specific CD4 T cells expressing another Vβ, (perhaps Vβ 8.1.2) into the cornea.
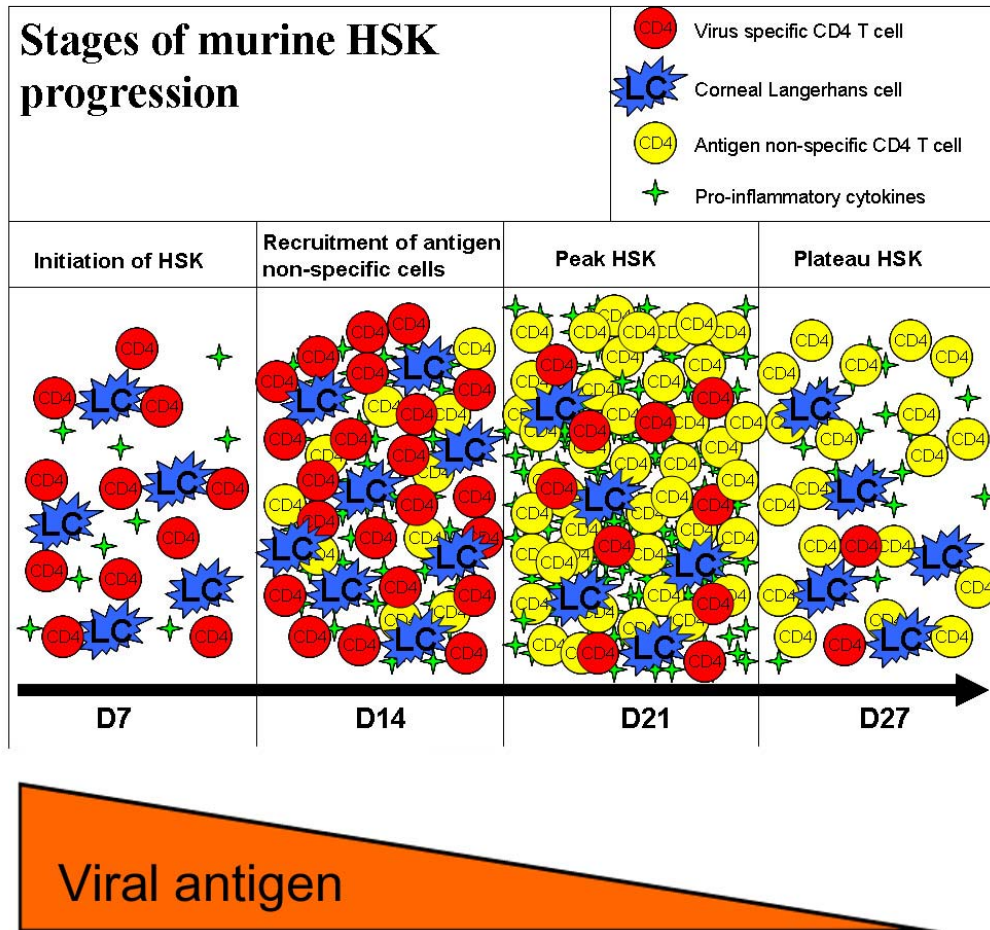
Figure 69: Proposed model for murine HSK in relation to the relative contribution of both virus specific and non-specific CD4 T cells.

We propose that the initiation of HSK occurs due to the infiltration of virus specific CD4 T cells that may express V beta 8.3. These cells are activated by corneal APCs that have been exposed to high levels of viral antigens during the primary infection. These virus specific CD4 T cells respond to these antigens and produce inflammatory cytokines including IL-2 and IFN-γ along with chemokines that induce the recruitment of virus non-specific CD4 T cells into the cornea. These virus specific CD4 T cells wane over time to decreasing viral antigen presence and the virus non-specific CD4 T cell predominate the CD4 infiltrate and maintain HSK.

This is consistent with our data (figure 24) and others (178) that show a preferential skewing of Vβ 8.1.2 expressing CD4 T cells in HSK lesions during peak disease (D+14). Correlative evidence that the Vβ 8.3 cells represent the virus specific CD4 T cell population in corneas with HSK can be seen when comparing the percentage of CD4 T cells that produce IFN-γ directly ex vivo at D+14 P.I. to the percentage of CD4 T cells expressing Vβ 8.3 also at D+14. Typically 10% of CD4 T cells express Vβ 8.3 at D+14 and ~10-15% of CD4 T cells produce IFN-γ after viral antigen stimulation at D+14. To test the hypothesis that Vβ 8.3$^+$ CD4 T cells are the virus specific cell population in corneas with HSK, corneal CD4 T cells were stimulated directly ex vivo with DC pulsed with viral antigen and were then costained for Vβ 8.3 vs IFN-γ or Vβ 8.1.2 vs IFN-γ. The prediction would be that only CD4 T cells expressing Vβ 8.3 produce IFN-γ in response to viral stimulation, however we were unable to effectively stain for any Vβ on CD4 T cells following stimulation due to TCR downregulation and loss from the surface (data not shown).

The next step to answering this question directly could involve two different approaches; 1) stain CD4 T cells for Vβ 8.3 at early time points to identify if indeed most of the CD4 T cells present in early HSK lesions express this particular Vβ, 2) sort Vβ 8.3$^+$ CD4 T cells from corneas at different times P.I. and stimulate that population with viral antigens to observe if a very high percentage of those cells respond to viral stimulation. Our predictions from these two experiments would be: a high percentage of CD4 T cells express Vβ 8.3 in early HSK lesions and following sorting on Vβ 8.3 CD4 T cells, a very high percentage of these cells will produce IFN-γ, while the rest of the CD4 T cells left over after the sort would show little to no viral reactivity.

The ability of the virus specific CD4 T cell clones to induce HSK in a normally resistant animal model, the nude mouse (79) was then tested. Adoptive transfer of clone AA, a virus specific CD4 T cell clone that produces high amounts of IFN-γ after virus specific stimulation, into nude mice resulted in HSK. Interestingly, not only did the nude mice develop HSK, but they resolved periocular skin disease and were protected from encephalitis (figure 26). The resolution of periocular skin disease is consistent with proper migration into the skin around the eye and production of IL-2 and IFN-γ which have been shown to provide protection in the skin after ocular HSV-1 infection (104). Additionally, a beneficial effect on nude mouse survival upon adoptive transfer of these virus specific CD4 T cell clones (figure 26) was detected, which is somewhat surprising as most literature suggests CD8 T cells to be the major contributor to viral control/maintenance in the TG (16,90,132,148,149). Confirmation that the adoptively transferred CD4 T cells did migrate into the both the TG and cornea is shown in figure 27, and is consistent with studies showing that CD4 T cells can protect mice from encephalitis following ocular HSV-1 infection (87,88). It is important to note that nude mice adoptively transferred with bulk CD4 T cells from D+6 P.I. lymph nodes had numerous CD4 T cells also within the TG; however these cells did not appear to provide as much protection from encephalitis as clone AA. This may be explained by the fact that the D+6 LN CD4 T cells contain a mix of virus specific and virus-nonspecific CD4 T cells and since 10^7 cells of either clone AA (all of which are virus specific) or LN CD4 (only some of which are virus specific) were transferred, the partial protection afforded by the adoptive transfer of D+6 LN CD4s may merely reflect a dose dependent effect.

Given the ability of the virus specific CD4 T cell clone AA to cause HSK in nude mice and its ability to protect nude mice from death, studies were initiated to identify what specific viral antigen is being recognized by these T cells. A preliminary study utilized cell lysates that

were generated from Vero cells infected for various periods of time with HSV-1 in order to separate the different classes of viral genes (see figure 22). This study provided preliminary evidence that an early or late viral gene product is the target of the CD4 T cell clones. In most cases, the CD4 T cell clones responded better to the 5 and 10 hour lysates, which would correspond to times at which the levels of early and late proteins would be highest. These findings are consistent with several reports illustrating CD4 T cell recognition of the late viral gene product gD (173,174). To better understand the identity of the CD4 T cell stimulus, plasmids encoding several different HSV-1 glycoproteins (including gD), have been obtained, expressed in 293T cells and cell lysates of these have been generated to test the CD4 T cell clones for specificity. These studies are currently underway.

5.3.   Are CD4 T cells absolutely required for HSK development?

Studies of HSK in mice have lead to the general conclusion that T cells play a requisite role (79), and that CD4^{+} T cells are the primary mediators of disease (80,102,103).   The involvement of CD8^{+} T cells in HSK is less clear. Numerous studies have demonstrated a large preponderance of CD4^{+} T cells over CD8^{+} T cells in HSK lesions. In our experience, CD8^{+} T cells are either undetectable or outnumbered by CD4^{+} T cells by almost 10:1 in HSV-1 infected corneas of wild type mice following infection with HSV-1 RE. This relative lack of CD8^{+} T cells in HSK lesions is particularly interesting in view of the fact that these cells are prominently present in the infected trigeminal ganglia of the same mice (figures 41-46). We demonstrate that in the absence of CD4^{+} T cells, CD8^{+} T cells can infiltrate HSV-1 infected mouse corneas, which subsequently develop HSK (figure 34). Since T cell-deficient mice including nude (79), SCID (80), or WT mice depleted of both CD4^{+} and CD8^{+} T cells (our unpublished observation) fail to develop HSK following HSV-1 corneal infection, we conclude that CD8^{+} T cells can infiltrate

infected corneas of CD4$^+$ T cell-deficient mice and mediate HSK. Thus, the paucity of CD8$^+$ T cells in HSK lesions of wild type mice does not appear to reflect an intrinsic capacity of infected mouse corneas to exclude CD8$^+$ T cells. In fact, the number of CD8$^+$ T cells in the infected corneas of CD4-deficient mice during the early stages of HSK was greater than the number of CD4$^+$ T cells in the infected corneas of WT mice (figure 34).

These findings invite conjecture that the presence of CD4$^+$ T cells within the infected cornea in some way inhibits the infiltration of CD8$^+$ T cells. In this regard, it is interesting to note that adoptively transferred HSV-1 specific CD8$^+$ T cells were absent from the HSV-1 infected corneas of DO11.10/SCID mice, in which apparent bystander activation of Ova-specific CD4$^+$ T cells lead to HSK (171). Thus, even Ova-specific CD4$^+$ T cells that have presumably never encountered antigen more efficiently accumulate in HSV-1 infected corneas than HSV-1 specific CD8$^+$ T cells.

In a recent study, HSV-1 corneal infection of OT-1 mice on a RAG$^{-/-}$ background resulted in infiltration and apparent bystander activation of Ova-specific CD8$^+$ T cells leading to the development of HSK (132). Since the OT-1/RAG mice are deficient in CD4$^+$ T cells, this again suggests that in the absence of CD4$^+$ T cells, CD8$^+$ T cells can infiltrate the infected cornea and be activated. Interestingly, when HSV-1 specific CD8$^+$ T cells were adoptively transferred into these mice, they were found in the trigeminal ganglion, but not in the infected corneas. The authors concluded that HSV-1 specific CD8$^+$ T cells were excluded from the infected corneas of these mice, whereas Ova-specific, presumably naïve CD8$^+$ T cells could enter and be activated. Although we did find a significant population of HSV-1 specific CD8$^+$ T cells in the infected corneas of CD4-deficient mice, the percentage of CD8$^+$ T cells that were HSV-1 specific was markedly lower in the infected corneas than in the infected trigeminal ganglia of these same mice

(compare figure 35 with figures 45 and 46). Moreover, the percentage of CD8$^+$ T cells that were HSV-1 specific in the corneas of CD4-deficient mice was significantly lower than the percentage of CD4$^+$ T cells that were HSV-1 specific in corneas of wild type mice. Together, these findings are consistent with the notion that activated CD8$^+$ T cells might be preferentially, though not absolutely excluded from the cornea.

What might be responsible for this apparent exclusion of activated CD8$^+$ T cells from the infected mouse corneas? A clue might be found in a previous study comparing the HSK induced in A/J mice by the KOS and RE strains of HSV-1 (103). The RE strain induced a predominantly neutrophilic infiltrate in which CD4$^+$ T cells greatly outnumbered CD8$^+$ T cells. In contrast, corneal infection with the KOS strain resulted in HSK lesions consisting of a largely mononuclear infiltrate in which CD8$^+$ cells were the dominant T cell population. Depletion of CD8$^+$ T cells prior to KOS HSV-1 corneal infection diminished the incidence and severity of HSK. It was noted that the KOS strain was a poor inducer of dendritic cell (DC) migration into the cornea (normally devoid of DC). Moreover, when DC migration into the cornea was induced prior to KOS HSV-1 corneal infection, the corneal infiltrate resembled that of RE infected corneas (mainly PMN and a preponderance of CD4$^+$ over CD8$^+$ T cells). In another study, depletion of DC from the peripheral cornea prior to HSV-1 infection abrogated the development of HSK (109). Together, these findings suggest that the infiltration of DCs might directly or indirectly create a microenvironment within the cornea that favors infiltration of CD4$^+$ T cells and PMN, while discouraging infiltration of activated CD8$^+$ T cells. This might also explain the lack of involvement of CD8$^+$ T cells in corneal allograph rejection, a situation also characterized by migration of DC into the grafted cornea (193,194).

Although CD8$^+$ T cells are able to mediate HSK, in our model the disease was somewhat milder and decidedly more transient than that mediated by CD4$^+$ T cells in wild type mice. One possible explanation for the reduced duration of HSK in this model is that the HSV-1 specific CD8$^+$ T cells that infiltrate the corneas of CD4-deficient mice destroy the APCs that are required for antigen presentation and/or bystander activation that leads to prolonged inflammation. This would account for the normal initiation, but short duration of HSK in CD4-deficient mice. In this regard, it is of interest that the HSK caused entirely by bystander activation of Ova-specific CD8$^+$ T cells in C57BL/6 mice, showed no signs of diminution within a 25 day observation period (132). We would propose that the prolonged inflammation in these corneas might reflect the inability of Ova-specific CD8$^+$ T cells to destroy HSV-1 infected APCs.

A second explanation for the short duration of HSK in CD4-deficient mice might relate to the impaired CD8$^+$ T cell memory response that is induced in the absence of CD4$^+$ T cells (136-138). In general it is found that CD4$^+$ T cells are not required for the initial development of effector CD8$^+$ T cells, but a long-term memory CD8$^+$ T cell response is not generated when CD4 T cells are absent during priming. We note a virtually complete loss of CD8$^+$ T cells in the corneas of the CD4-deficient mice late in infection when HSK was diminished, which is also accompanied by a loss of CD8 numbers in the TG (figure 41). In contrast, CD4$^+$ T cells were continuously present in the infected corneas of wild type mice, where HSK was chronic. In this scenario, the diminished HSK might result from a gradual exhaustion of the HSV-1 specific effector CD8$^+$ T cells, and failure to establish long-term memory.

An important observation in this study is that the requisite involvement of CD4$^+$ T cells in HSK is dependent on the dose of HSV-1 used to infect the cornea. Relatively low (perhaps more physiologic) doses of HSV-1 that uniformly induced HSK in wild type mice were

inefficient at inducing HSK in CD4-deficient mice. It is currently unclear why low dose infection fails to induce CD8$^+$ T cell-mediated HSK in the corneas of CD4-deficient mice. Some preliminary exploration into this question revealed that the total number of CD8 T cells was reduced in the DLNs of KO mice infected with a low dose of HSV compared to a high dose infection (figure 40). Additionally, the activation status of the CD8 T cells (CD69) was reduced in the draining lymph nodes of CD4 KO mice infected with a low dose of HSV. Unfortunately, we did not test the DLNs of WT BALB/c mice infected with high dose vs low dose. It is possible that a higher dose of virus is required to induce a potent effector CD8$^+$ T cell response in the absence of CD4$^+$ T cell help. Alternatively, less viral protein production in the cornea might be required to activate infiltrating CD4$^+$ T cells. Regardless of the explanation, it is important to note that most studies of HSK incorporate doses of HSV-1 that are more than two logs higher than that necessary to induce disease, and that the HSK induced at high doses of virus is not necessarily CD4$^+$ T cell-dependent. We would suggest that greater consistency in infectious dose, virus strain, and mouse strain used in studies of HSK might resolve some of the confusion that has hampered progress in understanding this blinding disease.

5.4. Do CD4 T cells influence CD8 T cell phenotype and function in the TG?

Recent work in our lab has clearly demonstrated a requisite role for CD8 T cells in the maintenance of HSV-1 latency in the TG (16,90,148,149). In this thesis we ask how do CD4 T cells regulate CD8 T cell responses that are important for the establishment (84) and maintenance of viral latency (16,90). Numerous studies have recently emerged addressing the role of CD4 T cell help in the generation (135,137,195) and maintenance of antigen specific CD8 T cell responses (66,138). The role of CD4 T cells during the three basic phases of a CD8 T cell

immune response; priming, contraction and maintenance/memory phase following ocular HSV-1 infection in both BALB/c and C57Bl/6 mice are addressed in this thesis.

5.4.1.   In BALB/c mice

The studies began in CD4 KO BALB/c mice, where equivalent numbers of CD8 T cells were detected in the TGs of both WT and KO mice at D+14 P.I., but then KO mice exhibited a sharp drop in T cell numbers (figure 41). This sharp decline in CD8 T cell numbers in the TGs of CD4 KO was also observed in CD4 depleted mice (figure 41). This data suggests that the effector population of CD8 T cells is generated in CD4 deficient mice, but they are gradually lost over time. This finding can be explained by one of several possibilities.

First, the CD8 T cells that were generated in the absence of CD4 T cell help are 'programmed' incorrectly and are thus unable to respond to viral antigen stimulation during latency. The production of viral transcripts during latency is well documented (and in some cases viral antigens are also detected) and is further supported by the findings of our lab and others that T cells expressing markers of recent activation are present in the TG throughout latency (14,90,91,148,149). We hypothesize that the low levels of viral antigen produced during latency represents a 'pseudo-rechallenge' to CD8 T cells that are in the TG. Since CD8 T cells are not programmed properly in CD4 deficient hosts, they are unable to respond to these 'pseudo-rechallenges' by proliferating and therefore wane over time. WT mice, however, have properly programmed CD8 T cells that respond to these 'pseudo-rechallenge' events in the TG by proliferation and effector cytokine secretion and is consistent with a very recent publication reporting fluctuations in CD8 T cell responses during HSV latency (196). This may explain why we find a stable pool of CD8 T cells in the TGs of latently infected WT mice and not in CD4

deficient animals. Additionally, 'unhelped' CD8 T cells in CD4 deficient mice have been shown to produce soluble TRAIL upon restimulation (144), which may result in the death of the CD8 T cells in the TG during latency and lead to the phenotype we observe in BALB/c mice.

A second possible explanation for the loss of CD8 T cells in BALB/c mice TGs is that chronic stimulation leads to CD8 T cell exhaustion. It has been well established in models of chronic infection that chronic stimulation of CD8 T cells can result in CD8 T cell exhaustion manifested as either physical deletion and/or functional inactivation of CD8 T cells. Clearly there appears to be different levels of exhaustion during a chronic infection based on amount of antigen present to stimulate CD8 T cells (155). We feel that latent HSV-1 infection in WT mice represents a situation of minimal chronic antigenic stimulation based on our inability to find any functional defects in CD8 T cells during latency and the very low frequency of viral antigen detected in latently infected TGs (14,15). When CD4 T cells are absent during the inductive phase, a gradual loss of CD8 T cells is observed during latency in BALB/c mice. Is this due to increased antigen persistence in the TGs of CD4 deficient BALB/c mice? Our data on viral genome copy number in the C57Bl/6 mice suggests the answer to this question may be yes. Additionally it should be noted that several studies have shown a role for CD4 T cells in the clearance of virus (89,197). This supports the hypothesis that CD4 deficiency during the establishment of latency can result in increased chronic antigen load within the ganglia that may ultimately result in CD8 T cell exhaustion. We unfortunately do not have data addressing viral genome copy number or viral antigen persistence in the TGs of CD4 deficient BALB/c mice, but we might expect to find increased amounts of viral antigen in these mice compared to WT BALB/c, which may be responsible for the exhaustion/deletion of CD8 T cells in the TGs of CD4 deficient mice over time.

A third possible explanation for the declining numbers of CD8 T cells in CD4 deficient BALB/c mice is that CD4 T cells are required to maintain CD8 T cells during viral latency as suggested (66,138). This study argues that memory CD8 T cells require constant 'help' from CD4 T cells in order to survive for long periods of time. Adoptive transfer of memory CD8 T cells that were generated in a 'helped' environment into CD4 deficient hosts resulted in a gradual loss of those cells, while transfer of either helped or unhelped memory CD8 T cells in CD4 competent mice resulted in a stable population of memory cells.

5.4.1.1. CD127 expression on CD8 T cells in the TGs of BALB/c mice

In addition to the dramatic reduction in the numbers of CD8 T cells in the TGs of CD4 deficient BALB/c mice compared to WT mice, CD4 deficiency resulted in the loss of expression of IL-7Rα (CD127). Expression of this marker on CD8 T cells in the TG of CD4 deficient mice was very low (less than 5% at both D14 P.I. and D33 P.I.) in CD4 deficient mice (figure 42). Additionally, depletion of CD4 T cells for only 12 days after infection was sufficient to reduce expression of CD127 on CD8 T cells in the TG at D+35 (figure 43), suggesting that the signal to CD8 T cells to express CD127 occurs very early and not during latency.

This marker has received newfound interest as its expression on effector CD8 T cells appears to mark cells that will survive contraction to become long lasting memory T cells (51). CD127 expression is restricted to naïve T cells, the small population of memory precursors within the effector T cell pool, and memory T cells (52). This lack of CD127 expression on the CD8 T cells at all times post-infection in the BALB/c mice is consistent with the hypothesis that memory precursor CD8 T cells are never generated in CD4 deficient mice, resulting in little to no memory CD8 T cell pool. This would manifest as reduced numbers of CD8 T cells during latency, which is what we observe in CD4 deficient BALB/c mice. This is consistent with a

recent publication that showed a need for CD4 T cell help in the generation of the effector memory CD8 T cell population in lymphoid tissue following an acute infection (185).

5.4.1.2. Does CD4 depletion during latency affect CD8 T cell phenotype in BALB/c mice?

Removal of CD4 T cells during viral latency in BALB/c mice (figure 43) resulted in a decrease in the absolute numbers of CD8 T cells in the TG; however no effect on the percentage of cells that express CD127 or CD69 was detected. This suggests that CD4 T cells may be playing a role in the maintenance of CD8 T cells in the TG of BALB/c mice. This would be consistent with a recent report claiming CD4 T cells maintain CD8 T cell memory (66). Future studies to repeat this are underway.

5.4.2. Results in C57Bl/6 mice

Given the findings in BALB/c mice, we moved our studies to C57Bl/6 mice which would allow us to analyze virus specific CD8 T cells using $gB_{498-505}$ tetramer staining (90). This provides a distinct advantage over BALB/c mice in that we can directly assess the effects of CD4 deficiency on both the virus specific and nonspecific CD8 T cell populations in the TG. Initial studies revealed that CD4 deficiency in C57Bl/6 mice does not result in the dramatic reduction in the numbers of CD8 T cells present in the TGs at late time points that was found in CD4 deficient BALB/c mice (compare figures 60 and 41). Instead, the absolute numbers of both total CD8s and virus specific ($gB_{498-505}$ specific) CD8 T cells did not differ between WT and CD4 depleted mice during latency (figure 60).

It was puzzling to find such a dramatic difference in the effect of CD4 deficiency on the CD8 T cell response in BALB/c and C57Bl/6 mice. Why do CD8 T cells in the TGs of CD4

deficient BALB/c mice decline over time while CD8s in CD4 deficient C57Bl/6 do not? This loss of CD8 T cells in the CD4 deficient BALB/c mice is strikingly similar to what is seen in LCMV clone 13 infected mice. Infection of C57Bl/6 mice with this strain of LCMV results in exhaustion of the CD8 compartment, as evidenced by loss of the NP396 specific CD8 T cells and loss of functionality of the GP33 specific population of virus specific CD8 T cells (155). Could the antigen load in CD4 depleted BALB/c mice be so much higher than the antigen load in CD4 depleted C57Bl/6 mice that it results in deletion of these cells? There is evidence of increased numbers of HSV antigen positive neurons in BALB/c mice vs C57Bl/6 mice at the peak of productive infection (82). Unfortunately, both this study and another have shown that BALB/c and C57Bl/6 mice contain equivalent viral genome copies during latency (82,198). It should be noted that both of those studies used the KOS strain of HSV-1, while all of the studies performed here were done with HSV-1 RE.

Unpublished work in our lab suggests that viral spread within the TG may be different between BALB/c and C57Bl/6 mice. We have observed that CD8 T cells are restricted to the ophthalmic branch of the TG in latently infected C57Bl/6 mice, but are found in all branches of the TG in latently infected BALB/c mice (unpublished observations). In addition, a much larger number of CD8 T cells are detected per ganglion in BALB/c vs C57Bl/6 mice. These observations might suggest that increased viral spread occurs within the TG of BALB/c mice, which presumably would result in higher amounts of viral antigen and may cause CD8 T cell exhaustion.

Work by Simmons' group has clearly shown that a major difference between BALB/c and C57Bl/6 mice in their resistance to lethal infection is located within the natural killer cell gene locus (75,76). They argue that NKT cells play a very important role in the clearance of

initial infection and prevent viral spread following flank infection. This reduced ability of BALB/c mice to control initial infection (coupled with CD4 deficiency) could conceivably result in high viral antigen loads within the TGs of BALB/c mice resulting in exhaustion of the CD8 T cells, while Bl/6 mice, which have this strong NKT response are capable of limiting the initial infection (even with CD4 deficiency), resulting in a low viral antigen load and no exhaustion of the CD8 T cell response.

5.4.2.1.   CD127 expression in Bl/6

Reduced expression of CD127 was observed in both CD4 depleted BALB/c and C57Bl/6 mice. At all time points tested, we found reduced expression of CD127 on $gB_{498-505}$ specific CD8 T cells in CD4 deficient C57Bl/6 mice compared to WT mice (figure 61). It is interesting to note that in Bl/6 mice, this reduction in the number of CD127^{+}CD8s early did not result in a reduction in the numbers of memory $gB_{498-505}$ specific CD8 T cells during latency as was observed in CD4 deficient BALB/c mice. This finding argues that the numbers of CD127^{+}CD8 T cells generated during the effector phase does not necessarily equate to the size of the memory pool. This is clearly shown in figures 60 and 61.

5.4.2.2.   Do CD4 T cells regulate contraction of virus specific CD8 T cells?

Another important finding from the studies in CD4 deficient C57Bl/6 mice is the effect CD4 T cells play during the contraction phase. CD4 deficient mice exhibited an accelerated contraction phase; however this accelerated contraction did not affect the size of the memory pool as defined at late time points in the TGs of these animals (figure 60). This is consistent with previous studies that have shown the initial burst size of the CD8 T cell response determines the size of the memory pool (199,200). These results suggest that CD4 T cells regulate the

contraction of the CD8 T cell pool, perhaps through production of cytokines such as IFN-γ (39-41) or perhaps TNF-α (44,45). Unpublished work in our lab suggests that a lack of IFN-γ during the contraction phase results in accelerated contraction of gB$_{498-505}$ specific CD8 T cells that is strikingly similar to the results observed when CD4 T cells are absent.

5.4.2.3. Are CD4 T cells needed during latency for maintenance of CD8s?

Given the high expression of MHC class II (figure 64) and the highly activated phenotype of the CD4 T cells (figure 63) present in the TG during latency, we next tested if CD4 T cells play an active role in the TG during viral latency, either as support cells for the maintenance of CD8 T cell memory (66) or perhaps even directly through the production of IFN-γ. The results here indicate that CD4 T cells are not needed for the maintenance of the absolute numbers, phenotype, or functionality of memory gB$_{498-505}$ specific CD8 T cells in the TG during latency (figures 65-68). Our results are more consistent with those of others (135-137) that found CD4 T cell help is instead necessary during the inductive phase of the immune response as evidenced by the decreased CD127 expression on gB$_{498-505}$ specific CD8 T cells and increased viral genome copy number.

This result is somewhat surprising given evidence of increased reactivation rate of HSV in HIV^{+} individuals (201). One study (202) showed that the recurrence rate of HSV keratitis was 2.48 times more frequent in HIV^{+} individuals; however the clinical course of disease was not different between HIV^{+} and HIV^{-} people. Other studies (203,204) have shown a direct relationship between CD4 T cell count and the rate of HSV-2 reactivation. Both studies clearly show that decreased CD4 T cell counts resulted in a higher reactivation rate of HSV-2 in both men and women. In relation to the work presented within this thesis, we may need to maintain CD4 depletion for a longer period of time to identify if reactivation will occur. Additionally, we

have not yet performed the analysis on the viral genome copy number of TGs that have been depleted of CD4 T cell during latency. It is conceivable that the HSV-1 may be reactivating in the face of a seemingly intact CD8 T cell response in the TG during latency as has been reported for MHV-68 infection of CD4 deficient mice (145-147). Alternatively, we have only examined the ability of the CD8 T cells to produce IFN-γ as a test of their functionality, but CD4 deficiency may affect other functional aspects of CD8 T cells such as the ability to be cytolytic (142).

5.4.2.4.   Why do CD4 depleted mice contain a higher HSV-1 genome copy number?

Figure 59 clearly demonstrates that viral genome copy number is elevated at all times P.I. in CD4 depleted C57Bl/6 mice compared to WT. This finding can be explained by one of several possibilities. First, CD4 T cells themselves may play a direct role in the initial clearance and establishment of viral latency in the TG. This is supported by recent work by Minagawa and Yanagi that showed adoptive transfer of CD4 T cells alone to SCID mice protected these mice from lethal encephalitis (88). Other studies have suggested that CD4 T cells play a role in viral clearance (87,89,197). This is also supported by data contained in this document in which adoptive transfer of virus specific CD4 T cells into nude mice resulted in protection from death (figure 26). The increased viral genome copy number observed in CD4 depleted C57Bl/6 mice at early times P.I. may be due to decreased initial control of the virus in the TG in the absence of CD4 T cells.

An additional explanation for the increase in copy number, especially at early time points, may be related to a functional defect in the effector CD8 T cells generated in CD4 deficient mice. Most current literature argues that the generation of effector CD8 T cell responses is CD4 independent, but this is a topic of contention. Notably, recent work by Marzo et al has shown

decreased primary CD8 T cells responses to *Listeria monocytogenes* in CD4 depleted mice (140). Additionally, work by Jennings et al has shown decreased cytolytic ability of primary CD8 T cells in CD4 depleted mice infected with HSV-1 (205). This reduction in the cytolytic capacity of the CD8 T cells may therefore result in reduced viral control during primary infection which manifests as increased viral genome copy number in the TG of CD4 depleted mice. It is notable that we find a significant decrease in the MFI of CD8 T cells producing IFN-γ in CD4 depleted mice at D+8 P.I. (figure 50), which again suggests a functional defect in the primary CD8 T cell response in CD4 depleted mice.

These points address why a higher genome copy number is detected at early times P.I. (D+8), but the data also shows increased copy number at later times in CD4 depleted mice, in fact it appears that the difference in copy number between WT and CD4 depleted mice increases as time goes by (figure 59). This might suggest reduced control of latency by the memory CD8 T cells even though CD8 T cells appear to be just as capable of producing IFN-γ in late term CD4 depleted hosts (figure 66). The cytolytic ability of the memory CD8 T cells in late term depleted mice needs to be addressed to identify if this may be reduced.

Another possible explanation for increased viral genome copy number in CD4 deficient mice may be due to the lack of a potent antibody response in these mice. Studies have shown that B cell KO mice exhibit increased mortality following ocular infection (206,207), cutaneous infection (208), and intraperitoneal infection (209), which is probably due to viral spread from the TG to the CNS in the absence of antibody as suggested (210,211). Importantly, anti-CD4 treated mice used in our studies contain B cells (unlike the studies using B cell KO mice) and would therefore have natural antibody to HSV (208); however isotype switching will be greatly impaired. This might explain why CD4 depleted mice survive initial infection (due to natural

antibody to HSV), but establish latency with a higher viral genome copy number. It should also be noted that high viral doses were used in the previous studies looking at survival of B cell KO mice, typically $> 10^6$ PFU. The authors did notice that the survival of B cell KO mice increased as viral dose was reduced (206,208) closer to the infectious dose used in our studies ($3X10^5$ PFU).

5.4.3. Why do we observe such a large influx of CD8 T cells after depletion runs out?

Our current hypothesis that predicts viral latency represents an active tug-of-war between the immune system and the virus is supported by the finding of a massive increase of CD8 and CD4 T cells into the TG (figure 55) once CD4 T cells recover in transiently depleted C57Bl/6 mice. This large increase in cells strongly suggests that an antigenic stimulus is still present during latency since we observe this replenishment into the TG and lung around 35 days P.I. Studies contained within this thesis indicate that depletion of CD4 T cells using an antibody treatment strategy of days -2, +1,+5,+8 P.I. caused depletion of CD4 T cells from mice at least as long as 23 days P.I. (i.e. no CD4 T cells could be detected in any tissue until D+23) with very few if any mice exhibiting CD4 T cell recovery in the TG until D+35. It is slightly confusing that increased numbers of CD8 and CD4 T cells were found in the lungs as well as the TG (figure 56). This data indicates that the increase in the numbers of cells in the TGs of transiently depleted mice at D+35 represents a non-specific T cell replenishment into all tissues once CD4 T cells recover from in vivo depletion.

This raised an important question: where is the expansion of these cells occurring? Lymph nodes and spleens of transiently CD4 depleted mice were tested between D+23 and D+32 for increased numbers of cells but no significant increases were detected in either tissue at any time point. This might suggest that upon CD4 recovery, CD4 T cells infiltrate tissues throughout the

body (including the TG and the lungs) and provide help (via cytokines perhaps) for the CD8 T cells present within those tissues resulting in proliferation of those cells within the tissues.

5.4.4. Why such low CD127 on CD8s in WT mice?

Figures 61 and 62 clearly demonstrate reduced CD127 on CD8 T cells (in terms of the low percentage and low MFI) in the TG during latency in both C57Bl/6 and BALB/c. Previous reports on expression of CD127 during the course of an acute infection indicate most if not all memory T cells express CD127 (51). Why then, don't we see high expression of CD127 on gB$_{498-505}$ specific CD8 T cells in the TG during latency? One possible explanation is the presence of antigen. Numerous reports have shown viral gene transcription and even in some rare cases, translation, occurs in the TG during latency. This low level antigen production does not appear to result in CD8 T cell exhaustion (at least in the C57Bl/6 mice), however we do observe one of the effects of chronic stimulation on gB$_{498-505}$ specific CD8 T cells: reduction in CD127 (153,184,212). It was shown in recent work that chronic antigenic stimulation resulted in reduced expression of CD127 both in terms of the percentage of CD8 T cells that express it and also in the MFI of expression per CD8 T cell (153). These findings correlate well with our observations that no more than 50% of CD8 T cells express CD127 in the TG during latency in either C57Bl/6 or BALB/c mice and the expression of this marker on a per cell basis is quite low. Another consideration is the fact that we have focused our studies here on expression of CD127 on CD8 T cells within the TG, while the vast majority of previous work has examined only lymphoid tissue. It is very likely that tissue specific expression of CD127 on pathogen specific CD8 T cells varies.

A summary diagram of the roles of CD4 T cells in mice following ocular HSV-1 infection of mice is shown in figure 70. This clearly shows the detrimental role of CD4 T cells in the development of HSK (figure 70A), but also depicts the important role of CD4 T cells in the initial priming of CD8 T cells in the lymph nodes by an unknown mechanism (figure 70C). Work provided in this thesis indicates that CD4 T cells are not required for the maintenance of CD8 T cells in the TG during latency in C57Bl/6 mice, however these studies need to be continued to identify if a longer period of time of CD4 depletion is necessary to identify if CD4 T cells do actively maintain CD8 T cell responses in the TG during latency (figure 70B). Additionally, preliminary evidence in BALB/c mice suggests that the requirement for CD4 T cell in the maintenance of CD8 T cells during latency may be mouse strain specific (figure 43) and warrants further investigation.
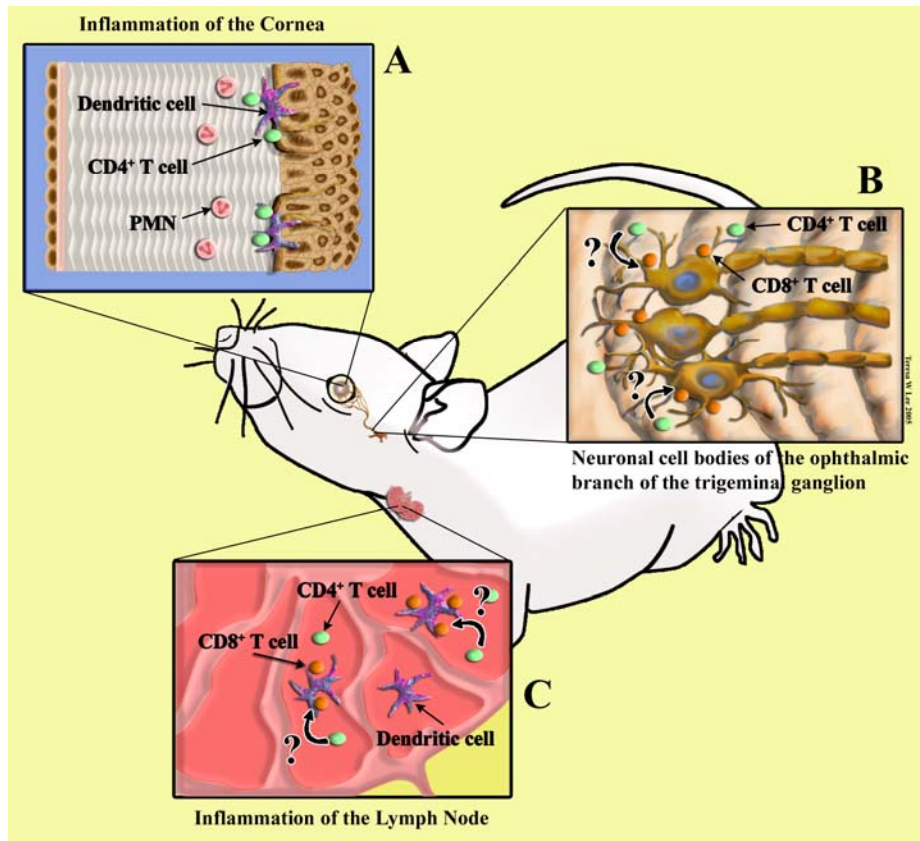
Figure 70: Proposed roles of CD4 T cells in mice following ocular HSV-1 infection.

CD4 T cells can be both detrimental and protective in mice following ocular HSV-1 infection. It is clear that CD4 T cells can mediate HSK (A) following ocular HSV-1 infection, however work in this thesis shows that CD8 T cells also appear to capable of mediating HSK when CD4 T cells are absent. In contrast to the pathologic effects of CD4 T cells in the cornea, we have shown that CD4 T cells are important regulators of CD8 T cell responses in the TG. We demonstrate that the absence of CD4 T cells during the priming of CD8 T cell responses in the lymph nodes (C) results in the generation of functionally compromised virus specific CD8 T cells in the TG (B). This functional impairment of virus specific CD8 T cells may explain the increased viral genome burden found within the TG at all times tested in CD4 deficient animals. Alternatively, CD4 T cells may play a direct role in the clearance of the virus early after infection. Our work has shown that CD4 T cells play a minimal role in the maintenance of CD8 T cells in the TG in C57Bl/6 mice (B) during viral latency at least following depletion of CD4 T cells for one to two weeks.

6.   Summary

This work has advanced the understanding of several aspects of the immune response to ocular HSV-1 infection in mice. First, blockade of CD134/OX40L costimulation following ocular HSV-1 infection does not appreciably affect the clinical course of herpes stromal keratitis. It does appear that only certain costimulatory interactions are required for the development of

HSK including CD28:B7 (38) and 4-1BB:4-1BBL(178), while others are largely dispensable such as CD40:CD154 (113) and CD134:OX40L. We have also characterized numerous virus specific CD4 T cell clones generated from BALB/c mice with clinical HSK that can induce HSK in resistant nude mice. These T cell clones will facilitate better understanding of the sequence of events culminating in HSK in mice and provides support for our animal model of HSK as human studies have clearly shown that virus specific CD4 and CD8 T cells are present in human corneas with HSK. Work contained within this thesis has shown, for the first time, that CD8 T cells can mediate HSK following HSV-1 RE infection of mice. These studies caution one to be cognizant of how viral dose can influence the development of HSK in mice and which T cell subset can mediate HSK at different viral doses. Finally, these studies provide compelling evidence that CD4 T cells are in fact needed to generate proper CD8 T cell responses resulting in proper development of viral latency. The consequences of CD4 deficiency in mice following ocular HSV-1 infection range from a massive loss in the numbers of CD8 T cells (in BALB/c mice) to increased viral genome copies that might be indicative of a higher viral burden during latency (in C57Bl/6 mice). This higher burden might result in a higher rate of reactivation in humans, thus increasing the likelihood of recurrent herpetic disease in CD4 deficient individuals (213-215).

APPENDIX A

Publications:

1. Brissette-Storkus CS, Reynolds SM, Lepisto AJ, Hendricks RL. Identification of a novel macrophage population in the normal mouse corneal stroma. Investigative Ophthalmology and Visual Sciences. 2002. July;43 (7):2264-71.
2. Xu M, Lepisto AJ, Hendricks RL. Co-stimulatory requirements of effector T cells at inflammatory sites. DNA and Cell Biology. 2002. May-June;21 (5-6):461-5.
3. Khanna KM, Lepisto AJ, Hendricks RL. Immunity to latent viral infection: many skirmishes but few fatalities. Trends in Immunology. 2004. May;25 (5):230-4.
4. Xu M, Lepisto AJ, Hendricks RL. CD154 signaling regulates the Th1 response to HSV-1 and inflammation in infected corneas. Journal of Immunology. 2004. July 15;173 (2):1232.
5. Khanna, KM, Lepisto AJ, Decman, V, Hendricks RL. Immune control of herpes simplex virus during latency. Current Opinion in Immunology.2004. Aug;16 (4):463-9.
6. Lepisto, AJ, Xu, M, Stuart, P.M. and Hendricks RL. CD8 T cells mediate HSK in BALB/c mice following HSV-1 RE infection. Manuscript in review.
7. Lepisto AJ, Hendricks RL. CD4 T cells control CD8 T cell memory development at site of HSV-1 latency. In preparation.

BIBLIOGRAPHY

Reference List

1. Schillinger, J. A., F. Xu, M. R. Sternberg, G. L. Armstrong, F. K. Lee, A. J. Nahmias, G. M. McQuillan, M. E. Louis, and L. E. Markowitz. 2004. National seroprevalence and trends in herpes simplex virus type 1 in the United States, 1976-1994. *Sex Transm.Dis.* 31:753-760.

2. Roberts, C. M., J. R. Pfister, and S. J. Spear. 2003. Increasing proportion of herpes simplex virus type 1 as a cause of genital herpes infection in college students. *Sex Transm.Dis.* 30:797-800.

3. Lowhagen, G. B., P. Tunback, K. Andersson, T. Bergstrom, and G. Johannisson. 2000. First episodes of genital herpes in a Swedish STD population: a study of epidemiology and transmission by the use of herpes simplex virus (HSV) typing and specific serology. *Sex Transm.Infect.* 76:179-182.

4. Scoular, A., B. G. Leask, and D. Carrington. 1990. Changing trends in genital herpes due to Herpes simplex virus type 1 in Glasgow, 1985-88. *Genitourin.Med.* 66:226.

5. Fleming, D. T., G. M. McQuillan, R. E. Johnson, A. J. Nahmias, S. O. Aral, F. K. Lee, and M. E. St Louis. 1997. Herpes simplex virus type 2 in the United States, 1976 to 1994. *N.Engl.J.Med.* 337:1105-1111.

6. Fisman, D. N., M. Lipsitch, E. W. Hook, III, and S. J. Goldie. 2002. Projection of the future dimensions and costs of the genital herpes simplex type 2 epidemic in the United States. *Sex Transm.Dis.* 29:608-622.

7. Roizman, B. and D. M. Knipe. 2001. Herpes simplex viruses and their replication. In *Fields Virology*. B. N. Fields, D. M. Knipe, P.M.Howley, S. E. Straus, and M. A. Martin, eds. Lippincott-Raven, Philadelphia, pp. 2399-2459.

8. Stevens, J. G., E. K. Wagner, G. B. Devi-Rao, M. L. Cook, and L. T. Feldman. 1987. RNA complementary to a herpesvirus alpha gene mRNA is prominent in latently infected neurons. *Science* 235:1056-1059.

9. Perng, G. C., C. Jones, J. Ciacci-Zanella, M. Stone, G. Henderson, A. Yukht, S. M. Slanina, F. M. Hofman, H. Ghiasi, A. B. Nesburn, and S. L. Wechsler. 2000. Virus-induced neuronal apoptosis blocked by the herpes simplex virus latency-associated transcript [In Process Citation]. *Science* 287:1500-1503.

10. Perng, G. C., B. Maguen, L. Jin, K. R. Mott, N. Osorio, S. M. Slanina, A. Yukht, H. Ghiasi, A. B. Nesburn, M. Inman, G. Henderson, C. Jones, and S. L. Wechsler. 2002. A Gene Capable of Blocking Apoptosis Can Substitute for the Herpes Simplex Virus Type

1 Latency-Associated Transcript Gene and Restore Wild-Type Reactivation Levels. *The Journal of Virology* 76:1224-1235.

11. Kramer, M. F. and D. M. Coen. 1995. Quantification of transcripts from the ICP4 and thymidine kinase genes in mouse ganglia latently infected with herpes simplex virus. *J.Virol.* 69:1389-1399.

12. Kramer, M. F., S. H. Chen, D. M. Knipe, and D. M. Coen. 1998. Accumulation of viral transcripts and DNA during establishment of latency by herpes simplex virus. *J.Virol.* 72:1177-1185.

13. Chen, S. H., M. F. Kramer, P. A. Schaffer, and D. M. Coen. 1997. A viral function represses accumulation of transcripts from productive-cycle genes in mouse ganglia latently infected with herpes simplex virus. *J.Virol.* 71:5878-5884.

14. Feldman, L. T., A. R. Ellison, C. C. Voytek, L. Yang, P. Krause, and T. P. Margolis. 2002. Spontaneous molecular reactivation of herpes simplex virus type 1 latency in mice. *Proc.Natl.Acad.Sci.U.S.A* 99:978-983.

15. Sawtell, N. M. 2003. Quantitative Analysis of Herpes Simplex Virus Reactivation In Vivo Demonstrates that Reactivation in the Nervous System Is Not Inhibited at Early Times Postinoculation. *J.Virol.* 77:4127.

16. Liu, T., K. M. Khanna, X. Chen, D. J. Fink, and R. L. Hendricks. 2000. CD8(+) T cells can block herpes simplex virus type 1 (HSV-1) reactivation from latency in sensory neurons. *J.Exp.Med.* 191:1459-1466.

17. Rooney, J. F., Y. Bryson, M. L. Mannix, M. Dillon, C. R. Wohlenberg, S. Banks, C. J. Wallington, A. L. Notkins, and S. E. Straus. 1991. Prevention of ultraviolet-light-induced herpes labialis by sunscreen. *Lancet* 338:1419-1422.

18. Sawtell, N. M. and R. L. Thompson. 1992. Rapid in vivo reactivation of herpes simplex virus in latently infected murine ganglionic neurons after transient hyperthermia. *J.Virol.* 66:2150-2156.

19. Padgett, D. A., J. F. Sheridan, J. Dorne, G. G. Berntson, J. Candelora, and R. Glaser. 1998. Social stress and the reactivation of latent herpes simplex virus type 1. *Proc.Natl.Acad.Sci.U.S.A* 95:7231-7235.

20. Pereira, D. B., M. H. Antoni, A. Danielson, T. Simon, J. Efantis-Potter, C. S. Carver, R. E. Duran, G. Ironson, N. Klimas, M. A. Fletcher, and M. J. O'Sullivan. 2003. Stress as a predictor of symptomatic genital herpes virus recurrence in women with human immunodeficiency virus. *J Psychosom.Res.* 54:237-244.

21. Sainz, B., J. M. Loutsch, M. E. Marquart, and J. M. Hill. 2001. Stress-associated immunomodulation and herpes simplex virus infections. *Med.Hypotheses* 56:348-356.

22. Sears, A. E., V. Hukkanen, M. A. Labow, A. J. Levine, and B. Roizman. 1991. Expression of the herpes simplex virus 1 α transinducing factor (VP16) does not induce reactivation of latent virus or prevent the establishment of latency in mice. *J.Virol.* 65:2929-2935.

23. Halford, W. P. and P. A. Schaffer. 2001. ICP0 is required for efficient reactivation of herpes simplex virus type1 from neuronal latency. *J.Virol.* 75:3240-3249.

24. Cai, W., Astor, T. D., Liptak, L. M., Cho, C., Coen, D. M., and Schaffer, P. A. The herpes simplex virus type 1 regulatory protein ICP0 enhances replication during acute infection and reactivation from latency. Journal of Virology 67, 7501-7512. 1993.
Ref Type: Journal (Full)

25. Harold A.Stein, B. J. S. R. M. S. 1992. Basic Anatomy and Physiology of the Eye. In *A Primer in Ophthalmology: A Textbook for Students*. Mosby-Year Book, pp. 1-40.

26. Hayashi, S., T. Osawa, and K. Tohyama. 2002. Comparative observations on corneas, with special reference to Bowman's layer and Descemet's membrane in mammals and amphibians. *J.Morphol.* 254:247-258.

27. Muller, L. J., C. F. Marfurt, F. Kruse, and T. M. Tervo. 2003. Corneal nerves: structure, contents and function. *Exp.Eye Res.* 76:521-542.

28. Charles A Janeway, Paul Travers, Mark Walport, and Mark Shlomchik. 2001. T cell mediated Immunity. In *Immunobiology*. Garland, New York, pp. 295-340.

29. Harty, J. T., A. R. Tvinnereim, and D. W. White. 2000. CD8+ T cell effector mechanisms in resistance to infection. *Annu.Rev.Immunol.* 18:275-308.

30. Russell, J. H. and T. J. Ley. 2002. Lymphocyte-mediated cytotoxicity. *Annu.Rev.Immunol.* 20:323-370.

31. Abul Abbas and Andrew Lichtman. 2003. Cytokines. In *Cellular and Molecular Immunology*. Saunders Elsevier Science, Philadelphia, pp. 243-274.

32. Mills, K. H. 2004. Regulatory T cells: friend or foe in immunity to infection? *Nat.Rev.Immunol.* 4:841-855.

33. Charles A Janeway, Paul Travers, Mark Walport, and Mark Shlomchik. 2001. Innate Immunity. In *Immunobiology*. Garland, New York, pp. 35-91.

34. Blattman, J. N., R. Antia, D. J. Sourdive, X. Wang, S. M. Kaech, K. Murali-Krishna, J. D. Altman, and R. Ahmed. 2002. Estimating the precursor frequency of naive antigen-specific CD8 T cells. *J.Exp.Med.* 195:657-664.

35. Appleman, L. J. and V. A. Boussiotis. 2003. T cell anergy and costimulation. *Immunol.Rev.* 192:161-180.

36. Xu, M., A. J. Lepisto, and R. L. Hendricks. 2002. Co-stimulatory requirements of effector T cells at inflammatory sites. *Dna and Cell Biology* 21:461-465.

37. Croft, M. and C. Dubey. 1997. Accessory molecule and costimulation requirements for CD4 T cell response. *Crit Rev.Immunol.* 17:89-118.

38. Chen, H. and R. L. Hendricks. 1998. B7 costimulatory requirements of T cells at an inflammatory site. *J.Immunol.* 160:5045-5052.

39. Harty, J. T. and V. P. Badovinac. 2002. Influence of effector molecules on the CD8(+) T cell response to infection. *Curr.Opin.Immunol.* 14:360-365.

40. Badovinac, V. P., A. R. Tvinnereim, and J. T. Harty. 2000. Regulation of antigen-specific CD8+ T cell homeostasis by perforin and interferon-gamma. *Science* 290:1354-1358.

41. Wodarz, D. 2001. Mechanisms underlying antigen-specific CD8+ T cell homeostasis. *Science* 292:595.

42. Badovinac, V. P., B. B. Porter, and J. T. Harty. 2002. Programmed contraction of CD8(+) T cells after infection. *Nat.Immunol.* 3:619-626.

43. Blattman, J. N., L. E. Cheng, and P. D. Greenberg. 2002. CD8(+) T cell responses: it's all downhill after their prime. *Nat.Immunol.* 3:601-602.

44. Reich, A., H. Korner, J. D. Sedgwick, and H. Pircher. 2000. Immune down-regulation and peripheral deletion of CD8 T cells does not require TNF receptor-ligand interactions nor CD95 (Fas, APO-1). *Eur.J.Immunol.* 30:678-682.

45. Suresh, M., A. Singh, and C. Fischer. 2005. Role of tumor necrosis factor receptors in regulating CD8 T-cell responses during acute lymphocytic choriomeningitis virus infection. *J.Virol.* 79:202-213.

46. Christensen, J. E., D. Wodarz, J. P. Christensen, and A. R. Thomsen. 2004. Perforin and IFN-gamma do not significantly regulate the virus-specific CD8+ T cell response in the absence of antiviral effector activity. *Eur.J.Immunol.* 34:1389-1394.

47. Badovinac, V. P. and J. T. Harty. 2000. Adaptive immunity and enhanced CD8+ T cell response to Listeria monocytogenes in the absence of perforin and IFN-gamma. *J.Immunol.* 164:6444-6452.

48. Stockinger, B., G. Kassiotis, and C. Bourgeois. 2004. CD4 T-cell memory. *Semin.Immunol.* 16:295-303.

49. Madakamutil, L. T., U. Christen, C. J. Lena, Y. Wang-Zhu, A. Attinger, M. Sundarrajan, W. Ellmeier, M. G. von Herrath, P. Jensen, D. R. Littman, and H. Cheroutre. 2004. CD8alphaalpha-mediated survival and differentiation of CD8 memory T cell precursors. *Science* 304:590-593.

50. Kim, S. V. and R. A. Flavell. 2004. Immunology. CD8alphaalpha and T cell memory. *Science* 304:529-530.

51. Kaech, S. M., J. T. Tan, E. J. Wherry, B. T. Konieczny, C. D. Surh, and R. Ahmed. 2003. Selective expression of the interleukin 7 receptor identifies effector CD8 T cells that give rise to long-lived memory cells. *Nat.Immunol.* 4:1191-1198.

52. Schluns, K. S., W. C. Kieper, S. C. Jameson, and L. Lefrancois. 2000. Interleukin-7 mediates the homeostasis of naive and memory CD8 T cells in vivo. *Nat.Immunol.* 1:426-432.

53. Petschner, F., C. Zimmerman, A. Strasser, D. Grillot, G. Nunez, and H. Pircher. 1998. Constitutive expression of Bcl-xL or Bcl-2 prevents peptide antigen-induced T cell deletion but does not influence T cell homeostasis after a viral infection. *Eur.J.Immunol.* 28:560-569.

54. Razvi, E. S., Z. Jiang, B. A. Woda, and R. M. Welsh. 1995. Lymphocyte apoptosis during the silencing of the immune response to acute viral infections in normal, lpr, and Bcl-2-transgenic mice. *Am.J.Pathol.* 147:79-91.

55. Wherry, E. J. and R. Ahmed. 2004. Memory CD8 T-cell differentiation during viral infection. *J.Virol.* 78:5535-5545.

56. Sallusto, F., D. Lenig, R. Forster, M. Lipp, and A. Lanzavecchia. 1999. Two subsets of memory T lymphocytes with distinct homing potentials and effector functions. *Nature* 401:708-712.

57. Masopust, D., V. Vezys, A. L. Marzo, and L. Lefrancois. 2001. Preferential localization of effector memory cells in nonlymphoid tissue. *Science* 291:2413-2417.

58. Wherry, E. J., V. Teichgraber, T. C. Becker, D. Masopust, S. M. Kaech, R. Antia, U. H. Von Andrian, and R. Ahmed. 2003. Lineage relationship and protective immunity of memory CD8 T cell subsets. *Nat.Immunol.* 4:225-234.

59. Unsoeld, H., S. Krautwald, D. Voehringer, U. Kunzendorf, and H. Pircher. 2002. Cutting edge: CCR7+ and CCR7- memory T cells do not differ in immediate effector cell function. *J.Immunol.* 169:638-641.

60. Roberts, A. D. and D. L. Woodland. 2004. Cutting edge: effector memory CD8+ T cells play a prominent role in recall responses to secondary viral infection in the lung. *J.Immunol.* 172:6533-6537.

61. Baron, V., C. Bouneaud, A. Cumano, A. Lim, T. P. Arstila, P. Kourilsky, L. Ferradini, and C. Pannetier. 2003. The repertoires of circulating human CD8(+) central and effector memory T cell subsets are largely distinct. *Immunity.* 18:193-204.

62. Murali-Krishna, K., L. L. Lau, S. Sambhara, F. Lemonnier, J. Altman, and R. Ahmed. 1999. Persistence of memory CD8 T cells in MHC class I-deficient mice. *Science* 286:1377-1381.

63. Swain, S. L., H. Hu, and G. Huston. 1999. Class II-independent generation of CD4 memory T cells from effectors. *Science* 286:1381-1383.

64. Bradley, L. M., L. Haynes, and S. L. Swain. 2005. IL-7: maintaining T-cell memory and achieving homeostasis. *Trends Immunol.* 26:172-176.

65. Sprent, J. 2003. Turnover of memory-phenotype CD8+ T cells. *Microbes.Infect.* 5:227-231.

66. Sun, J. C., M. A. Williams, and M. J. Bevan. 2004. CD4+ T cells are required for the maintenance, not programming, of memory CD8+ T cells after acute infection. *Nat.Immunol.* 5:927-933.

67. Brissette-Storkus, C. S., S. A. Reynolds, A. J. Lepisto, and R. L. Hendricks. 2002. Identification of a novel macrophage population in the normal mouse corneal stroma. *Investigative Ophthalmology & Visual Science* 43:2264-2271.

68. Allan, R. S., C. M. Smith, G. T. Belz, A. L. van Lint, L. M. Wakim, W. R. Heath, and F. R. Carbone. 2003. Epidermal viral immunity induced by CD8alpha+ dendritic cells but not by Langerhans cells. *Science* 301:1925-1928.

69. Thomas, J., S. Gangappa, S. Kanangat, and B. T. Rouse. 1997. On the essential involvement of neutrophils in the immunopathologic disease: herpetic stromal keratitis. *J.Immunol.* 158:1383-1391.

70. Tumpey, T. M., S. H. Chen, J. E. Oakes, and R. N. Lausch. 1996. Neutrophil-mediated suppression of virus replication after herpes simplex virus type 1 infection of the murine cornea. *J.Virol.* 70:898-904.

71. Shimeld, C., S. Efstathiou, and T. Hill. 2001. Tracking the spread of a lacZ-tagged herpes simplex virus type 1 between the eye and the nervous system of the mouse: comparison of primary and recurrent infection. *J.Virol.* 75:5252-5262.

72. Liu, T., Q. Tang, and R. L. Hendricks. 1996. Inflammatory infiltration of the trigeminal ganglion after herpes simplex virus type 1 corneal infection. *J.Virol.* 70:264-271.

73. Sciammas, R., P. Kodukula, Q. Tang, R. L. Hendricks, and J. A. Bluestone. 1997. T cell receptor-γ/δ cells protect mice from herpes simplex virus type 1-induced lethal encephalitis. *J.Exp.Med.* 185:1969-1975.

74. Kodukula, P., T. Liu, N. van Rooijen, M. J. Jager, and R. L. Hendricks. 1999. Macrophage control of Herpes simplex virus type 1 replication in the peripheral nervous system. *J.Immunol.* 162:2895-2905.

75. Pereira, R. A., A. Scalzo, and A. Simmons. 2001. Cutting edge: a NK complex-linked locus governs acute versus latent herpes simplex virus infection of neurons. *J.Immunol.* 166:5869-5873.

76. Grubor-Bauk, B., A. Simmons, G. Mayrhofer, and P. G. Speck. 2003. Impaired clearance of herpes simplex virus type 1 from mice lacking CD1d or NKT cells expressing the semivariant V alpha 14-J alpha 281 TCR. *J.Immunol.* 170:1430-1434.

77. Bouley, D. M., S. Kanangat, W. Wire, and B. T. Rouse. 1995. Characterization of herpes simplex virus type-1 infection and herpetic stromal keratitis development in IFN-gamma knockout mice. *J.Immunol.* 155:3964-3971.

78. Minagawa, H., K. Hashimoto, and Y. Yanagi. 2004. Absence of tumour necrosis factor facilitates primary and recurrent herpes simplex virus-1 infections. *J.Gen.Virol.* 85:343-347.

79. Metcalf, J. F., D. S. Hamilton, and R. W. Reichert. 1979. Herpetic keratitis in athymic (nude) mice. *Infect.Immun.* 26:1164-1171.

80. Mercadal, C. M., D. M. Bousley, D. Destephano, and B. Rouse. 1993. Herpetic stromal keratitis in the reconstituted SCID mouse model. *J.Virol.* 67:3404-3408.

81. Gangappa, S., J. S. Babu, J. Thomas, M. Daheshia, and B. T. Rouse. 1998. Virus-induced immunoinflammatory lesions in the absence of viral antigen recognition. *J.Immunol.* 161:4289-4300.

82. Ellison, A. R., L. Yang, C. Voytek, and T. P. Margolis. 2000. Establishment of latent herpes simplex virus type 1 infection in resistant, sensitive, and immunodeficient mouse strains. *Virology* 268:17-28.

83. Gesser, R. M., T. Valyi-Nagy, and N. W. Fraser. 1994. Restricted herpes simplex virus type 1 gene expression within sensory neurons in the absence of functional B and T lymphocytes. *Virology* 200:791-795.

84. Simmons, A. and D. C. Tscharke. 1992. Anti-CD8 impairs clearance of herpes simplex virus from the nervous system: Implications for the fate of virally infected neurons. *J.Exp.Med.* 175:1337-1344.

85. Goldsmith, K., W. Chen, D. C. Johnson, and R. L. Hendricks. 1998. Infected cell protein (ICP)47 enhances herpes simplex virus neurovirulence by blocking the CD8^{+} T cell response. *J.Exp.Med.* 187:341-348.

86. Ghiasi, H., G. Perng, A. B. Nesburn, and S. L. Wechsler. 1999. Either a CD4(+)or CD8(+)T cell function is sufficient for clearance of infectious virus from trigeminal ganglia and establishment of herpes simplex virus type 1 latency in mice. *Microb.Pathog.* 27:387-394.

87. Ghiasi, H., S. Cai, G. C. Perng, A. B. Nesburn, and S. L. Wechsler. 2000. Both CD4+ and CD8+ T cells are involved in protection against HSV-1 induced corneal scarring. *Br.J.Ophthalmol.* 84:408-412.

88. Minagawa, H. and Y. Yanagi. 2000. Latent herpes simplex virus-1 infection in SCID mice transferred with immune CD4+T cells: a new model for latency. *Arch.Virol* 145:2259-2272.

89. Nash, A. A., A. Jayasuriya, J. Phelan, S. P. Cobbold, and H. Waldmann. 1987. Different roles for L3T4+ and Lyt 2+ T cell subsets in the control of an acute herpes simplex virus infection of the skin and nervous system. *J.Gen.Virol.* 68:825-833.

90. Khanna, K. M., R. H. Bonneau, P. R. Kinchington, and R. L. Hendricks. 2003. Herpes simplex virus-specific memory CD8+ T cells are selectively activated and retained in latently infected sensory ganglia. *Immunity.* 18:593-603.

91. Shimeld, C., J. L. Whiteland, S. M. Nicholls, E. Grinfeld, D. L. Easty, H. Gao, and T. J. Hill. 1995. Immune cell infiltration and persistence in the mouse trigeminal ganglion after infection of the cornea with herpes simplex virus type 1. *J.Neuroimmunol.* 61:7-16.

92. Cantin, E. M., D. R. Hinton, J. Chen, and H. Openshaw. 1995. Gamma interferon expression during acute and latent nervous system infection by herpes simplex virus type 1. *J.Virol.* 69:4898-4905.

93. Theil, D., T. Derfuss, I. Paripovic, S. Herberger, E. Meinl, O. Schueler, M. Strupp, V. Arbusow, and T. Brandt. 2003. Latent herpesvirus infection in human trigeminal ganglia causes chronic immune response. *Am.J.Pathol.* 163:2179-2184.

94. Liu, T., K. M. Khanna, B. N. Carriere, and R. L. Hendricks. 2001. Gamma interferon can prevent herpes simplex virus type 1 reactivation from latency in sensory neurons. *J.Virol.* 75:11178-11184.

95. Halford, W. P., B. M. Gebhardt, and D. J. J. Carr. 1996. Persistent cytokine expression in trigeminal ganglion latently infected with herpes simplex virus type 1. *J.Immunol.* 157:3542-3549.

96. Halford, W. P., B. M. Gebhardt, and D. J. Carr. 1997. Acyclovir blocks cytokine gene expression in trigeminal ganglia latently infected with herpes simplex virus type 1. *Virology* 238:53-63.

97. Chen, S. H., D. A. Garber, P. A. Schaffer, D. M. Knipe, and D. M. Coen. 2000. Persistent elevated expression of cytokine transcripts in ganglia latently infected with herpes simplex virus in the absence of ganglionic replication or reactivation. *Virology* 278:207-216.

98. Cook, W. J., M. F. Kramer, R. M. Walker, T. J. Burwell, H. A. Holman, D. M. Coen, and D. M. Knipe. 2004. Persistent expression of chemokine and chemokine receptor RNAs at primary and latent sites of herpes simplex virus 1 infection. *Virol.J.* 1:5.

99. Bauer, D., S. Mrzyk, N. van Rooijen, K. P. Steuhl, and A. Heiligenhaus. 2000. Macrophage-depletion influences the course of murine HSV-1 keratitis. *Curr.Eye Res.* 20:45-53.

100. Inoue, T., Y. Inoue, R. Kosaki, Y. Inoue, K. Nishida, Y. Shimomura, Y. Tano, and K. Hayashi. 2001. Immunohistological study of infiltrated cells and cytokines in murine herpetic keratitis. *Acta Ophthalmol.Scand.* 79:484-487.

101. Russell, R. G., M. P. Nasisse, H. S. Larsen, and B. T. Rouse. 1984. Role of T-lymphocytes in the pathogenesis of herpetic stromal keratitis. *Invest.Ophthalmol.Vis.Sci.* 25:938-944.

102. Newell, C. K., S. Martin, D. Sendele, C. M. Mercadal, and B. T. Rouse. 1989. Herpes simplex virus-induced stromal keratitis: role of T-lymphocyte subsets in immunopathology. *J.Virol.* 63:769-775.

103. Hendricks, R. L. and T. M. Tumpey. 1990. Contribution of virus and immune factors to herpes simplex virus type 1 induced corneal pathology. *Invest.Ophthalmol.Vis.Sci.* 31:1929-1939.

104. Hendricks, R. L., T. M. Tumpey, and A. Finnegan. 1992. IFN-gamma and IL-2 are protective in the skin but pathologic in the corneas of HSV-1-infected mice. *J.Immunol.* 149:3023-3028.

105. Tang, Q. and R. L. Hendricks. 1996. IFN-gamma regulates PECAM-1 expression and neutrophil infiltration into herpes simplex virus-infected mouse corneas. *J.Exp.Med.* 184:1435-1447.

106. Tang, Q., W. Chen, and R. L. Hendricks. 1997. Proinflammatory functions of IL-2 in herpes simplex virus corneal infection. *J.Immunol.* 158:1275-1283.

107. Niemialtowski, M. G. and B. T. Rouse. 1992. Predominance of Th1 cells in ocular tissues during herpetic stromal keratitis. *J.Immunol.* 149:3035-3039.

108. Tamesis, R. R., E. M. Messmer, B. A. Rice, J. E. Dutt, and C. S. Foster. 1994. The Role of Natural-Killer-Cells in the Development of Herpes-Simplex Virus Type-1 Induced Stromal Keratitis in Mice. *Eye* 8:298-306.

109. Hendricks, R. L., M. Janowicz, and T. M. Tumpey. 1992. Critical role of corneal Langerhans cells in the CD4- but not CD8-mediated immunopathology in herpes simplex virus-1-infected mouse corneas. *J.Immunol.* 148:2522-2529.

110. Koch, F., U. Stanzl, P. Jennewein, K. Janke, C. Heufler, E. Kämpgen, N. Romani, and G. Schuler. 1996. High level IL-12 production by murine dendritic cells: Upregulation via MHC class II and CD40 molecules and downregulation by IL-4 and IL-10. *J.Exp.Med.* 184:741-746.

111. Cella, M., D. Scheidegger, K. Palmer-Lehmann, P. Lane, A. Lanzavecchia, and G. Alber. 1996. Ligation of CD40 on dendritic cells triggers production of high levels of interleukin-12 and enhances T cell stimulatory capacity: T-T help via APC activation. *J.Exp.Med.* 184:747-752.

112. Karni, A., D. N. Koldzic, P. Bharanidharan, S. J. Khoury, and H. L. Weiner. 2002. IL-18 is linked to raised IFN-gamma in multiple sclerosis and is induced by activated CD4(+) T cells via CD40-CD40 ligand interactions. *J.Neuroimmunol.* 125:134-140.

113. Xu, M., A. J. Lepisto, and R. L. Hendricks. 2004. CD154 signaling regulates the Th1 response to herpes simplex virus-1 and inflammation in infected corneas. *J.Immunol.* 173:1232-1239.

114. Mallett, S., S. Fossum, and A. N. Barclay. 1990. Characterization of the MRC OX40 antigen of activated CD4 positive T lymphocytes--a molecule related to nerve growth factor receptor. *EMBO J.* 9:1063-1068.

115. Latza, U., H. Durkop, S. Schnittger, J. Ringeling, F. Eitelbach, M. Hummel, C. Fonatsch, and H. Stein. 1994. The human OX40 homolog: cDNA structure, expression and chromosomal assignment of the ACT35 antigen. *Eur.J.Immunol.* 24:677-683.

116. Calderhead, D. M., J. E. Buhlmann, A. J. van den Eertwegh, E. Claassen, R. J. Noelle, and H. P. Fell. 1993. Cloning of mouse Ox40: a T cell activation marker that may mediate T-B cell interactions. *J.Immunol.* 151:5261-5271.

117. Ohshima, Y., Y. Tanaka, H. Tozawa, Y. Takahashi, C. Maliszewski, and G. Delespesse. 1997. Expression and function of OX40 ligand on human dendritic cells. *J.Immunol.* 159:3838-3848.

118. Brocker, T., A. Gulbranson-Judge, S. Flynn, M. Riedinger, C. Raykundalia, and P. Lane. 1999. CD4 T cell traffic control: in vivo evidence that ligation of OX40 on CD4 T cells by OX40-ligand expressed on dendritic cells leads to the accumulation of CD4 T cells in B follicles. *Eur.J.Immunol.* 29:1610-1616.

119. Murata, K., N. Ishii, H. Takano, S. Miura, L. C. Ndhlovu, M. Nose, T. Noda, and K. Sugamura. 2000. Impairment of antigen-presenting cell function in mice lacking expression of OX40 ligand. *J.Exp.Med.* 191:365-374.

120. Imura, A., T. Hori, K. Imada, T. Ishikawa, Y. Tanaka, M. Maeda, S. Imamura, and T. Uchiyama. 1996. The human OX40/gp34 system directly mediates adhesion of activated T cells to vascular endothelial cells. *J.Exp.Med.* 183:2185-2195.

121. Baum, P. R., R. B. Gayle, III, F. Ramsdell, S. Srinivasan, R. A. Sorensen, M. L. Watson, M. F. Seldin, E. Baker, G. R. Sutherland, K. N. Clifford, and . 1994. Molecular characterization of murine and human OX40/OX40 ligand systems: identification of a human OX40 ligand as the HTLV-1-regulated protein gp34. *EMBO J.* 13:3992-4001.

122. Yoshioka, T., A. Nakajima, H. Akiba, T. Ishiwata, G. Asano, S. Yoshino, H. Yagita, and K. Okumura. 2000. Contribution of OX40/OX40 ligand interaction to the pathogenesis of rheumatoid arthritis. *Eur.J.Immunol.* 30:2815-2823.

123. Weinberg, A. D., K. W. Wegmann, C. Funatake, and R. H. Whitham. 1999. Blocking OX-40/OX-40 ligand interaction in vitro and in vivo leads to decreased T cell function and amelioration of experimental allergic encephalomyelitis. *J.Immunol.* 162:1818-1826.

124. Tittle, T. V., A. D. Weinberg, C. N. Steinkeler, and R. T. Maziarz. 1997. Expression of the T-cell activation antigen, OX-40, identifies alloreactive T cells in acute graft-versus-host disease. *Blood* 89:4652-4658.

125. Sugamura, K., N. Ishii, and A. D. Weinberg. 2004. Therapeutic targeting of the effector T-cell co-stimulatory molecule OX40. *Nat.Rev.Immunol.* 4:420-431.

126. Weinberg, A. D., A. T. Vella, and M. Croft. 1998. OX-40: life beyond the effector T cell stage. *Semin.Immunol.* 10:471-480.

127. Tsukada, N., H. Akiba, T. Kobata, Y. Aizawa, H. Yagita, and K. Okumura. 2000. Blockade of CD134 (OX40)-CD134L interaction ameliorates lethal acute graft-versus-host disease in a murine model of allogeneic bone marrow transplantation. *Blood* 95:2434-2439.

128. Verjans, G. M., L. Remeijer, R. S. van Binnendijk, J. G. Cornelissen, H. J. Volker-Dieben, S. G. Baarsma, and A. D. Osterhaus. 1998. Identification and characterization of herpes simplex virus-specific CD4+ T cells in corneas of herpetic stromal keratitis patients. *J.Infect.Dis.* 177:484-488.

129. Verjans, G. M., L. Remeijer, C. M. Mooy, and A. D. Osterhaus. 2000. Herpes simplex virus-specific T cells infiltrate the cornea of patients with herpetic stromal keratitis: no evidence for autoreactive T cells. *Invest Ophthalmol.Vis.Sci.* 41:2607-2612.

130. Koelle, D. M., S. N. Reymond, H. Chen, W. W. Kwok, C. McClurkan, T. Gyaltsong, E. W. Petersdorf, W. Rotkis, A. R. Talley, and D. A. Harrison. 2000. Tegument-specific, virus-reactive CD4 T cells localize to the cornea in herpes simplex virus interstitial keratitis in humans. *J Virol* 74:10930-10938.

131. Stuart, P. M., B. Summers, J. E. Morris, L. A. Morrison, and D. A. Leib. 2004. CD8(+) T cells control corneal disease following ocular infection with herpes simplex virus type 1. *J.Gen.Virol.* 85:2055-2063.

132. Banerjee, K., P. S. Biswas, U. Kumaraguru, S. P. Schoenberger, and B. T. Rouse. 2004. Protective and pathological roles of virus-specific and bystander CD8+ T cells in herpetic stromal keratitis. *J.Immunol.* 173:7575-7583.

133. Huster, K. M., V. Panoutsakopoulou, K. Prince, M. E. Sanchirico, and H. Cantor. 2002. T cell-dependent and -independent pathways to tissue destruction following herpes simplex virus-1 infection. *Eur.J.Immunol.* 32:1414-1419.

134. Deshpande, S., M. Zheng, S. Lee, K. Banerjee, S. Gangappa, U. Kumaraguru, and B. T. Rouse. 2001. Bystander activation involving t lymphocytes in herpetic stromal keratitis. *J Immunol* 167:2902-2910.

135. Janssen, E. M., E. E. Lemmens, T. Wolfe, U. Christen, M. G. von Herrath, and S. P. Schoenberger. 2003. CD4+ T cells are required for secondary expansion and memory in CD8+ T lymphocytes. *Nature* 421:852-856.

136. Shedlock, D. J. and H. Shen. 2003. Requirement for CD4 T cell help in generating functional CD8 T cell memory. *Science* 300:337-339.

137. Sun, J. C. and M. J. Bevan. 2003. Defective CD8 T cell memory following acute infection without CD4 T cell help. *Science* 300:339-342.

138. Bevan, M. J. 2004. Helping the CD8(+) T-cell response. *Nat.Rev.Immunol.* 4:595-602.

139. Keene, J. A. and J. Forman. 1982. Helper activity is required for the in vivo generation of cytotoxic T lymphocytes. *J.Exp.Med.* 155:768-782.

140. Marzo, A. L., V. Vezys, K. D. Klonowski, S. J. Lee, G. Muralimohan, M. Moore, D. F. Tough, and L. Lefrancois. 2004. Fully functional memory CD8 T cells in the absence of CD4 T cells. *J.Immunol.* 173:969-975.

141. Riberdy, J. M., J. P. Christensen, K. Branum, and P. C. Doherty. 2000. Diminished primary and secondary influenza virus-specific CD8(+) T-cell responses in CD4-depleted Ig(-/-) mice. *J.Virol.* 74:9762-9765.

142. Serbina, N. V., V. Lazarevic, and J. L. Flynn. 2001. CD4(+) T cells are required for the development of cytotoxic CD8(+) T cells during Mycobacterium tuberculosis infection. *J.Immunol.* 167:6991-7000.

143. Bourgeois, C., B. Rocha, and C. Tanchot. 2002. A role for CD40 expression on CD8+ T cells in the generation of CD8+ T cell memory. *Science* 297:2060-2063.

144. Janssen, E. M., N. M. Droin, E. E. Lemmens, M. J. Pinkoski, S. J. Bensinger, B. D. Ehst, T. S. Griffith, D. R. Green, and S. P. Schoenberger. 2005. CD4+ T-cell help controls CD8+ T-cell memory via TRAIL-mediated activation-induced cell death. *Nature* 434:88-93.

145. Cardin, R. D., J. W. Brooks, S. R. Sarawar, and P. C. Doherty. 1996. Progressive loss of CD8+ T cell-mediated control of a gamma-herpesvirus in the absence of CD4+ T cells. *J.Exp.Med.* 184:863-871.

146. Belz, G. T., H. Liu, S. Andreansky, P. C. Doherty, and P. G. Stevenson. 2003. Absence of a functional defect in CD8+ T cells during primary murine gammaherpesvirus-68 infection of I-A(b-/-) mice. *J.Gen.Virol.* 84:337-341.

147. Stevenson, P. G., G. T. Belz, J. D. Altman, and P. C. Doherty. 1998. Virus-specific CD8(+) T cell numbers are maintained during gamma-herpesvirus reactivation in CD4-deficient mice. *Proc.Natl.Acad.Sci.U.S.A* 95:15565-15570.

148. Khanna, K. M., A. J. Lepisto, V. Decman, and R. L. Hendricks. 2004. Immune control of herpes simplex virus during latency. *Curr.Opin.Immunol.* 16:463-469.

149. Khanna, K. M., A. J. Lepisto, and R. L. Hendricks. 2004. Immunity to latent viral infection: many skirmishes but few fatalities. *Trends Immunol.* 25:230-234.

150. Fuller, M. J. and A. J. Zajac. 2003. Ablation of CD8 and CD4 T cell responses by high viral loads. *J.Immunol.* 170:477-486.

151. Khanolkar, A., M. J. Fuller, and A. J. Zajac. 2002. T cell responses to viral infections: lessons from lymphocytic choriomeningitis virus. *Immunol.Res.* 26:309-321.

152. Fuller, M. J., A. Khanolkar, A. E. Tebo, and A. J. Zajac. 2004. Maintenance, loss, and resurgence of T cell responses during acute, protracted, and chronic viral infections. *J.Immunol.* 172:4204-4214.

153. Wherry, E. J., D. L. Barber, S. M. Kaech, J. N. Blattman, and R. Ahmed. 2004. Antigen-independent memory CD8 T cells do not develop during chronic viral infection. *Proc.Natl.Acad.Sci.U.S.A* 101:16004-16009.

154. van der Most, R. G., K. Murali-Krishna, J. G. Lanier, E. J. Wherry, M. T. Puglielli, J. N. Blattman, A. Sette, and R. Ahmed. 2003. Changing immunodominance patterns in antiviral CD8 T-cell responses after loss of epitope presentation or chronic antigenic stimulation. *Virology* 315:93-102.

155. Wherry, E. J., J. N. Blattman, K. Murali-Krishna, M. R. van der, and R. Ahmed. 2003. Viral persistence alters CD8 T-cell immunodominance and tissue distribution and results in distinct stages of functional impairment. *J.Virol.* 77:4911-4927.

156. Welsh, R. M. 2001. Assessing CD8 T cell number and dysfunction in the presence of antigen. *J.Exp.Med.* 193:F19-F22.

157. Zhang, D., P. Shankar, Z. Xu, B. Harnisch, G. Chen, C. Lange, S. J. Lee, H. Valdez, M. M. Lederman, and J. Lieberman. 2003. Most antiviral CD8 T cells during chronic viral infection do not express high levels of perforin and are not directly cytotoxic. *Blood* 101:226-235.

158. Lieberman, J., P. Shankar, N. Manjunath, and J. Andersson. 2001. Dressed to kill? A review of why antiviral CD8 T lymphocytes fail to prevent progressive immunodeficiency in HIV-1 infection. *Blood* 98:1667-1677.

159. Chen, G., P. Shankar, C. Lange, H. Valdez, P. R. Skolnik, L. Wu, N. Manjunath, and J. Lieberman. 2001. CD8 T cells specific for human immunodeficiency virus, Epstein-Barr

virus, and cytomegalovirus lack molecules for homing to lymphoid sites of infection. *Blood* 98:156-164.

160. van Baarle, D., A. Tsegaye, F. Miedema, and A. Akbar. 2005. Significance of senescence for virus-specific memory T cell responses: rapid ageing during chronic stimulation of the immune system. *Immunol.Lett.* 97:19-29.

161. Matloubian, M., R. J. Concepcion, and R. Ahmed. 1994. CD4+ T cells are required to sustain CD8+ cytotoxic T-cell responses during chronic viral infection. *J.Virol.* 68:8056-8063.

162. Zajac, A. J., J. N. Blattman, K. Murali-Krishna, D. J. Sourdive, M. Suresh, J. D. Altman, and R. Ahmed. 1998. Viral immune evasion due to persistence of activated T cells without effector function [see comments]. *J.Exp.Med.* 188:2205-2213.

163. Haskova, Z., N. Usiu, J. S. Pepose, T. A. Ferguson, and P. M. Stuart. 2000. CD4+ T cells are critical for corneal, but not skin, allograft rejection. *Transplantation* 69:483-487.

164. Fu, T. M., R. H. Bonneau, M. J. Tevethia, and S. S. Tevethia. 1993. Simian virus 40 T antigen as a carrier for the expression of cytotoxic T-lymphocyte recognition epitopes. *J.Virol.* 67:6866-6871.

165. Flynn, S., K. M. Toellner, C. Raykundalia, M. Goodall, and P. Lane. 1998. CD4 T cell cytokine differentiation: the B cell activation molecule, OX40 ligand, instructs CD4 T cells to express interleukin 4 and upregulates expression of the chemokine receptor, Blr-1. *J.Exp.Med.* 188:297-304.

166. Yu, S., B. Medling, H. Yagita, and H. Braley-Mullen. 2001. Characteristics of inflammatory cells in spontaneous autoimmune thyroiditis of NOD.H-2h4 mice. *J.Autoimmun.* 16:37-46.

167. Kaleeba, J. A., H. Offner, A. A. Vandenbark, A. Lublinski, and A. D. Weinberg. 1998. The OX-40 receptor provides a potent co-stimulatory signal capable of inducing encephalitogenicity in myelin-specific CD4+ T cells. *Int.Immunol.* 10:453-461.

168. Nohara, C., H. Akiba, A. Nakajima, A. Inoue, C. S. Koh, H. Ohshima, H. Yagita, Y. Mizuno, and K. Okumura. 2001. Amelioration of experimental autoimmune encephalomyelitis with anti-OX40 ligand monoclonal antibody: a critical role for OX40 ligand in migration, but not development, of pathogenic T cells. *J.Immunol.* 166:2108-2115.

169. Lane, P. 2000. Role of OX40 signals in coordinating CD4 T cell selection, migration, and cytokine differentiation in T helper (Th)1 and Th2 cells. *J.Exp.Med.* 191:201-206.

170. Zhao, Z.-S., F. Granucci, L. Yeh, P. A. Schaffer, and H. Cantor. 1998. Molecular mimicry by herpes simplex virus-type 1: Autoimmune disease after viral infection. *Science* 279:1344-1347.

171. Gangappa, S., S. P. Deshpande, and B. T. Rouse. 1999. Bystander activation of CD4(+) T cells can represent an exclusive means of immunopathology in a virus infection. *Eur.J.Immunol.* 29:3674-3682.

172. Maertzdorf, J., G. M. Verjans, L. Remeijer, K. A. van der, and A. D. Osterhaus. 2003. Restricted T cell receptor beta-chain variable region protein use by cornea-derived CD4+ and CD8+ herpes simplex virus-specific T cells in patients with herpetic stromal keratitis. *J.Infect.Dis.* 187:550-558.

173. Johnson, R. M., D. W. Lancki, F. W. Fitch, and P. G. Spear. 1990. Herpes simplex virus glycoprotein D is recognized as antigen by CD4+ and CD8+ T lymphocytes from infected mice. Characterization of T cell clones. *J.Immunol.* 145:702-710.

174. Heiligenhaus, A., S. Jayaraman, S. Soukiasian, M. Dorf, and C. S. Foster. 1995. [Glycoprotein D (5-23) specific Th2-T-cell line induces HSV-1 keratitis]. *Ophthalmologe* 92:484-491.

175. Foster, C. S., G. A. Rodriguez, M. Pedroza-Seres, A. Berra, A. Heiligenhaus, S. Soukiasian, and S. Jayaraman. 1993. Murine herpes simplex virus keratitis is accentuated by CD4+, V beta 8.2+ Th2 T cells. *Trans.Am.Ophthalmol.Soc.* 91:325-348.

176. Heiligenhaus, A., A. Berra, and C. S. Foster. 1994. CD4+V beta 8+ T cells mediate herpes stromal keratitis. *Curr.Eye Res.* 13:711-716.

177. Pedroza-Seres, M., S. Goei, J. Merayo-Lloves, J. E. Dutt, S. J. Lee, V. Arrunategui-Correa, and C. S. Foster. 1995. T cell receptor V beta gene expression in experimental herpes stromal keratitis. *Eye* 9 (Pt 5):599-604.

178. Seo, S. K., H. Y. Park, J. H. Choi, W. Y. Kim, Y. H. Kim, H. W. Jung, B. Kwon, H. W. Lee, and B. S. Kwon. 2003. Blocking 4-1BB/4-1BB ligand interactions prevents herpetic stromal keratitis. *J.Immunol.* 171:576-583.

179. Gangappa, S., S. P. Deshpande, and B. T. Rouse. 2000. Bystander activation of CD4+ T cells accounts for herpetic ocular lesions. *Invest Ophthalmol.Vis.Sci.* 41:453-459.

180. Rouse, B. T. 1996. Virus-induced immunopathology. [Review] [121 refs]. *Advances in Virus Research* 47:353-376.

181. Locksley, R. M., S. L. Reiner, F. Hatam, D. R. Littman, and N. Killeen. 1993. Helper T cells without CD4: Control of Leishmaniasis in CD4- deficient mice. *Science* 261:1448-1451.

182. Tyznik, A. J., J. C. Sun, and M. J. Bevan. 2004. The CD8 population in CD4-deficient mice is heavily contaminated with MHC class II-restricted T cells. *J.Exp.Med.* 199:559-565.

183. Rahemtulla, A., T. M. Kundig, A. Narendran, M. F. Bachmann, M. Julius, C. J. Paige, P. S. Ohashi, R. M. Zinkernagel, and T. W. Mak. 1994. Class II major histocompatibility complex-restricted T cell function in CD4-deficient mice. *Eur.J.Immunol.* 24:2213-2218.

184. Lang, K. S., M. Recher, A. A. Navarini, N. L. Harris, M. Lohning, T. Junt, H. C. Probst, H. Hengartner, and R. M. Zinkernagel. 2005. Inverse correlation between IL-7 receptor expression and CD8 T cell exhaustion during persistent antigen stimulation. *Eur.J.Immunol.* 35:738-745.

185. Huster, K. M., V. Busch, M. Schiemann, K. Linkemann, K. M. Kerksiek, H. Wagner, and D. H. Busch. 2004. Selective expression of IL-7 receptor on memory T cells identifies early CD40L-dependent generation of distinct CD8+ memory T cell subsets. *Proc.Natl.Acad.Sci.U.S.A* 101:5610-5615.

186. Gramaglia, I., A. D. Weinberg, M. Lemon, and M. Croft. 1998. Ox-40 ligand: a potent costimulatory molecule for sustaining primary CD4 T cell responses. *J.Immunol.* 161:6510-6517.

187. Weinberg, A. D. 2002. OX40: targeted immunotherapy--implications for tempering autoimmunity and enhancing vaccines. *Trends Immunol.* 23:102-109.

188. Malmstrom, V., D. Shipton, B. Singh, A. Al Shamkhani, M. J. Puklavec, A. N. Barclay, and F. Powrie. 2001. CD134L expression on dendritic cells in the mesenteric lymph nodes drives colitis in T cell-restored SCID mice. *J.Immunol.* 166:6972-6981.

189. Streilein, J. W., M. R. Dana, and B. R. Ksander. 1997. Immunity causing blindness: five different paths to herpes stromal keratitis. *Immunol.Today* 18:443-449.

190. Deshpande, S., M. Zheng, S. Lee, K. Banerjee, S. Gangappa, U. Kumaraguru, and B. T. Rouse. 2001. Bystander activation involving T lymphocytes in herpetic stromal keratitis. *J Immunol.* 167:2902-2910.

191. Panoutsakopoulou, V., M. E. Sanchirico, K. M. Huster, M. Jansson, F. Granucci, D. J. Shim, K. W. Wucherpfennig, and H. Cantor. 2001. Analysis of the Relationship between Viral Infection and Autoimmune Disease. *Immunity.* 15:137-147.

192. Avery, A. C., Z.-S. Zhao, A. Rodriguez, E. K. Bikoff, M. Soheilian, C. S. Foster, and H. Cantor. 1995. Resistance to herpes stromal keratitis conferred by an IgG2a-derived peptide. *Nature* 376:431-433.

193. He, Y. G., J. Ross, and J. Y. Niederkorn. 1991. Promotion of murine orthotopic corneal allograft survival by systemic administration of anti-CD4 monoclonal antibody. *Invest Ophthalmol.Vis.Sci.* 32:2723-2728.

194. He, Y. G. and J. Y. Niederkorn. 1996. Depletion of donor-derived Langerhans cells promotes corneal allograft survival. *Cornea* 15:82-89.

195. Bourgeois, C., H. Veiga-Fernandes, A. M. Joret, B. Rocha, and C. Tanchot. 2002. CD8 lethargy in the absence of CD4 help. *Eur.J.Immunol.* 32:2199-2207.

196. Crough, T., J. M. Burrows, C. Fazou, S. Walker, M. P. Davenport, and R. Khanna. 2005. Contemporaneous fluctuations in T cell responses to persistent herpes virus infections. *Eur.J.Immunol.* 35:139-149.

197. Manickan, E. and B. T. Rouse. 1996. Roles of different T-cell subsets in control of herpes simplex virus infection determind by using T-cell-deficient mouse models. *J.Virol.* 69:8178-8179.

198. Halford, W. P., J. W. Balliet, and B. M. Gebhardt. 2004. Re-evaluating natural resistance to herpes simplex virus type 1. *J.Virol.* 78:10086-10095.

199. Hou, S., L. Hyland, K. W. Ryan, A. Portner, and P. C. Doherty. 1994. Virus-specific CD8+ T-cell memory determined by clonal burst size. *Nature* 369:652-654.

200. Doherty, P. C., S. Hou, and R. A. Tripp. 1994. CD8+ T-cell memory to viruses. *Curr.Opin.Immunol.* 6:545-552.

201. Celum, C. L. 2004. The interaction between herpes simplex virus and human immunodeficiency virus. *Herpes.* 11 Suppl 1:36A-45A.

202. Hodge, W. G. and T. P. Margolis. 1997. Herpes simplex virus keratitis among patients who are positive or negative for human immunodeficiency virus: an epidemiologic study. *Ophthalmology* 104:120-124.

203. Augenbraun, M., J. Feldman, K. Chirgwin, J. Zenilman, L. Clarke, J. DeHovitz, S. Landesman, and H. Minkoff. 1995. Increased genital shedding of herpes simplex virus type 2 in HIV-seropositive women. *Ann.Intern.Med.* 123:845-847.

204. Schacker, T., J. Zeh, H. L. Hu, E. Hill, and L. Corey. 1998. Frequency of symptomatic and asymptomatic herpes simplex virus type 2 reactivations among human immunodeficiency virus-infected men. *J.Infect.Dis.* 178:1616-1622.

205. Jennings, S. R., R. H. Bonneau, P. M. Smith, R. M. Wolcott, and R. Chervenak. 1991. CD4-positive T lymphocytes are required for the generation of the primary but not the secondary CD8-positive cytolytic T lymphocyte response to herpes simplex virus in C57BL/6 mice. *Cell Immunol.* 133:234-252.

206. Deshpande, S. P., M. Zheng, M. Daheshia, and B. T. Rouse. 2000. Pathogenesis of herpes simplex virus-induced ocular immunoinflammatory lesions in B-cell-deficient mice. *J.Virol.* 74:3517-3524.

207. Daheshia, M., S. Deshpande, S. Chun, N. A. Kuklin, and B. T. Rouse. 1999. Resistance to herpetic stromal keratitis in immunized B-cell-deficient mice. *Virology* 257:168-176.

208. Deshpande, S. P., U. Kumaraguru, and B. T. Rouse. 2000. Dual role of B cells in mediating innate and acquired immunity to herpes simplex virus infections. *Cell Immunol.* 202:79-87.

209. Beland, J. L., R. A. Sobel, H. Adler, N. C. Del Pan, and I. J. Rimm. 1999. B cell-deficient mice have increased susceptibility to HSV-1 encephalomyelitis and mortality. *J.Neuroimmunol.* 94:122-126.

210. Shimeld, C., T. J. Hill, W. A. Blyth, and D. L. Easty. 1990. Passive immunization protects the mouse eye from damage after herpes simplex virus infection by limiting spread of virus in the nervous system. *J.Gen.Virol.* 71:681-687.

211. McKendall, R. R., T. Klassen, and J. R. Baringer. 1979. Host defenses in herpes simplex infections of the nervous system: effect of antibody on disease and viral spread. *Infect.Immun.* 23:305-311.

212. Fuller, M. J., D. A. Hildeman, S. Sabbaj, D. E. Gaddis, A. E. Tebo, L. Shang, P. A. Goepfert, and A. J. Zajac. 2005. Cutting Edge: Emergence of CD127high Functionally Competent Memory T Cells Is Compromised by High Viral Loads and Inadequate T Cell Help. *J.Immunol.* 174:5926-5930.

213. Sawtell, N. M. 1998. The probability of in vivo reactivation of herpes simplex virus type 1 increases with the number of latently infected neurons in the ganglia. *J.Virol.* 72:6888-6892.

214. Sawtell, N. M. and R. L. Thompson. 2004. Comparison of herpes simplex virus reactivation in ganglia in vivo and in explants demonstrates quantitative and qualitative differences. *J.Virol.* 78:7784-7794.

215. Sawtell, N. M., D. K. Poon, C. S. Tansky, and R. L. Thompson. 1998. The latent herpes simplex virus type 1 genome copy number in individual neurons is virus strain specific and correlates with reactivation. *J.Virol.* 72:5343-5350.